Truly Innovative Engineering
for Exceptional Performance

University of Maryland
June 1, 2009

GRIFFIN

VERITAS

FASTER STRONGER FARTHER LONGER QUIETER SAFER GREENER

University of Maryland
Alfred Gessow Rotorcraft Center
Department of Aerospace Engineering
University of Maryland
College Park, Maryland 20742

GRIFFIN
VERITAS
Truly Innovative Engineering for Exceptional Performance

In Response to the 2009 American Helicopter Society
Student Design Competition – Graduate Student Category
NON-CONVENTIONAL ROTOR DRIVE
June 1, 2009

Louise Ahuré, Graduate Student

LCDR A. C. Dutko, USN, Graduate Student

Eric Greenwood, Graduate Student

Timothy E. Lee, Graduate Student (Team Leader)

Ria P. Malhan, Graduate Student

Kumar Ravichandran, Graduate Student

Anand Saxena, Graduate Student

Dr. Inderjit Chopra, Faculty Advisor

Dr. J. Gordon Leishman, Faculty Advisor

Dr. V. T. Nagaraj, Faculty Advisor

All students received academic credit for ENAE 634 "Helicopter Design" through submission of this design proposal.

Acknowledgements

The *Griffin* design team wishes to acknowledge the following people and thank them for their guidance and assistance.

Dr. Vengalattore T. Nagaraj - Senior Research Scientist, Dept. of Aerospace Engineering, University of Maryland, College Park

Dr. Inderjit Chopra - Interim Chair, Gessow Professor, and Director of Gessow Rotorcraft Center (AGRC), Dept. of Aerospace Engineering, University of Maryland, College Park

Dr. J. Gordon Leishman - Minta Martin Professor of Engineering, Dept. of Aerospace Engineering, University of Maryland, College Park

Dr. Roberto Celi - Professor, Dept. of Aerospace Engineering, University of Maryland, College Park

Dr. Fredric Schmitz - Senior Research Professor, Dept. of Aerospace Engineering, University of Maryland, College Park

Dr. James Baeder - Associate Professor, Dept. of Aerospace Engineering, University of Maryland, College Park

Dr. Darryll J. Pines - Dean, Clark School of Engineering and Professor, Dept. of Aerospace Engineering, University of Maryland, College Park

Dr. Norman Wereley - Professor, Dept. of Aerospace Engineering, University of Maryland, College Park

Dr. Christopher Cadou - Associate Professor, Dept. of Aerospace Engineering, University of Maryland, College Park

Dr. Sean Humbert - Assistant Professor/Director, Autonomous Vehicle Laboratory, Dept. of Aerospace Engineering, University of Maryland, College Park

Dr. Shreyas Ananthan - Assistant Research Scientist, Dept. of Aerospace Engineering, University of Maryland, College Park

Jaye Falls, Jason Pereira, Peter Copp, Arun Jose, Monica Syal, Abhishek Roy, Moble Benedict, Vikram Hrishikeshavan, Brandon Bush, Nicholas Wilson, Daniel C. Sargent, Richard Sickenberger, Evan Ulrich, Ben Woods, Bradley Johnson, Ben Berry : Graduate students at the Dept. of Aerospace Engineering, University of Maryland, College Park

Dr. Manikandan Ramasamy - NASA AMES

Dr. Jinsong Bao - Dynamics and Acoustics, Sikorsky Aircraft, Co.

Dr. Preston B. Martin - Research Scientist, NASA Ames Research Center

Dr. A.R. Manjunath - Additional General Manager, Hindustan Aeronautics Limited, Bangalore, India.]

LCDR Scott Stringer - MH-60S Class Desk, Naval Air Systems Command, NAS Patuxent RIver, MD

Mr. Jeffrey DeBruin - Air Vehicle Engineering Department, Aeromechanics Division, Rotary Wing Performance Branch, Naval Air Systems Command, Patuxent River, MD

Maryland State Police Aviation Command, Fredrick Station Section “Trooper 3”.

Contents

List of Figures

List of Tables

RFP Requirements and Compliance

RFP Requirements	Design Solutions Taken to Comply	Reference
Retain rotorcraft capabilities	Griffin is fully capable of vertical and omni-directional flight, hover, and autorotation	Sec. 4, 5.2, 9, 7
Derivative of a current, in-service helicopter between 3500 kg to 5500 kg	EC145 is selected as baseline helicopter with MTOW = 7887 lbs (3585 kg)	Sec. 2.2
Alternative, non-conventional rotor/drive system:	Variable Energy Rotor and Innovative Transmission ArchitectureS (VERITAS)	
• Rotors	Variable energy rotor with integrated trailing edge flaps, de-icing system, innovative blade tip (TALON), swiveling tail prop	Sec. 5.1,5.3
• Rotor control system	Fly-by-wire system using electrohydrostatic actuators	Sec. 5.9, 9
• Drivetrain	Innovative multi-speed gearboxes with a dual clutch mechanism, novel split-torque transmission	Sec. 4
• Engines	Baseline helicopter engines replaced with more efficient, lightweight, and suitable Rolls-Royce 250-C30 engines, which can operate in off-design conditions with FADEC	Sec. 4.2
Substantiate improved performance compared to baseline helicopter in:		
• Speed	Cruise speed increased by 15% (from 131 to 150 knots); Never Exceed Speed (V_{NE}) increased by 17% (from 150 to 176 knots)	Sec. 12,7
• Range	Maximum range increased by 64% (from 360 to 590 nm)	Sec. 12, 7
• Payload	Payload capability increased by 4% (from 2242 to 2332 lb)	Sec. 9, 11, 7
• Endurance	Maximum endurance increased by 76% (from 4 h 12 min to 7 h 24 min)	Sec. 11, 12, 7
• Noise	Perceived noise level reduced by 82%	Sec. 8
Mission considerations	Safety features : OEI capability, degraded visibility landing aid, crash survivability and vibration reduction seats, rotor speed manual override capability	Sec. 4, 10.2, 13.1
Capable of undergoing a certification process with Aviation Authority	Designed under CFR Title 14, PART 29 - Airworthiness Standards: Transportation Category Rotorcraft	Sec. 5.1, 5.9, 11, 12, 13.1
New design is not increased in size and/or power	Compared to baseline helicopter, Griffin's MTOW is within 4.4 lbs (2 kg), hover power remains the same, and power required is reduced by 50% at maximum endurance speed	Sec. 3, 14, 7
Materials utilized must be functionally, mechanically and thermally feasible	Drivetrain and swiveling tail prop function and mechanism clearly explained; current materials, manufacturing processes, and engines utilized	Sec. 4, 5.2, 6.2, 11
Final design must focus on describing the new rotor/drive system to substantiate performance claims	Detailed description of improved performance of designed VERITAS is provided	Sec. 4, 5.1, 5.2, 7

– continued

RFP Requirements	Design Solutions Taken to Comply	Reference
Final design must substantiate claims and clarify functions and construction details	VERITAS construction and functions explained and performance analysis substantiated	Sec. 4, 5.1, 5.2, 7, Foldouts

Answers to RFP Questions (RFP-Q)	Design Solutions Taken to Comply	Reference
Initial Operational Capability 2015	*Griffin* utilizes existing technologies to minimize developmental risks	Sec. 4, 4.2, 5.3, 9, 13.1
Demonstrate rotorcraft "power-off autorotation" landing capabilities	"Power-off autorotation" landing capabilities shown even with 85% of hover main rotor speed	Sec. 7
Final design must range within MTOW class of 3500 kg to 5500 kg	Final design MTOW of 7891 lbs (3587 kg)	Sec. 14
Rotorcraft of the same class as baseline helicopter with same mission capabilities	Baseline helicopter is a two-engine light utility class specifically for transportation, and Griffin is a two-engine light utility class fulfilling the same mission requirements with improved performance	Sec. 4.2, 11, 7, 14
Proposed design must not claim performance improvements on expected technology progress not based on realistic data	Physics-based design performance analysis clearly explained, and data and assumptions realistic and justified	Sec. 4.2, 10.1, 11, 7
Airframe changes should be functional to the integration of the new system, and should retain the baseline airframe as much as possible	Airframe designed to retain EC145 airframe while integrating structural modifications for tail prop, engine and exhaust location and streamlining to contribute to performance improvement	Sec. 11, 12, 6.2
Proposal should attempt to improve performance in as many parameters (speed, range, endurance, payload, noise) as possible	Improved performance over baseline in ALL five categories: speed (15% increase), maximum range (64% increase), maximum endurance (76% increase), payload (4% increase), and noise (82% reduction)	Sec. 7

List of Main Symbols

A	Disk Area
AR	Aspect ratio
c	Chord
C_T / σ	Blade loading coefficient
EA	Axial stiffness
EI_y	Flap-bending stiffness
EI_z	Lead-lag bending stiffness
f	Flat plate area
GJ	Torsion bending stiffness
H	Harris and Scully's function
I_R	Rotor Inertia
J	Vibration objective function
L	Roll moment
$L_{\theta_{1c}}$	Derivative of roll moment with respect to lateral cyclic pitch
L/D	Lift-to-drag
m	Local mass per unit-length
m_0	Reference mass per unit-length
M_{dd}	Mach drag divergence
M	Pitch moment
N	Yaw moment
N_2	Operating turbine output speed
N_b	Number of blades
N_R	Nominal Speed
P	Power
r	Spanwise location
R	Radius
SFC_{NR}	Specific Fuel Consumption at nominal speed
V_{tip}	Tip speed
W	Takeoff Weight
W_o	Empty Weight
W_z	Matrix of penalties for hub loads
W_θ	Matrix of penalties for flap harmonics
X, Y, Z	Longitudinal, lateral, vertical forces
$\bar{Z}$	Vector of hub loads
$\bar{\theta}$	Vector of trailing edge flap harmonics
θ_0	Blade collective pitch
θ_{1c}	Lateral cyclic pitch
θ_{1s}	Longitudinal cyclic pitch
θ_t	Tail collective pitch
ν_ξ	Blade rotating lag frequency
σ	Solidity
Ω	Rotor speed

Subscripts

p, q, r	Roll, pitch, yaw rates
u, v, w	Longitudinal, lateral, vertical translational velocities

List of Abbreviations

AACVS	Attitude and Acceleration Command/Velocity Stabilization
ACAH	Attitude Command/Attitude Hold
ACP	Autopilot Control Processor
ACPS	Attitude Command/Position Stabilization
ADC	Air Data Computer
AEA	Adaptive Energy Absorbing
AFCS	Automatic Flight Control System
AGMA	American Gear Manufactures Association
AHRS	Attitude and Heading Reference System
A.I.	Autorotation Index
Al-Li	Aluminum Lithium
AMD	Advance Micro Devices
APU	Auxiliary Power Unit
ASI	Airspace Situation Indicator
BVI	Blade Vortex Interaction
CATIA	Computer Aided Tridimensional Interactive Application
CBM	Condition Based Maintenance
CDS	Control Displacement Panel
CFD	Computational Fluid Dynamics
CG	Center of Gravity
CO2	Carbon Dioxide
COTS	Commercial Off-The-Shelf
CPI	Consumer Price Index
CSC	Control Storage Computer
CSIC	Controlled Solidification Investment Casting
CVT	Continuously Variable Transmission
DARPA	Defense Advanced Research Projects Agency
DAU	Data Acquisition Unit
DECV	Digital EC Controller Velocity
DeVLA	Degraded Visibility Landing Aid
DH	Double Helical
DL	Disk Loading
DOC	Direct Operating Cost
EH	Electrohydrostatic
EHA	Electrohydrostatic actuators
EMI	Electromagnetic Interference
ESFI	Electronic Standby Flight Instrument
GTOW	Gross Takeoff Weight
GPS	Global Positioning System
FADEC	Full Authority Digital Engine Control
FAR	Federal Aviation Regulations
FBW	Fly-By-Wire
FCC	Flight Control Computer
FCC	Fray-Farthing-Chen
FLEA	Fixed Load Energy Absorbing
FLIR	Forward-looking infrared
FMC	Flight Management Computer
FRTP	Fiber Reinforced Thermoplastic
FRTS	Fiber Reinforced Thermoset
FWH	Ffowcs Williams and Hawkings
HOGE	Hover-Out of-Ground Effect
HUD	Heads-up display
HUMS	Health and Usage Monitoring System
H-V	Height-Velocity
ICS	Internal Communication System
ICWS	Integrated Caution and Warning System
IEFM	Interactive Electronic Flight Manual
IFR	Instrument Flight Rules
IGB	Intermediate Gearbox
ILS	Instrument Landing System
IOC	Indirect Operating Cost
IOP	Input/Output Processor
ISA	International Standard Atmosphere
ips	Inches per second
Li-Po	Lithium Polymer
MAC	Modular Aerospace Control
MAR	Mission Adaptive Rotor
MFD	Multi-function display
MEMS	Microelectromechanical Systems
MPD	Magnetic Particle Detectors
MR	Magnetorheological
MRACC	Main Rotor Actuator Control Computer
MTBR	Mean time between Repairs
MTBF	Mean time between Failures
MTOW	Maximum Takeoff Weight
NASA	National Aeronautics and Space Administration

List of Abbreviations (*continued*)

NOx	Nitrous oxide
NOTAR	NO-Tail Rotor
PEEK	Polyetheretherketone
PFD	Primary Flight Display
p-p	peak-to-peak
PPS	Polyphenylene Sulfide
OA	ONERA
OEI	One-Engine Inoperative
OPAS	Obstacle Proximity Awareness System
RACC	Rudder Actuator Control Computer
RAE	Royal Aircraft Establishment
RPM	Revolution per Minute (engine)
RFP	Request for Proposal
RFP-Q	Request for Proposal Questions
RR	Rolls Royce
RTM	Resin Transfer Molding
SAS	Stability Augmentation System
SJA	Synthetic Jet Actuators
SOx	Sulfur Oxide
SFC	Specific Fuel Consumption
SPL	Sound Pressure Level
shp	Shaft Horsepower
TALON	Thinned-Anhedral Lift-Optimized Notched
TAWS	Terrain Avoidance Warning System
TCAS	Traffic Collision Advisory System
TEF	Trailing Edge Flaps
TM	Turbomeca
TOP	Takeoff Power
TPACC	Tail Prop Actuator Control Computer
UHF	Ultra High Frequency
UMARC	University of Maryland Advanced Rotorcraft Code
VAC	Voltage (Alternating Current)
VAC	Vibration Analysis Computer
VDC	Voltage (Direct Current)
VERITAS	Variable Energy Rotor and Innovative ArchitectureS
VHF	Very High Frequency
V.I.I.	Vibration Intrusion Index
VLEA	Variable-Load Energy Absorber
VPEA	Variable Profile Energy Absorbing
VOC	Volatile Organic Compound
VOR	VHF Omnidirectional Range
VVCAS	Vertical Velocity Command/Altitude Stabilization
YRCHS	Yaw Rate Command/Heading Stabilization
YRCTC	Yaw Rate Command/Turn Coordination

Introduction

Tragedy has struck islands in the South Pacific. A tsunami of epic proportions has left thousands without basic necessities and challenges their very survival. Maritime vessels from allied nations immediately deploy, but only those with embarked aviation assets possess the capability of rendering effective humanitarian assistance to the survivors. Luckily, *Griffin* is onboard a number of the first responders' ships. The range and high speed of this advanced rotorcraft permit it to launch and arrive on scene before any other vertical takeoff platforms. Its extended endurance enable it to remain on station longer than all other search and rescue helicopters, and its expansive payload capability increases the effective reach of the responders. The *Griffin*'s reduced noise signature minimizes the obtrusiveness of 24-hour recovery efforts. While such a catastrophe is not without precedent, the capability of those assets relying on the *Griffin* most certainly is. This quantum leap in rotorcraft performance is powered by the innovative rotor system and drivetrain at the heart of the *Griffin*.

The Griffin: Part Lion, Part Eagle, All Performance

The griffin is the legendary creature traditionally portrayed as a fantastic hybrid of a lion and an eagle. In heraldry, griffins symbolize strength and courage. Though their portrayal in literature is diverse, griffins are most often depicted as guardians of treasure. The *Griffin* is thus aptly named, as it too is a hybrid of seemingly disparate entities working to power the whole system. *Griffin*'s innovative rotor system and variable energy drivetrain combine to propel it to unparalled performance. The *Griffin* exemplifies innovative engineering just as the mythological creature embraces its unique, non-conventional nature. Moreover, the *Griffin* serves as a true guardian by rendering priceless rotorcraft assistance to those in need during their darkest hour.

Concept Design

In response to the 2009 AHS Student Design Competition Request for Proposal (RFP) for a non-conventional rotor/drive system, a team from the University of Maryland consisting of seven graduate students — one of whom is a military rotary-wing aviator — was assembled to develop the skills required for successful helicopter design. Their individual specialties included aerodynamics, aeromechanics, acoustics, crash safety, and flight test. To most effectively design a helicopter, these graduate students enrolled in a one-semester Helicopter Design course, ENAE 634. This formal education, coupled with the students' technical specializations and the pilot's extensive operational experience accrued from over 1000 flight hours, culminated in the *Griffin* and its VERITAS: Variable Energy Rotor and Innovative Transmission ArchitectureS. All claims are substantiated by in-house design analyses which were extensively tested and verified with existing data wherever possible to ensure realistic analysis and, ultimately, physical meaning. The primary design method is a comprehensive coupled computer code that incorporates Tishchenko

sizing and blade element performance predictions. The illustrations of the *Griffin* and its components were generated from a variety of computer-aided design applications including CATIA, Pro/ENGINEER, and SolidWorks.

The critical technical parameters of improved speed, range, endurance, payload, and noise signature detailed in the RFP drove selection of the *Griffin*'s primary mission. Humanitarian assistance missions typically require helicopters to launch from air-capable ships, transit expeditiously to an assigned location, deliver or retrieve a payload, and rapidly recover for subsequent tasking. The advanced performance required by the RFP — and the need for the proposed vehicle to retain the hallmark capabilities of a helicopter — are those same improvements needed to increase the ability of rotorcraft to render effective humanitarian assistance. The *Griffin* carries a greater payload over longer distances in shorter time than comparable light utility rotorcraft, and offers extended flight endurance with a minimal noise signature.

The VERITAS of *Griffin* emerged from careful analysis of numerous potential vehicle architectures in light of the following five criteria derived from either the RFP or the AHS Response to RFP Questions:

- ✓ Any potential architecture must empower the aircraft to better achieve the representative mission of humanitarian aid delivery. For the *Griffin*, these critical performance areas are its payload, speed, range, and endurance.
- ✓ Performance increases should not only be limited to those critical areas necessary for the helicopter's primary mission. Any potential architecture must endow *Griffin* with increased speed, range, payload, endurance, and noise signature to improve its overall utility.
- ✓ The proposed rotorcraft must be a derivative of an existing in-service helicopter. To maintain its derivative nature, structural modifications should be limited to those required to support integration of the advanced rotor/drive system.
- ✓ Feasibility, producibility, and maintainability must be key discriminators when examining potential architectures from an engineering perspective. These design drivers arose from the need to meet the required Initial Operational Capability of 2015.
- ✓ Though innovation must be considered at every design level of a potential architecture, increased performance — particularly as a payload delivery vehicle — must outweigh non-conventional solutions. That is, innovation must improve the capability of the derivative rotorcraft and should not be implemented simply for the sake of innovation.

The selection of an in-service helicopter and its existing architecture, from which a derivative rotorcraft and its non-conventional rotor system and drivetrain are designed, is not trivial. Indeed, the baseline aircraft bounds the possible missions of its derivatives and has traditionally dictated the rotor/drive system enabling mission completion. Among helicopters within the 3- to 5-ton weight class, the Eurocopter EC145 was selected as the baseline rotorcraft. It is a leader among light twin-engine utility helicopters and currently employed in a wide variety of roles,

including search and rescue, civil transport, and para-military operations. The primary mission of the EC145 ultimately remains, however, payload delivery. Its commercial success lies in its class-leading productivity and impressive payload delivery efficiency. Nevertheless, the physical limitations that restrict the performance of all conventional helicopters affect the EC145. These phenomena ultimately prevent it from reaching across the capability gap between rotary- and fixed-wing aircraft to offer truly remarkable performance. The *Griffin*, however, not only improves upon the most capable rotorcraft in this weight class, but its innovative rotor system and drivetrain empowers the advanced rotorcraft to bridge the performance divide previously thought too expansive. Moreover, it retains the hallmark performance of rotorcraft: vertical takeoff and landing, omni-directional flight, and autorotational capability for safety.

Considering the application of the RFP requirements and derived criteria to the chosen baseline aircraft within its primary role, the VERITAS of *Griffin* emerged as the non-conventional rotor system and drivetrain best suited to enhancing payload delivery capability. From a technical viewpoint, VERITAS is an optimally-reduced rotational speed, thrust compounding rotor and drive system. The rotor system incorporates advanced rotor blades with Thinned Anhedral Lift-Optimized Notched (TALON) blade tips and trailing edge flaps for vibration suppression. The thrust-compounding tail prop swivels to provide anti-torque in low-speed flight regimes. Through automated engine modulation and transmission gear reduction, VERITAS lowers the main rotor speed in a manner that optimizes the associated power reduction while maintaining safe rotor stall margin. The thrust compounding tail prop amplifies this effect at higher forward flight speeds with an automatic swiveling schedule that enables the main rotor to operate at progressively lower thrust levels. This simultaneously decreases *Griffin*'s acoustic signature and the main rotor's profile power. As such, the *Griffin* operates at its optimal capability throughout the flight envelope and enables a quantum leap in performance over all helicopters in the weight class. *Griffin* is the multi-mission rotary wing platform of the future — capable of carrying a greater payload over longer distances in shorter time than traditional light helicopters — while offering extended flight endurance and minimal external noise.

Performance

VERITAS is designed to maximize the *Griffin*'s payload delivery capability. The complimentary benefits offered by rotor speed reduction and thrust compounding optimize the energy use of the *Griffin* in all flight regimes without sacrificing any capability inherent in the EC145. In fact, the VERITAS of *Griffin* maximizes the range and endurance of the advanced rotorcraft, while significantly improving its speed and payload, and minimizing its acoustic signature.

- ✓ **Faster**: With a maximum speed of 176 knots, *Griffin* sprints 26 knots faster than the baseline aircraft, permitting greater payload delivery in less time than the EC145.
- ✓ **Stronger**: Superior strength-to-weight material advancements endow *Griffin* with a 90 lbs improvement in payload capability over the EC145.

- ✓ **Farther**: *Griffin*'s maximum range is 64% greater than the EC145, allowing the helicopter to impact previously inaccessible regions.
- ✓ **Longer**: With a maximum endurance of 7 hours and 24 minutes, the *Griffin* soars 76% longer than the EC145.
- ✓ **Quieter:** Lower main rotor blade tip speeds reduce the size of *Griffin*'s noise footprint by up to 85%, significantly reducing its environmental impact.
- ✓ **Safer**: *Griffin*'s advanced rotor system retains nearly an identical autorotational index as the baseline EC145, maintaining its industry-leading safety rating.
- ✓ **Greener**: *Griffin* consumes 50% less power and 17% less fuel per flight hour than the EC145, vaulting it to the top of an increasingly energy-sensitive marketplace.

Core Features

The *Griffin* implements an extensive array of innovative technologies designed to optimize its capability. The technical, developmental, and flight safety risks associated with adoption of advanced technology has been minimized through careful system selection and design. Rather than employ technologies that have yet to fully mature, *Griffin*'s system architectures have been adapted from those commercially available, or currently employed on advanced technology demonstrators or rotorcraft in developmental test. In addition, commercial off-the-shelf (COTS) components are utilized where feasible within these advanced subsystem architectures. The performance calculations include a measure of engineering conservatism. As such, even greater performance may be realized by a production *Griffin*.

VERITAS — Main Rotor

The *Griffin*'s innovative 4-bladed main rotor is a primary contributor to its enhanced performance. It is an aerodynamically synthesized system that promotes performance at reduced rotor speeds. The *Griffin*'s rotor hub is designed to enhance effective payload delivery and permit stowage aboard air-capable ships.

- ✓ **Innovative TALON blade tip** avoids drag divergence penalties and increases the rotor figure of merit by incorporating elements of sweep, taper, and anhedral. It also features a notch that delays retreating blade stall, further improving rotor performance by addressing performance limits on either lateral side of the main rotor disk.
- ✓ **Integrated trailing edge flaps** are capable of extensive vibration suppression, eliminating the need for costly and weighty stationary frame vibration reduction systems. Driven by lightweight electric direct current motors rather than expensive smart actuators, the flaps are an innovative yet fiscally responsible solution.
- ✓ **Semi-articulated hub with small hinge offset** featuring established elastomeric bearings capable of a lifetime of 5,000 hours with minimal maintenance, provides lower vibration levels and eliminates the strong control cross couplings inherent in the EC145.

- ✓ **Blade folding capability** shrinks the footprint of the rotorcraft, a critical consideration for shipboard operations where storage space is at a premium.

VERITAS — Engine and Drivetrain

VERITAS is the heart of the *Griffin*, providing the capability for continuous variation in main rotor speed. The *Griffin* consumes 50% less power than the EC145 in forward flight, permitting replacement of the baseline Turbomeca Arriel 1E2 engines with more efficient Rolls Royce 250-C30 engines. This COTS engine is lighter than the baseline, contributing to the improved performance of *Griffin*. Moreover, it operates with a lower specific fuel consumption (SFC), permitting a nearly 5% savings in life-cycle cost through decreased energy consumption. Not only then does *Griffin* outperform the EC145, it is significantly "greener" than the baseline.

- ✓ **Low-maintenance drivetrain** designed for 5,000 hour overhaul intervals and usage of universal MIL-L-23699 oil. VERITAS features easy component access and relies on an extensive Health and Usage Monitoring System (HUMS) to enable Condition Based Maintenance.
- ✓ **Multi-speed main rotor gearbox** provides continuous and efficient rotor speed modulation over a 20% range of rotational speed.
- ✓ **Innovative dual-clutch mechanism** permits smooth and uninterrupted power delivery at all flight and rotor speeds.
- ✓ **Superior corrosion resistance and significant weight reduction** realized through the use of controlled solidification investment cast aluminum gearbox housings.
- ✓ Advanced electronics automate rotor drivetrain control and offer **"hands-off" rotor speed scheduling** based on flight condition with a manual override capability.
- ✓ Modular drivetrain controls allow for **more convenient and safer operation** with automatic start-up, engine relight, and surge detection and recovery features.
- ✓ Drive system architecture requires **no significant changes to the existing EC145 airframe**.

VERITAS — Tail Propeller

The dual-functional tail prop provides anti-torque in hover and propulsion in forward flight. Conversion from anti-torque to thrust compounding mode is performed automatically. The vertical stabilizers, which are mounted at an angle, begin to generate lift as forward airspeed increases, eventually providing sufficient anti-torque to permit the tail prop to swivel aft. Rudders on the vertical stabilizers trim the helicopter in forward flight. *Griffin*'s flight control laws accommodate control switching from the tail prop to the rudders, permitting a single cockpit controller for yaw authority. The tail prop provides ample yaw authority throughout its operational envelope. This increased anti-torque capability dramatically improves upon EC145's widely criticized loss of tail rotor effectiveness during high density altitude operations.

VERITAS — Avionics and Flight Controls

The avionics and flight control systems employed on *Griffin* were specifically designed to decrease the overall aircraft weight while increasing the capability of a fully equipped EC145. Reducing *Griffin*'s weight permits the reallocation of critical vehicle mass in support of the RFP's performance goals. To enable this weight redistribution and optimize *Griffin*'s safety, capability and life cycle costs, the avionics suite and flight controls feature:

- ✓ Aviation-certified and flight-proven **MEMS-based sensors** that improve system reliability and reduce component weight by 64% over comparable equipment in the EC145.
- ✓ Advanced **Health and Usage Monitoring System** that permits reduction of installed component redundancy and contributes to a 4.5% decrease in life cycle costs from the EC145's while improving operator safety.
- ✓ Exclusive **Obstacle Proximity Awareness System** that leverages recent advances in infrared energy sensing technology to offer the operator a 360° representation of objects in the vicinity of the aircraft at low altitude.
- ✓ **Lithium-Polymer batteries** that provide 20 minutes of generator-out power for all installed electrical components at *one-third* the weight of the EC145's battery.
- ✓ FAR Part 29-certified **Automatic Flight Control System** that provides true 'hands-off' capability with force-feel trim and embedded provisions for attitude, altitude, and airspeed hold as well as GPS way-point and glide slope tracking capability at 20% the weight of the baseline system.
- ✓ Innovative, commercially available electrohydrostatic actuators for primary flight control that **virtually eliminate environmentally hazardous hydraulic fluid**.
- ✓ 'Dual-triple' redundant **Fly-By-Wire** architecture that permits rapid incorporation of mission-specific flight control laws and reduces system weight by nearly 40% from EC145's traditional flight control system.
- ✓ Unique **3-axis side-stick flight controller** that increases the safety of ground personnel in close proximity to the rotor system while providing satisfactory handling qualities.

VERITAS — Safety

While historical pioneering helicopter architectures have not always included safety as a critical design driver, VERITAS employs a plethora of fail-safe features to ensure that *Griffin* guards its treasured payload.

- ✓ Twin Rolls Royce 25-C30 engines provide **OEI capability required for FAR Part 29 Category A certification** in the unlikely event of an engine failure.
- ✓ Variable Load Energy Absorbing (VLEA) seats provide *Griffin*'s passengers and crew **crashworthy protection from vertical loads** by limiting occupant lumbar loads to safe levels during decelerations of up to 12 g's.

- ✓ **Innovative "dual-triple" flight control processor approach** achieves the failure coverage of a quadruple cross-channel monitored system without the danger of cross-channel failure propagation or the complexity of a quad voter.
- ✓ **Rotor speed manual override capability** accelerates the main rotor to its maximum operating speed in only seconds to enhance pilot emergency response.
- ✓ **Light-weight swiveling tail prop gearbox** features a fail-safe recall function that returns the tail prop to its traditional antitorque configuration in the unlikely event of an actuation failure.

Comparison Metrics

Multiple metrics are utilized to quantify and compare the exceptional performance of the *Griffin* with other rotorcraft in the weight class. Two measures that are widely accepted in the helicopter industry are used to assess the design: Payload Delivery Efficiency and Productivity.

$$Payload\ Delivery\ Efficiency = \frac{Payload \times Range}{Fuel\ Weight}$$

$$Productivity = \frac{Payload \times Cruise\ Velocity}{Empty\ Weight + Fuel\ Weight}$$

The first is the best metric to compare payload transportation helicopters such as the *Griffin*. It details the effective range per unit of energy consumed as a measure of efficiency in terms of cost. The second is a widely-used metric to assess the overall capability of helicopters across weight classes. It is best viewed as a measure of utility. These two metrics were computed for the *Griffin*, the baseline EC145, and representative light utility helicopters from the other primary manufacturers. As such, calculations for Agusta Westland's AW109E, Bell Helicopter's 430, and the Sikorsky S-76C++ are also included below.

Helicopter		***Griffin***	**Eurocopter EC145** (baseline)	**Bell 430**	**Agusta Westland AW109E**	**Sikorsky S-76C++**
PDE	*nm*	901	529	486	569	647
	Griffin Improvement	—	**70%**	85%	58%	39%
Productivity	*kts*	62.9	51.6	46.0	59.8	43.1
	Griffin Improvement	—	**22%**	37%	5%	46%

Additionally, *Griffin*'s gains in the targeted performance capabilities of speed, range, payload, endurance, and noise signature are compared to the baseline EC145 through a Composite Utility Index. This is a simple index derived to specifically address the performance parameters in the RFP, that weights each capability equally in the following manner:

Composite Utility Index =

$$\left(\frac{Cruise\ Velocity_{Griffin}}{Cruise\ Velocity_{EC145}}\right)\left(\frac{Payload_{Griffin}}{Payload_{EC145}}\right)\left(\frac{Range_{Griffin}}{Range_{EC145}}\right)\left(\frac{Endurance_{Griffin}}{Endurance_{EC145}}\right)$$

Griffin's performance improvements are decomposed into the components of the comparative index and detailed below

Helicopter		***Griffin***	**Eurocopter EC145** (baseline)
Cruise Velocity	*kts (km/h)*	150 (278)	131 (243)
	Griffin Improvement	—	**15%**
Payload	*lb (kg)*	2332 (1060)	2242 (1019)
	Griffin Improvement	—	**4%**
Maximum Range	*nm (km)*	590 (1093)	360 (666)
	Griffin Improvement	—	**64%**
Maximum Endurance	*h:min*	7:24	4:12
	Griffin Improvement	—	**76%**
		CUI = 3.45	

Regardless of the comparison method, *Griffin* truly offers a quantum leap in rotorcraft performance. It offers a 77% increase in payload delivery efficiency, a 22% increase in productivity, and an astounding 245% increase in composite utility index over the baseline EC145. Although not within the target weight class, *Griffin*'s performance is so exceptional that it already meets, and in some cases exceeds, the requirements of the DARPA Mission Adaptive Rotor (MAR) Program.

Desired MAR Attributes	**Fulfilled**	***Griffin* Feature**
40% increase in specific range (range/fuel)	✓	64% increase
50% reduction in acoustic detection range	✓	50% reduction
90% reduction in vibration	✓	100% reduction capabile
Morphing rotor system	✓	RPM variability, Integrated trailing edge flaps
Availability	✓	Minimum significant fuselage changes, COTS equipment
Marinization	✓	Blade and empennage folding, Drivetrain corrosion resistance

Griffin's amazing capability enhancements are also cost-effective. The mere eight percent increase in acquisition cost from the equipped price of an EC145 is fully justified by the performance gains realizable immediately upon fielding *Griffin*. Regardless of this slightly increased initial investment, the total cost of ownership over an assumed 20 year service life with a 400 annual flight hour usage rate is calculated to be $18.6 million for *Griffin* — nearly a 5% savings over the life cycle costs of the EC145. Despite the additional complexity accompanying VERITAS fabrication, operating costs are optimized by relying on an extensive HUMS. This robust COTS system improves safety and thus lowers insurance rates. In addition, the HUMS permits implementation of Condition Based Maintenance. This approach significantly decreases maintenance costs and improves operational availability, further reducing direct-operating costs. Ultimately, the *Griffin* is practical to own and operate — a true testament to its balance between

innovation and feasibility. Careful materials selection, system design, fabrication techniques, and implementation of advanced yet reliable COTS components provides *Griffin* a quantum leap in helicopter capability at a lower cost to own and operate than all other helicopters in the weight class.

Conclusion

Since the earliest hoppers and hoverers, scientists, engineers, and inventors have endeavored to improve the capabilities of the helicopter. Although blessed with a relatively efficient hovering ability for its weight and good low speed maneuverability, the maximum speed — and therefore range — of the conventional helicopter is constrained by a variety of aerodynamic phenomena. Combined with a relatively harsh vibratory environment — one that can impose drastic dynamic component life limits and decrease operator comfort — these drawbacks have prompted the introduction of a plethora of vertical lift concepts seeking to mitigate the helicopter's most undesirable attributes. Few concepts, however, have gained widespread acceptance and this inhospitable environment has served to quash innovation in the rotorcraft marketplace. As a consequence, the notable advances — quantum leaps — in performance accompanying such innovation have been largely missing from the recent history of helicopter development. Indeed, despite decades of continued advances in power generation, rotor design, and materials technology, no recent quantum leap has been achieved. Innovation has been largely curtailed by the perception of excessive risk. Reliable and staid thinking has replaced confident advances in helicopter capability. *Enter the Griffin.*

The *Griffin* fills the capability gap that exists between traditional helicopters and fixed wing platforms while retaining the hallmark performance of rotorcraft: vertical takeoff and landing, omnidirectional flight, and autorotational capability. Indeed, *Griffin* is the multi-mission rotary wing platform of the future — capable of carrying a greater payload over longer distances in shorter time than traditional light utility helicopters — while offering extended flight endurance with minimal noise signature.

Ultimately, the *Griffin* represents more than a vastly improved EC145 derivative. It represents a true paradigm shift in helicopter design, one that trades cautious re-packaged designs for an innovative systemic perspective encompassing all flight regimes, aerodynamic phenomena, and physical configurations. *Griffin* represents an engineering marvel that strikes the ideal balance between creativity and practicality, innovation and feasibility, and embodies imagination tempered with producibility.

Welcome to the next quantum leap.

The VERITAS of Griffin:
Truly Innovative Engineering for Exceptional Performance

		Griffin	EC145
Standard Accommodation		1 + 9	
WEIGHTS			
Design Gross Weight	lb (kg)	7891 (3587)	7887 (3585)
Empty Weight		3858 (1753)	3951 (1792)
Payload (no fuel)		2332 (1060)	2242 (1019)
Fuel		1527 (694)	
SPEEDS			
Speed for Best Endurance	kts (kmph)	65 (120)	
Speed for Best Range		100 (185)	110 (204)
Recommended Cruise Speed		150 (278)	131 (243)
Never Exceed Speed		176 (326)	150 (279)
PERFORMANCE			
Maximum Range	nm (km)	590 (1093)	360 (666)
Maximum Endurance	h:min	07:24	04:12
HOGE Ceiling	ft (m)	7400 (2256)	9200 (2800)
Rate of Climb @ VBE	ft/min (m/min)	2600 (793)	1800 (549)
MAIN ROTOR			
Diameter	ft (m)	36.08 (11)	
Chord		1.05 (0.32)	
Number of Blades	–	4	
Tip Speed (hover)	ft/s (m/s)	723.5 (220.6)	
TAIL PROP/ROTOR			
Diameter	ft (m)	5.74 (1.75)	6.43 (1.96)
Chord		0.43 (0.13)	0.66 (0.20)
Number of Blades	–	2	
Tip Speed	ft/s (m/s)	751.4 (229.1)	730.1 (222.6)
POWERPLANT (x 2)			
Model	–	RR 250-C30	TM Arriel 1E2
Weight	lb (kg)	253 (115)	276 (125.5)
Takeoff Power	hp (kW)	650 (485)	748 (550)
Max. Continuous Power		557 (416)	701 (516)
SFC @ TOP	lb/hp/hr (kg/kw/hr)	0.592 (0.361)	0.573 (0.349)
LIFE CYCLE COSTS			
Acquisition Cost (base)	2009 USD	5.07M	4.24M
Direct Operating Cost / FH		1065	1166
Indirect Operating Cost /Year		0.36M	0.36M

Griffin Airframe View

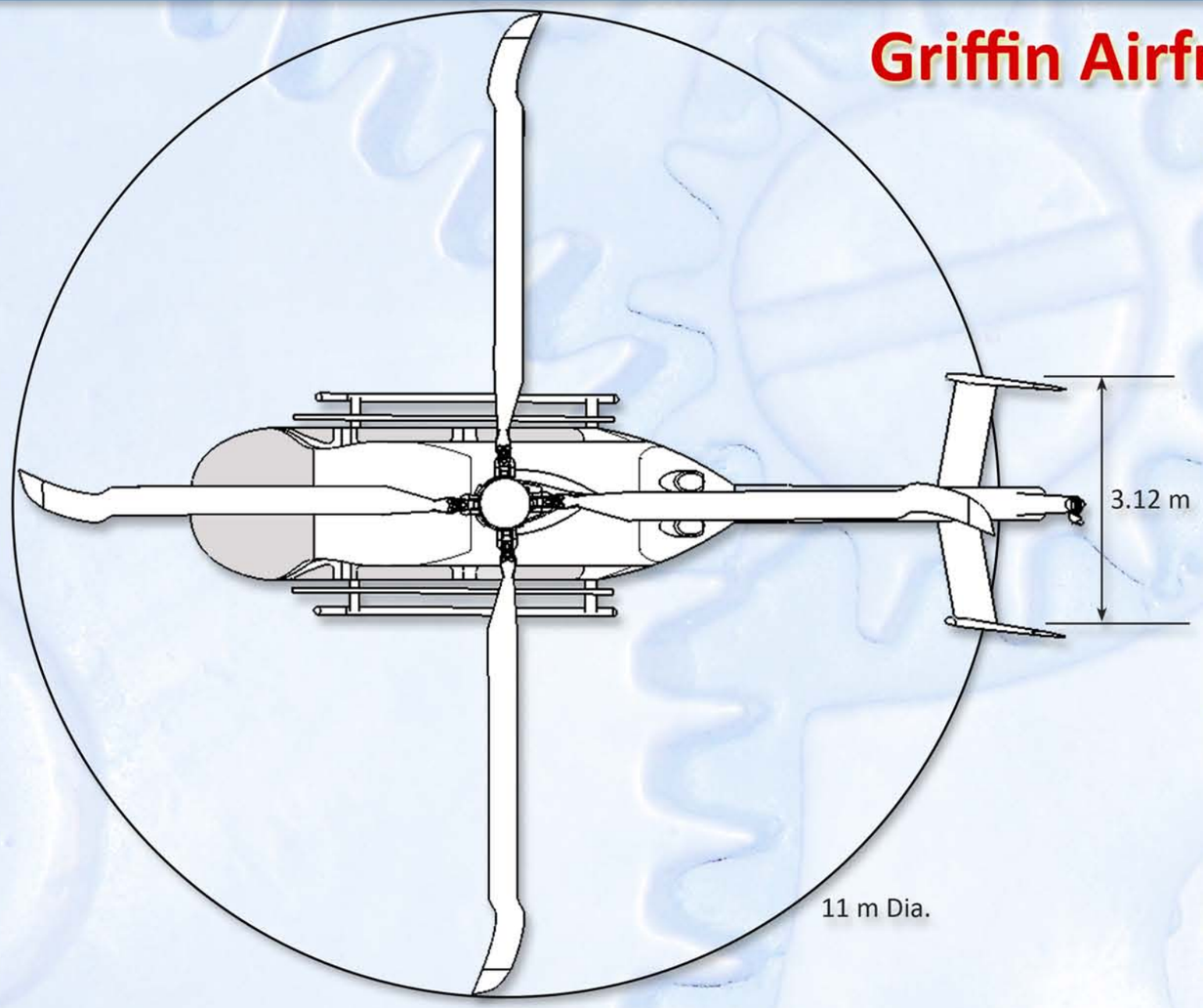

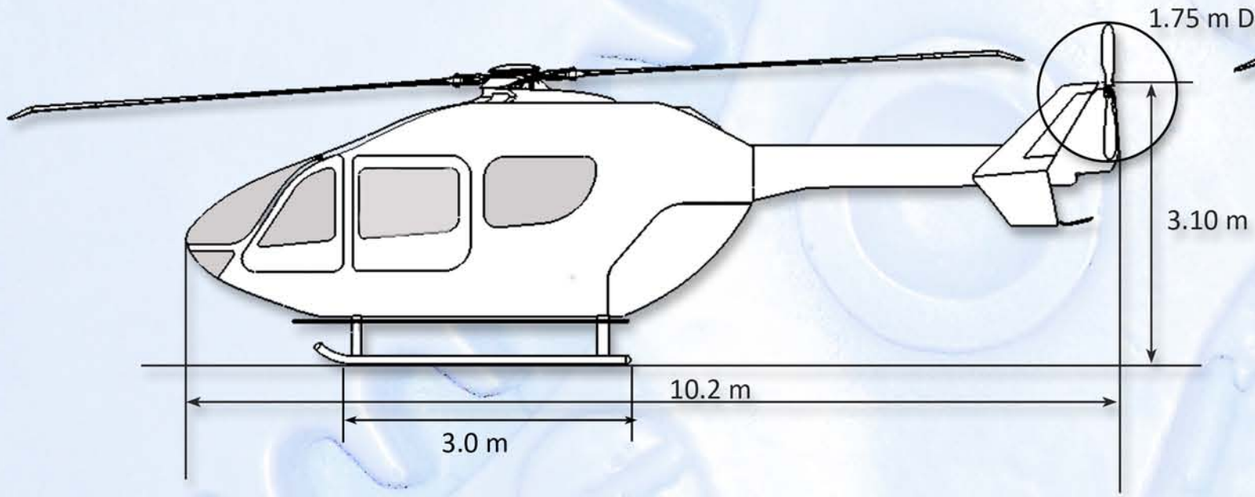

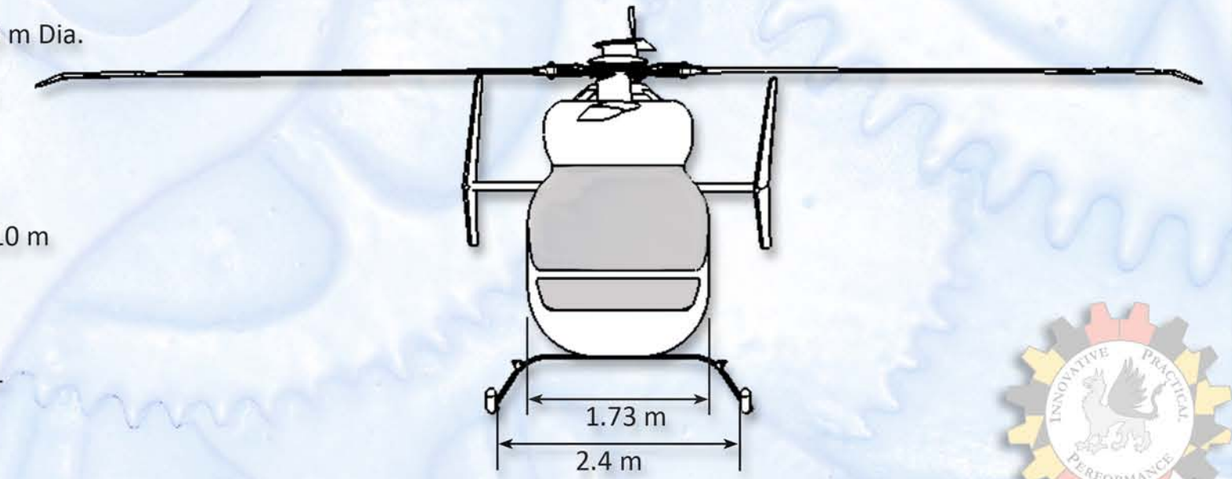

Griffin's Exterior Layout

Thrust Compounding Configuration (High Speed)

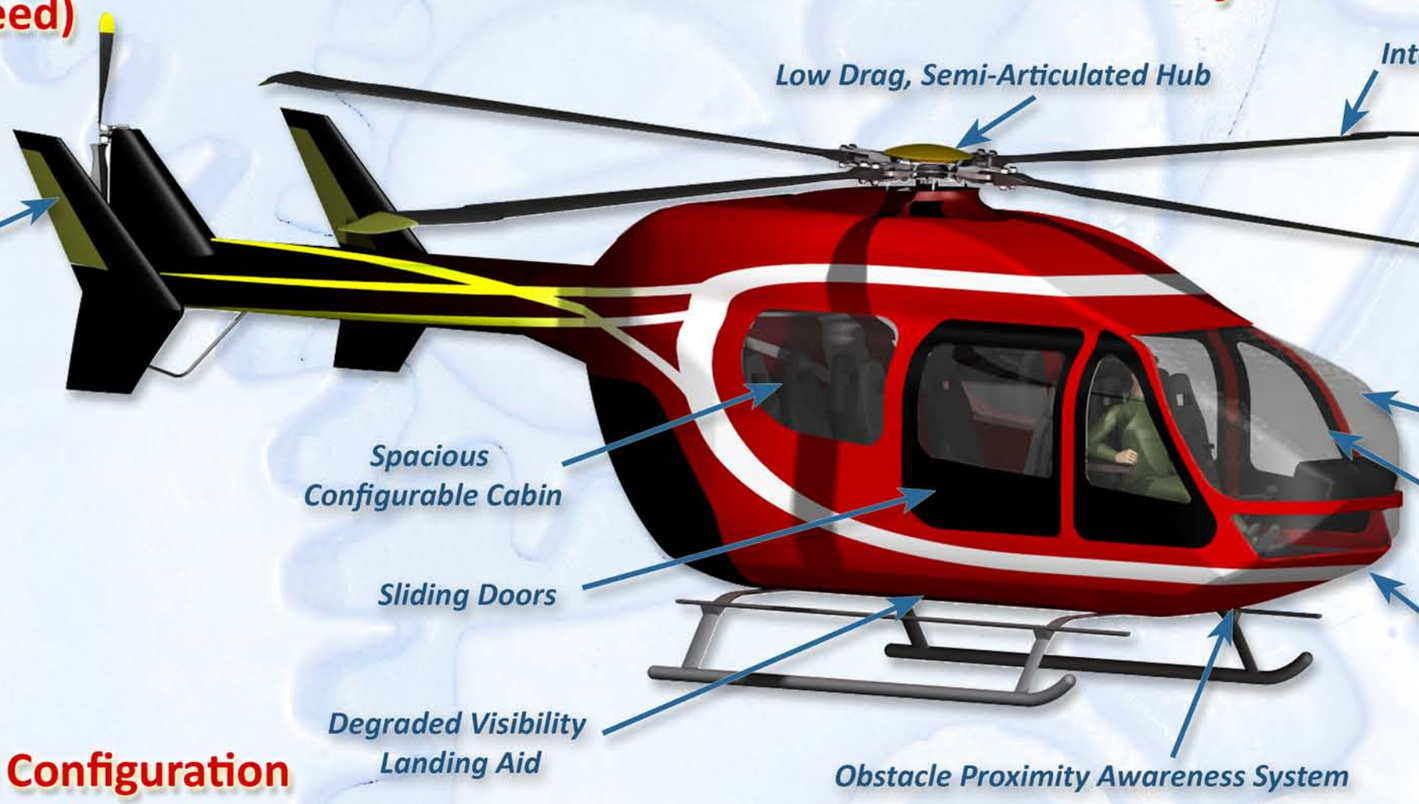

Anti-Torque Configuration (Hover/Low Speed)

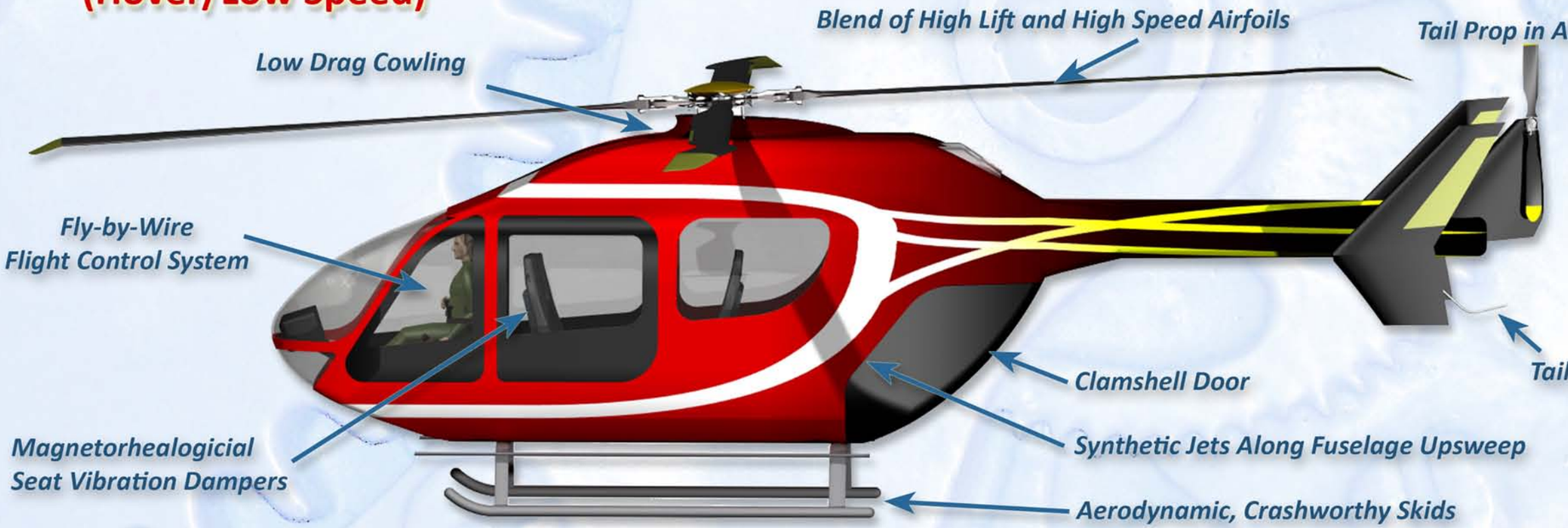

Empty Weight: 1753 kg
Fuel Weight: 694 kg
Payload: 1060 kg
MTOW: 3587 kg

1 Introduction

The physical phenomena that dictate the maximum speed, range, endurance, payload, and noise signature of conventional helicopters are well understood. The performance arising from these engineering limitations contrasts starkly with the growing demands on rotorcraft operators to travel farther, faster, and longer with greater payloads while minimizing environmental impact. The 26^{th} annual AHS Student Design Competition Request for Proposals (RFP), sponsored by AgustaWestland, addresses this global trend by requesting a non-conventional rotor and drive system that improves the performance of an in-service helicopter in terms of speed, range, payload, endurance, and noise signature. This derivative aircraft must also remain at the forefront of rotorcraft technology by leveraging advanced materials and design techniques to provide superior efficiency - as well as operational safety and maintainability.

The *Griffin* and its Variable Energy Rotor and Innovative Transmission ArchitectureS (VERITAS) were designed keeping the mind the requirements of the RFP by utilizing both modern multi-disciplinary technologies as well as proven rotorcraft concepts. The resulting vehicle provides the customer with an ideal synergy of innovation and reliability in a highly efficient, practical and affordable platform.

2 Vehicle Configuration Selection

The conventional single main rotor-tail rotor helicopter has historically proven to be a highly versatile and efficient platform for a variety of VTOL missions. Nevertheless, numerous other rotorcraft concepts have been proposed and in some cases, developed and flown. Notably, the tandem, coaxial, and intermeshing rotor configurations have gained acceptance within the rotorcraft industry and among helicopter operators. Regardless, the RFP requires a non-conventional rotor/drive system that does not fall within these categories. Thus, careful consideration of the specific design criteria in light of the primary mission profile of the existing aircraft is required to develop the optimum vehicle configuration. This section first identifies the primary design drivers based on the RFP requirements and the responses to questions posed to AHS regarding the RFP. The selection of the baseline aircraft and the primary mission of the proposed derivative rotorcraft are then detailed. These considerations are finally used to quantify the relative merits of potentially feasible technologies and derive the ultimate design: the *Griffin*.

2.1 Identification of Design Drivers

The RFP seeks an alternative, non-conventional rotor/drive system, and all necessary subsystems, that will improve the performance of a current, in-service helicopter. The proposed derivative rotorcraft must retain the traditional capabilities of a helicopter: hovering and omni-directional flight, as well as safe autorotational capability. Feasibility and practicality must be considered in order to offer initial operational capability by 2015. To maintain its derivative nature, structural modifications should be limited to those required to support integration of the non-conventional rotor/drive system. Nevertheless, the primary emphasis is on the performance improvements - as quantified by speed, range, payload, endurance, and noise signature. Advanced materials, design techniques, and manufacturing processes should also be leveraged. Ultimately, the rotorcraft must strike the ideal balance between innovation and practicality, creativity and feasibility, and promote safety and energy efficiency to guarantee an extended service life.

2.2 Selection of Baseline Helicopter

The selection of a current, in-service helicopter, from which a derivative is designed, is of critical importance because its representative mission influences the design drivers that ultimately dictate the proposed non-conventional rotor/drive system. To wisely select the baseline aircraft, helicopters within the required maximum take-off weight (MTOW) range of 3500-5500 kg were assessed on three metrics: empty weight fraction, payload delivery efficiency, and productivity.

Empty weight fraction is the ratio between a helicopter's empty weight and its MTOW. A general indicator of helicopter

capability, a low empty weight fraction suggests a relatively large payload capability. Specifically, it is expressed as:

$$Empty\ Weight\ Fraction = \frac{Empty\ Weight}{MTOW} = \frac{MTOW\ -\ Payload\ -\ Fuel\ Weight}{MTOW}$$

Historically, many non-conventional architectures have not gained acceptance because of the weight penalty of implementing bulky and mechanically complex technologies, increasing their empty weight fraction and thus reducing their capability. Therefore, of these metrics, empty weight fraction is perhaps the most important in selecting a baseline from which a non-conventional derivative is designed. Figure 2.1 shows the empty weight fraction of helicopters in the specified weight range.[91] The Eurocopter EC145 clearly leads its class this metric, suggesting that implementing a more complex architecture would not compromise the viability of the derivative helicopter.

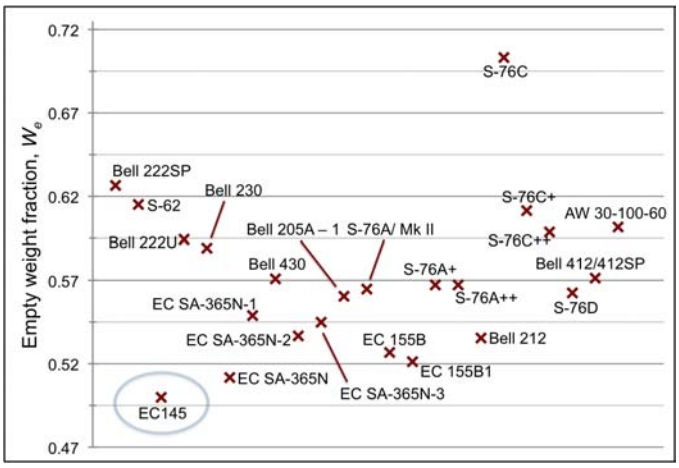

Figure 2.1: Empty weight fraction of a variety of helicopters in the 3- to 5-ton weight class.

In addition, the performance of the baseline aircraft should be representative of its weight class to ensure that the proposed derivative is legitimate for consumer purchase. Two performance metrics which broadly encompass helicopter performance are payload delivery efficiency and productivity. Payload delivery efficiency is defined as:

$$Payload\ Delivery\ Efficiency = \frac{Payload \times Range}{Fuel\ Weight}$$

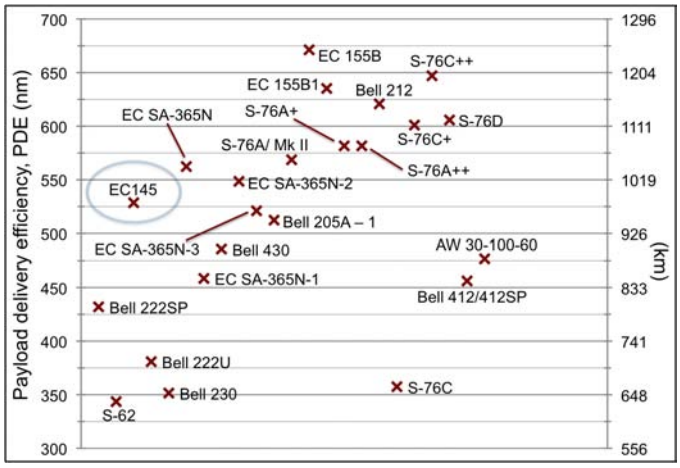

(a) Payload delivery efficiency of a variety of helicopters in the 3.5 to 5.5 ton weight class

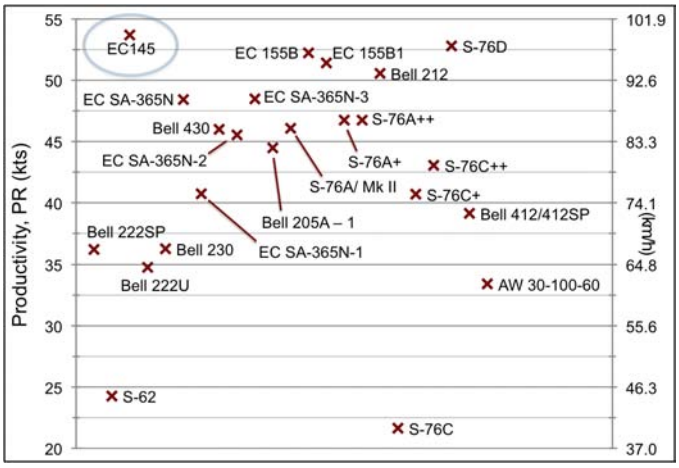

(b) Productivity of a variety of helicopters in the 3.5 to 5.5 ton weight class.

Figure 2.2: Performance metrics.

This metric represents the ability of a helicopter to ferry payload on the basis of fuel weight. As such, it is a measure of efficiency on the basis of both cost and energy for the purchase and consumption of fuel. Payload delivery efficiency, however, does not incorporate speed, which is a critical component of helicopter utility. Indeed, speed is a valuable parameter for many missions, ultimately decreasing time and cost. Productivity incorporates this performance parameter and is defined as:

$$Productivity = \frac{Payload \times Cruise\ Velocity}{Empty\ Weight + Fuel\ Weight}$$

Used together, these metrics demonstrate that the EC145 is a state-of-the-art high-performing helicopter (Figs. 2.2a and 2.2b).

With this information at hand, the EC145 is selected as the baseline helicopter based on its low empty weight and class-leading performance. Indeed, selection of the EC145 as a baseline aircraft offers a true engineering challenge as its employed technology has already vaulted it to prominence within the industry. Indeed, the U.S. Army's award of a $2 billion contract to Eurocopter for 322 militarized versions of the EC145 - the newly christened UH-72 Lakota - validates the baseline Eurocopter as a performance leader in the light utility helicopter market.

2.3 Primary Mission Profile Determination

Humanitarian assistance missions typically require helicopters to launch from a remote location - often an air-capable ship - and transit to an assigned location to deliver or retrieve a payload. Further tasking follows recovery to the original launch site or alternate forward staging area. Examination of the components of this mission reveals that the advanced performance required by the RFP - coupled with the need for the proposed vehicle to retain the hallmark capabilities of a helicopter - are those same improvements needed to enhance the ability of rotorcraft to render effective humanitarian aid.

- Operating from increasingly remote locations - or offshore vessels - compels extended range to reach disaster-affected areas.
- Required transit times to and from devastated areas diminish with increased speed, extending the "golden hour" reach of the vehicle.
- Improved payload capability increases the aid - in the form of basic necessities or medical attention - deliverable, as well as search and rescue utility.
- Minimization of noise signature decreases the obtrusiveness of 24-hour recovery efforts.
- Maximum endurance enables extended "on-station" time and minimizes the turnaround time between tasking.

Retention of hovering and omni-directional flight capability is required to operate in the shipboard environment and in confined areas with unprepared surfaces. Naval operations additionally require ruggedized components and corrosion-resistant materials in a compact design to withstand the maritime environment and minimize vehicle footprint on vessels with limited hangar space. The *Griffin*, therefore, has been designed to carry a greater payload over longer distances in shorter time than the EC145. In addition, it offers extended flight endurance with a reduced noise signature in a compact, ship-capable package.

2.4 Quality Function Deployment

Quality function deployment (QFD) is a value engineering tool that allows designers to translate design requirements into specific engineering parameters. At this design stage, only the House of Quality (HOQ) and the Pugh decision matrices were employed to determine and rank the criteria that were then used to obtain the final vehicle configuration.

2.4.1 Design Criteria - Value Engineering

Three steps are required in the typical construction of a HOQ:

1. Identify and rank the requirements.
2. Identify engineering parameters that are capable of affecting the requirements.

3. Rank the relative impact of each engineering parameter on each customer requirement.

The completed HOQ is shown in Fig. 2.3. The requirements and their relative rankings are given in the left column. A rank of five signifies critical importance, while progressively lower values indicate reduced importance. Although the weightings and values of the requirements were inherently subjective, the effect of this subjectivity was minimized by utilizing the unique assessments of all seven design team members, whose areas of expertise range from piloting helicopters to aeroacoustics to aerospace structures. Regardless, all operational requirements were treated as absolute needs and given the highest possible weighting. Among the cost considerations, the total life cycle cost (LCC) received the highest weighting.

The relevant engineering parameters needed to complete the HOQ are listed near the top of Fig. 2.3. Care was taken to eliminate highly correlated parameters that could potentially skew the results of the analysis. The ability of each parameter to affect each requirement was ranked from zero to three, corresponding to its increasing effect on the requirement. Those numerical rankings are displayed in Fig. 2.3. Based on the requirement weights, a raw score was then calculated for each engineering parameter. Higher scores represent a more significant impact of the given parameter on the ability of the final design to meet the RFP requirements. The results of the HOQ make it clear that to best meet the needs of the customer, the final design must be one that focuses on airframe weight, vehicle lift-to-drag ratio, rotor tip speed, materials, and the selected powerplant. The rank of these design parameters reinforces the RFP's focus on the delivery of performance improvements over existing rotorcraft.

2.5 Feasible VTOL Technology

The strict prohibition of conventional helicopter configurations prompted consideration of a number of rotor/drive systems that have yet to see widespread acceptance within the rotorcraft industry. Six broad categories of VTOL technologies encompassing the majority of experimental and developmental test vehicles were considered for inclusion in the final decision matrix. This qualitative assessment of the viability of each category is primarily based on first-order aerodynamic principles taken within the context of the RFP requirements. The feasibility of the potential technologies received similar scrutiny.

2.5.1 Compounding

The compound helicopter offers a solution to overcoming the rotor stall limits through thrust compounding and/or the cruise speed barrier imposed by retreating blade stall by lift compounding. Modifying the baseline helicopter in such a manner adds weight and reduces efficiency at low to moderate speeds. The primary drawbacks of a compound configuration are the increased fuel consumption and empty weight, and the associated deleterious effects on payload and/or range. Leveraging recent advances in materials and avionics technology that previously limited past compound rotorcraft, however, offers an attractive engineering option to satisfy RFP requirements. The additional cost and complexity of a compounded vehicle limits the appeal of this option.

2.5.2 Stopped Rotor

Designs that achieve high cruise speeds by converting the rotor to a fixed wing in forward flight require a compromise in terms of the blade and airfoils that may be used. The decision to employ elliptical airfoils on X-50, for example, was driven by the requirement to provide uni-directional rotor blade sections for use as wing sections upon stopping the rotor. These airfoils limit low to moderate flight speed performance and significantly restrict hovering efficiency. The mechanical problems encountered with slowing the rotating wings while sustaining controlled flight during the transition to fixed wing flight on the few developmental test vehicles of this type make the feasibility questionable. In addition, the implications of the dynamics of stopping a rotor blade completely are not understood well enough to ensure safe flight operation. Further detracting from this rotorcraft concept is the RFP requirement to maintain traditional autorotational capability.

Requirements	*Weighting*	Empty Weight	Cruise/Dash Speed	Disc Loading	Power Loading	Engine Selection	Installed Power	Engine SFC	Blade Tip Speed	Autorotative Capability	Aircraft L/D Ratio	Flat Plate Area	MTBF, MTBR	Transmission Efficiency	Engine Fuel Efficiency	Emissions	Alternate Materials (strength/weight)	Control Effectiveness	Stability
Improved Speed	5	3	3	1	2	2	2	1	2	1	3	2	0	2	1	0	1	1	1
Improved Range	5	3	3	1	2	2	1	1	2	1	3	1	0	2	2	0	1	1	1
Improved Endurance	5	2	1	2	2	2	1	2	1	1	3	1	0	3	2	0	1	1	1
Improved Payload	5	3	1	2	2	3	3	2	1	1	2	1	0	1	2	0	1	0	0
Improved Noise	5	0	2	1	2	2	0	0	3	1	1	1	1	1	0	0	0	0	0
Cruise Altitude	3	2	3	1	2	2	3	0	2	1	3	2	0	3	3	0	1	1	1
Hover Out-of-Ground-Effect	3	3	0	3	3	3	3	0	3	0	1	0	0	3	0	0	0	1	1
Service Ceiling	3	1	0	2	1	1	3	0	3	1	3	0	0	3	0	0	0	1	1
Autorotational Capability	5	1	2	3	1	0	1	0	3	3	3	1	3	1	0	0	1	3	2
Initial Acquisition Cost	5	3	2	1	3	2	1	0	0	1	1	1	1	1	1	0	1	3	2
Life Cycle Cost	5	1	1	1	1	3	1	3	0	3	2	1	3	1	3	1	1	1	1
Fast Time to Market (2015)	5	0	0	0	0	1	0	0	0	0	0	0	0	0	0	0	3	0	0
Environmental Signature	5	0	0	0	0	0	0	3	0	0	0	0	2	1	2	3	2	0	0
Internal Volume	5	2	0	0	0	1	0	0	0	0	0	0	0	0	0	0	1	0	0
Passenger Comfort	3	2	1	0	0	1	0	0	3	0	3	1	1	1	0	0	2	0	3
Pilot Workload/Handling Qualities	4	1	1	0	1	1	3	0	3	3	0	0	1	1	0	0	0	3	3
Crashworthiness	5	2	0	0	0	0	1	0	2	3	0	0	0	1	0	0	3	0	0
Ground Handling/Ground Personnel Safety	4	0	0	0	0	1	0	1	0	0	0	0	0	0	0	1	0	3	1
Multirole Capability/Versatility of Design	5	2	3	1	1	3	3	1	3	3	2	1	3	1	1	3	3	3	3
Derivative	5	2	0	0	0	0	0	0	1	0	1	1	2	1	0	0	3	2	3
	Raw Score	148	106	83	102	134	109	69	135	108	135	64	82	114	79	39	119	108	104
	Relative Importance	8%	6%	5%	6%	7%	6%	4%	7%	6%	7%	3%	4%	6%	4%	2%	6%	6%	6%
	Rank	*1*	10	13	12	*4*	7	16	*2*	8	*2*	17	14	*6*	15	18	*5*	8	11

Figure 2.3: House of Quality decision matrix in determining critical engineering parameters from RFP requirements.

2.5.3 Tip Speed Modulation

Tip speed modulation allows a helicopter to adapt the tip speed of the rotor blades to best suit the flight condition. The tip speed of rotary wings has a strong impact on the profile power required to drive the rotor in all flight regimes, as well as the level of external noise radiated. A reduction of rotor tip speed can lead to a substantial decrease in the power required by the helicopter and a dramatic reduction of its noise signature. A rotor tip speed reduction, however, increases the blade loading for the same level of thrust, pushing the rotor closer to stall and limiting the altitude, payload, and maneuvering capability of the helicopter. Moreover, a lower rotor tip speed reduces the kinetic energy stored in the rotor, negatively impacting autorotational performance. The selection of rotor tip speed in a conventional helicopter design is a compromise between efficiency and noise on one hand, and lift carrying capability, maneuverability, and safety on the other.

The tip speed of the rotor can be modulated by varying the rotational speed or the diameter of the rotor. While variable rotation speed does not mandate any change to the helicopter rotor, it does require a drivetrain capable of efficient operation across a range of output speeds. This need drives the use of advanced engine designs capable of efficient operation across a wide range of output speeds, or a transmission capable of smoothly varying the reduction ratio from the engine output to the rotor without interruption of power. Although drivetrains with this functionality currently exist in automobiles, they have yet to see implementation in the aerospace industry beyond Boeing's A160. Varying rotor diameter does not necessarily require modification of the drivetrain. The rotor blades, however, must be capable of changing length during flight. The high centrifugal loading on the rotor blades demands a robust system to vary blade length. Telescoping blade designs also impose significant geometric limitations on the choice of blade taper and twist, creating the potential for additional design compromises that may detrimentally impact performance. To date, such designs have yet to see incorporation on full-scale helicopter rotors beyond the wind tunnel.

2.5.4 Tilting Thrust

Tilt-rotor, tilt-wing and tilt-fan technologies employ tandem rotors and require many of the same performance compromises. While tandem rotorcraft have extensive operational records, tilting thruster configurations, such as Bell Helicopter's new Hybrid Tandem Rotor, have yet to prove themselves beyond the Bell-Boeing V-22. And though greater engine power can be dedicated to propulsive thrust for a given empty weight, the multiple rotor system suffers from significant aerodynamic interference losses. In addition, numerous control linkages, gearboxes and driveshafts are required in any tandem configuration, greatly increasing mechanical complexity and maintenance costs. Although tilting thruster rotorcraft may cruise at speeds in excess of those achieved by helicopters, the mechanism required for tilting the thrusting components similarly adds complexity and empty weight. These complexities may be offset by comparable gains in lift-to-drag ratio, though adoption of this technology would require a truly remarkable increase in the fixed-wing flight efficiency. The potentially increased propulsive efficiency and lift-to-drag ratio must, therefore, significantly outweigh the increased structural weight and fuel consumption to satisfy the RFP requirements. Incorporation of this technology would also mandate substantial structural modifications from the baseline helicopter, decreasing the derivative nature of the design. The ultimate detractor for this technology, however, is an inability to offer the RFP-required autorotation capability.

2.5.5 Vectored Thrust

Vectored thrust fixed-wing vehicles are by far the fastest of any VTOL aircraft. This speed contributes to the highest range of any technology considered, but sacrifices hovering efficiency by increasing the effective disk loading. The significant mechanical complexity required to efficiently direct the thrust further detracts from this technology. Moreover, the significant fuel consumption of large thrust-oriented jet engines hampers the endurance of fixed-wing VTOL aircraft. Without a true autorotational capability - a clearly defined RFP requirement - this technology is ultimately not appropriate for the current design.

2.5.6 Torqueless Rotor

Tip jets are one method of driving the main rotor without requiring an anti-torque device. This method is ultimately less efficient than employing shaft-driven rotors because of the lower efficiency inherent in the conversion of mechanical compressor power to chemical propulsive power. Although they are a technically feasible concept, as evidenced by the relative experimental success of the Fairey Rotodyne, tip jets are obtrusively noisy. Moreover, existing methods of quieting tip jets, such as employing cooled exhaust gases, have not been successfully demonstrated on full-sized aircraft.

A more innovative solution for eliminating the torque on the main rotor is the "Ornicopter." This experimental concept is a single rotor whose powerplant forces the blades to flap rather than rotate. Both a lifting force and an average propulsive force are generated by the flapping motion of the blades. The propulsive force propels the blades in the rotating frame, eliminating the need to transfer torque from the fuselage to the rotor. Though scale experiments have demonstrated the feasibility of the concept, the mechanical complexity and weight of the flapping swashplate mechanism effectively prevents their application on full-scale helicopters in near future.

2.6 Pugh Decision Matrix

Although the preceding qualitative assessment of the potential VTOL technologies eliminated further consideration of stopped rotor and vectored thrust, it failed to identify the final vehicle architecture. As such, the QFD analysis was continued to consider the remaining technologies: compounding, tip speed modulation, tilting thrust, and no torque rotors. The engineering parameters from the previous HOQ assessment that directly affect configuration were modified for inclusion as the ultimate selection criteria in a standard Pugh decision matrix. As shown in Fig. 2.4, the weightings are based on the relative HOQ rankings of the selected engineering parameters. The original requirements thus directly impacted the resulting scores of each technology. Each technology was then ranked as it impacted the engineering parameters considered. As before, a rank of five signifies critical importance, while progressively lower values indicate reduced importance. The weighted sum of the scores for each technology were then prioritized.

The results shown in Fig. 2.5 clearly indicate that thrust compounding with tip speed modulation through variable rotor speed are the preferred technologies for satisfying the RFP requirements. Although the variable speed rotor was judged the best candidate technology to couple with thrust compounding, the similarity of its raw score with that of the variable diameter rotor did not make it the clear winner. Trade studies were conducted to narrow down to the choice of a variable speed rotor system.

2.7 Trade Study of Tip Speed Modulation Concepts

Both tip speed modulation concepts were evaluated in greater detail, to compare the potential for improvement in both performance and noise over conventional helicopters. Figure 2.6a shows the results of a simple momentum theory analysis of both the variable diameter and variable rotational speed concepts in comparison to the baseline. For both concepts the tip speed was chosen to provide a 15% margin between the maximum thrust capability of the rotor and the weight of the helicopter.

The variable speed rotor provides better performance than the variable diameter rotor at all but the highest airspeeds, particularly at the moderate speed flight conditions where the variable speed rotor offers the lowest possible rotor power requirements, and hence the maximum endurance.

The noise reduction potential of each concept was also evaluated. Main rotor ground noise level contours were generated for each concept at the EC-145's cruise speed of 131 kts using a combined blade-element theory / Ffowcs Williams - Hawkings method, as described in Sec. 8. The 65 dBA sound pressure level contours are shown in Fig. 2.6b. The variable speed rotor offers a significantly lower noise footprint than the variable diameter concept. This is because the variable diameter rotor achieves a tip speed reduction by reducing the rotor diameter, increasing disk loading and thereby increasing rotor steady loading noise.

	Technology	Compounding			Tip Speed Modulation		Tilting Thrust			Torqueless	
Technical Parameters	*Parameter Relative Weighting*	Thrust	Lift	Thrust and Lift	Variable Rotor Speed	Variable Rotor Diameter	Tilt-Rotor	Tilt-Wing	Tilt-Fan	Tip Jet	Ornicopter
Low Empty Weight	0.08	3	2	1	2	2	1	1	1	2	2
High Speed	0.06	5	3	4	4	4	5	5	4	2	1
Low Disk Loading	0.05	3	3	3	3	3	2	2	2	3	3
High Power Loading	0.06	2	3	3	3	3	2	2	2	2	3
Low Blade Tip Speed	0.07	3	3	3	5	4	2	2	2	3	4
Good Autorotation Capability	0.06	5	2	1	2	3	1	1	1	4	1
High L/D	0.07	3	4	3	4	4	3	3	3	3	3
Low Fuselage Drag	0.03	4	1	1	3	3	2	3	2	3	3
Low Mechanical Complexity	0.04	3	3	2	2	1	2	3	2	2	1
Level 1 Handling Qualities	0.06	3	3	3	3	3	3	3	3	3	2
Highly Stable Platform	0.06	3	3	3	3	3	2	2	2	3	2
Minimal Structural Changes	0.05	3	3	2	3	3	1	1	1	3	2
	Raw Score	2.28	1.93	1.68	2.16	2.10	1.49	1.57	1.44	1.89	1.57
	Relative Importance	13%	11%	9%	12%	12%	8%	9%	8%	10%	9%
	Rank	**1**	4	6	**2**	**3**	9	7	10	5	8

Figure 2.4: The Pugh Decision Matrix favors thrust compounding and variable tip speed or diameter rotors.

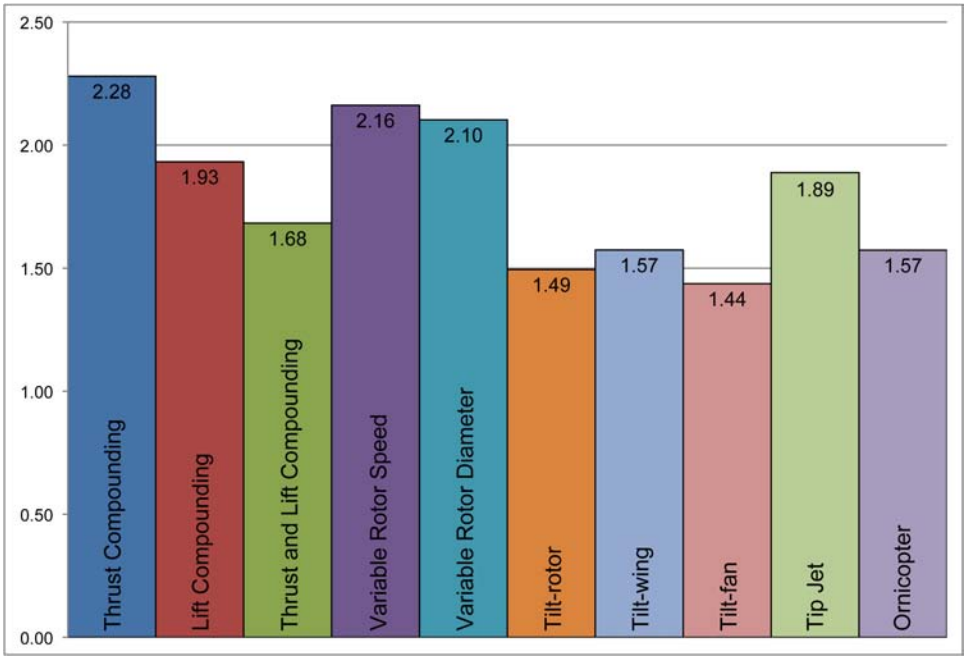

Figure 2.5: Ranking the feasible VTOL technologies.

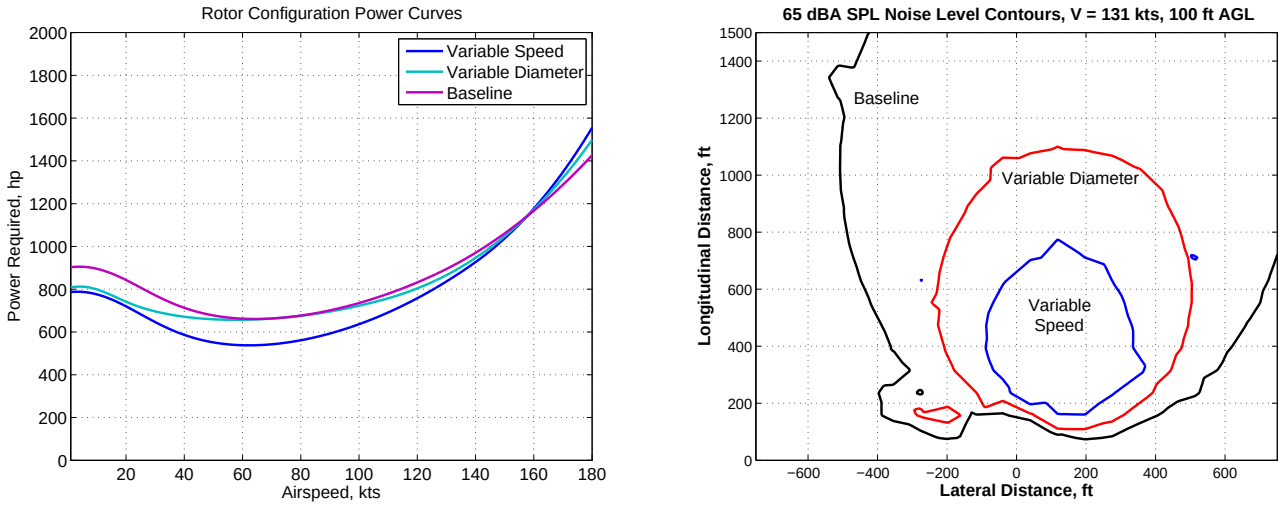

(a) Tip speed modulation concept power curves.

(b) Tip speed modulation concept noise footprint comparison.

Figure 2.6: Tip speed modulation concept trade-off.

Overall, the variable speed rotor concept requires less power and generates less noise than the variable diameter concept. As such, the variable speed rotor outperforms the variable diameter concept and is clearly the best choice to couple with thrust compounding to meet the RFP performance requirements.

2.8 *Griffin*'s Rotor/Drive System: VERITAS

The VTOL concepts of a variable speed rotor and thrust compounding are identified as the best technologies to form the non-conventional architecture for the derivative EC145. However, such a concept requires anti-torque, and traditional methods of anti-torque, such as the use of a tail rotor, are not permitted by the RFP. To this end, an innovative solution is to design a dual-mode thruster system which propels the helicopter at high speeds and provides anti-torque in hover and low forward speeds. This is done by a swiveling tail propeller. The helicopter vertical fins are aerodynamically designed to produce lift in forward flight, providing the anti-torque to the variable speed main rotor and permitting the tail prop to swivel to its thrust compounding configuration.

Ultimately, these two concepts are not simply discrete technologies. Thrust compounding in forward flight offloads the main rotor and reduces its power consumption. The tail prop thrust reduces the helicopter angle of attack and decreases parasitic drag. In this way, the variable speed rotor is seen as a *variable energy* rotor. As such, the non-conventional rotor/drive system was dubbed Variable Energy Rotor and Innovative Transmission ArchitectureS (VERITAS). It is a rotor-to-rotor system consisting of a variable energy rotor, a swiveling tail prop, and the non-conventional drivetrain powering both. The individual components of VERITAS synergistically drive exceptional performance increases over the baseline EC145. Together, they are greater than the sum of their parts - as is the mythological griffin. Indeed, the VERITAS of *Griffin* bridges the performance gap that exists between hover and forward flight which has previously eluded hybrid architectures. Optimal modulation of main rotor speed and swiveling tail thrust makes *Griffin* a truly flight- and mission-adaptive helicopter.

3 Initial Sizing

3.1 Description of Methodology

An iterative procedure was developed to carry out the initial sizing of the helicopter based on mission requirements and user inputs, which is shown in the flow chart (Fig. 3.1). It begins with specification of mission requirements, such as cruise speed, payload, and range of the helicopter. The original method (Tishchenko's method[1]) was used to size conventional single main rotor-tail rotor configurations. The capability to analyze various configurations such as conventional main rotor–tail rotor, fenestron, NOTAR, lift and thrust compounding concepts, variable speed drive and variable diameter rotor was added to the analysis. This provides versatility to the design procedure, allowing the user to choose a particular configuration or combination of these configurations to be analyzed. The methodology is described below:

(a) **Sizing Module:** The module is initialized with estimates of parameters such as lift-to-drag ratio, figure of merit, propulsive efficiency, weight efficiency, etc. A series of sizing and performance calculations are then conducted to meet mission requirements and user choices. The analysis can carry out wing sizing if lift compounding is selected as an option. Once these calculations are complete, component weight calculations are performed based on correlation equations obtained from historical data and technological considerations.[1]

(b) **Trim Module:** A coupled rotor-fuselage trim analysis was developed to achieve force and moment equilibrium in x, y and z–directions. The user can specify helicopter center of mass location, height of hub above the center of mass, rotor type, etc, to carry out the trim calculations. The trim procedure takes into consideration lift and thrust compounding, if selected. If a variable speed drive is specified, optimum rotor speed is also calculated. The user can specify the range of operating speed. The maximum rotor speed is limited by advancing side tip Mach number. At any given speed, minimum safe operational rotor speed is decided based on two key considerations namely, rotor stall margin and rotor blade dynamics. This trim procedure computes primary controls, blade flap responses, and shaft angles. These values are used in the performance calculations and to set the shaft inclinations.

(c) **Performance Module:** A blade element analysis was developed to calculate the induced and profile drag of the rotor. The user can specify the airfoil section, and a table lookup procedure is incorporated to calculate the lift and drag characteristics based on flow velocity and angle of attack at each blade element. The default option is thin airfoil theory with appropriate corrections for stall and compressibility effects. Uniform inflow and Drees' inflow models are also incorporated in the analysis. Various planform shapes and twist distributions can also be specified. For estimation of parasitic power, the user can input the flat plate area based on wind–tunnel tests, CFD calculations, or from drag estimated from detailed CAD drawings.[2] The default option is to estimate equivalent flat plate area based on historical data.[3] For thrust compounding configuration, the propeller design and performance subroutine is used. An analysis was developed to carry out an iterative blade element propeller design procedure and calculates the propeller pitch, thrust produced, and the power required by the propeller. The performance module calculates the power required to cruise at given flight speed as well as the power required to hover out of ground effect at a specified altitude. This result is used as an estimate of minimum installed power on the helicopter. Next, the specific range and endurance are calculated, and these are used to determine the amount of fuel required, the range, and the endurance of the helicopter.

(d) **Weight Module:** Detailed component weight breakdown is obtained from the sizing module. The component weights are used to calculate the empty weight. In the case that certain subsystems are already chosen or known exactly, their weights are updated accordingly. The fuel weight calculated in the performance module is added to the empty weight and the specified payload to calculate the new gross takeoff weight of the helicopter.

(e) **Convergence Check and Update:** This updated gross takeoff weight is then compared to the initial estimate of the weight. If the weight has not converged to within a specified tolerance, then the aerodynamic and performance quantities such

as lift-to-drag ratio, figure of merit, power estimates, etc, are updated and re-input to the sizing module. The process is repeated until the gross weight converges. This entire process is repeated for various combinations of number of blades, rotor solidity, and tip speeds. This process allows direct comparisons of various configurations, and ultimately, the selection of best overall design to meet the mission requirements.

(f) **Noise Module:** Once the weight converges, steady harmonic noise estimation is carried out. The acoustics solver developed uses Farassat's Formulation–1 of the Ffowcs Williams and Hawkings (FW-H) equation.[4] The solver takes as inputs the rotor advance ratio, rotor speed and the spanwise distribution of loads at each azimuth angle from the performance module to perform the calculation of loading noise. The thickness noise is also calculated based on airfoil coordinates. The method then calculates the pressure time history at one observer location. This process is repeated for a number of ground based observers, and the A-weighted Sound Pressure Level (SPL) at each point is calculated to generate the ground noise contours.

(g) **Cost Module:** The cost of the helicopter "from the cradle to the grave" is calculated using the Conklin & de Decker cost evaluator method.[5] The method calculates the development cost, production cost, operational cost, and recycling cost.

3.2 Trade Studies

Using the analysis developed, trade studies were carried out to investigate the design space based on the variation of critical rotor parameters such as blade loading, number of blades, and rotor solidity.

3.2.1 Choice of Blade Loading Coefficient

Blade loading was chosen based on a specified rotor stall margin. The greater the blade loading, the closer is the rotor to stall, and the lower is the stall margin. While choosing blade loading, two flight condiions were considered: hover-out-of-ground effect and maneuvering flight. In these flight regimes, the rotor should have enough sufficient thrust margin.

Because the RFP requires the design of a derivative helicopter that has at least the same capabilities as the baseline helicopter, a blade loading coefficient of 0.084 (same as that of the EC145) was chosen for the *Griffin*. This value ensures enough margin for the *Griffin* to effectively carry out all the missions of the EC145.

3.2.2 Choice of Tip Speed

For a given blade area, a high hover tip speed helps to lower the angle of attack on the blade as well as to provide good autorotational capabilities. However, a higher tip speed resulting in a greater tip Mach number increases the noise levels. For conventional helicopters, tip speed is also limited by forward flight conditions. However, *Griffin* has a unique Variable Energy Rotor and Innovative Transmission ArchitectureS (VERITAS) (Sec. 4). VERITAS allows reductions of the rotor tip speed in forward flight, thereby pushing the penalties associated with compressibility effects to higher cruise speeds. This allows *Griffin* to cruise at least 20 knots faster than the baseline EC 145.

Because the derivative helicopter has to retain the same autorotational capability as the baseline helicopter, the hover tip speed was chosen to be 220.6 m/s (same as the baseline EC145). The noise level in hover is reduced by use of innovative TALON tip shape (Sec. 5.1.5) which greatly reduced the thickness noise making *Griffin* a remarkably quiet helicopter compared to the EC145.

3.2.3 Choice of Number of Blades

After the selection of the blade loading coefficient and rotor tip speed, a design space was generated (Fig. 3.2a) by varying number of blades and aspect ratio for given blade loading and tip speed. Each point on Fig. 3.2a represents a configuration that meets the performance requirements. As the number of blades increases, the main rotor diameter decreases (Fig. 3.2b). On one hand, this increases the disk loading and the power required by the main rotor, and hence the fuel weight increases. On the

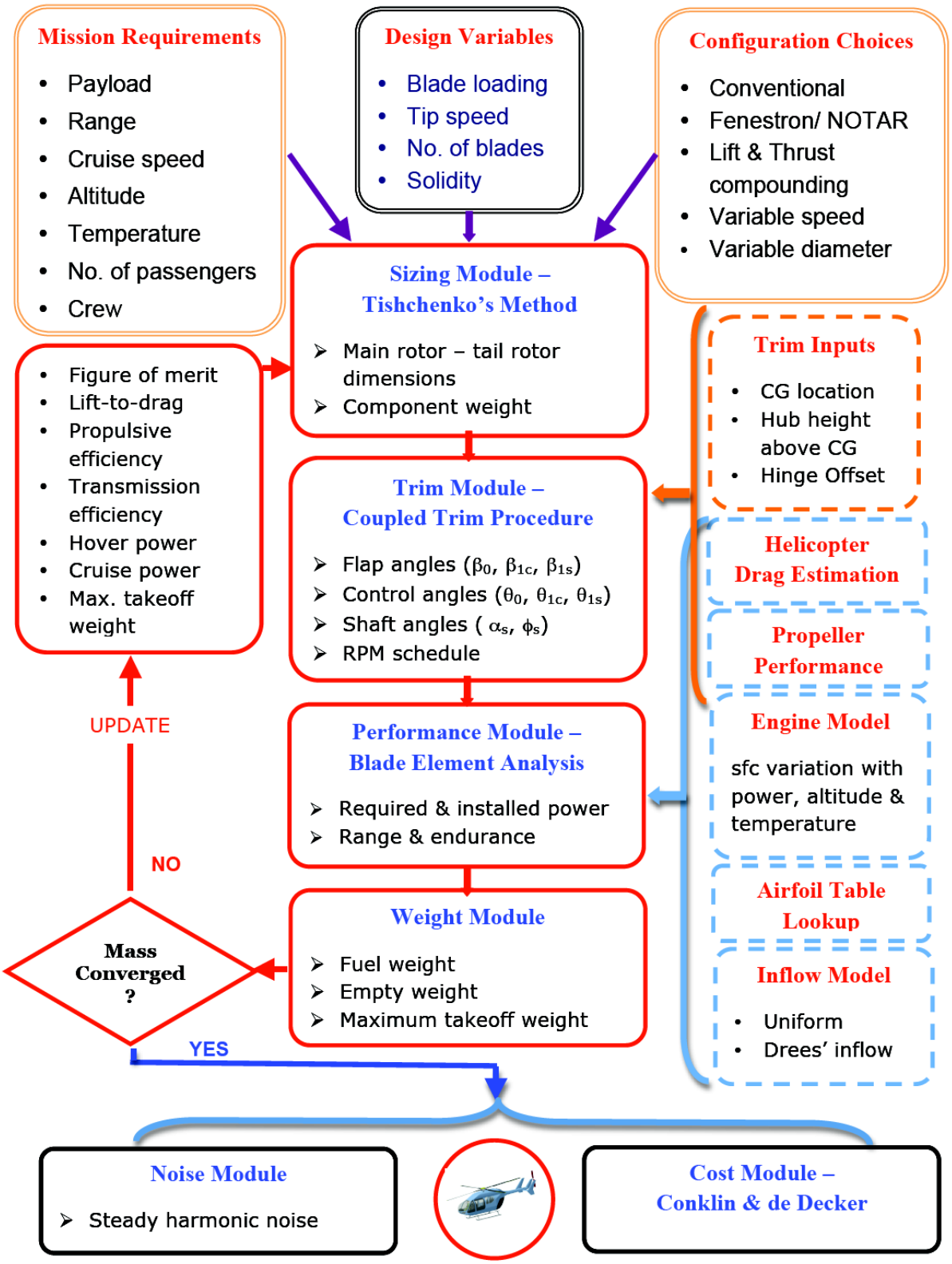

Figure 3.1: Design Methodology

other hand, a reduction in the main rotor diameter reduces the empty weight. The gross weight was found to be a minimum for a 3-bladed rotor.

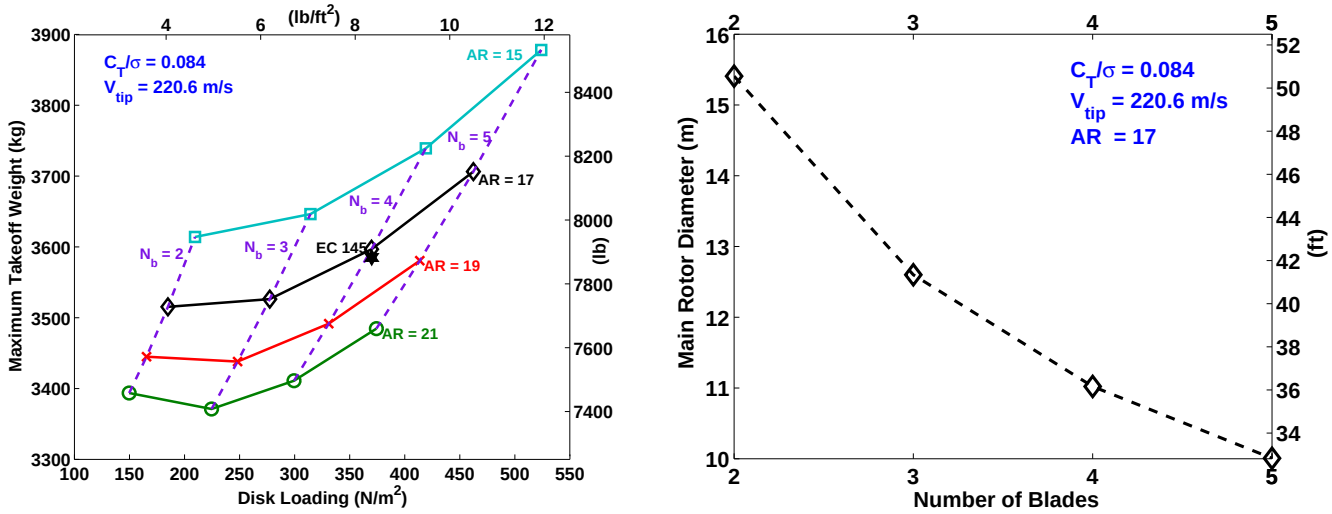

(a) Variation of MTOW with aspect ratio and number of blades.

(b) Variation of Rotor Diameter with number of blades.

Figure 3.2: Choice of number of blades.

Because the primary mission of the *Griffin* is maritime-based, a compact footprint is highly desirable. In addition, a large diameter rotor would mean a heavier hub, and the fuselage would have to be reinforced, making it bulkier and heavier. Keeping this in mind, two and three bladed rotors were rejected. A five bladed rotor was heavier and would also be costlier than a four bladed rotor and this was also rejected. Therefore, a four bladed rotor system was selected for the *Griffin*.

3.2.4 Choice of Rotor Solidity

The rotor solidity (σ) is related to number of rotor blades (N_b) and aspect ratio (AR) using

$$\sigma = \frac{N_b}{\pi AR}$$

where aspect ratio is the ratio of rotor radius (R) to the blade chord (c), $AR = R/c$. After the number of blades was decided, the choice of solidity was made by varying the aspect ratio of the blades. As the solidity reduces, the power requirement reduces (Fig. 3.3a). This in turn reduces the fuel consumption and decreases the gross takeoff weight (Fig. 3.3b).

Therefore, from the perspective of reduced fuel consumption and weight, it was desirable to choose highest possible aspect ratio and/or lowest possible solidity for the rotor. However, a high aspect ratio blade would have lead to either a larger diameter or to a smaller blade chord. As discussed earlier, a large diameter rotor was not desirable from perspective of mission, weight and cost.

The *Griffin* is equipped with active trailing edge flaps used to reduce vibration levels at all flight speeds. These active flaps needed an actuator that had to be accommodated within the blade profile, so reduced chord blades was undesirable. As a result, a rotor diameter of 11 m and a rotor solidity of 0.0741 was chosen based on the trade studies.

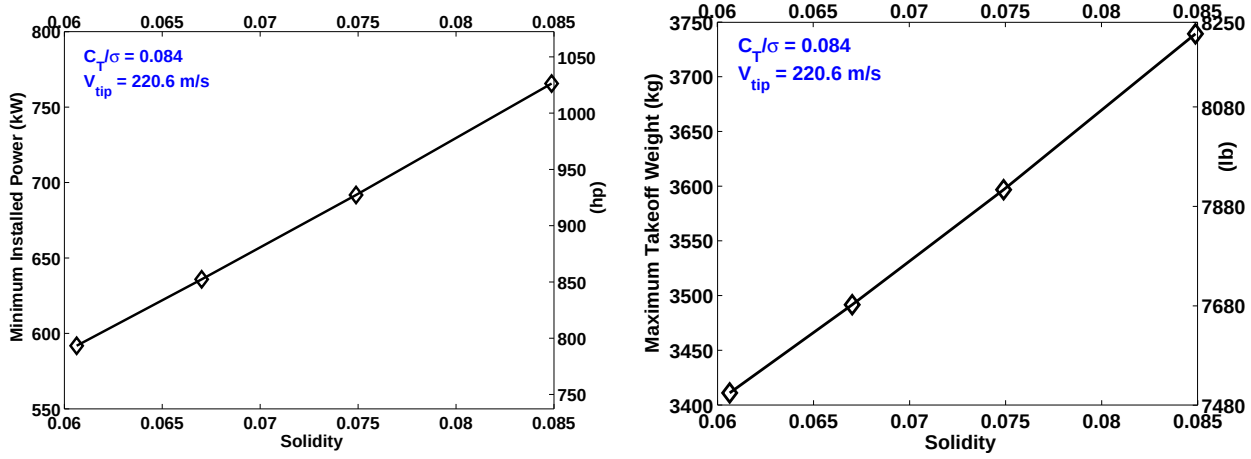

(a) Variation of installed power with solidity.

(b) Variation of MTOW with solidity.

Figure 3.3: Choice of main rotor solidity.

3.3 Final Configuration

Based on both the trade studies and the RFP requirements, a four-bladed rotor with a blade loading coefficient of 0.084 was chosen. A hover tip speed of 220.6 m/s (723.6 ft/s) and a diameter of 11 m (36.08 ft) was chosen to ensure minimum changes to the airframe and provide a compact footprint. The sizing of the *Griffin* was carried out to ensure that the gross takeoff weight doesn't increase much compared with the baseline EC145. This allows using the same airframe structure and landing gear on the *Griffin* as the EC145, without any reinforcements. Judicious choice of design parameters and use of non-conventional VERITAS enpowers the *Griffin*'s quantum leap in flight performance. For the same amount of fuel, the *Griffin* is capable of carrying 40 kg more payload, cruises 20 knots faster with 164% better range and 176% better endurance compared with the EC 145 (Sec. 7).

4 Drivetrain

The *Griffin* achieves its significant improvements in performance and efficiency by implementing an innovative and non-conventional rotor drivetrain, the Variable Energy Rotor and Innovative Transmission ArchitectureS (VERITAS). VERITAS allows power to be smoothly and efficiently transmitted from the engines to the rotors across a wide range of operating rotor speeds, from 82 to 103% of the hovering rotor speed, to tailor the operating state of the rotor to the flight condition. In addition to allowing for a smooth and continuous variation in rotor speed, VERITAS features a swiveling tail prop which provides anti-torque and directional control at low speeds and propulsive force at high speeds. VERITAS has been designed to have a minimal impact on the existing airframe of the baseline helicopter and could be readily adapted to any other conventional helicopter design at low cost.

4.1 Configuration

The VERITAS configuration consists of two engines, two multi-speed dual-clutch gearboxes, a single main rotor gearbox, and the swiveling tail prop gearbox (Fig. 4.1). All components are designed to be lubricated with MIL-L-23699 standard turbine engine oil to ease maintenance requirements. Additionally, all gearboxes are designed to exceed a 5,000 hour MTBR with at least 30 minutes of dry operation possible in the event of an oil system failure. VERITAS is tightly integrated with a Health and Usage Monitoring System (HUMS), as described in Sec. 9.11.3. Overall transmission efficiency during steady flight is

Engine and Transmission System

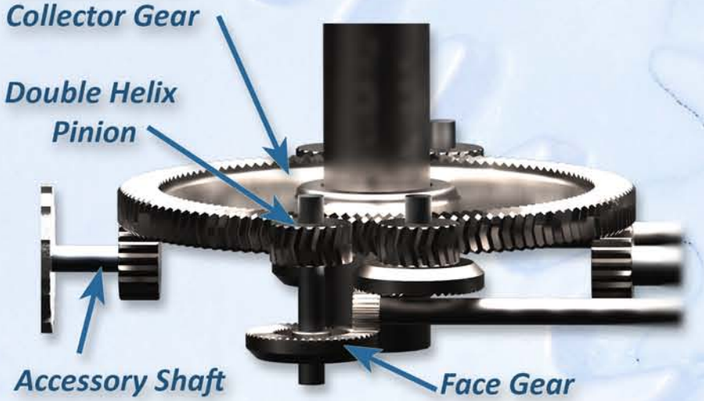

Split-Torque Gearbox

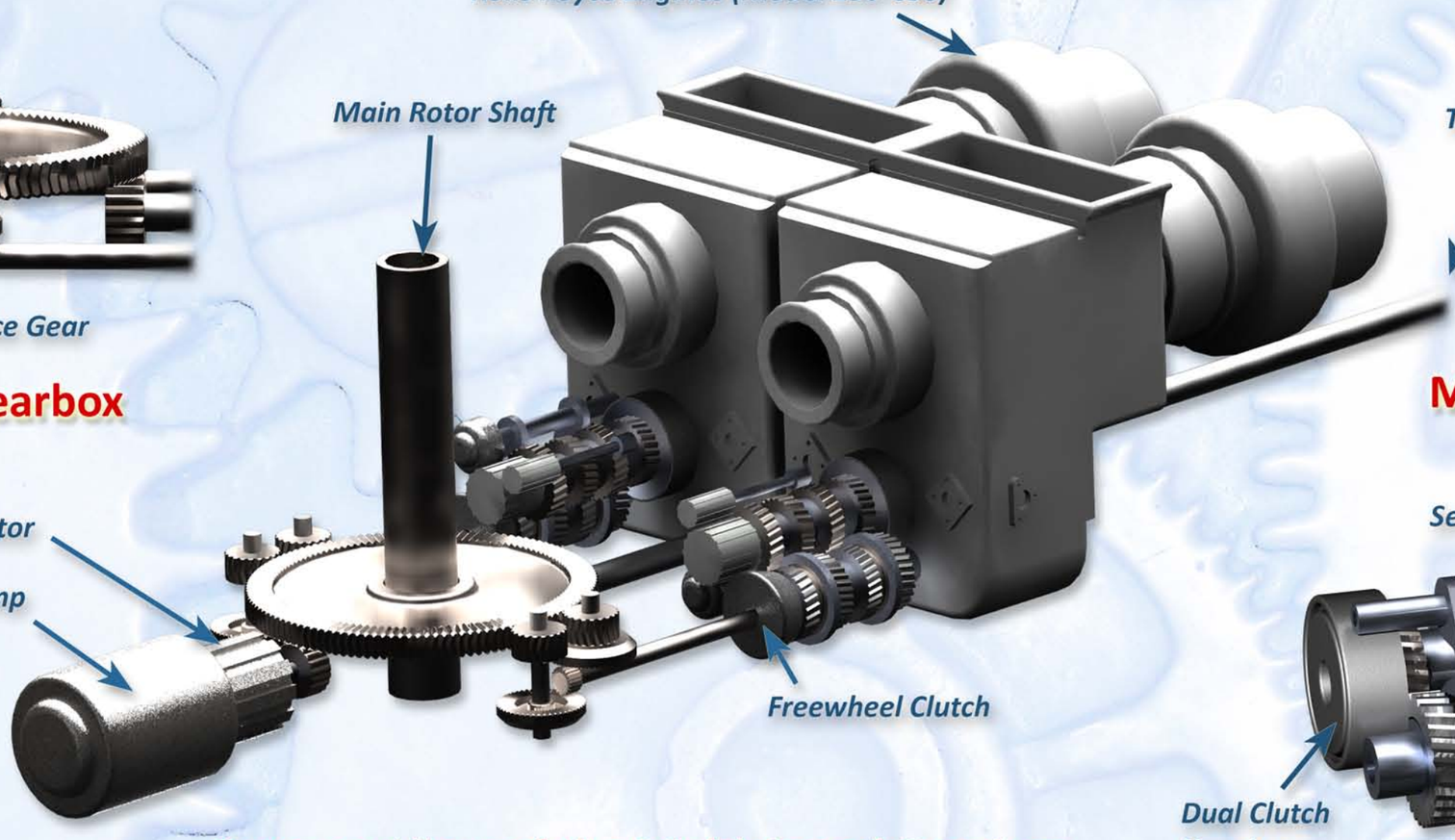

Multi-Speed Gearbox

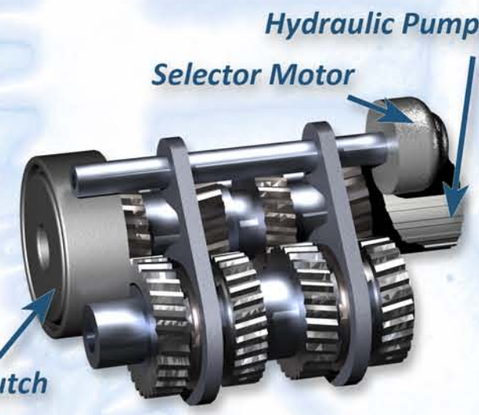

Green: Engaged Gear
Red: Disengaged Gears

Cutaway View of the Multi-Speed Gearbox

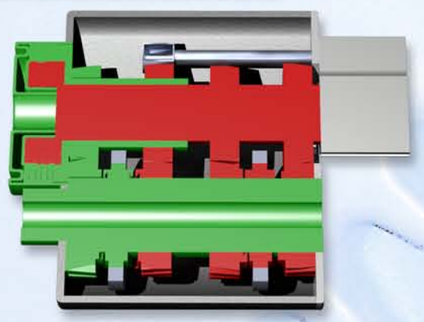

First Gear
(83% - 88% N_R)

Second Gear
(88% - 93% N_R)

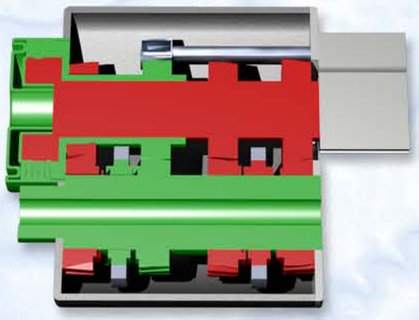

Third Gear
(93% - 98% N_R)

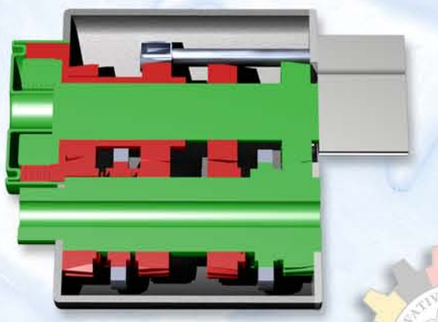

Fourth Gear
(98% - 103% N_R)

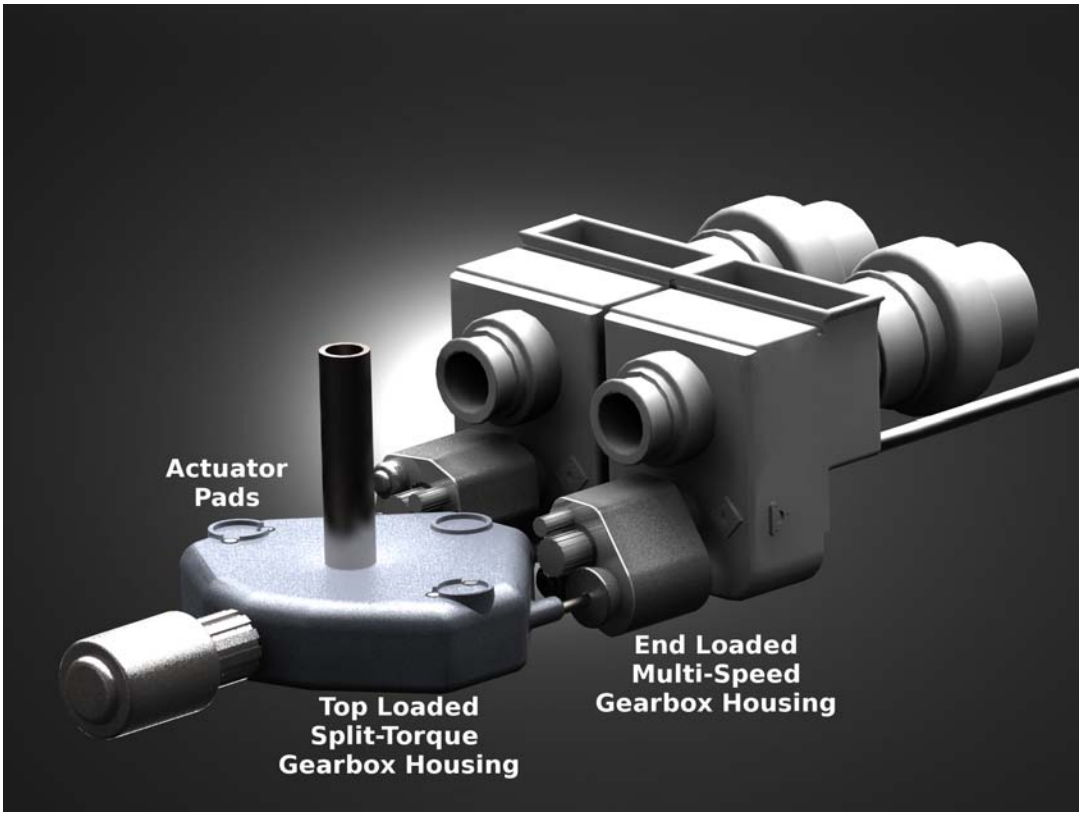

Figure 4.1: External view of the VERITAS.

estimated to exceed 98%.

4.2 Engines

The Rolls Royce 250-C30 engine was selected to replace the Turbomeca Arriel 1E2 of the baseline aircraft. The 250-C30 offers improved specific fuel consumption and reduced weight, increasing the range, endurance, and payload capability of the *Griffin*, as shown in Fig. 4.2a and Table 4.1. While the maximum continuous power output of the 250-C30 is slightly less than that of the Arriel 1E2, the improved efficiency of VERITAS enables the *Griffin* to significantly exceed the performance of the baseline helicopter under all flight conditions.

Table 4.1: Engine data.

Engine	Takeoff power (shp)	Continuous power (shp)	Output RPM	Weight (lb)	Length (in)	Width (in)	Height (in)
Arriel 1E2	738	692	6000	276	46.7	18.2	27.3
250-C30	650	557	6016	252	43.2	22.0	25.5

The 250-C30 is equipped with a manufacturer supplied gearbox reducing the power turbine output from 30,650 RPM to 6,016 RPM. The continuous engine output speed may be varied by $\pm 3\%$ of the nominal value without significantly impacting specific fuel consumption[6] (Fig. 4.2b) or engine life[7] - larger excursions from the nominal speed lead to degraded performance and may require additional maintenance actions. The hydromechanical control unit of the engine is retained; however, the functions of the electronic control unit are replaced by VERITAS to coordinate speed and power changes with the advanced transmission (Sec. 4.5).

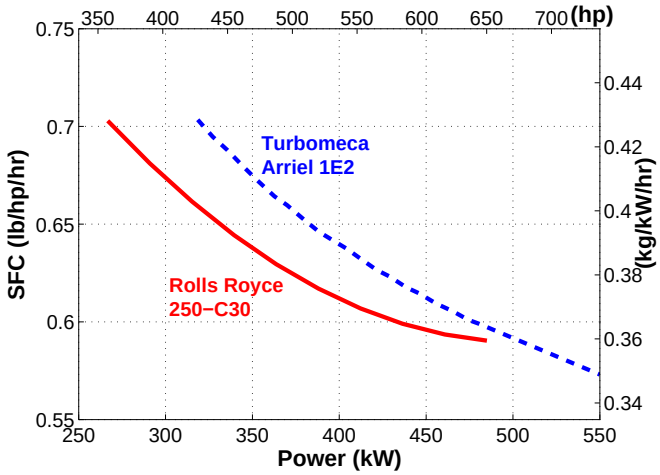

(a) Engine SFC vs. power output.

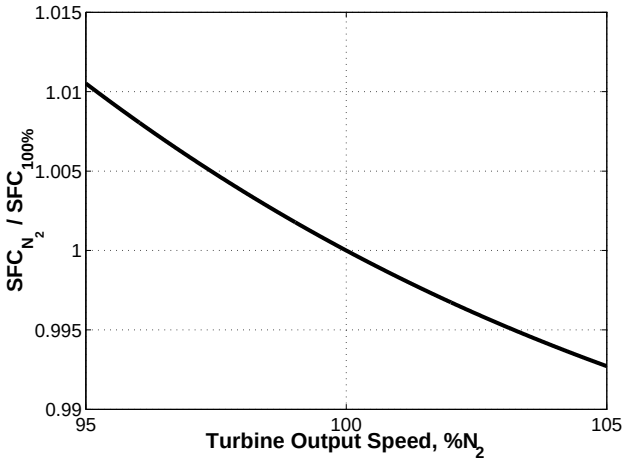

(b) Off-design engine SFC trend vs. turbine output speed.

Figure 4.2: Engine SFC.

4.3 Multi-Speed Gearbox

VERITAS features two multi-speed gearboxes, one connected to power takeoff of each engine. The multi-speed gearbox provides four discrete output speeds at 86, 90, 96, and 100% of the input speed. In conjunction with the capability of the engines to provide an efficient range of rotor speed adjustment of $\pm 3\%$, a continuous variation in rotor speed from 83% to 103% of nominal is possible. A robust dual-clutch mechanism allows for smooth transitions between output speeds without interruption in power delivery during the gear shifting process. The multi-speed gearboxes were designed to AGMA aerospace gearing standards for the calculation of bending and contact stresses (AGMA 911-A94, AGMA 2001-D04) and the design was optimized for minimum weight and size using a hybrid pattern-search/genetic algorithm.[8] Component weights were estimated using a solid rotor model.[9] Because the multi-speed gearboxes operate at high speed and low torque, each gearbox weighs only 108 lb, including oil.

4.3.1 Alternative Approaches

In addition to the multi-speed gearbox, several alternative variable speed drive configurations were considered. Continuously Variable Transmissions were found to be ill suited to the high continuous torque loads required to maintain helicopter rotor speed in flight. Heavy-duty CVT units employ toroidal rollers which transmit torque through a friction contact between two rounded disks. Since both the disks and roller are rounded, the size of the contact patch between friction surfaces is small. In addition, the surfaces are continuously slipping against each other. A high normal force must be applied in order to effectively transmit a large torque, as required to drive the rotor. This leads to a high actuation force requirement, a high rate of heat generation, and a high rate of wear making CVTs inviable for helicopter applications. Other alternatives include fluidic couplings or “no contact” electric drives; both of these concepts dramatically reduce the transmission efficiency and increase the weight substantially.

4.3.2 Operation

A dual clutch transmission is composed of two tightly integrated torque transfer paths. Power can be seamlessly transferred from one path to the other through use of the dual clutch mechanism. Each path consists of a clutch which transfers the input torque to a layshaft. Affixed to the layshaft are laygears which are continuously engaged with idler gears that are attached to the output shaft using bearings and are free to rotate about the shaft. The output shaft is driven by engaging a dog gear which rotates with the shaft to the desired idler gear, which then transfers torque to the output shaft. By using the dog gear to select

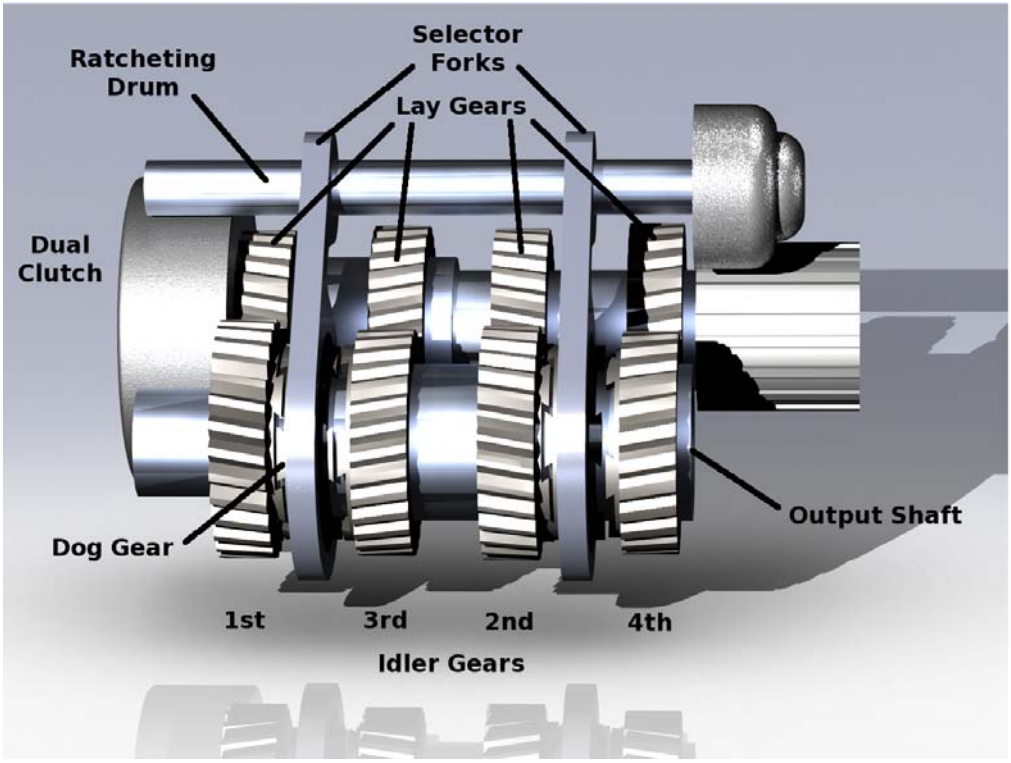

Figure 4.3: Multi-speed gearbox internals.

different idler gears, different gear ratios may be chosen.

In the VERITAS dual-clutch transmission, shown in Fig. 4.3, a single input drives both clutches which each drive a separate layshaft. The clutches and layshafts are arranged coaxially for compactness. The outer layshaft drives the first and third laygears and the inner layshaft the second and fourth laygears. All four idler gears rotate about the single output shaft. One dog gear is used to select between first and third gears and another to select between second and fourth gears.

The process of speeding the rotor from 83% to 103% nominal speed (N_R) is as follows. When the helicopter is in fourth gear (83% - 88% N_R) the inner clutch will be engaged to the inner layshaft and the fourth idler gear connected to the output shaft by engagement with the adjacent dog gear. (See the Engine and Transmission System Foldout.) At this time, the other dog gear will be engaged with the third idler gear, but no torque will be transferred through this path as the outer clutch will be disengaged from the outer layshaft. To shift to third gear (88% - 93% N_R), the outer clutch will be engaged as the inner clutch is simultaneously disengaged. During the engagement process, both clutches will slip, allowing torque to be transferred through both paths despite the difference in gear ratio. Once the outer clutch is fully engaged, the transmission will now pre-select second gear (93% - 98% N_R) for a subsequent shift by disengaging the dog gear from the now unloaded fourth gear and engaging the second gear. Once the gear is pre-selected, the process is repeated with the inner clutch now engaged and the outer clutch simultaneously disengaged in order to shift into second gear. First gear (98% - 103% N_R) may now be pre-selected, the outer clutch engaged, and the inner clutch disengaged in order to accelerate the rotor to full speed. The process for slowing the rotor is the same, but performed in reverse. The VERITAS-equipped *Griffin* can operate continuously in any gear ratio and may speed up or slow down the rotor at any time, but gear changes must be performed sequentially to enable a smooth transfer of power from one ratio to the next. Changes in the reduction ratio of the multi-speed gearbox are coordinated with changes in engine speed to provide a continuous variation of rotor speed (Sec. 4.5).

4.3.3 Dual Clutch

Table 4.2: Wet clutch properties.

Clutch	Inner diameter (in)	Outer diameter (in)	Clutch load (lb)	# of plates	Thickness (in)
Inner	2.04	4.14	5000	7	0.14
Outer	4.16	5.50	5000	5	0.20

The dual clutch unit (Fig. 4.4) provides the multi-speed gearbox with the capability of providing an uninterrupted flow of power to the rotor even as the gear reduction ratio is changed. The dual clutch unit consists of of a pair of coaxial multi-plate hydraulically actuated wet clutches. The larger outer clutch is sized to carry the higher torque of 1st gear, while the inner clutch is sized to withstand the reduced torque applied by 2nd gear. The clutches have been sized by the genetic algorithm using a non-linear model of clutch friction and heat generation based on experimental data[10] - the results are shown in Table 4.2.

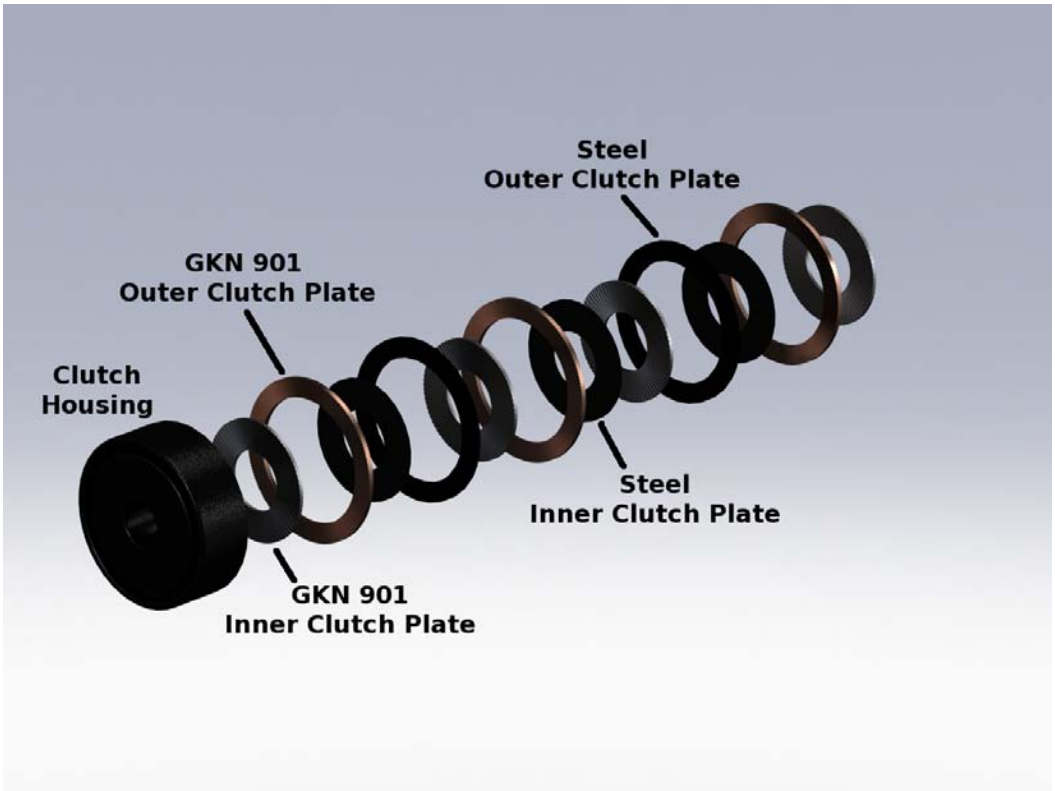

Figure 4.4: Wet clutch exploded view.

Overheating of the friction surfaces is the primary source of clutch wear and reduces the torque holding capability of the clutch. To improve the durability of the clutch under high loads, as well as to allow for prolonged engagement times, the wet clutches used in the VERITAS system are suspended in oil to cool the surface of the clutch during operation. The friction surfaces of the clutch have radial fluid pumping grooves to improve the rate of heat transfer while the clutch is engaged. The addition of oil for cooling reduces the coefficient of friction of the clutch surfaces - to provide the same torque capacity as a dry clutch, multiple clutch plates are installed in each clutch pack. Five clutch plates are used for the larger outer clutch pack, and seven clutch

plates for the inner clutch packs. The plates in each clutch pack are stacked with alternating composition of GKN 901 sintered metal and steel material. This arrangement allows for a greater torque capacity with a very low rate of wear (Table 4.3); each clutch is designed to allow for 50,000 full-power engagements with a maximum permissible slip time of five seconds. Reducing the slip time during an upshift results in reduced clutch wear, but requires more power from the engines (Table 4.4). During a downshift, the both clutches may be disengaged within five milliseconds allowing the rotor to coast down to the desired speed. The appropriate clutch may then be reengaged, minimizing clutch slip time and prolonging clutch life.

Table 4.3: Clutch material properties comparison. (Adapted from.[11])

Characteristic	Molded semi-metallic	Sintered metal	Graphite paper	Polymeric
Dynamic friction	Low	Medium	Medium	High
Static friction	Medium	Medium	Medium	Medium
Heat resistance	Good	Excellent	Good	Good
Durability	Good	Excellent	Moderate	Moderate
Compressive strength	High	High	Medium	High
Mating surface	Rough	Rough	Smooth	Rough to smooth
Optimal grooving	Spiral	Sunburst	Waffle	Waffle

The clutches are hydraulically actuated. The dual clutch unit employs a set of solenoid 3/2-way valves to control the hydraulic pressure applied to each wet clutch pack against a return spring built into the wet clutch housing. For redundancy, a pair of 3/2-way valves are used to actuate each clutch pack - in the event that a solenoid fails, the attached 3/2-way valve will be closed by the built in spring, sealing the clutch housing and allowing the other 3/2-way valve to control clutch actuation without any degradation in performance.

Table 4.4: Clutch engagement time vs. power to overcome rotor/drive inertia for a 5% increase in rotor speed.

Clutch time (sec)	Additional power (shp)
5.0	34
2.5	69
1.5	114
0.5	343

4.3.4 Geartrain

All gears within the multi-speed gearbox have a 20° helix angle to improve the contact ratio between teeth, yielding reductions in both noise and vibration. The gears are constructed from VASCO X-2M gear steel, which offers excellent fatigue and scuffing resistance across a wide range of temperatures. The layshaft gears are fitted to the layshafts using splines, whereas the idler gears ride on bearings affixed to the output shaft. The dog gears are allow to slide on the output shaft along a straight-grooved spline and are mounted within bearings set in each selector fork. The design of the geartrain is shown in Table 4.5.

4.3.5 Gear Selection

Gear ratio selection is accomplished by engaging the dog teeth of the dog gear and the desired idler gear. The dog teeth have a trapezoidal dovetail profile, drawing the dog and idler gears together as torque is transmitted through the gears. The dog gear is moved into engagement with the idler gear along the output shaft by movement of the selector fork.

One selector fork is used to engage gears one and three, the other engages gears two and four. The selector fork is cammed between each gear pair through the rotation of the ratcheting drum assembly; one full rotation of the ratcheting drum moves the

Table 4.5: Multi-speed gearbox geartrain.

Gear	Ratio	Lay gear diameter (in)	# of teeth	Idler gear diameter (in)	# of teeth	Face width (in)
First	1.00	4.01	25	4.01	25	1
Second	0.96	3.93	25	4.09	26	1
Third	0.90	3.80	27	4.22	30	1
Fourth	0.86	3.71	25	4.31	29	1

two selector forks through all four possible gear engagement combinations. The movement of the ratcheting drum is controlled by a small electric motor which is affixed to the gearbox housing and is externally accessible for inspection and maintenance. The selector fork and ratcheting drum are constructed from Aluminum T7075 and sized to withstand the maximum possible actuation loads.

4.3.6 Gear Synchronization

To reduce transmission wear and noise during gear engagement, it is necessary to synchronize the speeds of the idler and dog gears before meshing the dog teeth together. In a conventional automotive transmission, individual conical clutch synchronizers within each idler gear are used to match speeds during engagement. Clutch-based synchronizers allow for rapid gear engagements, but are fragile and difficult to maintain as they are inaccessible without complete disassembly of the gearbox.

Instead, the VERITAS multi-speed gearbox makes use of central synchronization. During the gear pre-selection process, the inactive dog gear and idler gear pair are disengaged. A hydraulic pump-motor attached to the inactive layshaft is then used to adjust the speed of the inactive shaft to match that required to synchronize the dog gear with the idler gear to be pre-selected. Because the inertia of the inactive gears and layshaft is small, the power requirements for synchronization are low and the pre-selection operation can be completed within 1/4 second. The pump-motor on the inactive layshaft is driven by a pump-motor connected to the active layshaft, which also provides the required oil flow for lubrication and cooling of the gearbox and dual-clutch mechanisms. The pump-motor driven by the shorter outer layshaft is connected through a small gear drive affixed to the third lay gear and operates at a higher RPM than the larger pump-motor connected directly to the longer inner layshaft. Both pump-motors are affixed to the gearbox housing and can be externally inspected and maintained.

4.3.7 Lubrication

Oil is distributed throughout the gearbox using small channels built into the housing. Spray nozzles mist oil inside the gearbox to leave a thin film on all gear contact surfaces. The oil flow rate is sufficient to remove all heat generated by the gears and clutch when the transmission is operating at peak power without heating the oil above 140° F.

4.3.8 Housing

The transmission housing supports the bearings which hold all shafts in the transmission, provides for the distribution and retention of oil, and protects transmission components from corrosion. The housing is an end-loaded configuration, which allows for a precise and self-aligning installation of the shafts and bearings and reduces the assembly and maintenance time required to install or replace internal components.[12] The housing is cast from Aluminum A357 using a Controlled Solidification Investment Casting (CSIC) process. CSIC allows for a substantially thinner, more uniform, more complex and lighter-weight aluminum housing than is possible with conventional casting methods without significant change in cost. CSIC gearbox housings may be as much as 20% lighter than comparable magnesium housings, since additional corrosion protection is not required for the aluminum housing. The shape of the housing is carefully designed for quiet operation, avoiding flat panels which may be excited by the meshing frequencies of the gears and radiate acoustic energy.

4.3.9 Failure Modes and Effects Analysis

In the event of a failure of any subsystem, the VERITAS multi-speed gearbox retains the capability to operate at a single fixed reduction ratio until the helicopter is able to safely land. The hydraulically actuated dual-clutch mechanism is designed to hold clutch pressure and remain engaged to the currently active layshaft for at least 30 minutes after the failure of either pump-motor or a loss of oil from the transmission housing. Likewise, in the event of a failure of the gear selection system, the profiles of the teeth of the dog and idler gears are designed so as to remain engaged under load. Under fixed-ratio operation, the helicopter may still vary rotor speed by variation of turbine speed. The Rolls-Royce 250-C30 engine may operate continuously from 91.5% to 112.7% of nominal output speed with reduced efficiency and increased wear.[7] This allows the rotor to be operated at speeds up to 96% N_R from a failure fixing the reduction ratio to the worst-case of 0.86.

The two multi-speed gearboxes may be controlled independently by VERITAS for redundancy. Near the speed for best range, where only one engine is required for flight, the fixed-ratio gearbox and engine may be taken offline in order to minimize fuel consumption and retain the exceptional range and endurance of the *Griffin* without degradation. As the pilot prepares for landing, the fixed-ratio gearbox and engine may be brought back online to provide the power required for hover at a safe rotor speed of at least 96% N_R by operating the 250-C30 up to its maximum continuous power turbine speed limit .

4.4 Main Rotor Gearbox

The main rotor gearbox is responsible for providing the majority of the speed reduction from the engine power take-off output of 6,016 RPM to the main rotor speed of 383 RPM. The transmission is designed to accommodate a continuous power input from each engine of 600 shp at any input speed for 5,000 hours. In addition, the transmission can accept up to 700 shp from either one or both engines at an accelerated rate of wear. The transmission also provides power take-offs for both the tail rotor drive shaft and electrical generator at 2,400 RPM.

4.4.1 Design

Hybrid pattern-search/genetic algorithm optimization routines were developed to assess three alternative main rotor gearbox configurations: a conventional planetary gearbox configuration with a spiral bevel input combiner, a non-conventional split-torque configuration utilizing a single double-helix collector gear, and a hybrid configuration with a split-torque stage combining the power inputs and providing some reduction with a planetary stage providing the final reduction to 383 RPM. The estimated size and weight of the three configurations is tabulated below, in Table 4.6. As in the multi-speed gearbox, all helical gears were constructed from VASCO X-2M because of its excellent scuffing resistance. Spiral bevel gears are not commonly available in VASCO X-2M, and where used, were made from Grade 3 case hardened steel. The main rotor shaft in all three configurations was constructed from forged titanium 6 A1-4V, and other shafts from aluminum alloy T7075.

Table 4.6: Main rotor gearbox configuration comparison.

Configuration	Overall weight (lb)	Length (in)	Width (in)	Height (in)
Planetary	416	26.1	18.8	18.4
Split-torque	**315**	**21.3**	**26.4**	**13.2**
Hybrid	363	22.4	26.4	14.7

The split-torque configuration results in the lowest overall weight, as a result of the lack of a separate input combiner stage and because the torque-splitting layout reduces gear tooth stresses allowing for the use of smaller and lighter gears. In addition, the split-torque configuration eliminates the use of less robust spiral bevel gears and reduces overall noise by enabling the use of helical gears with a high contact ratio. Helical gears are not typically used in planetary gearboxes because the thrust loads produced by the helical profile are not easily supported from within a planetary gearset.

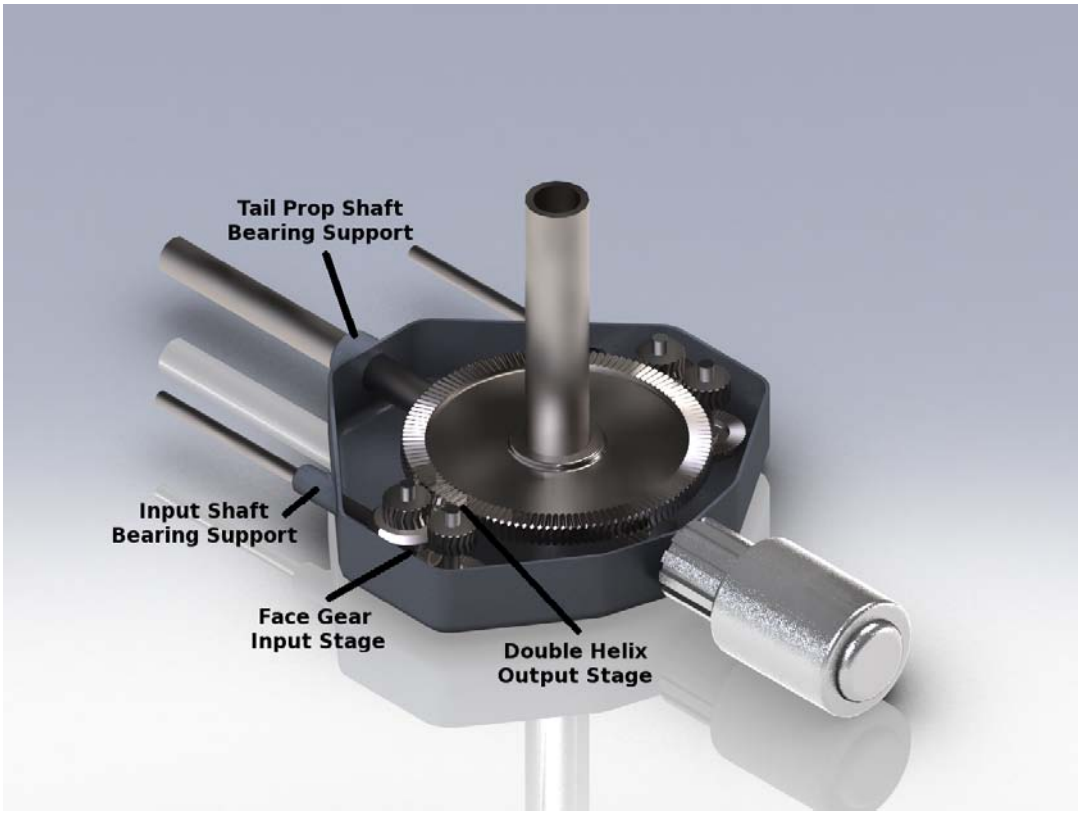

Figure 4.5: Main rotor gearbox open view.

The VERITAS split-torque design, shown in Fig. 4.5 and on the Engine and Transmission System Foldout, follows the McDonnel Douglas Advanced Rotorcraft Transmission configuration,[17] and can be divided into two stages. The input stage connects the input shafts to input pinions and uses each pinion to drive two face gears as an alternative to the use of a spiral bevel gear drive. A similar configuration tested by Boeing showed that torque loads applied to each face gear remained within 4% of one another.[16] This small imbalance of torque loads was taken into account in the design of the VERITAS split-torque gearbox. The VERITAS split-torque configuration balances the shear forces applied to the input pinion, reducing the amount of support required to retain the input shafts. The face gear concept has been well studied by NASA Glenn[13] and several manufacturers[14,15] and should pose no barrier to practical implementation of the gearbox. The second stage of the split-torque design is the output stage. Four double-helix pinions, affixed to the face gear support shafts, drive a double-helix collector gear attached to the main rotor shaft. The division of torque across the four pinions reduces the bending and contact stresses seen by any single tooth, allowing light-weight gearing to be employed. Face teeth are cut into the collector gear so that it can drive output pinions for the tail rotor and accessory output shafts. Shear loads applied to collector gear are balanced reducing the loads applied through the shaft supports of the gearbox housing. The optimized design generated by the genetic algorithm is shown in Table 4.7.

The VERITAS split-torque transmission accepts input from two parallel Al 7075 shafts connected to sprag-type overrunning clutches which are affixed to the multi-speed gearbox output shafts. The split-torque input shafts are connected to the overrunning clutches using Kaman KAflex® maintenance-free non-lubricated couplings. These couplings allow the some structural flexing between the rigidly mounted multi-speed gearboxes and engines, and the vibration-isolated main rotor transmission. Similar couplings are used to connect the segments of the tail prop drive shaft.

Table 4.7: Split-Torque Gearbox Geartrain

Gear	Pitch diameter (in)	# of teeth	Face Width (in)
DH collector	19.34	125	1.5
DH pinion	3.09	20	1.5
Face	3.91	50	1.0
Input	1.56	25	1.0
Tail shaft	3.09	20	1.0
Accessory	3.09	20	1.0

4.4.2 Housing

Like the multi-speed gearbox, the main rotor gearbox housing is manufactured from Aluminum A357 using the CSIC process for superior corrosion resistance, light weight, and low cost. The gearbox uses a top-loaded configuration, allowing for easy assembly and precise fitment.[12] Internal support ribs are cast into the housing to provide stiffening, to accommodate cored passages for oil distribution, and reduce noise radiation.

The titanium main rotor shaft is supported by a bearing contained inside of a steel standpipe, supported at four points on the upper surface of the gearbox housing, in order to transfer shaft side-forces and moments to the reinforced sections of the gearbox housing. The main rotor swashplate control actuators are affixed to pads set in the upper portion of the housing. The main rotor shaft is also retained by two bearings mounted in the upper and lower surfaces of the housing. Below the lower bearing and transmission housing, and outside of the load path, is an electrical slip ring to allow electrical power and command signals to be sent to the trailing edge flaps and de-icing equipment. The transmission housing is attached to the transmission deck through vibration isolators. The internal double helix input pinion, multi-speed gearbox, tail rotor output, and accessory drive shafts are also supported by bearings set in reinforced sections of the housing.

4.4.3 Accessories

The accessory power takeoff supports the main rotor gearbox oil pump and a hybrid output generator[18] producing 15A of 400 VAC power at a constant 60 Hz to supply power to the actuators as well as 45A 28 VDC for front panel equipment.

4.5 Electronic Controls

Electronic controls for both the multi-speed gearboxes and engine are integrated using Honeywell's Modular Aerospace Control (MAC). MAC allows different replaceable and reprogrammable modules to be installed depending on system configuration. The VERITAS MAC will include a MIL-STD-1553B communications link to the pilot's manual controls, front panel avionics, trailing edge flap controller, and HUMS. Additional modules are used to control the speed of each engine and gear selection of the multi-speed transmission units to coordinate rotor speed changes continuously from 82% to 103% N_R. The engine control modules will also provide several advanced features: automatic engine start-up, cold temperature start-up, engine load balancing, emissions control, engine overspeed and overtorque protection, auto-relight and surge detection and recovery capability, engine condition monitoring, and allow for consistent engine performance and response regardless of ambient conditions or fuel quality.

4.6 Tail Prop Gearbox

The tail prop gearbox, shown in Fig. 4.6 and on the Tailprop and Empennage Assembly Foldout, enables the tail prop to be swiveled 90° for use as an anti-torque device at low speeds and as a propulsor at high speeds. The swiveling mechanism must be robust and be able to return to an anti-torque configuration upon failure.

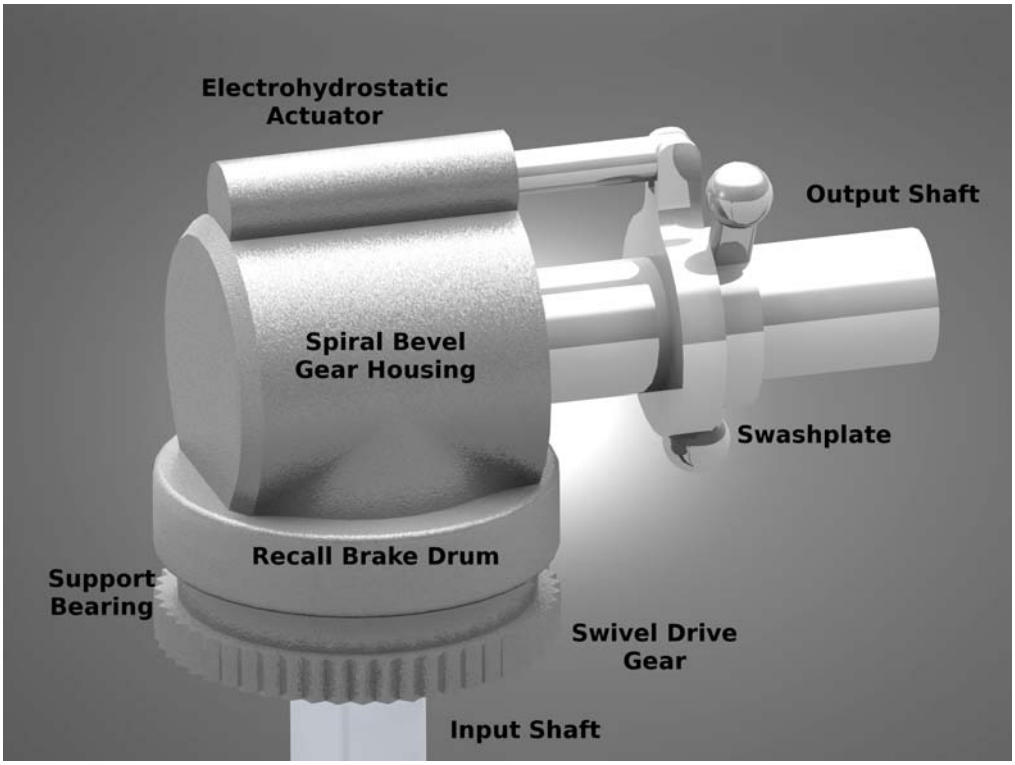

Figure 4.6: Tail prop swiveling gearbox.

4.6.1 Intermediate Gearbox

The VERITAS intermediate gearbox is similar to the spiral bevel gearbox of the baseline aircraft, but with a 90° shaft angle in order to allow the swiveling mechanism to rotate about the output shaft axis.

4.6.2 Swiveling Mechanism

The VERITAS swiveling mechanism is derived from the existing tail rotor gearbox. The 90° spiral bevel tail rotor gearbox allows the tail prop to rotate about the input shaft axis. The spiral bevel gears are splash lubricated with the same MIL-L-26399 oil common to the other drivetrain components. The gear box is supported by a bearing at the base which is affixed to the airframe. Rotation is accomplished by driving a gear affixed to the base of the gearbox housing with a pinion and electric motor. Rotor drag forces are relatively low at the transition speeds (3.5 lb), so a relatively lightweight and compact electric motor with a holding torque of 20 in-lb is employed to accomplish transition within 30 seconds. A pair of solenoid actuated locking mechanisms hold the gearbox against stops in both the anti-torque and propulsor configurations to eliminate unwanted motion of the rotor during flight.

4.6.3 Emergency Recall Mechanism

An electrically actuated braking caliper is installed in the swiveling gearbox which clamps to a rotor affixed to the tail rotor drive shaft. In case the swiveling drive mechanism fails, the prop-motor may be recalled to the anti-torque configuration by activating the brake thereby applying a torque to the swiveling gearbox until it engages with the anti-torque configuration swivel stop.

4.7 Maritime Considerations

VERITAS is designed to allow for shipboard helicopter operation. Corrosive materials have not been used in the design of VERITAS in order to allow for operation near sea-water without additional maintenance procedures. Shipboard storage and maintenance facilities are limited, so special care has been taken to limit maintenance requirements. By duplicating components on both the port and starboard side of the drivetrain, the number of parts that need to be stocked has been reduced. In addition, tight integration with HUMS allows part replacements to be anticipated, eliminating unscheduled maintenance and increasing availability. VERITAS has been designed to achieve a high degree of reliability to prevent failures over water, and to allow the *Griffin*'s crew the maximum possible range in order to find a suitable landing site in the unlikely event of a systems failure.

5 Main Rotor and Hub Design

A key innovation in the *Griffin* rotor aerodynamic design is the TALON tip. The *Griffin* also features integrated trailing edge flaps which, in conjunction with creative composite couplings, provide near 100% vibration suppression capability. The structural design of the blade and semi-articulated hub is crucial to the successful operation of the VERITAS and is detailed below. A stability analysis was performed to ensure that all dynamic instabilities are avoided.

5.1 Main Rotor Aerodynamic Design

The *Griffin*'s main rotor operates at a higher cruise speed (150 kts) than that of the baseline EC145 (131 kts). To enable the rotor to have this capability, the main rotor was re-designed to maximize the performance for the expanded flight envelope of the *Griffin*. Great performance gains are partly attributed to judicious airfoil selection and the non-conventional TALON (Thinned Anhedral Lift-Optimized Notched) tip geometry which greatly mitigates drag divergence penalties. The critical parameters of the main rotor are summarized in Table 5.1.

Table 5.1: Critical main rotor parameters.

Diameter	36.1 ft 11.0 m
Chord	1.05 ft 0.32 m
Number of blades	4
Solidity (thrust weighted)	0.074
Blade twist	-10°/+1° bilinear
Airfoils	SC-1095 SC-1095R8

5.1.1 Airfoil Selection

A variety of airfoils exist for rotorcraft use, most stemming from the OA (ONERA), RAE (Royal Aircraft Establishment), RC (NASA), SC (Sikorsky), or VR (Boeing-Vertol) airfoil families. However many, they can generally be categorized into two types:[19]

- High-lift airfoils. These typically have thicknesses between 8–16% chord and notable amounts of camber. The OA-214, RAE 9645, RC(4)-10, and VR-12 are examples of such airfoils that are utilized for their high maximum lift capability.
- High-speed airfoils. These are characterized by Mach drag divergence numbers above 0.80 as a result of thicknesses of 8% chord or smaller. A selection of high-speed airfoils include the OA-206, RAE 9634, RC(5)-10, and VR-15.

These two separate types of airfoils exist because of the competing aerodynamic environments at the rotor disk in forward flight. The middle portion of the blade contributes significantly to the generation of thrust, requiring airfoils with high maximum lift capabilities (high-lift airfoils). Airfoils that postpone stall to relatively high angles of attack are greatly desirable in this section of the blade to avoid stall on the retreating side of the rotor disk. At the tip, high incident Mach numbers imply that airfoils must have excellent drag divergence properties (high-speed airfoils). Overall, well-performing rotorcraft airfoils must also exhibit good lift-to-drag characteristics. Considering the nature of the rotor disk in forward flight, the *Griffin*'s airfoils consist of a pair of airfoils, one of each general type, appropriately positioned so rotor performance is maximized.

Griffin Main Rotor

Swashplate Assembly

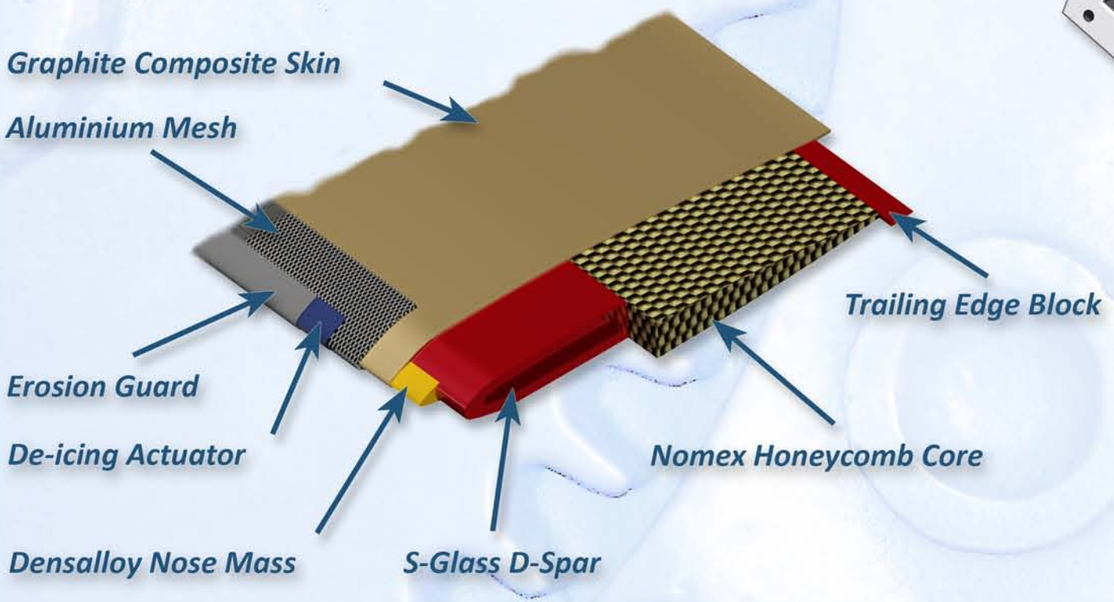

Main Rotor Blade Cross Section

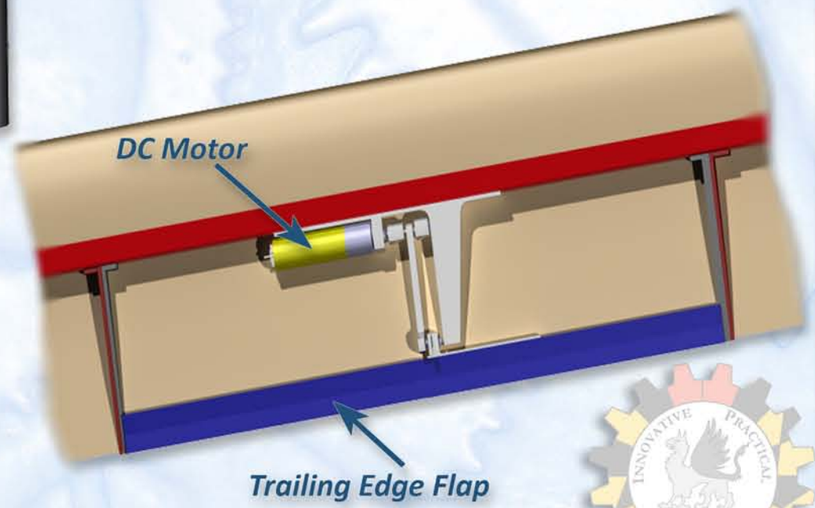

Trailing Edge Flap Actuation Assembly

The rotor of the baseline EC145 incorporates several airfoils, beginning with the OA-415 at the blade root and ending with the OA-407 at the tip. A blend of the OA-312 and OA-409 airfoils is used intermediately.[20] The required aerodynamic data for these OA airfoils were not available; therefore, these airfoils were not used in the *Griffin*. The VR-12 and VR-15 airfoils were considered, but not chosen because of high pitching moments which would cause undesirable root stress at the hub. Ultimately, the SC-1095R8 and SC-1095 airfoils were chosen. In addition to readily available aerodynamic performance data, these airfoils are proven performers as evidenced by the success of the Sikorsky UH-60 Blackhawk.

5.1.2 Planform Design

The placement of airfoils to form the main rotor planform is a procedure which begins at the blade root and continues along the blade span. The final planform is summarized in Fig. 5.1.

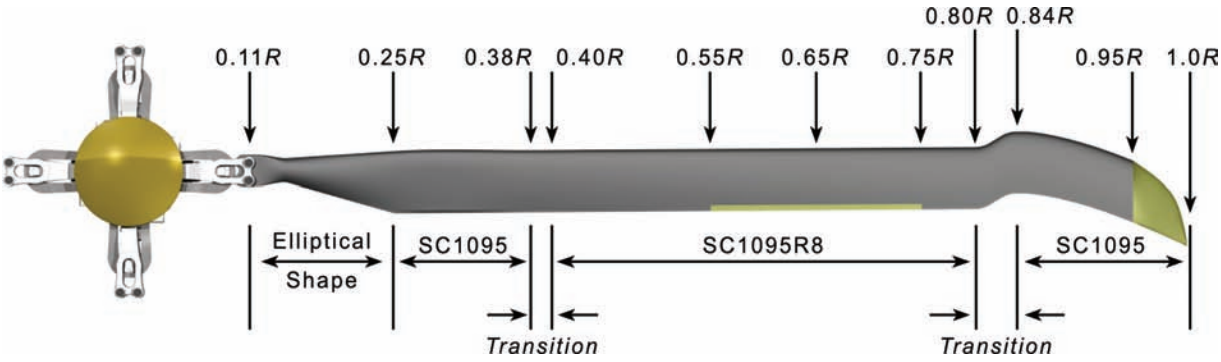

Figure 5.1: Main rotor planform.

- The root sections provide modest amounts of lift in hover. In forward flight, the retreating blade experiences reverse flow near the root, producing only drag. This reverse flow region is a circle of diameter approximately equal to $\mu_{cr}R = 0.38R$. Therefore, this section must limit an otherwise large drag penalty on the retreating side while producing meaningful lift in hover. The best solution is to have an elliptical shape from the root cutout at $0.11R$ to $0.25R$. This shape is a transition between an ellipse and the SC1095 airfoil, which has better lift-to-drag qualities than the SC1095R8 at low Mach numbers (Fig. 5.2a). The SC1095 is then carried through to the end of the reverse flow region at $0.38R$. Using this airfoil, rather than extending the elliptical shape to $0.38R$, ensures that in hover the root sections still produce meaningful lift.

- The middle section of the blade produces the most lift. Reducing drag in this region is also important. Thus, the SC1095R8 is used as the representative high-lifting airfoil because of its better maximum lift and lift-to-drag characteristics over the SC1095 (at $M = 0.4$, the maximum lift coefficient of the SC1095 and SC1095R8 is 1.19 and 1.30, respectively).[21] A transition is incorporated from $0.38R$ to $0.40R$, so the SC1095R8 begins at $0.40R$. The end point is chosen after determining the location for the tip airfoil. However, it must be located after $0.75R$ so the entire trailing edge flap module operates in a section without geometry blends.

- The tip of the rotor blade experiences high incident Mach numbers; mitigating drag divergence becomes the priority in this location. Therefore, the SC1095 is utilized as the blade tip airfoil rather than the SC1095R8 because of its superior Mach drag divergence number ($M_{dd} = 0.80$, instead of $M_{dd} = 0.78$ for the SC1095R8).[21] To determine where this crossover occurs, the required blade sweep is computed at cruise for the SC1095 airfoil, as shown in Fig. 5.2b with the SC1095R8 sweep for comparison. The radial location where sweep becomes necessary is $0.84R$, so the SC1095 airfoil is used from this location through to the blade tip.

- The transition region between the SC1095R8 and SC1095 is larger than $0.02R$, which was utilized previously. A transition

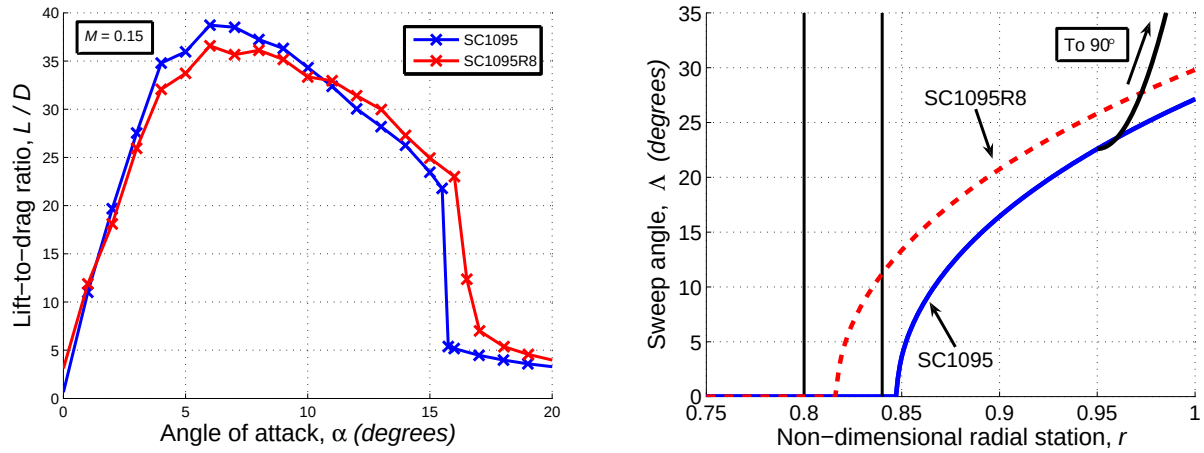

(a) Lift-to-drag vs. angle of attack for the selected SC airfoils.

(b) Ideal and implemented tip sweep for the *Griffin*.

Figure 5.2: Airfoil lift-to-drag and tip sweep.

region of 0.04R is found to be preferable to avoid stress concentrations which may result from a rapid geometry change. Thus, the SC1095R8 ends at 0.80R such that this second transition region spans 0.80R and 0.84R.

5.1.3 Blade Twist

The selection of blade twist is a matter of optimizing hovering and/or forward flight performance at some cost to the other. Highly twisted blades aid the helicopter in hover by minimizing its induced power requirements, allowing greater climb rates and higher hover out-of-ground-effect (HOGE) altitude. However, highly twisted blades are penalized in forward flight, leading to steeper power requirements and a lower cruise velocity. Conversely, blades with little-to-no twist perform well in forward flight, but they suffer a larger penalty in hover.

It is clear that striking a balance between these two by choosing a moderate twist distribution is the best solution. No twist was used from the root cutout to 0.250R. A distribution of -10° linear twist begins at 0.250R. To reduce the negative lift that occurs at the very tip of the blade at high forward speeds, the portion of the blade beyond 0.95R is linearly twisted by +1°. The resulting bilinear twist distribution is simply manufactured because the tip is fabricated separately and attached after applying the relieving twist.

5.1.4 Blade Taper

Blade taper, like twist, is another factor which may be controlled to improve the performance of the helicopter in either hovering or forward flight. An ideal hovering helicopter has hyperbolic taper which minimizes profile power, yielding blade stations which operate at maximum lift-to-drag ratios. Yet, the *Griffin* employs trailing edge flaps which are very sensitive to changes in blade chord. Taper would also complicate the composite layup practice and increase manufacturing time and cost. Thus, the *Griffin* benefits from a largely untapered blade.

5.1.5 Design of the TALON Tip

The baseline Eurocopter EC145 cruises only at 130 kts, so a swept tip is not necessary. By increasing the *Griffin*'s cruise speed to 150 kts and dash speed to 176 kts, the tip region of the blade now must be designed to mitigate compressibility effects. Figure 5.2b prescribes the necessary blade sweep for the incident Mach number of all sections to be under the Mach drag

divergence number for the SC1095 airfoil, i.e. $M_{dd} = 0.80$. However, only sweeping the tip causes unfavorable torsional effects as a result of offsetting the blade center of gravity and aerodynamic center. Thus, the tip is moved forward relative to the main rotor quarter-chord line to decrease these torsional effects.[22]

This forward movement also yields a notch which delays stall to higher angles of attack by acting as an "aerodynamic fence".[22] This notch is critically important as it addresses the concerns of the retreating blade. Because blade sweep is designed from only the advancing blade, some experiments have shown that a rectangular blade may outperforms a notchless swept tip.[23] Indeed, any tip design must address both the advancing and retreating sides of the rotor disk. The addition of the notch to the rotor appropriately addresses the aerodynamics of the retreating blade; it is a proven solution as evidenced by the performance of the matured design of the BERP rotor.

The remaining 5% of the blade span has a 20 degree anhedral, which gives a modest improvement in the figure of merit. Anhedral also introduces the rolled-up tip vortices farther below the tip-path-plane of the rotor, reducing BVI noise in level flight. The leading edge of this tip section is also rounded so the very edge of the blade is streamwise to the incident airflow. Tip taper such as this has shown to modestly improve the rotor lift-to-drag ratio by offloading the tip and reducing vortex drag.[24,25] Lastly, this portion of the tip is also thinned to reduce thickness and high-speed impulsive noise. This design yielded the final tip geometry as shown in Figs. 5.3 and 5.4.

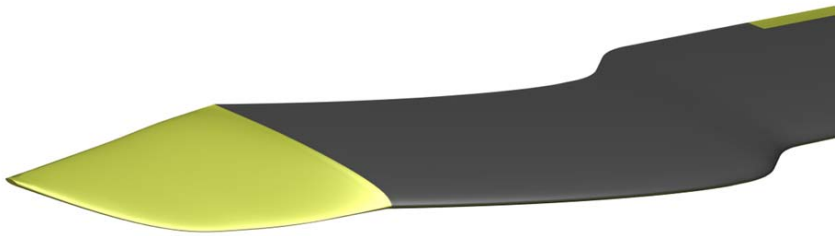

Figure 5.3: The TALON tip.

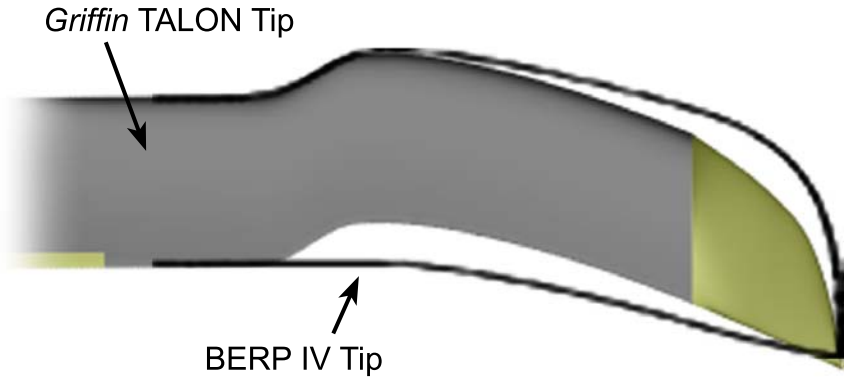

Figure 5.4: Comparison of the BERP IV and TALON tips.

The *Griffin*'s main rotor tip shape is appropriately named the TALON tip — for Thinned Anhedral Lift-Optimized Notched tip — as it encompasses the critical features which endow *Griffin* great performance at high speeds. Its unique shape is a result of an innovative approach to aerodynamic rotor design by addressing the entire rotor disk in hover and forward flight. Figure 5.4 illustrates the similarities with the BERP IV tip, evidence that such a unique shape can also be functional.[25] Other complex tip shapes, such as the ERATO or the Sikorsky Growth tip, further suggest that combined use of sweep, anhedral, thickness

reduction, and tip taper are indeed beneficial to rotor performance.

5.2 Blade Structural Design

The rotor blade structure was designed to withstand the centrifugal forces and the steady and oscillatory flap, lead-lag and torsional moments and shear stresses from the aerodynamic and inertial loads.
The primary load-carrying members of the *Griffin's* rotor blade are:

(i) Spar: It spans the length of the blade and carries the bulk of the centrifugal loads, the flap bending and lead-lag bending stresses and the torsional moments. The baseline aircraft, the EC145, uses a C-spar section; however, a D-spar was selected for the blades of the *Griffin*, since the spar-web provides an excellent anchor for the actuators of the trailing edge flaps. The required blade section properties were tailored to accommodate the D-spar design.

(ii) Skin: It helps distribute the shear and torsional moments.

(iii) Core filling: It helps preserve the blade profile by preventing the deformation of the skin under shear.

5.2.1 Choice of Materials

The main rotor blades were designed using fiber-reinforced composites. They have superior specific strength, stiffness, and fatigue properties. The composite construction has excellent corrosion resistance, an important consideration for the maritime missions of the *Griffin*. A thermoplastic matrix PEEK (Poly-Ether-Ether-Ketone) was chosen for the ease of manufacturability and recyclability. The blade spar was constructed of unidirectional S-glass/PEEK, the skin of woven graphite/PEEK fabric, and the filler of Nomex honeycomb. Densalloy, an alloy of tungsten, nickel and iron was used as the leading-edge mass because of its superior ductility and machinability. The materials used in the *Griffin*'s rotor blade and their mechanical properties are listed in Table 5.2. For a comparison, the other candidate materials are also listed.

Table 5.2: Materials used for *Griffin* blade construction

Material	**Density** (Mg/m^3)	**Tensile modulus** (GPa)	**Tensile strength** (GPa)	**Specific modulus**	**Specific strength**	**Shear modulus** (GPa)
S-2/APC-2 Glass/PEEK	2	55.2	1.17	27.6	0.59	6.55
IM7/APC-2 Graphite/PEEK	1.6	172	2.9	107.5	1.81	5.5
Nomex Honeycomb	0.032	-	-	-	-	0.03
S-2/8552 Glass/Epoxy	1.9	49.2	-	25.9	-	6.24
IM7/APC-2 Graphite/PEEK	1.53	144	-	94.1	-	5.4
Carbon/PPS	1.6	114.5	1.84	71.6	1.15	-
E-Glass/PP	1.5	39.3	1	26.2	0.67	-

5.2.2 Composite Coupling

The *Griffin* incorporates elastic flap bending-torsion couplings in the blades to reduce vibratory loads. Wind tunnel studies on Mach-scaled rotors have demonstrated significant reductions in 4/rev vibratory loads (reductions of 14% in vertical shear, 12% in in-plane shear and 18% in head moment) through the integration of multiple spanwise segmented pitch-flap couplings along composite blades.[26] AgustaWestland has successfully investigated the composite tailoring concept in the BERP IV blade design.[25] In the *Griffin* blades, the coupling was introduced by designing the spar to have negative pitch-flap coupling from

20% to 75% of the span and positive pitch-flap coupling from 75% to the tip. The *Griffin* is also equipped with trailing edge flaps to reduce vibrations. The use of composite coupling lowers the deflections and the actuation power required by the flaps. This coupling is also expected to offer performance benefits by reducing the negative lift at the advancing blade tip. The effect of the blade composite coupling has not been modeled in the vibration reduction studies and performance calculations for the *Griffin* and hence, the estimates are conservative.

5.2.3 Composite Lay-Up and Sizing

A composite tailoring procedure was developed to design the blade with required sectional stiffnesses, in particular, flap bending (EI_y), lead-lag bending (EI_z) and torsion bending stiffnesses (GJ), and axial stiffness (EA). The basic design parameters in the blade construction were the spar section dimensions, the number of plies in the spar and skin, the skin fiber orientation and leading-edge masses. The section shear center and center of gravity were designed to be located at the quarter-chord point. In conjunction with the estimation of the structural properties, the blade natural frequencies were suitably placed to allow safe "on-the-fly" modulation of rotor speed.

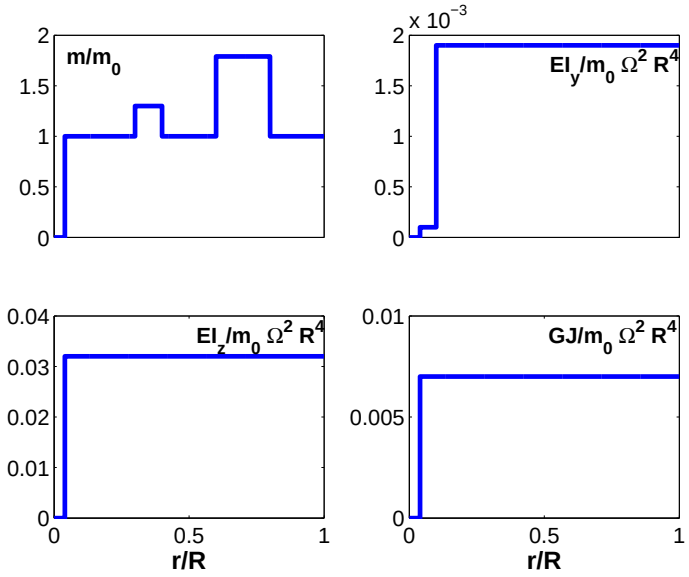

Figure 5.5: Blade mechanical properties.

Detailed 3D CATIA drawings of the blade including the blade planform, twist and tip shape were made and used to form a closed die mold of the blade. The spar is made of unidirectional $[0^\circ]_{18}$ plies of S-glass/PEEK with inner and outer torsion wraps made of woven $[\pm 45^\circ]$ graphite/PEEK fabric. Layers of unidirectional $[20]_6$ plies were used to introduce elastic flap bending-torsion coupling. The layup of the D-spar is $[45/0_{18}/\text{-}20_6/\text{-}45]$ inboard and $[45/0_{18}/+20_6/\text{-}45]$ outboard. A silicone rubber mandrel was used to form the D-spar during the curing stage and the spar was then laid up with the rest of the blade. The spar wall thickness is 10 mm. The chordwise extent of the spar is from 5% to 40% chord. A uniformly distributed nose weight of 4 kg was bonded to the spar and covered by the skin. The skin was made of woven $[\pm 45^\circ]_2$ graphite/PEEK plies. The designed spanwise stiffness and mass distributions are given in Fig. 5.5. The cross-sectional detail of the *Griffin*'s blade is shown in the Griffin Main Rotor Foldout.

5.2.4 De-icing system

Common de-icing methods for helicopter blades include freezing-point depressants, thermal melting, and surface deformation. The *Griffin* uses a novel de-icing method. It employs a 79 mil (2 mm) thick piezo-actuators, between the blade skin and leading-edge erosion guard, to generate ultrasonic waves that shear the skin at high frequencies, causing the accumulated ice layers to crack and be carried away by the flow. Compared to thermal de-icing (26 W/in^2), this system uses much less power (1.2 W/in^2) per unit blade area de-iced.[28]

5.2.5 Leading-edge erosion guard

Rotor blades are protected from water and sand erosion by bonding a titanium, steel or nickel sheet to the nose of the blade. The *Griffin*'s blade erosion guard is a 0.5 mm titanium sheet, covered with a 0.56 mm thick polyurethane tape (3M 8542HS MB) for enhanced sand erosion resistance. The tip is also capped with a metallic strip to preserve the shape and minimize damage

in case of a rotor strike.

5.2.6 Lightning Protection

Electrical bonding of the helicopter is crucial for lightning protection. The *Griffin* blade's outer skin is covered with a co-cured aluminum mesh to conduct the electrical charge to the metal abrasion guard, and thus to the blade root. The root is electrically bonded to the hub which conducts the charge to the airframe and finally to the ground through metallic skid landing gears.

5.2.7 Electromagnetic Shielding

A nickel-filled conductive coating[29] is applied to the motor enclosures to eliminate radio frequency interference. The spray cures at room-temperature and is electrically stable even at high temperatures. It is resistant to corrosion, abrasion, jet fuel, hydraulic fluids, oils, and greases, making it highly desirable.

5.2.8 Slip Ring

The main rotor leading edge de-icing system and trailing-edge flap actuators require electrical power which is supplied by the aircraft's alternator. It is therefore necessary to transfer power from the fixed frame to the rotating frame. This is achieved through an electrical slip ring, comprising of a stationary housing with brushes, which contact a conducting ring in the rotating frame. Electrical connections to the blade are made from this conducting ring. The slip ring is sealed against sand and water intrusion to ensure operation even under harsh environmental conditions.

5.3 Active Flaps for Vibration Control

The main rotor operates in an asymmetric and unsteady flow environment thus exciting the blade at all rotor harmonics. However, the rotor also acts as a filter, transmitting only loads at multiples of the blade passage frequency to the hub and the fuselage. The active vibration control cancels vibratory hub loads by secondary hub loads generated by aerodynamic on-blade actuation, eliminating the vibrations at the source itself. Eurocopter recently demonstrated the successful use of trailing-edge flaps for reducing the vibratory loads and BVI noise on a full-scale BK-117.[30] More recently, Boeing demonstrated the successful application of smart flaps on a full-scale MD-900 to minimize vibratory hub loads and BVI noise in the 40 x 80 ft wind

Active vibration control system of the *Griffin* incorporates on-blade trailing-edge flaps commanded by a robust adaptive control scheme to suppress vibration. An innovative flap actuation mechanism using brushless DC motors as actuators was designed as is detailed in Sec. 5.5.

It is possible to use trailing-edge flaps for swashplateless control, however, this concept requires torsionally soft blades. This makes the blades more susceptible to pitch-flap instabilities and flutter at high speeds. Designed for high speed flight, the *Griffin* employs a traditional swashplate design for primary control and trailing-edge flaps for vibration suppression.

5.3.1 Selection of Trailing-Edge Flap Configuration

The important design parameters for the *Griffin*'s trailing edge flaps were:

(i) Flap length: A larger spanwise length for a flap reduces the deflections needed to produce the same rotating frame loads.

(ii) Flap chord ratio: A smaller chord length of the flap makes it more effective in producing section pitching moments because of the larger moment arm from the elastic axis, and the needed deflections are therefore reduced.

(iii) Flap spanwise location: The further outboard a flap is located, the more effective it is as a result of the higher dynamic pressure it operates in, thus reducing the deflections needed for comparable forces.

(iv) Flap overhang: The designed flap is hinged at its quarter-chord point, making it aerodynamically balanced. This ensures low hinge moments.

The University of Maryland Advanced Rotorcraft Code (UMARC[27]) was used to conduct trade studies to determine a suitable flap design. The indices used to compare the different flap configurations were the Vibration Intrusion Index (V.I.I.), the flap hinge moment, and the flap deflection requirements. Propulsive trim was performed at a moderate thrust level and the vibratory hub loads and flap actuation requirements were monitored for different flight speeds.

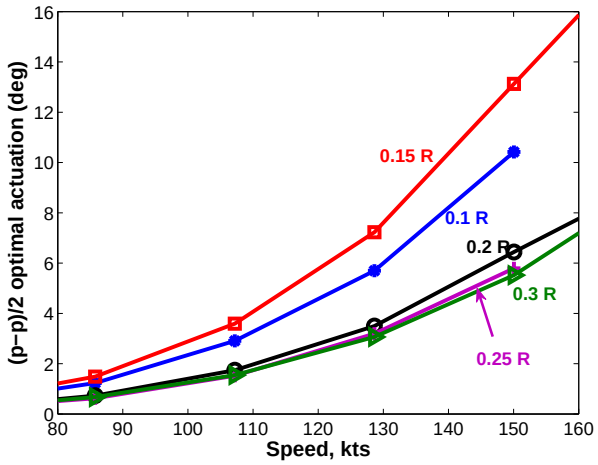

(a) Optimal trailing-edge flap deflections for different span

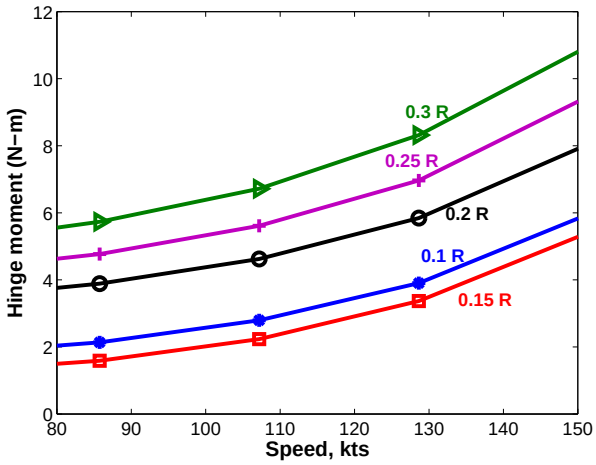

(b) Trailing-edge flap hinge moments for different span

Figure 5.6: Choice of trailing-edge flap span.

5.3.1.1 Choice of Flap Span Various flap lengths were examined for different flight speeds to determine the flap deflection angles required and hinge moments for the reduction of the vibration levels at cruise (150 knots). Figures 5.6a and 5.6b show that larger span flaps required smaller deflections but higher hinge actuations. A span length of 20% rotor radius (R) was chosen for the *Griffin* as a compromise between moderate flap deflections and hinge moments.

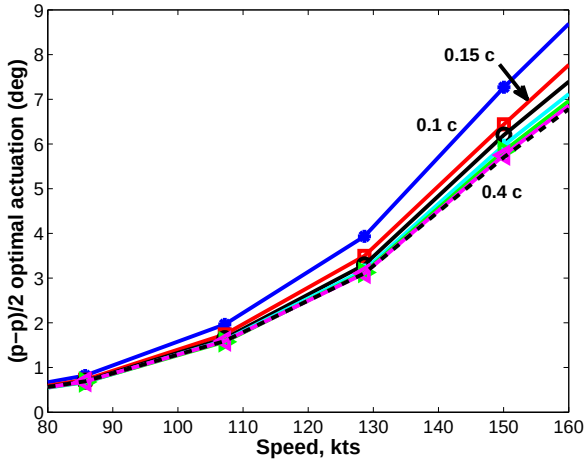

(a) Optimal trailing-edge flap deflections for different chord

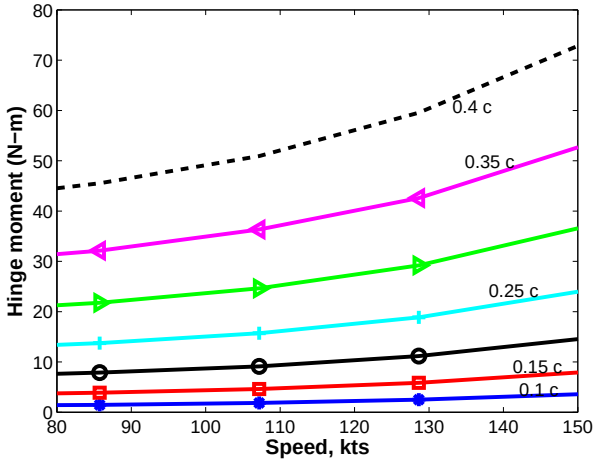

(b) Trailing-edge flap hinge moments for different chord

Figure 5.7: Choice of trailing-edge flap chord.

5.3.1.2 Choice of Flap Chord Ratio Figures 5.7a and 5.7b show that choice of flap chord largely affects the hinge moment. A smaller chord reduces significantly the hinge moment, without a huge penalty in the flap deflections required. Therefore, a flap chord of 10% blade chord (c) was chosen for the *Griffin*.

5.3.1.3 Choice of Flap Midspan Location Flaps with their midspan located at 60% to 85%*R* were examined and the most effective flaps were found to be at the 65% to 75% radial locations (Figs. 5.8a and 5.8b). The *Griffin*'s swept blade tip extends from around 80%*R*, therefore the flap midspan was located at 65%*R*.

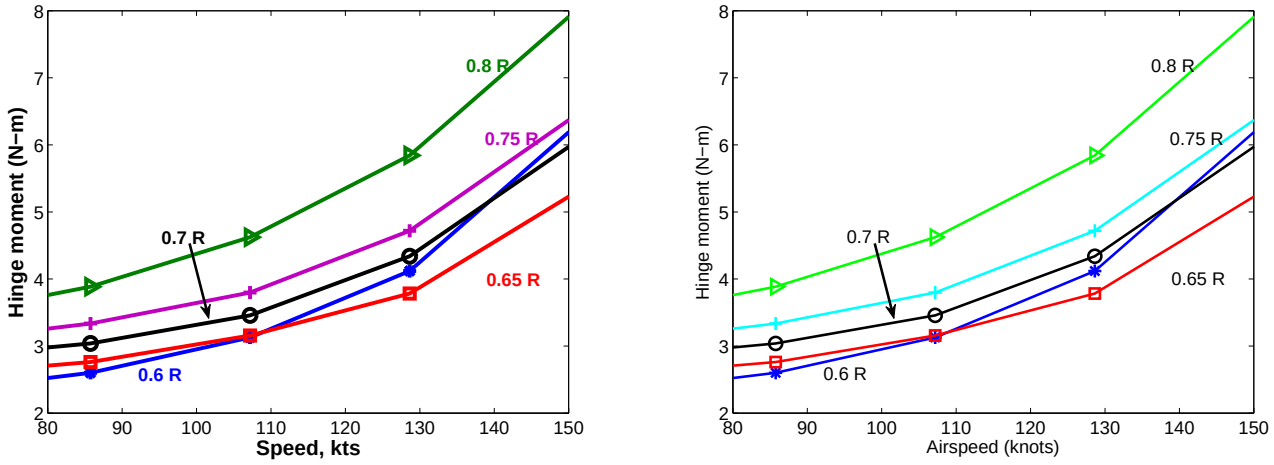

(a) Optimal trailing-edge flap deflections for different midspan locations

(b) Trailing-edge flap hinge moments for different midspan locations

Figure 5.8: Choice of trailing-edge flap midspan location.

The flap parameters selected are listed in Table 5.3.

Table 5.3: Trailing-edge flap sizing.

Flap chord	10% blade chord
Flap midspan location	65% blade radius
Flap length	20% blade radius
Overhang	25% flap chord

5.4 Vibration Reduction in the *Griffin*

5.4.1 Definition of Vibration Levels

The level of vibration in the airframe is usually specified in terms of one of several indices :

(i) *ips*: inches per second, is the value of the peak vibration velocity at a desired location.

(ii) *g-level*: This represents the vibratory accelerations measured at desired locations on the vehicle in terms of *g*.

(iii) *Vibration Intrusion Index (V.I.I.)*: It includes the effects of all frequencies below 60 Hz excluding the 1/rev contributions. The measured vibration spectrum (in 'ips') up to 60 Hz for each of three orthogonal directions at a specific location is normalized by standard levels prescribed in relevant normalization curves.[32] The four largest peaks excluding the 1/rev

peak, for each of the 3 spectra is calculated and the root-mean-squared value of these measurements is defined as the Intrusion Index.

To predict the exact levels of vibration at key fuselage locations such as the cabin floor and cockpit, knowledge of the complete fuselage mode shapes is necessary to determine the response of the airframe to vibratory loads. As an approximation in this preliminary analysis, the vibration levels due to the 4/rev hub loads at the gearbox are estimated and vibration intrusion index is used as the vibration metric.

5.4.2 Vibration Reduction Attained Using Trailing-Edge Flaps

The vibration intrusion index of the baseline EC145 and the *Griffin* employing the designed trailing-edge flaps, is shown in Fig. 5.9. The baseline vibration level peaks in two different speed regimes:

- Transition (20-40 knots): At these low speeds, the rotor is in close proximity to its own wake, and the rotor-wake interactions result in highly unsteady blade loads and consequently, high vibratory hub loads.
- High speed ($>$ 140 knots): At high speeds, retreating blade stall is the major cause of vibration.

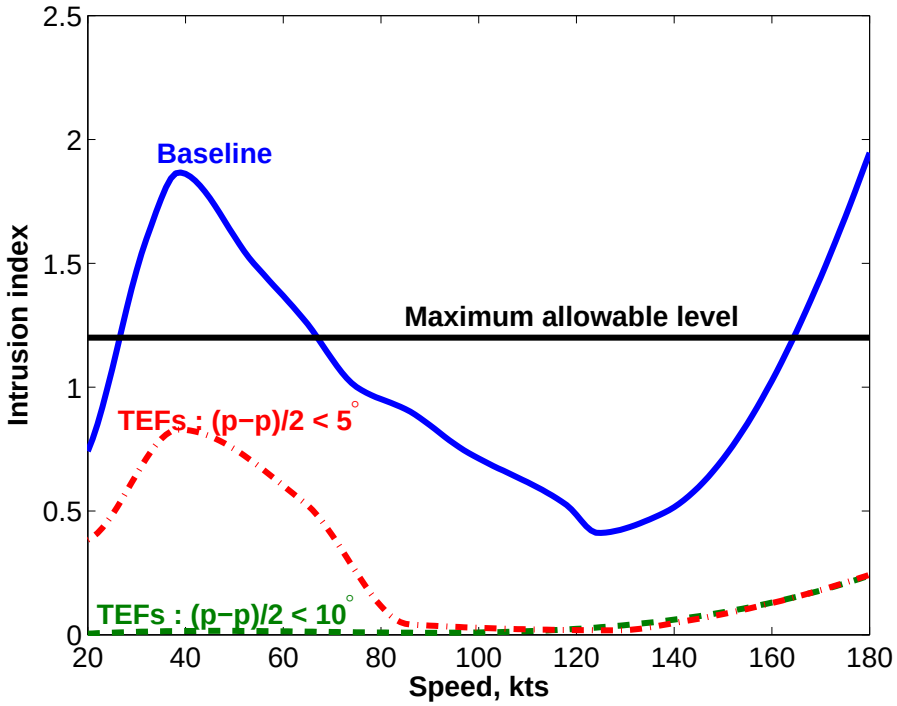

Figure 5.9: Intrusion index of the *Griffin* for different forward speeds, with and without trailing-edge flaps.

Historically, the problem of suppressing high-speed vibrations has been addressed more extensively than those during transition because the exact mechanism of blade-vortex interactions has not been fully understood. However, most helicopters experience comparable or higher vibrations in the transition regime than at high forward speeds. This is reflected in Fig. 5.9.

Figure 5.9 shows the exceptional capability of the *Griffin*'s trailing edge flaps in substantially reducing vibrations at all flight speeds. It has also, been demonstrated that by suitable phasing of trailing-edge flap inputs at multiple frequencies, the critical

rotor-induced vibratory loads can be completely eliminated. However, the target vibration levels were limited by the consideration of maintaining the flap deflections within reasonable limits. Using moderate flap deflections ($\pm 5^\circ$), the Intrusion Index at the gearbox is still maintained well below the maximum allowable value of 1.2.

It is seen that the use of active trailing-edge flaps enables the *Griffin* to achieve the goal of jet-smooth flight.

5.5 Flap Actuation Mechanism

The trailing-edge flap actuator must be lightweight, structurally robust, provide sufficient stroke and bandwidth and fit within the blade internal volume. Existing trailing-edge flap actuation systems for vibration reduction are based on smart actuators[30] like piezostacks and magnetostrictives.[33]

An attractive, unconventional approach adopted is to incorporate brushless DC motors as actuators for trailing-edge flaps. DC motors are lightweight, compact, easy to use, have high stroke, low cost and long operational life, making them highly desirable. Ongoing research at the Alfred Gessow Rotorcraft Center on Mach-scaled rotors has demonstrated the feasibility of using electric motors for trailing-edge flap actuation. The motor is electronically commanded to actuate the flaps using a motor controller. The amplitude of flapping is controlled by the DC voltage supplied to the motor. The direction of flapping is controlled by a digital logic signal sent by the Active Vibration Control System to the motor controller. The frequency of flapping is set by the frequency of the logic signal. The instantaneous angular position of the flap is sensed using Hall sensors and is fed back to the control system, which then suitably constructs the logic signal (Fig. 5.11b).

The motor to be used on the *Griffin* was restricted to a diameter of about 28 mm, in order to fit within the SC1095R8 airfoil profile. Based on the calculated power requirements for trailing-edge flap actuation and the available blade internal volume, Maxon Motors EC-powermax 22[34] was chosen. It is rated at 120 W, 20V, weighs 160 g and has a diameter of 22 mm. The motor is supplied with a pre-installed planetary gearhead for output torque amplification, and the DECV 50/5 motor controller. Melexis[34] tri-axis rotary Hall sensors were used to sense the flap angular state.

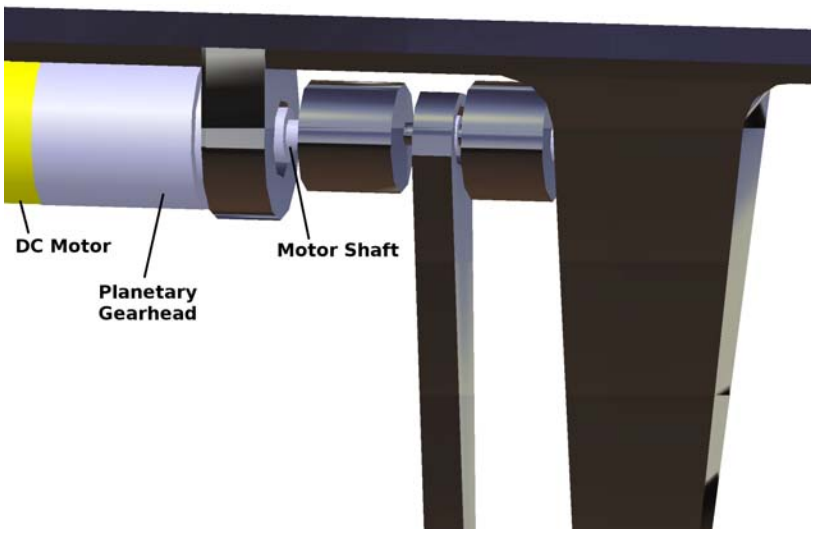

Figure 5.10: Eccentric arrangement at motor shaft.

A simple yet innovative method of transferring the motor shaft motion to the trailing-edge flap is incorporated in the *Griffin*. It consists of a lever arrangement with eccentric rotations with respect to the motor shaft (Fig. 5.10), and the flap hinge (Fig. 5.11a). Thrust bearings attached to the gearhead ensure the centrifugal forces do not cause the planetary gears to lock up.

The motor assembly is mounted on brackets bonded to the blade spar. The flap is constructed in two sections and the actuation is effected at the center. The entire mass of the trailing-edge flap module, including the trailing-edge flaps themselves, is estimated at about 3 kg per blade. The section mass balance therefore requires an additional 2.6 kg distributed uniformly with the nose mass from 55% – 75%R.

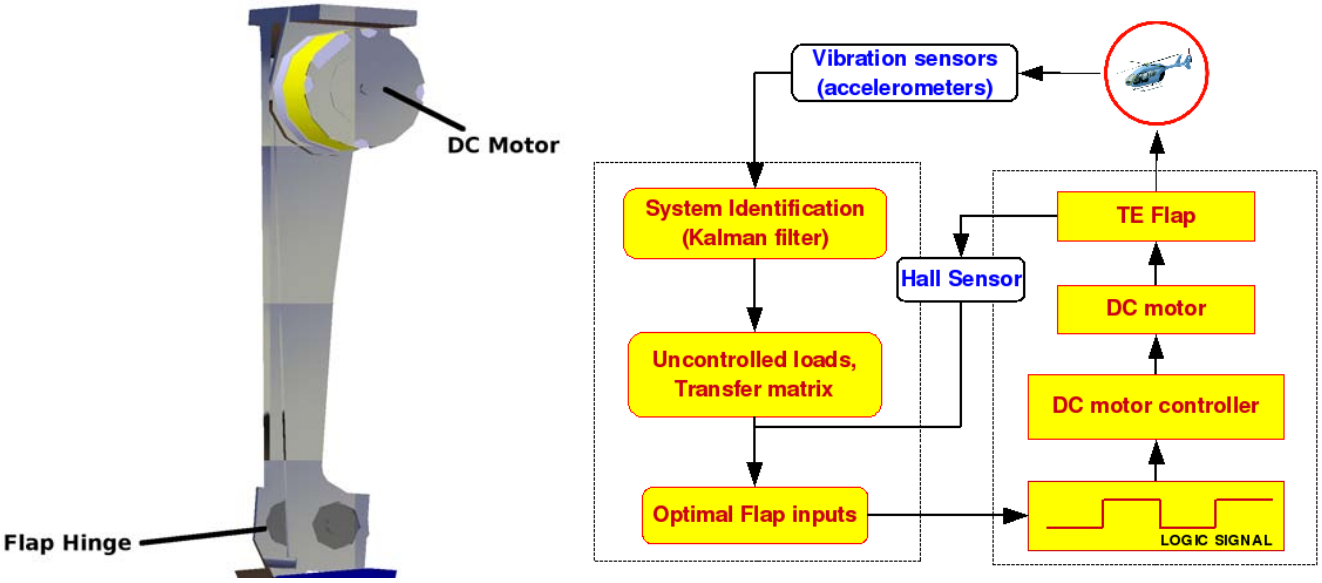

(a) Eccentric arrangement at trailing-edge flap hinge

(b) Schematic of the *Griffin*'s Active Vibration Control System

Figure 5.11: Active Vibration Control

5.6 Active Vibration Control Scheme

The helicopter vibration is modeled as a linear, quasi-static system in the hub loads and the flap inputs, related by a transfer matrix. The transfer matrix varies with the operating flight condition, so system identification is performed in real time. System identification is carried out using a robust Kalman filter method, which recursively estimates the uncontrolled vibratory loads at any operating condition from the applied flap inputs and the measured fixed frame vibratory loads. The transfer matrix from the flap deflections to the hub loads is then determined, and the optimal flap control deflections ($N_b, N_b \pm 1$/rev sine and cosine amplitudes for N_b-bladed rotor to minimize N_b/rev vibratory loads) are obtained by minimizing an objective function in the vibratory hub loads and the flap deflection amplitudes. This objective function was defined as

$$J = \bar{Z}^T W_z \bar{Z} + \bar{\theta}^T W_\theta \bar{\theta}$$

where the vectors $\bar{Z}$ and $\bar{\theta}$ contain the target N_b/rev hub loads and the flap input harmonics respectively, and W_z, W_θ are diagonal matrices with weights for the individual loads and control harmonics respectively. The optimal flap deflection schedule is sent to the motor controller in the form of a logic signal. A schematic of the vibration control scheme is shown in Fig. 5.11b.

5.7 Performance Improvement with Trailing-Edge Flaps

The work in[35] demonstrated the benefits of using 2/rev trailing-edge flap inputs to improve the rotor lift-to-drag ratio at high speeds. The negative angles of attack on the advancing side were reduced using the flaps with suitably phased inputs, thus reducing local profile drag. To this end, the performance assessment of 2/rev trailing-edge flap inputs

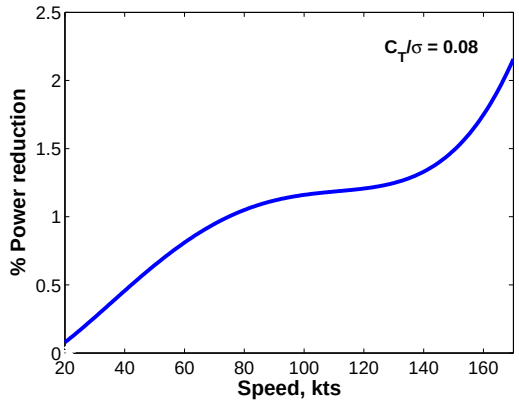

Figure 5.12: % L/D increase with 2/rev TEF inputs.

on the *Griffin*'s rotor was performed using UMARC, trimming the rotor to the cruise blade loading. The improvement is quantified in terms of the reduction in power from the baseline value (i.e., without flaps) at the same thrust state. This could also be interpreted as an increase in vehicle L/D in forward flight. Figure 5.12 shows the typical improvements in L/D using 2/rev flap deflections of at most $\pm 3^{\circ}$.

5.8 Safety Aspects

The brushless DC motor used for trailing-edge flap actuation is reliable and long-lasting. The simplicity of the actuation mechanism and provision for thrust bearings ensure safe operation. However, in the event of a failure of the flap system, the performance of the vehicle is not severely compromised because the flaps only provide vibration control, which is not a flight safety issue.

5.9 Hub Design

The main rotor hub assembly is a critical sub-system of VERITAS, the novel rotor/drive system of the *Griffin*. The rotor hub provides the connection between the mast and the rotor, transfers the blade loads from the rotating frame to the fixed frame, transfers the torque to the rotor, and transmits blade control inputs from fixed to rotating frame. These functions must be performed while maintaining a low weight, low drag, mechanical simplicity, low part count, low cost, and long fatigue life. A carefully designed hub is crucial to the success of the *Griffin*.

The "Bölkow" hub on the EC145 is a bearingless hingeless design with a high hinge offset making it extremely maneuverable. However, such a high hinge offset causes vibrations and strong cross-coupling of lateral and longitudinal dynamics, deteriorating passenger comfort and handling qualities. The *Griffin* was therefore designed with an elastomeric, semi-articulated rotor hub to minimize mechanical complexity and time-intensive maintenance procedures.

The primary elements of the *Griffin* hub are: the rotor mast and swashplate assembly, the clover plate, the elastomeric frequency adapters, and the conical bearings.

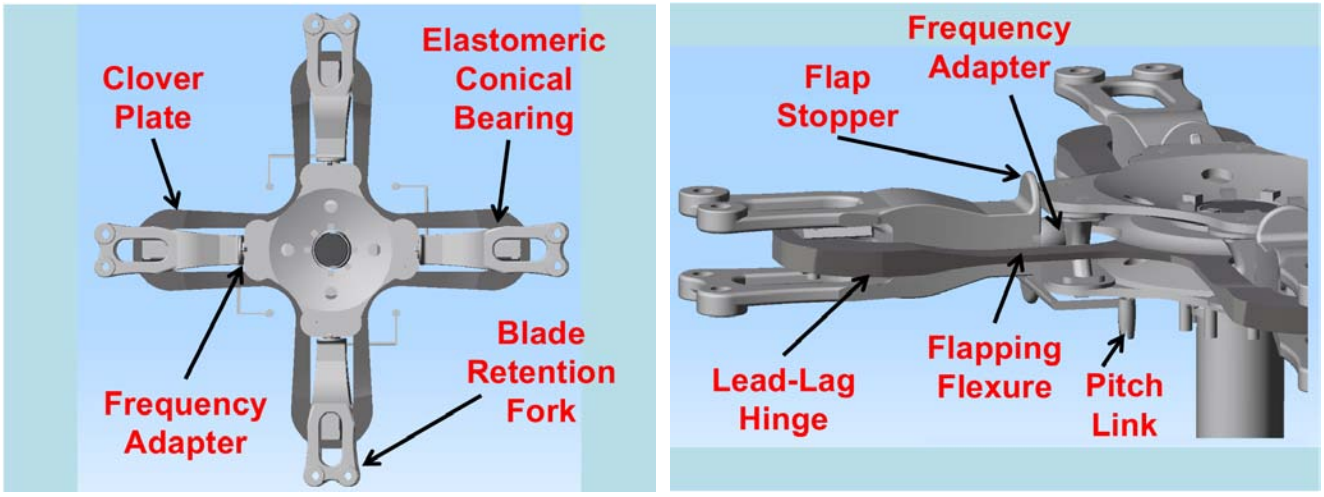

(a) Semi-articulated hub with elastomeric bearings.

(b) Semi-articulated hub – blade hinges.

Figure 5.13: *Griffin* rotor hub.

5.9.1 Rotor Mast and Swashplate Assembly

The main rotor mast is a hollow titanium shaft that transmits rotary motion from the transmission to the main rotor and reacts the mast moments. The mast has three sets of splines and a flange. The lower splines fit into the transmission gearbox to provide

the mast drive source. The center splines are master-splined and drive the rotating portion of the swashplate. The upper splines and flange drive the main rotor. The mast is supported in the transmission by single ball bearings, bearing liner, and retainer. It is aligned by a roller bearing mounted in the lower mast bearing case.

A graphite/epoxy composite swashplate assembly transmits the collective and cyclic pitch controls from the fixed frame to the main rotor blades. The non-rotating portion of the controls are mounted on the top of the transmission and receive control inputs from the electro-hydrostatic actuators. The electro-hydrostatic actuator uses an electric motor to drive a hydraulic pump and relies on local hydraulics for force transmission. Collective pitch changes are effected by raising or lowering the swashplate ball sleeve; the cyclic pitch changes are made by tilting the swashplate. The rotating controls are spline adapted to and driven by the rotor mast and follow the vertical and tilting motion of the swashplate. This motion is transfered to the main rotor blades through the corrosion resistant steel pitch rods.

5.9.2 Clover Plate

The clover plate provides the flap bending stiffness, bears centrifugal loads, and transmits shaft torque. The flap-bending stiffness plate is tailored to accommodate a virtual hinge offset of 5%. The conical bearing is secured to the clover plate by two bolts, which carry the centrifugal load (See the Griffin Main Rotor Foldout); the clover plate is therefore made thicker at this connection point to distribute the bearing stress over a greater surface area. The flap plate is sandwiched between the top and bottom hub plates, which all mate together with the rotor shaft through a series of floating bolts, allowing torque to be transmitted to the rotor (see Fig. 5.13a).

The clover plate is constructed of S-glass composite material and has a symmetric layup of alternating [0°, ±45°, 90°] plies to provide superior strength for axial and in-plane loads. A droop stop is integrated into the hub to alleviate static stresses on the blades while not in operation.

5.9.3 Elastomeric Frequency Adapter – Lead-Lag Damper

The elastomeric lead-lag damper unit provides an in-plane complex stiffness that has two functions. First, it provides stiffness to tune the rotor in-plane frequency acting as a frequency adapter. Second, it attenuates in-plane vibrations through in-plane shearing of the silicone elastomeric damper. This damping is critical for the stability of the rotor in-plane modes. The radial bearing in the lead-lag damper allows unrestricted feathering motion while orienting the blade and connecting the blade to the lead-lag damper.

5.9.4 Elastomeric Conical Bearing

The conical bearing directly connects to the outermost portion of the clover plate and features an elastomer and stainless steel shim construction. It includes an outer race supported on the hub and an inner race spaced axially from the outer race supported by a shackle attached to the blade root. The laminates-shims assembly is bonded to the races at radially opposite ends. The bearing shims are oriented in a conical fashion to provide both torsional stiffness and support high centrifugal loads. The alignment of the lead-lag damper and the conical bearing defines the pitch axis. The conical bearing also acts as the blade lead-lag hinge (Fig. 5.13b).

Both lead-lag and conical elastomeric bearings have long service life, high reliability, and are fully effective through a temperature range of -65 $^{\circ}F$ to +200 $^{\circ}F$. They are silicon coated for protection against salt water corrosion, and provide maintenance-free operation and fail-safe system degradation.

5.9.5 Blade folding

The simple design of the hub assembly facilitates folding of the blades. In the folded position, the two unfolded blades are aligned with the helicopter centerline, and the folded blades are swiveled 90° around the blade bolts (Fig. 5.14). For pivoting the blades to the folded position, one of the two retention bolts attaching the rotor blade to the hub is a quick-release bolt.

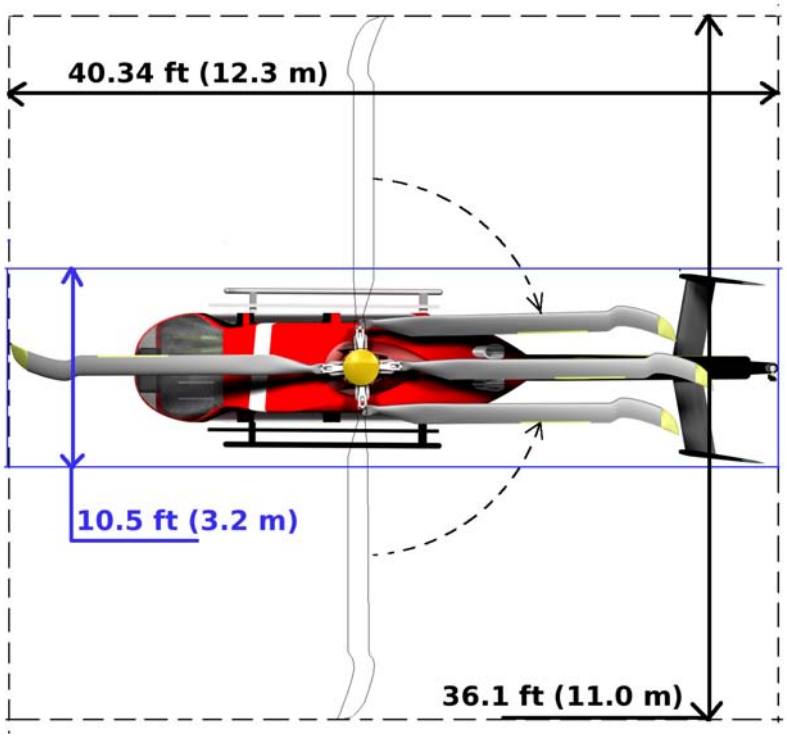

Figure 5.14: Reduction in footprint with blade folding.

These bolts are removed during the folding process and stowed on the blade retention device. The folding mechanism provides the *Griffin* with a compact footprint, allowing it to be effectively stowed on the ship. The folded blades are supported on the tailboom.

5.10 Rotor Dynamics

The spanwise distributions of the blade mass and section stiffnesses are shown in Fig. 5.5. The root cutout of the blade is 20%*R*. The additional mass from 55%*R* to 75%*R* results from the flap actuation assembly and the extra leading-edge mass in the flap section for chordwise balance. It was found during preliminary calculations that the third flap mode intersected the 5/rev line in the operating range of 85% – 100% hovering rotor speed. Two anti-nodal masses of 1.4 kg each were distributed over 10% radial sections near the anti-nodes (30%*R* and 75%*R*) of the third flap mode. Figure 5.15 shows the fan plot of the *Griffin*'s rotor. All the blade frequencies are well separated from the rotor harmonics throughout the operating speed range. The first six natural frequencies at the maximum and minimum (85%) rotor speed are given in Table 5.4.

Table 5.4: *Griffin* main rotor blade natural frequencies (/rev).

RPM	**Flap**			**Lag**		**Torsion**
	1	2	3	1	2	1
100%	1.03	2.70	4.65	0.74	4.60	4.11
85%	1.03	2.75	4.85	0.83	5.19	4.81

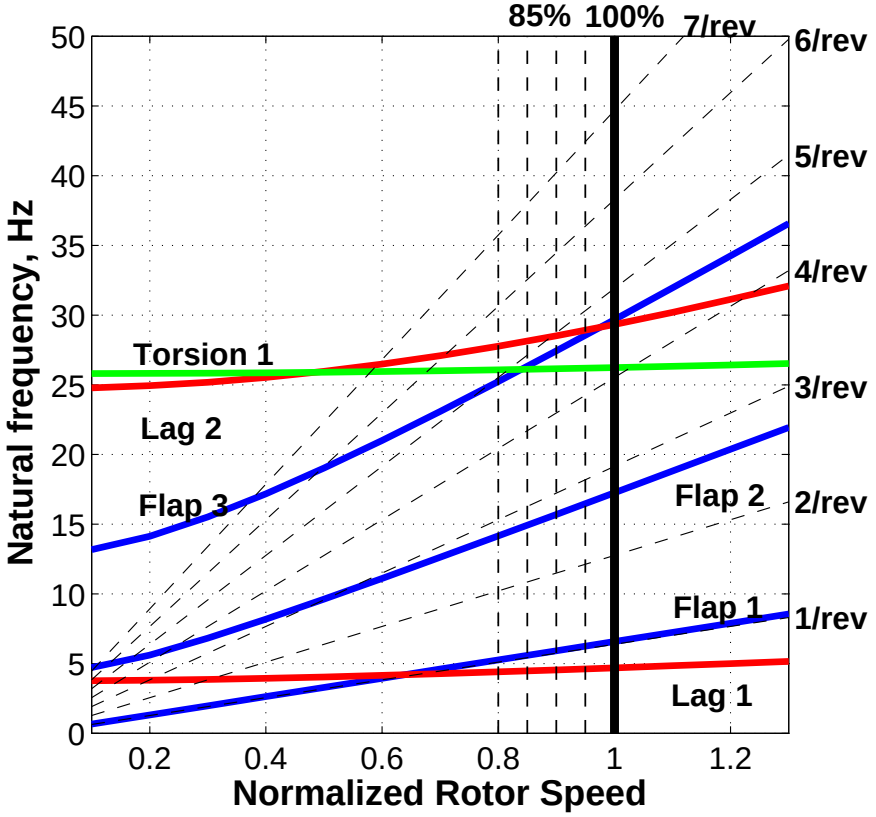

Figure 5.15: Fan plot of the *Griffin* rotor.

5.10.1 Aeroelastic Stability Analysis

The interactions between the aerodynamic, inertial and elastic forces acting on the rotor cause aeroelastic responses. An analysis was developed to study aeroelastic stability of the blade and the results are discussed below.

5.10.1.1 Pitch-Flap Stability The critical design parameters that affect the rotor flap-torsion couplings are the chordwise offset of the blade section center of gravity and aerodynamic center (quarter-chord) and the blade torsional frequency. Stability boundaries for both static (pitch divergence) and dynamic (pitch-flap flutter) instabilities were obtained by modeling the coupled flap-torsion dynamics of the rotor. Figure 5.16a shows that with the *Griffin*'s design torsional frequency of 4.1/rev and a $-0.01c$ c.g. offset aft of the quarter chord, there is no possibility of either divergence or flutter.

5.10.1.2 Flap-Lag Stability The soft in-plane first lag mode of the *Griffin*'s rotor blades (ν_ζ =0.74/rev) needs to be damped to avoid flap-lag flutter and resonance with the body modes. The coupled flap-lag dynamics of the rotor and body roll and pitch in forward flight was analyzed by using the perturbation equations about the trim state at the operating speed, determined by a complete six degree-of-freedom trim calculation for the vehicle. The damping of the flap and lag perturbation modes as a function of forward speed was determined, and is shown in Fig. 5.16b. As expected, the flap mode is highly damped due to aerodynamic forces. The lag mode is positively damped by the elastomeric frequency adapter, thus avoiding any possibility of instability.

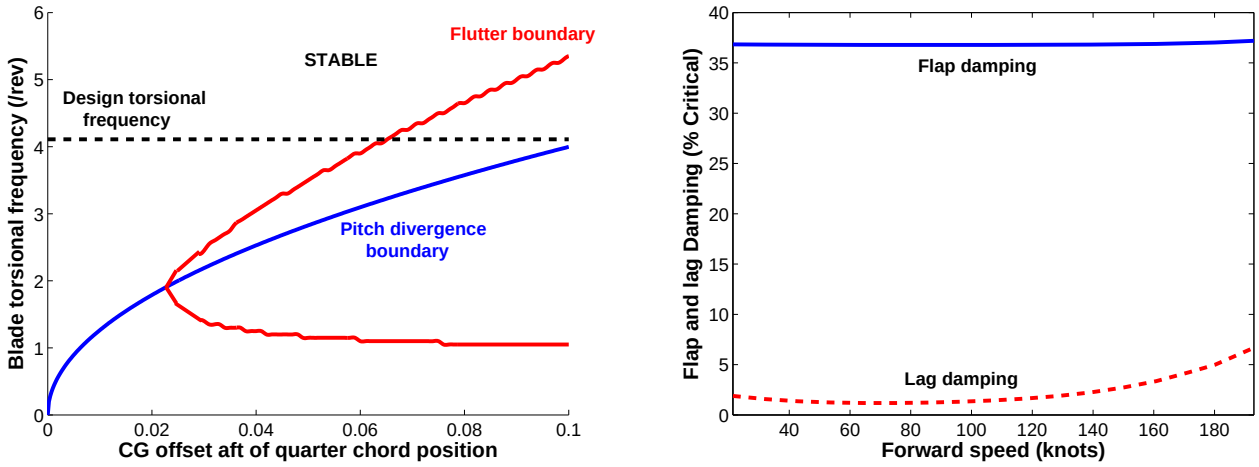

(a) Pitch-flap stability at hover

(b) Damping of flap and lag modes in forward flight

Figure 5.16: Aeroelastic stability analysis for the *Griffin*

5.10.2 Ground Resonance

Ground resonance is a dynamic instability caused by the coupling of the blade lag motion, and the inplane motion of the hub. It is pronounced in rotors with low lag frequencies. The stiffness and damping characteristics of the body and support modes are important factors; inclusion of rotor lag dampers and careful design of landing gears is critical to avoiding ground resonance. In particular, the ship-based *Griffin* must be free of ground resonance across the operating rotor speed regime.

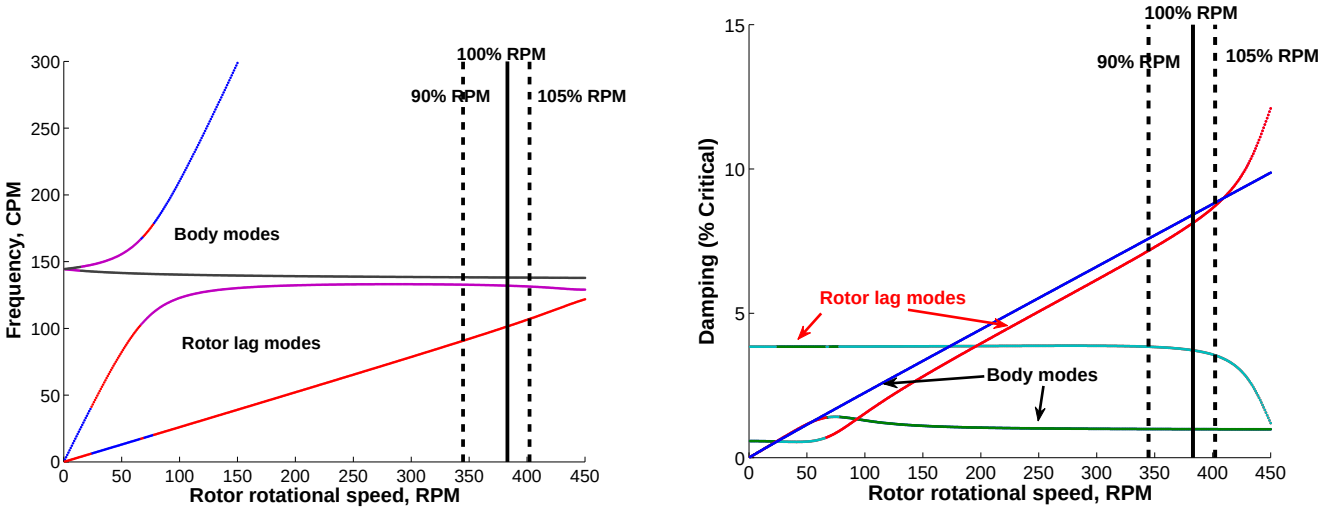

(a) Coleman diagram

(b) Damping of body and inplane modes

Figure 5.17: Ground resonance analysis for the *Griffin*.

Coupled rotor lag-body roll and pitch dynamics were simulated with representative values of frequencies and damping of the body roll and pitch modes. The elastomeric lag damper helps tune the low lag frequency to 0.74/rev and provides a lag damping of 2%. Figures 5.17a and 5.17b show that the *Griffin* lag frequencies and body pitch and roll frequencies are well-separated and

all modes are well damped, thus avoiding ground resonance.

6 Empennage and Tail Prop Design

The *Griffin* features a novel swiveling tail prop which provides the required anti-torque at low flight speeds and acts as a pusher propeller at high speeds. The use of this innovative feature requires careful design of the empennage. The empennage surfaces were initially sized using the sizing analysis and later checked to provide sufficient stability and control. Minimum structural changes, if required, were made. The composite tail prop was designed and construction details are discussed.

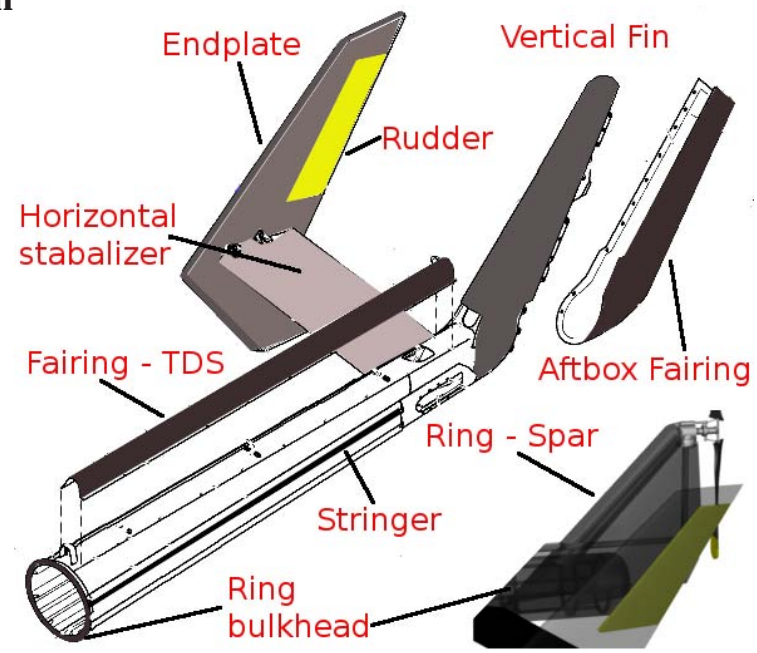

Figure 6.1: Empennage – *Griffin*.

6.1 Empennage Construction

The empennage of the *Griffin* consists of a tailboom, a vertical fin, and a horizontal stabalizer with end plates (Fig. 6.1). Each endplate has a rudder to provide directional control at high forward flight speeds, when the tail prop is used as a pusher propeller. The tailboom was sufficiently reinforced to withstand the loads arising in the tail prop mode. The horizontal stabalizers were sized to provide stability of the phugoid mode and vertical fins were checked to ensure sufficient weathercock and dutch-roll stability (Sec. 10.1).

6.1.1 Tailboom

The tailboom is a semi-monocoque structure, consisting of ring bulkheads and stringers that run along the boom length. This structure is covered with a carbon fiber reinforced composite skin. The boom is designed to take bending and fatigue loads. It houses the tail prop drive shaft and actuators to move the rudders and is attached to the main body by bolts.

6.1.2 H–tail

The horizontal stabilizer is designed to resist bending loads. It has a unidirectional carbon fiber/epoxy spar that attaches to the tailboom at the ring bulkhead and is covered with composite skin. They are bolted to the tailboom bulkhead and can be easily attached/detached for maintenance and repair. The vertical end plates are of a similar construction and are secured to the horizontal tail. Each end plate has a 30% chord rudder hinged along its quarter-chord. The rudder is actuated using push-pull rods and bell-crank arrangement. The actuator is placed in the tailboom, securely bolted to one of the bulkheads.

6.1.3 Central Fin

The central fin is designed for bending and torsional loads arising due to the tail prop. The central fin has a single piece spar cum bulkhead acting as the spar for the fin as well as the rearmost ring of the tailboom. It provides a simple load path and ease of manufacturing. The fin is covered with a $\pm 45^{\circ}$ composite skin, and together with the spar, provides torsional stiffness and thereby help avoiding any aeroelastic instability.

Tail Propeller and Empennage Assembly

Anti-Torque Configuration

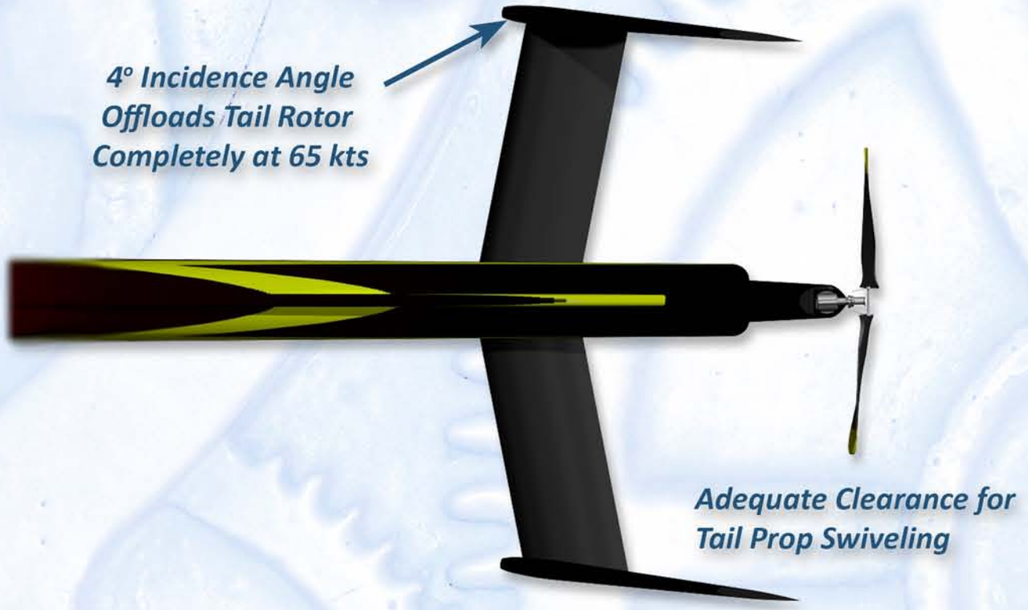

Thrust Compounding Configuration

Swiveling Tail Gearbox

Variable Pitch Propeller Designed for
Maximum Efficiency at 100 kts
for Best Range

Diameter: 5.74 ft (1.75 m)
Chord: 0.41 ft (0.125 m)
RPM: 2500
Airfoil: Clark Y
Hyberbolic Twist

Unispar Composite Tail Prop

Tail Propeller

Tail Boom Construction

6.2 Tail Prop Design

The tail prop on the *Griffin* performs dual roles. It provides adequate anti-torque and directional control in low airspeed regimes and serves as an effective pusher propeller in high-speed flight. A traditional tail rotor uses blades with little to no twist to minimize drag penalties from the edgewise flow in which it operates. Propellers, however, operate in a predominantly axial flow field and are highly twisted to maximize their propulsive efficiency. The design of the *Griffin*'s tail prop was, therefore, a compromise between maximizing propeller efficiency and minimizing the penalties inherent in the tail rotor. Since the tail prop only has to operate as a tail rotor at low flight speeds, a variable pitch design with a moderate built-in twist was chosen. The distribution of *Griffin*'s tail prop twist is detailed in Fig. 6.2. The tail prop was designed for maximum efficiency at 100 knots, the *Griffin*'s speed for best range, and is a good compromise between hover and never exceed airspeed. Throughout the flight envelope, the flight control system automatically adjusts the tail prop pitch to generate sufficient thrust to identically overcome the helicopter's parasitic drag. Since the parasitic power requirement grows with the cube of the flight speed, it is a major fraction of the total power at high airspeeds.

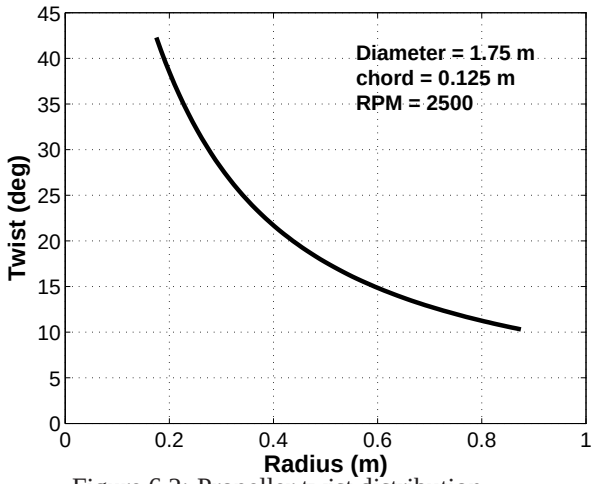

Figure 6.2: Propeller twist distribution.

6.3 Tail Prop Construction

Figure 6.3: 3D CATIA drawing of the *Griffin's* tail prop.

The single piece two-bladed tail prop consists of two "mirror image" carbon fiber spars and a central polyurethane foam core which are enclosed by a glass/epoxy shell forming the airfoil profile. Detailed CATIA drawings (Fig. 6.3) defining the shape, size, and construction details of the tail prop are used to produces detailed CNC cutting patterns. This allows carbon fiber prepreg to be automatically cut on a computer controlled cutting table to form the complex layered shapes required for each spar. The spar was made in two stages. The carbon fiber layers were laid up using the shaped mold, and heat cured, which bonded together the layers in each spar. Once heat treatment was complete, the two spars were brought together within a single heated mold. A polyurethane foam core was then injected under heat and pressure.

The injection process involves the use of a precision formed heated mold containing the blade assembly held vertically. Resin was forced into the mold under pressure, progressing through a three stages of mold preheat, resin injection, and resin cure. Temperatures need to be controlled to within $\pm 2^{\circ}$C throughout the cycle.

The blade was then removed from its mold, and post cured at high temperature. The internal structure of the blade is now complete. After curing and de-flashing, the prop was subjected to nondestructive testing. It examines each blade comprehensively using dimensional, ultrasonic, X-ray and other techniques, rejecting any that show internal faults such as air bubbles, micro cracks, etc.

6.4 Accessibility

Special care was taken to provide easy access to the drive components in the tailboom and are listed below:

- The tail drive shaft is mounted above the tailboom and the tail drive shaft fairing can be easily removed. The vertical shaft between IGB and TGB can also be similarly accessed by removing aftbox fairing. This allows easy access to the drive shaft for inspection, maintenance, and repair.
- The tail prop gear box and the swiveling mechanism is mounted at the top of the central fin and can be easily inspected and/or serviced without any requirement of disassembling the empennage.
- Active use of HUMS to monitor the tail drive shaft, central fin, and prop gearbox allows regular health monitoring and faster pre-flight checks.

Extensive use of composites ensures light structure, long life, corrosion resistance, ease of maufacturing, and fail safe degradation. Active HUMS usage reduces the time between operations, and increases safety.

7 Performance Analysis

A comprehensive method for evaluating helicopter performance was developed and subsequently utilized to ascertain the capabilities of the *Griffin*. Performance data of the baseline EC145, provided by Eurocopter, was used to validate the analysis. The analysis incorporates the ability of the Variable Energy Rotor and Innovative Transmission ArchitectureS (VERITAS) of *Griffin* to modulate the main rotor rotational speed throughout the flight envelope. The use of the tail prop as a pusher propeller for thrust compounding was also included. Judicious scheduling of both the main rotor speed variation and tail prop swiveling is crucial to maximizing the performance benefits attained from these advanced technologies, and as such, an optimal schedule was determined. The calculations showed that for the same amount of fuel carried, the *Griffin* is capable of sprinting 30 knots faster than the EC145, has 64% more range and 76% more endurance. These extraordinary improvements empower the *Griffin*'s quantum leap in rotorcraft capability.

7.1 Drag Estimation

Table 7.1: Component drag breakdown.

Component	**f (ft^2)**	**f (m^2)**	**f/A**	**% of total**
Fuselage	0.283	3.045	0.0030	40.0
Rotor hub and shaft	0.220	2.367	0.0023	31.1
Horizontal stabilizer	0.027	0.290	0.0003	3.8
Vertical stabilizer	0.055	0.592	0.0006	7.8
Rotor-fuselage interference	0.067	0.721	0.0007	9.5
Exhaust	0.003	0.032	0.0000	0.4
Landing gear	0.040	0.430	0.0004	5.6
Miscellaneous	0.013	0.140	0.0001	1.8
Total	**0.708**	**7.617**	**0.0075**	**100.0**
Additional 20%	0.850	9.140	0.0089	–

In Table 7.1, f is the *Griffin's* flat plate area presented in both english and SI units, and A is its main rotor area.

The equivalent flat plate drag area was estimated for the calculation of the helicopter parasitic power. An estimate of the helicopter drag area was calculated using detailed CAD drawings. Frontal areas of the various components were calculated from the drawings and combined with appropriate drag coefficients to determine the flat plate area of the entire helicopter. A factor of 20% was then added to the total to account for component interference effects.[2]

Table 7.1 shows the component breakdown of the equivalent parasitic area. The fuselage, rotor hub, pylon, and shaft are the largest drag-producing components in the helicopter, followed by the landing gear and rotor-fuselage interference effects. The predicted drag area of the *Griffin* was found to be 9.14 ft^2 (0.85 m^2). This value was used for all the performance calculations. The drag estimation procedure was validated by the subsequent calculation of EC145's flat plate drag area of 9.47 ft^2 (0.88m^2), as detailed in Sec. 7.4. During the design process of the *Griffin*, special emphasis was placed on making minimum structural changes to the fuselage in accordance with the RFP requirements. Nevertheless, several other innovative concepts were incorporated into the design to minimize the drag.

7.2 Drag Reduction

Figure 7.1: Drag reduction in the *Griffin*.

7.2.1 Fuselage Drag – Synthetic Jet Actuators

Innovative active flow control devices like zero-mass synthetic jet actuators (SJA) were considered[39] for reduction of fuselage drag. They are ultra lightweight pneumatic jets and generate oscillatory momentum injection through slots over the upswept ramp region of the fuselage. Wind tunnel studies have proved their effectiveness in reducing pressure drag from turbulent boundary layer separation and lowering the fuselage drag coefficient by 30%.[39] In addition, no modification of the existing fuselage would be required to accommodate them. This huge reduction in drag translates in to increased range as well as endurance of the helicopter.

However, SJA are not off-the-shelf components and are extremely expensive. It's a maturing technology and if desired, these can be included as an upgrade to the *Griffin*. All the performance estimates, made in the following sections, would then be conservative for this upgraded version of the *Griffin*.

7.2.2 Rotor Hub, Pylon and Engine Installation

- By streamlining the exposed hub components, adding a fairing, reducing the height of the hub above the pylon, and keeping the portion of the main rotor shaft which is exposed to free-stream as thin as possible, the rotor hub was made low profile.
- The top of the pylon is flat to minimize the Venturi effect between hub and pylon and hence leads to reduction of dynamic pressure of the flow in this region that hence reduces drag.
- Additionally, the pylon lip (Fig. 7.2) guides the direction of the flow as it passes over it and makes it move away from the main rotor, and reduces upwash into main rotor.
- The intake and exhaust were designed low in profile, which reduces drag significantly.

7.2.3 Main Rotor Drag

- The VERITAS lowers the main rotor speed which reduces the profile drag.
- The rotor blade airfoils have a high lift-to-drag ratio and drag divergence Mach number.
- The innovative Talon tip avoids drag divergence penalties and increases rotor figure of merit. The notch in the design aids in reducing the drag by postponing the retreating blade stall.
- Trailing edge flaps used for vibration control can be used to get a 3% increase in rotor *L/D*.
- Distributed bending-torsion composite couplings can enhance lift on advancing side at high speed and thereby increse L/D.

7.2.4 Tail Prop Drag

- Thrust compounding from the tail prop offloads the main rotor, increasing its effective *L/D*.
- A variable pitch propeller is used to overcome the parasitic drag of the fuselage, and is significantly more efficient than main rotor in providing the horizontal force.

7.2.5 Landing Gear and other Drag Reduction Efforts

- Skid landing gear used on the *Griffin* was aerodynamically faired to reduce the drag.

7.3 Performance Analysis Methodology

At each flight speed, the *Griffin* was first trimmed using a coupled rotor-fuselage trim procedure to achieve force and moment equilibrium in the *x*, *y* and *z* directions and a blade element analysis was carried out to calculate the rotor induced and profile power requirements. Airfoil table lookup, Drees' inflow model, and a 10° linear nose down blade twist were used. Parasitic power was calculated based on the helicopter drag area of 9.14 ft^2 (0.85 m^2) as estimated in Sec. 7.1. The effects of changes in rotor speed and thrust compounding were included in both the trim and blade element analysis. An optimum schedule was then calculated (Secs. 7.5 and 7.6.2). The trim procedure computed controls, blade flap reponse, and shaft angles, which were then used in the blade element calculations and to establish the shaft inclinations to level the fuselage in cruise flight. To ascertain the performance of the tail prop, an iterative blade element analysis was performed. The procedure calculated the propeller pitch angles, thrust produced, and the power required.

7.4 Validation of Performance Analysis

The analysis was validated using performance data for EC145[37] that relates percentage reference torque required to forward flight speeds. The EC145 Technical Data presents curves at various combinations of gross takeoff weights, temperature and pressure altitude. The data corresponding to maximum gross takeoff weight at sea-level ISA conditions were reconstructed and displayed as a power curve in Fig. 7.2. 100% reference torque was used as the take off power rating of the transmission. Figure 7.2 shows the EC145 power curve predicted by our performance analysis. It shows very good correlation with the available data from the manufacturer. All the following comparisons are made using the calculated values. Only the maximum endurance is overpredicted by the analysis, but other values are fairly close to the reported EC145 values.

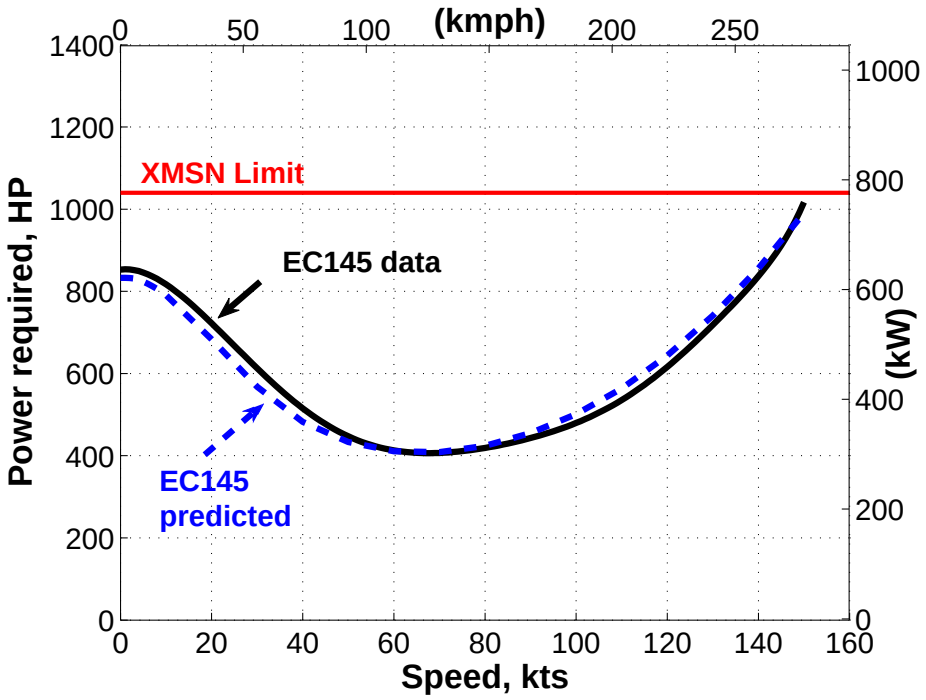

Figure 7.2: Validation of the performance analysis.

7.5 Rotor Speed Schedule

At any given flight speed, the minimum safe operational rotor speed is determined from three major considerations: capability to perform safe autorotation, rotor stall margin, and rotor blade dynamics. The safe autorotational envelope at forward flight speed is usually detailed in a height–velocity (H–V) diagram. Those combinations of height and velocity where safe autorotation cannot be performed are shown as avoid regions. The maximum speed associated with EC145's avoid region is 50 knots (Sec. 7.10). Since the MTOW, main rotor dimensions and hover tip speed for the *Griffin* are the same as the EC145, this flight speed should correspond to that for the *Griffin*. As such, the rotor speed is not reduced until this flight speed of 50 knots. As detailed in Sec. 7.10, this design endows *Griffin* with the similar autorotational capabilities as the EC145.

Above 50 knots, the minimum possible rotor speed was determined from main rotor stall and dynamics considerations. For a given gross weight and flight conditions, lowering the rotor speed increases the blade loading, pushing the rotor closer to stall. In addition, at the operational rotor speed, the blade flap and lag frequencies should be sufficiently separated from rotor order frequencies to avoid resonance (Sec. 5.10). Ultimately, these considerations limit the minimum operational rotor speed.

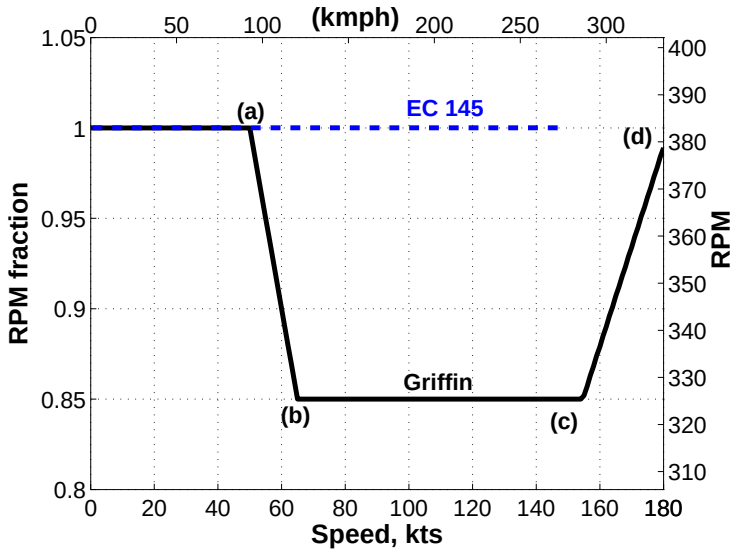

Figure 7.3: Rotor speed schedule for the *Griffin*.

For the *Griffin* rotor blades, the lower rotor speed limit was found to be 85% of the hovering rotor speed. The rotor speed schedule was so engineered that at any operational rotor speed, the blade loading coefficient was at least 15% lower than the maximum attainable thus, maintaining a safe stall margin. Figure 7.3 shows the optimal rotor speed schedule for the *Griffin*. The rotor speed reduction is initiated at a flight speed of 50 knots (point (a)). The rotor speed is gradually lowered to the minimum allowable speed of 85% of hover rotor speed. It reaches this lower limit at a flight speed of 65 knots(point (b)), the speed for best endurance. This is the optimal speed for search and rescue operations as it maximizes "on station time" and optimizes the ability of rescue personnel to identify objects.[83] The rotor speed remains constant untill a flight speed of about 156 knots (point(c)). At flight speeds greater than 156 knots, the rotor speed is increased, as required, to maintain a 15% stall margin. The never-exceed speed is 176 knots due to the transmission torque limit (Fig. 7.7).

7.6 Tail Prop Design and Swivel Schedule

7.6.1 Tail Prop Design

The tail prop on the *Griffin* performs dual roles. It must provide adequate anti-torque and directional control in low airspeed regimes and serve as an effective pusher propeller in high-speed flight. A traditional tail rotor uses blades with little to no twist to minimize drag penalties from the edgewise flow in which it operates. Propellers, however, operate in a predominately axial flow field and are highly twisted to maximize their propulsive efficiency. The design of the *Griffin's* tail prop was, therefore, a compromise between maximizing propeller efficiency and minimizing the penalties inherent in the tail rotor. Since the tail prop only has to operate as a tail rotor at low flight speeds, a variable pitch design with a moderate built-in twist was chosen. The distribution of *Griffin's* tail prop twist is detailed in Fig. 7.4. The tail prop was designed for maximum efficiency at 100 knots, the *Griffin's* speed for best range, and is also a good compromise between hover and never exceed airspeed. Throughout the flight envelope, the flight control system automatically adjusts the tail prop pitch to generate sufficient thrust to identically overcome the helicopter's parasitic drag. Since the parasitic power requirement grows with the cube of the flight speed, it is a major fraction of the total power at high airspeeds.

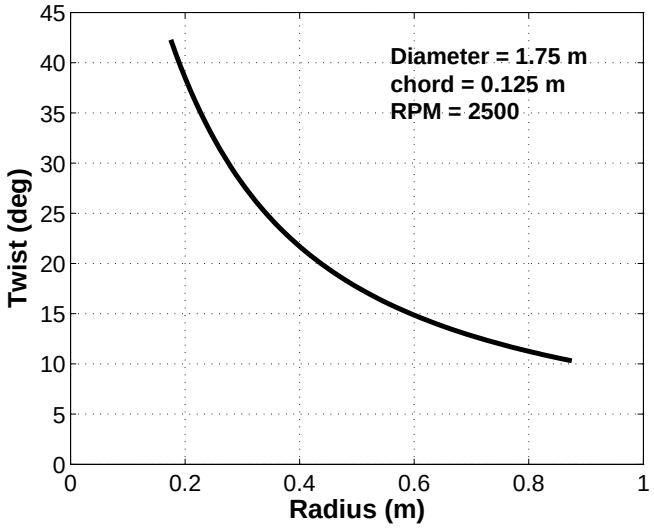

Figure 7.4: Propeller twist distribution.

7.6.2 Tail Prop Swivel Schedule

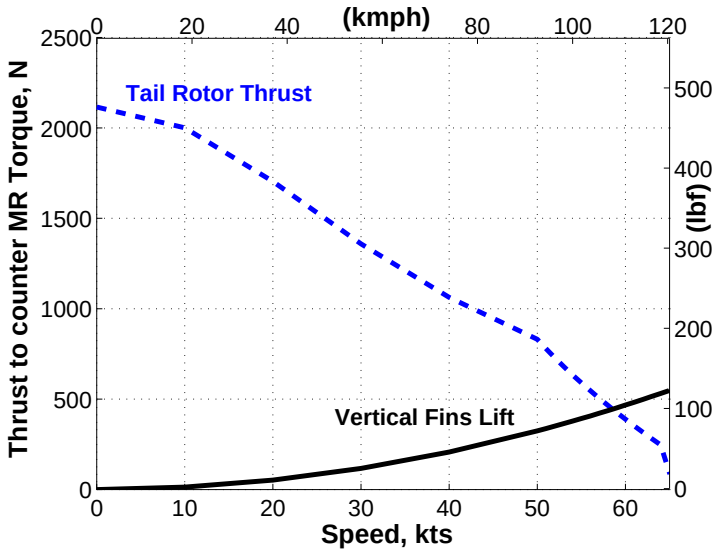

Figure 7.5: Thrust required to counter main rotor torque.

Traditional tail rotors provide not only the thrust required to counteract the main rotor torque, they also impart directional control and stability. The EC145 empennage has two vertical fins that augment the helicopter's directional stability and additionally serve to progressively offload the tail rotor as forward flight speed increases. Figure 7.5 shows the thrust required from the tail rotor to counter the main rotor torque. As forward airspeed increases, the required main rotor power - and hence torque - decreases. Reducing the main rotor speed lowers the power requirement (Fig. 7.7) further, decreasing the thrust required from the tail rotor. The lift generated by the vertical fins increases with airspeed and at approximately 65 knots, they provide enough force to offload the tail rotor completely. No longer required for directional stability, the tail prop thus swivels to a pusher propeller configuration for thrust compounding at 65 knots. This offloads the main rotor by effectively reducing the propulsive component of its thrust and manifests as a large improvement in the range and endurance of the *Griffin*.

7.7 Hover Performance

The *Griffin* has the same main rotor diameter, blade aspect ratio, solidity and hover tip-speed as the baseline EC145. Careful selection of materials, coupled with implementation of an advanced MEMS-based avionics suite, a "dual-triple" redundant fly-by-wire control system, and environmentally-friendly electrohydrostatic flight control actuators, endow *Griffin* with improved capability without any weight penalty. The hover performance is thus comparable to the baseline EC145.

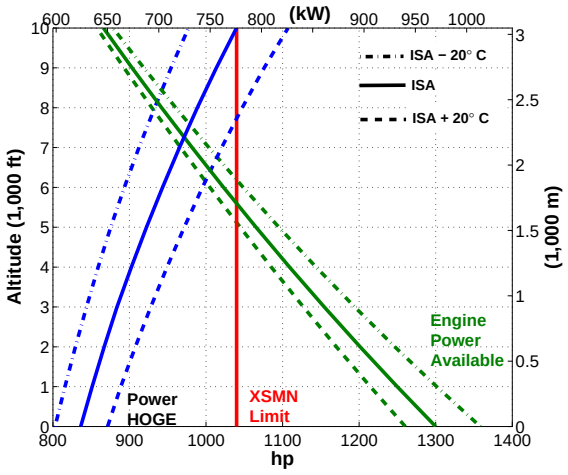

(a) HOGE power required with altitude MTOW = 3587 kg.

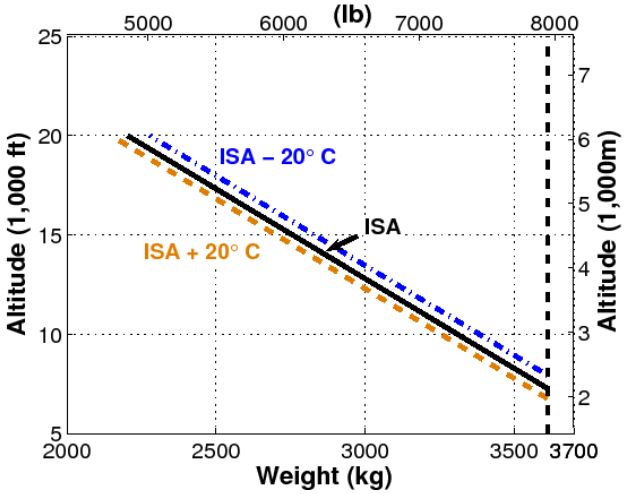

(b) Weight-Altitude-Temperature Curves

Figure 7.6: Hover performance – *Griffin*.

The power required to hover out-of-ground effect (HOGE) is a function of temperature and altitude. With increasing altitude, the power required to hover increases and the power available from the engine decreases. The calculated HOGE power is

displayed in Fig. 7.6a for three separate temperatures. The power available from the engines is also shown as a function of altitude for the same conditions. *Griffin*'s HOGE ceiling with MTOW 3585 kg is engine limited to 7,000 ft (2,134 m) at ISA conditions. As seen in Fig. 7.6b, however, at a gross weight of 5,060 lb (2,300 kg), the *Griffin* can hover out-of-ground effect at an altitude of 20,000 ft (6,096 m).

7.8 Forward Flight Performance

Although the *Griffin* and EC145 have the same MTOW and main rotor dimensions, VERITAS bestows significant forward flight performance improvements upon *Griffin*. Figure 7.7 details the total power required for both aircraft as a function of forward flight speed at sea-level ISA conditions. Reducing the main rotor speed at point (a) and initiating thrust compounding at point (b) dramatically lowers *Griffin*'s power requirements when compared to the EC145. While the rotor speed reduction decreases the profile power of the rotor blades, thrust compounding offloads the main rotor. This increases the effective lift-to-drag ratio (*L/D*) of the main rotor, making it more aerodynamically efficient. Moreover, the tail prop is significantly more efficient than the main rotor in overcoming the fuselage parasitic drag. This propulsive efficiency improvement translates directly into lower power consumption than EC145 when operating above 65 knots airspeed.

7.8.1 Speed – 20 knots *faster*

The *Griffin*'s recommended cruise and never-exceed speeds are 150 and 180 knots, respectively. These flight conditions are shown in Fig. 7.7 as points (c) and (d). The *Griffin* cruises 20 knots faster than the baseline and is capable of exceeding the top speed of the EC145 by 26 knots. These are truly quantum leaps in attainable flight speed. The increased speed is critical to the successful completion of *Griffin*'s primary humanitarian assistance mission as it increases its "golden hour" reach by 30 nm over that of the EC145.

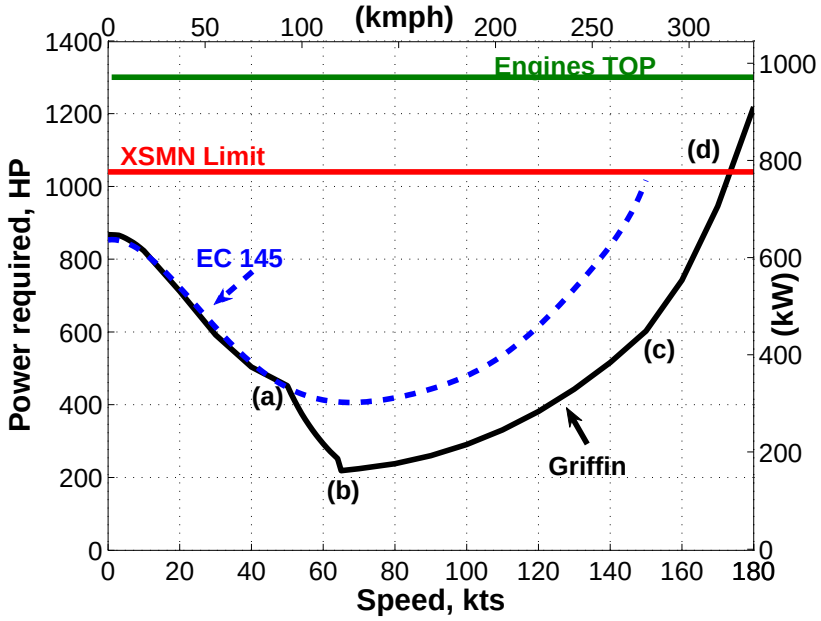

Figure 7.7: Power curve.

7.8.2 Range – 164% *farther*

The EC145 employs twin Turbomeca Arriel 1E2 engines. The *Griffin*, however, is equipped with more fuel efficient Rolls Royce 250C–30 engines. This state-of-the-art power plant consumes less fuel than an Arriel 1E2 (Fig. 4.2a) when producing

the same amount of power. Strategic engine selection reduces the fuel cost per flight hour by over 17% and, when combined with the reduced power consumption of VERITAS, results in another quantum leap in capability. The increased range of the *Griffin* over the EC145 is clearly detailed in Fig. 7.8.

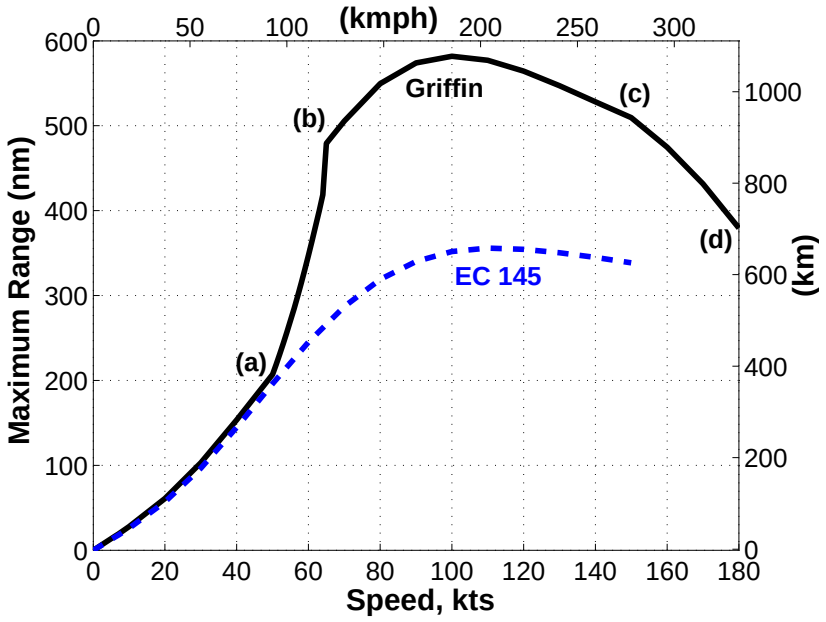

Figure 7.8: Variation of range with forward speed.

7.8.3 Endurance – 176% *longer*

The *Griffin*'s VERITAS and its fuel efficient engines endow the advanced rotorcraft with outstanding efficiency. Figure 7.9 details the extraordinary increase in the endurance of the *Griffin* over the baseline EC145.

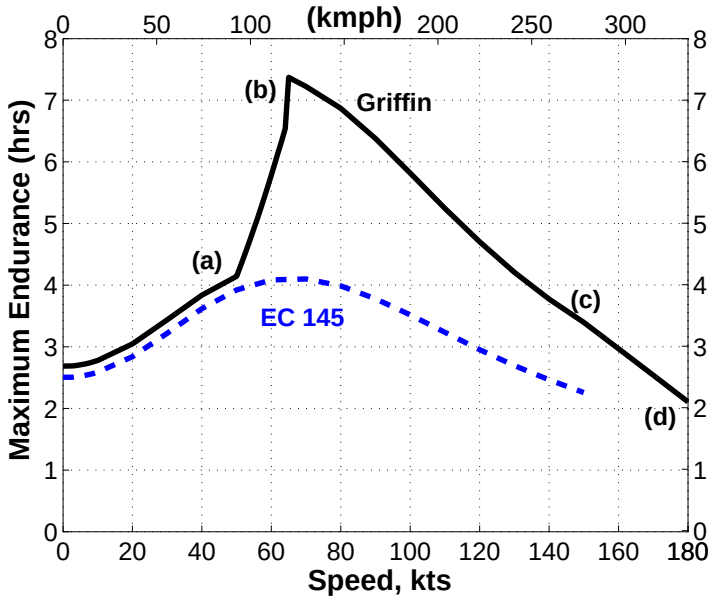

Figure 7.9: Variation of endurance with forward speed.

The slopes of the payload–range and payload–endurance curves are inversely proportional to helicopter *L/D*. That is, a greater *L/D* corresponds to a higher helicopter efficiency, and a shallower curve slope. The *Griffin*'s reduced rotor speed and thrust compounding increases its *L/D*, decreasing the slopes in Figs. 7.10 and 7.11.

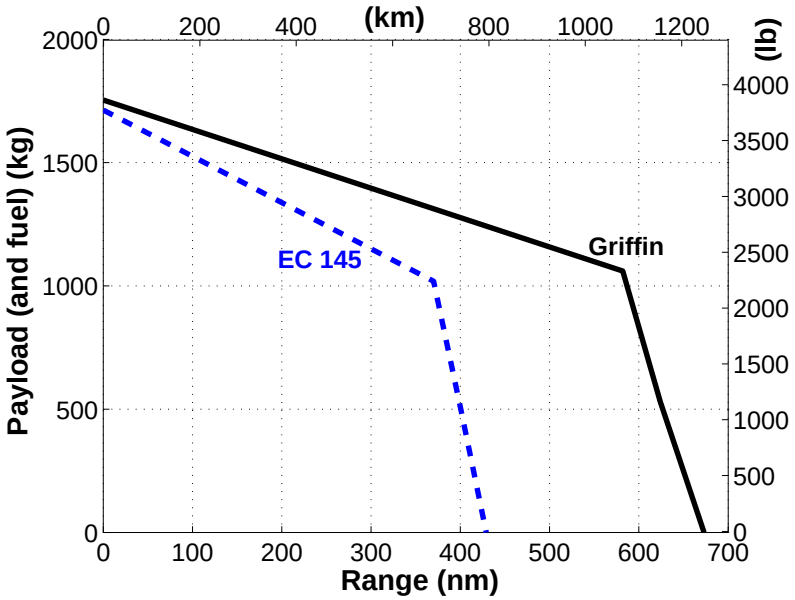

Figure 7.10: Payload – range plot.

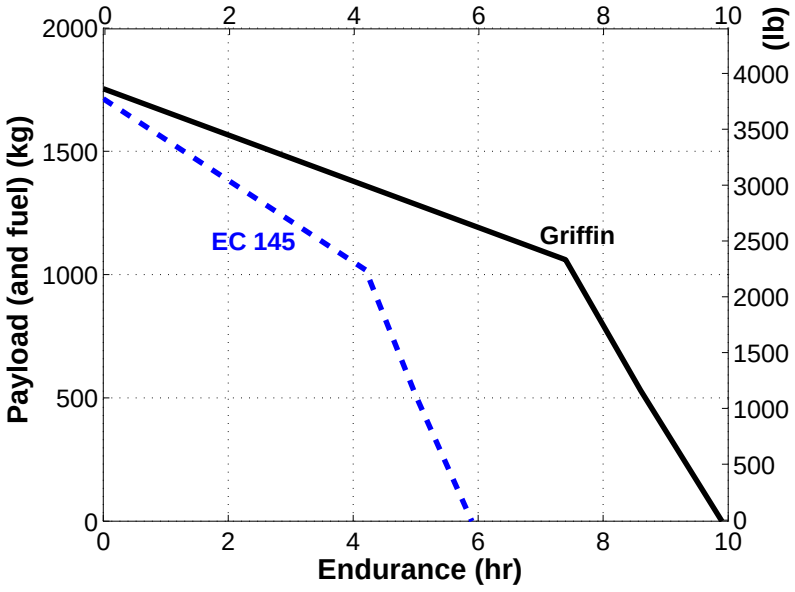

Figure 7.11: Payload – endurance plot.

Its improved *L/D* is the prime driver for the *Griffin*'s remarkably improved performance when compared to the baseline EC145.

At any airspeed, the *Griffin* is capable of flying farther and longer than an EC145. VERITAS truly powers the *Griffin*'s quantum leap in rotorcraft performance.

7.8.4 Comparison Metrics

For the same MTOW and same fuel capacity, the *Griffin* is capable of carrying 40 kg more payload than EC145. The maximum range is 64% more and the maximum endurance is 76% better than the EC145. Two widely accepted metrics are utilized to quantify and compare the exceptional performance of the *Griffin* with the baseline EC145. These are Payload Delivery Efficiency and Productivity:

$$Payload\ Delivery\ Efficiency = \frac{Payload \times Range}{Fuel\ Weight}$$

$$Productivity = \frac{Payload \times Cruise\ Velocity}{Empty\ Weight + Fuel\ Weight}$$

Payload delivery efficiency is the effective range per unit of energy consumed and is a measure of efficiency in terms of cost. Productivity is used to assess the overall capability of helicopters in terms of payload, speed and empty weight fraction.

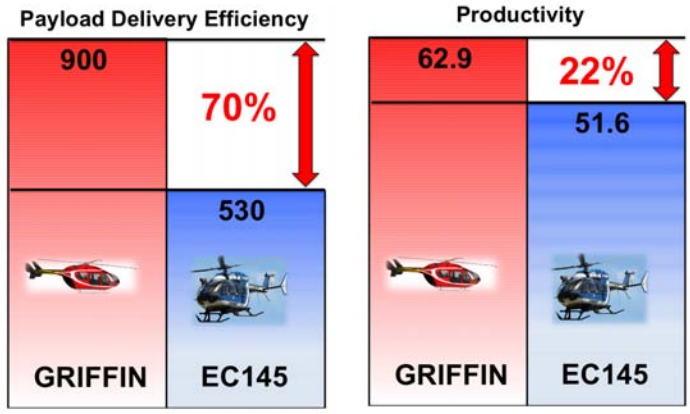

(a) Payload delivery efficiency. (b) Productivity.

Figure 7.12: Comparison metrics.

Figure 7.12 shows that *Griffin* offers a 70% increase in payload delivery efficiency and a 22% increase in productivity. These metrics show that to ferry a given payload over a specified range, the *Griffin* consumes much less fuel and time as compared to the EC145. It highlights both economical and enviromental friendly feature of the *Griffin*. A simple RFP-specific index was used as a measure of increase in utility of the *Griffin*. The composite utility index quantifies the aggregate increase in the utility of the aircraft due to improvements in specified parameters. Speed, payload, range, endurance and noise signature are weighed equally to fairly claim that a high composite utilitiy index represents an overall improvement in the helicopter utility.
Composite Utility Index =

$$\left(\frac{Cruise\ Velocity_{Griffin}}{Cruise\ Velocity_{EC145}}\right)\left(\frac{Payload_{Griffin}}{Payload_{EC145}}\right)\left(\frac{Range_{Griffin}}{Range_{EC145}}\right)\left(\frac{Endurance_{Griffin}}{Endurance_{EC145}}\right)$$

Composite utility index for the *Griffin* is calculated to be 3.45. It shows that the *Griffin*, due to its exemplary performance, has over 300% more utility compared to the baseline EC145 with 82% reduction in percieved noise compared to EC145. Regardless of the comparison method, *Griffin* truly offers a quantum leap in rotorcraft performance.

7.9 Climbing Flight Performance

Rate of climb is an important operating parameter for all flight operations. The best rate of climb is a function of the excess power available at the speed for best endurance [Fig. 7.7 point (b)]. At lower altitudes, the maximum power that can be extracted is established by the transmission torque limit. At higher altitudes, however, the available engine power typically limits rate of climb. Figure 7.13 details the best rate of climb for the *Griffin* and the EC145 at various altitude and temperature conditions. As seen in Fig. 7.7, the variable rotor speed capability given by the VERITAS reduces the power consumption of the *Griffin* when compared to the EC145. Greater excess power is thus available for the *Griffin*, permitting it to climb at much higher rates. Clearly, the climb performance of *Griffin* is superior to that of the EC145.

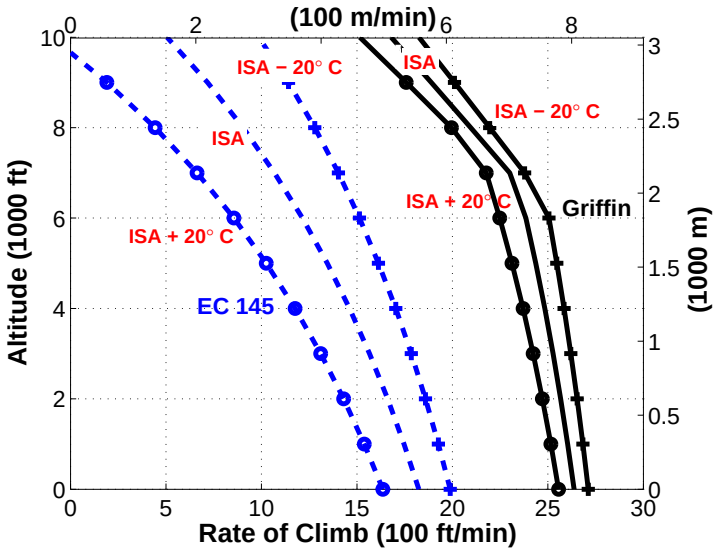

Figure 7.13: Best rate of climb.

7.10 Autorotational Performance

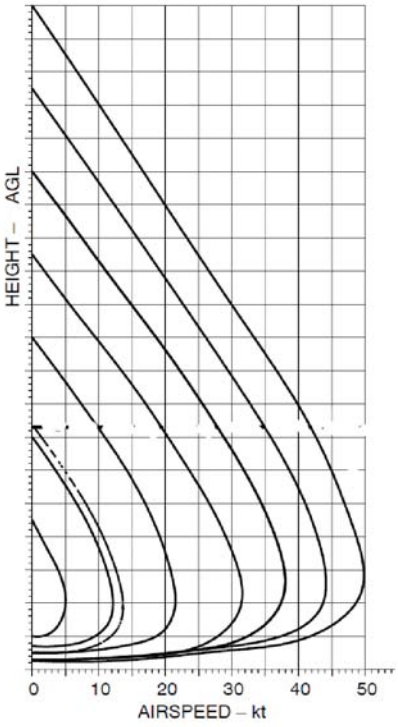

Figure 7.14: Height–velocity curve for EC145.

Autorotation is an essential requirement for helicopter certification. This capability depends on the stored kinetic energy in the rotor system, kinetic energy of helicopter and the flight altitude. The capability of the helicopter to autorotate can be measured using an Autorotation Index (A.I.),[22]

$$A.I. = \frac{I_R \Omega^2}{2W(DL)}$$

where I_R is the rotor inertia, Ω is the angular velocity of the rotor, W is the takeoff weight and DL is the disk loading of the helicopter. For a multi engine helicopter, the value of the A.I. should atleast be 10. The A.I. for *Griffin* is 16.4 which is comparable to other helicopters in the same weight class. In an unlikely event of a dual-engine failure and/or loss of anti-torque capability at 85% hovering rotor speed, the *Griffin* retains safe autorotational characteristics; it has an A.I. of 10.6 which is higher than the minimum recommended for a twin-engine helicopter.

Figure 7.14 is the H–V diagram for the EC145[40] and clearly depicts the region where autorotation cannot be safely performed in the unlikely event of a single engine failure. As mentioned in section 1.5, the *Griffin* has the same MTOW, main rotor dimensions, and hover tip speed as the EC145. Since *Griffin* does not implement main rotor speed reduction until after the maximum speed of the "avoid" region (Fig. 7.3), the VERITAS permits virtually identical autorotation capability as that of the EC145.

7.11 *Griffin* exceeds DARPA-MAR objectives

Recently, the Defense Advanced Research Projects Agency (DARPA) announced its Mission Adaptive Rotor (MAR) program:[88] "The goal of the Mission Adaptive Rotor (MAR) program is to develop "on-the-fly" morphing rotor technology and demonstrate the dramatic benefits possible using this capability to reconfigure the rotor in flight, either during each rotor revolution, between mission phases, or both." Table 7.2 lists the desired performance attributes and corresponding *Griffin's* capabilities.

Table 7.2: Mission Adaptive Rotor (MAR) goals – DARPA.

Desired MAR Attributes	Fulfilled	*Griffin* Feature
40% increase in specific range	✓	64% increase
50% reduction in acoustic detection range	✓	82% reduction
90% reduction in vibration	✓	100% reduction capable
Morphing rotor system	✓	RPM variability, TEFs
Availability	✓	Minimum fuselage changes, COTS equipment
Marinization	✓	Blade folding, corrosion resistant materials

Table 7.3: Performance comparison of the *Griffin* and EC145

		Griffin	**EC145**
MTOW	kg	3587	3585
	lb	7891	7887
Payload	kg	1060	1019
	lb	2332	2242
Fuel capacity	kg	694	694
	lb	1527	1527
Speed for best range	kmph	185	204
	knots	100	110
Speed for best endurance	kmph	120	120
	knots	65	65
Recommended cruise speed	kmph	278	241
	knots	150	131
Rate of climb	m/min	792	549
	ft/min	2600	1800
Maximum range	km	1093	667
	nm	590	360
Maximum endurance	–	7 hr 24 min	4 hr 12 min

Although not within the weight class, *Griffin's* revolutionary performance capability already meets and in some cases far exceeds the DARPA MAR requirements. The unique ability of the *Griffin* to retain the hover characteristics of the rotorcraft and have exceptional forward flight performance makes it not just a mission adaptive rotor architecture rather a *mission adaptive rotorcraft* that offers a quantum leap in helicopter performance.

7.12 Conclusions

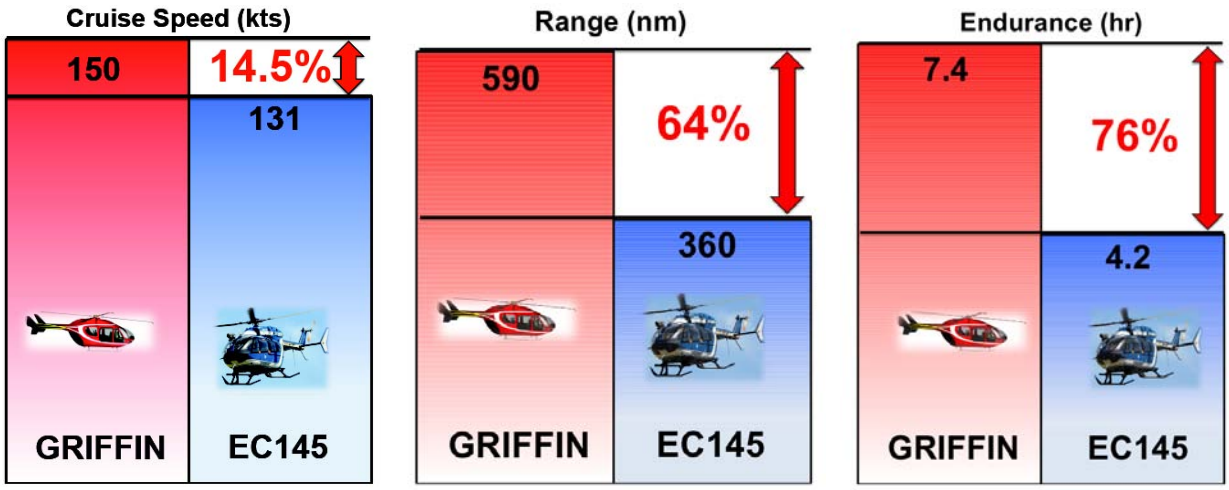

Figure 7.15: Comparison of key performance parameters.

The use of novel Variable Energy Rotor and Innovative Transmission ArchitectureS (VERITAS) endows upon *Griffin* the outstanding capabilities (Fig. 7.15, Table 7.3) consuming the same amount of fuel as EC145. The *Griffin* demonstrates this extraordinary performance with minimum structural changes to fuselage and no increase in the gross takeoff weight over the baseline EC145. As will be seen in Sec. 8.2, the *Griffin* also has 82% *smaller* percieved noise level compared to EC145. The *Griffin* truly, satisfies the RFP's demand of improvement in speed, range, payload, endurance, and noise in totality.

8 Acoustics

The *Griffin*'s innovative variable speed rotor drive and thrust-compounding tail prop have provided new opportunities to dramatically reduce the high levels of external noise radiation typically associated with rotorcraft operations. The use of these new technologies allow the *Griffin* an unprecedented capability to operate in noise sensitive communities and to avoid aural detection. An acoustic analysis developed in order to assess the noise radiation of the *Griffin* indicates that large improvements in external noise radiation are achieved relative to the baseline EC145: an estimated reduction in ground noise levels by 25 dBA in steady level flight, an estimated reduction of the aural detection distance by 85%, and the capability to nearly eliminate Blade-Vortex Interaction (BVI) noise during typical landing approaches. This exceptional reduction in noise reduces the environmental impact of the *Griffin* during it's primary humanitarian aid mission. The *Griffin*'s low noise footprint enables commercial operators of the *Griffin* to operate more frequently and in more localities without violating noise ordinances while improving their public image. Law enforcement and military operators will also benefit from the *Griffin*'s capability to perform missions in closer proximity to opposing forces without detection.

8.1 Acoustic Analysis

The estimation of helicopter external noise radiation is a complex problem. Helicopter noise radiation originates from a number of different sources: rotor steady harmonic noise, rotor impulsive noise, and mechanical noise. Each source has a different mechanism and radiation characteristics - without detailed experimental data it is not possible to predict overall noise levels exactly. However, simplified models of the noise sources may be developed independently in order to estimate the relative improvement in the helicopter's noise signature.

8.2 Steady Harmonic Noise

Rotor steady harmonic noise originates through two mechanisms: the steady thrust and torque loads the blades apply to the air as they rotate and the displacement of the air around the blades as they pass through the medium. While steady harmonic noise is not the dominant noise source in high speed flight or moderate speed descending flight, where impulsive noise sources dominate, it is the major source of noise in the low to moderate speed level flight regime where the *Griffin* is expected to spend most of its time operating. These sources of noise are well understood; given knowledge of the steady loads on the rotor and the airfoil profiles along the blade, this noise may be predicted using a discretized form of the Ffowcs Williams - Hawkings equation.[4] The inputs to this acoustic analysis were provided by the blade element momentum theory analysis described in Sec. 7, for both the main rotor and tail prop.

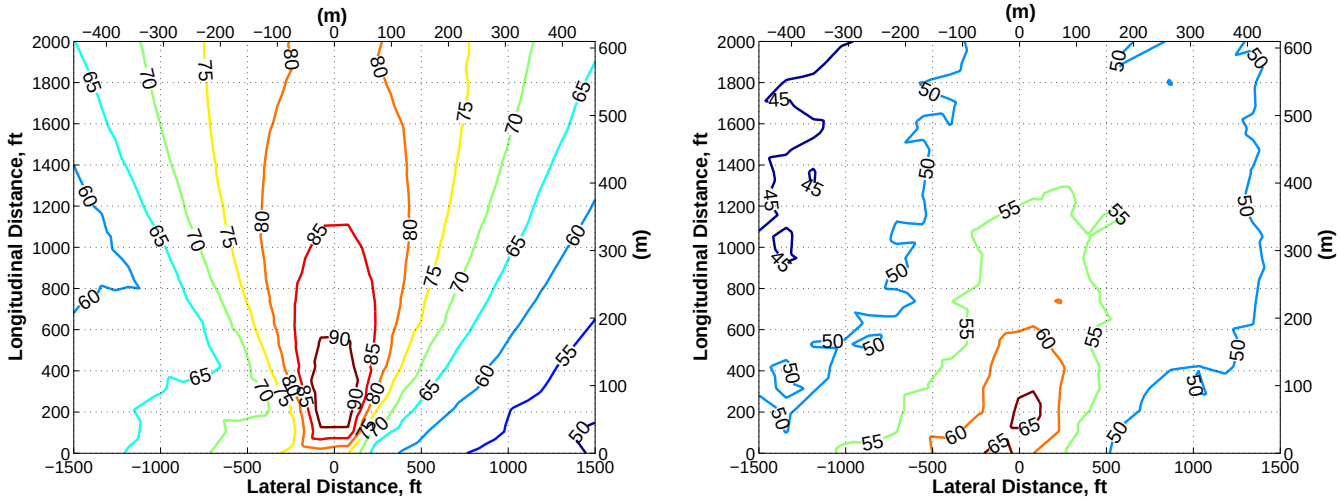

(a) Predicted EC-145 ground noise contours.

(b) Predicted *Griffin* ground noise contours.

Figure 8.1: Ground noise contours.

Time-history acoustic pressure data was calculated for both the *Griffin* and the baseline helicopter at a number of ground-based observer locations. From this data, the A-weighted sound pressure level ground noise footprints were calculated for both helicopters. A-weighting adjusts the sound pressure levels to account for the frequency response of the human ear, and reflects human annoyance and aural detection. Figure 8.1a shows the predicted ground noise contours for the EC145's during 100 kts flight. Figure 8.1b shows the contours for the *Griffin*. The noise levels for both helicopters are largely set by the higher frequency tail rotor, as is typically for light helicopters. The reduced main and tail rotor tip-speed of the *Griffin* during steady cruise results in a dramatically smaller ground noise footprint, with A-weighted sound pressure levels about 25 dB less than those of the EC145 at most observer locations. Consequently, the *Griffin* is perceived by the human ear to be 5.5 times quieter than the EC145. In addition to a reduction in tip speed, the swiveling tail prop yields a reduction in noise because the blade tip Mach number is uniform when operating in the propeller mode, as compared to a conventional tail rotor where the Mach number on the advancing side is increased.

Steady harmonic noise will also set the aural detection distance for moderate speed cruising flight. The chance of aural detection is determined by noise level of the helicopter above the noise level of the background. In general, when the helicopter is 5 dBA louder than ambient noise, there is a 50 % chance of detection.[84] For a quiet ambient level of 60 dBA, the detection distance of the *Griffin* is estimated to be less than 400 ft - more than 85% less than that estimated for the EC145.

8.3 Impulsive Noise

Rotor impulsive noise sources are more difficult to assess than their steady counterparts. High Speed Impulsive (HSI) noise is due to the formation of local shocks about the blades. It is the dominant source of noise at high speeds, where the advancing tip Mach number approaches the speed of sound. The *Griffin* is expected to have exceptionally low levels of HSI noise radiation, due to the reduced rotor tip speed and the thinned and swept tips of the TALON blade.

The other major source of impulsive noise is Blade-Vortex Interaction (BVI) noise. BVI occurs when the main rotor blades on the aft portion of the rotor disk pass close to the tip vortices shed from the preceding main rotor blades. The vortices cause a rapid change of loads on the blades, which is realized as impulsive noise as well as increase vibration. BVI does not typically occur during level flight, as inflow through the rotor convects the wake well away from the blades. However, during typical landing approaches where the helicopter descends to the landing zone at low or moderate speed, the inflow through the rotor is reduced, reducing the separation distance between the wake and the blades and yielding high levels of BVI noise.

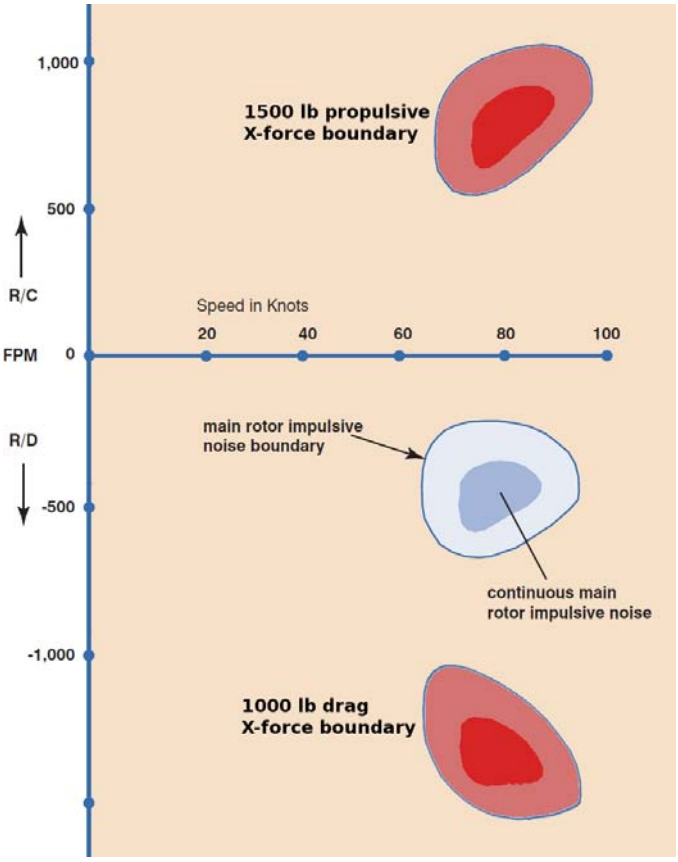

Figure 8.2: Range of BVI noise boundary displacement by X-force control.

The thrust compounding of the *Griffin* allows for a unique opportunity to eliminate most BVI. The tail prop may be swiveled to the propeller configuration at speeds above 50 kts. During typical 60 kts to 100 kts descending flight, the swiveling tail prop may provide anywhere between 1500 lb of propulsive force to 1000 lb of additional drag force. This "X-force" may be applied to adjust the trim state of the main rotor, thereby controlling the inflow and changing the separation distance between the rotor and its wake.[85] The Helicopter Association International's *Fly Neighborly* guidelines for light helicopter BVI noise were adapted, using the Quasi-Static Acoustic Mapping method, to shown how flight envelop where BVI noise occurs may be shifted away from the desired flight condition using the *Griffin's* X-force control. The results are plotted in Fig. 8.2 (adapted from[86]).

For any practical approach flight path selected by the pilot, the tail prop provides sufficient X-force to shift the BVI noise boundary well away from the trajectory. Unlike other helicopters, the *Griffin* does not require fight-path management to avoid BVI noise - the pilot simply chooses the desired trajectory to reach the landing zone and X-force control is applied automatically to steer the main rotor away from BVI. Since the HAI guidelines shown in Fig. 8.2 are general for all light helicopters, flight testing will be required to determine the precise X-force schedule that best avoids BVI for the *Griffin*. However, the general trends show that there will be more than sufficient X-force control authority to achieve an unprecedented level of BVI noise and vibration avoidance.

8.4 Mechanical Noise

Mechanical noise is generated by the engines and transmission, and occurs at high frequencies which are readily absorbed by the atmosphere. For this reason, it is not an important source of external noise radiation except at very close distances to the helicopter, such as those experienced by ground crew working near operating helicopters. Several steps have been taken to

minimize this source of noise on the *Griffin*. The engine intake and exhaust ducts are located on top of the helicopter, allowing the fuselage to block high frequency engine noise radiated from these openings. The VERITAS drivetrain makes extensive use of helical gearing throughout to increase gear contact ratios and reduce gear meshing noise. Additionally, all drive train housings feature reinforcing ribs designed to eliminate flat surfaces which may radiate noise outside the transmission housing. The cabin of the helicopter is also acoustically treated to reduce interior noise levels. Altogether, these measures result in low external and interior noise levels for the comfort and safety of both the passengers and crew.

9 Avionics

Every avionics system should clearly provide the pilot with the timely information required to safely and effectively operate the aircraft. The avionics suite of the *Griffin* was designed in close coordination with an active-duty U.S. Navy rotary-wing aviator and maximizes operator situational awareness while minimizing pilot workload. *Griffin*'s suite of state-of-the art flight and aircraft health sensors and multi-function displays leverage MEMS technology to minimize vehicle weight. COTS equipment usage was maximized to reduce development and integration risks. These advancements were specifically implemented to optimize *Griffin*'s safety, capability and operational availability, while minimizing life cycle costs.

9.1 Cockpit Layout

The cockpit of the *Griffin* is detailed in the Avionics and Cockpit Foldout as configured for all-weather single pilot operations. By minimizing clutter, promoting "heads-up" operation, facilitating mission data recall and usage, and incorporating logical flight controls, the *Griffin*'s cockpit is designed for mission success.

9.2 Instrument Panel

As shown in the Avionics and Cockpit Foldout, the instrument panel contains four multi-function displays (MFDs). Also included are rechargeable battery-powered electronic standby flight instruments (ESFI). The ESFI consist of backup airspeed, altitude, attitude, and horizontal situation indicators. A traditional magnetic compass is mounted to the top of the glare shield and a digital clock is also included for instrument navigation. Heads-up display (HUD) provisions are located in the upper portion of the instrument panel on the right (pilot) side of the cockpit for flight path management and to facilitate single-pilot instrument flight rules (IFR) operations.

9.3 Consoles

An upper console, located between the pilot and co-pilot/passenger, is provided for internal communication system (ICS) connections. The lower console, as shown in Fig. (panel), is located next to the base of the instrument panel and extends through the cockpit between the pilot and co-pilot/passenger and includes a backup battery-powered VHF radio and various mission equipment control panels. A backlit, programmable keypad is provided to simplify preflight mission system programming and to facilitate in-flight navigational aid and communication system operation. The primary electrical system controls including internal and external light rheostats – are also included. Several circuit breakers are provided for a variety of helicopter systems to ensure FAR 29 compliance.

9.4 Flight Displays

Mission, flight, and aircraft status can be interchangeably displayed on any cockpit MFD. The pilot at the controls can, however, designate a primary flight display (PFD) and configure it as desired within a range of output. Nominally, the PFD presents:

- Flight instruments: artificial horizon with embedded heading and sideslip indicators, vertical speed, radar and barometric altitude and airspeed.

Avionics and Cockpit Layout

Electrohydrostatic Primary Flight Control Actuators

Health & Usage Monitoring System (HUMS)

MEMS Based Sensors

Single Pilot IFR Capable

Unobstructed Pilot View

Obstacle Proximity Awareness System

Degraded Visibility Landing Aid

3 Axis Side Stick Controller

Crashworthy Variable Load Energy Absorbing Seats

"Dual-Triple" Redundant Fly-by-wire Flight Control System

Cockpit

Primary Flight Display with Airspace Situation Indicator

Vehicle Systems Status (From HUMS Sensors)

GPS-Linked Moving Map

Communication & Navigation Controls

Electronic Standby Flight Instruments

Autopilot Control

Electrical and Lighting Controls

Circuit Breakers

Instrument Panel

- Airspace Situation Indicator (ASI): offers a realistic, real-time, three-dimensional view of the aircraft and its relation to the surrounding terrain from an onboard database of satellite topographical photographs and GPS data.
- Terrain Avoidance Warning System (TAWS): provides aural and visual cueing to the operator when pre-determined ground proximity thresholds are breached. When coupled with the Degraded Visibility Landing Aid (DeVLA), this advanced synthetic vision significantly increases aircraft capability and drastically improves operator safety.
- Obstacle Proximity Awareness System (OPAS): leverages recent advances in infrared energy sensing technology to offer the operator a 360° representation of objects in the vicinity of the aircraft at low altitude.

The upper center MFD typically displays the status of *Griffin*'s Variable Energy Rotor and Innovative Transmission ArchitectureS (VERITAS) through graduated color strip light indicators and Health and Usage Monitoring System (HUMS) data. The lower center MFD defaults to controlling and displaying the primary navigation, mission planning, and communications systems. A GPS-linked moving map with embedded Traffic Collision Advisory System (TCAS) is typically displayed on the left MFD. Forward-looking infrared (FLIR) camera imagery or flight path director information can similarly be displayed at the pilot's discretion.

Because the pilot's ability to easily access and manipulate logically presented task-oriented data is critical to mission completion, the MFDs can be operated by selecting icons on pressure sensitive screens or by a control stick-mounted castle switch. This control method maximizes cockpit resource functionality while minimizing hands-off control operation during critical flight regimes. The MFDs accept mission, navigation, and communications input from the programmable, backlit keypad located on the center console. Warnings of subsystem faults are displayed at the top of the top center MFD and are linked to an embedded Interactive Electronic Flight Manual (IEFM) that can direct real-time operator diagnosis and prompt corrective actions. These warnings, displayed by the Integrated Caution and Warning System (ICWS), have the highest level of interrupt priority and continually display the fault code until corrected, regardless of any other currently active tasks.

To limit risk and reduce life-cycle costs, the *Griffin* leverages manufacturers' research and development activities and uses multi-function displays developed by Chelton Flight Systems for minimal pilot workload and maximum productivity. Each COTS unit can display data from any subsystem processor and thus enables mission completion despite the unlikely in-flight failure of multiple displays. Should all MFDs fail, the continued flight safety of the pilot and passengers is assured by battery-powered ESFI that offer the same functionality as the primary flight instruments on a smaller scale. Additionally, the navigation capability of the operator following a complete failure of the aircraft electrical system is guaranteed by the magnetic compass, and battery-powered digital clock and VOR-capable VHF radio.

9.5 Instrument Flight Rules (IFR) Equipment

The *Griffin*'s avionics suite complies fully with FAR Part 29 and VFR equipment requirements, permitting rapid IFR certification for single pilot operations. Flight displays and the associated sensors provide indications of altitude, airspeed, free air temperature, heading, non-tumbling flight attitude, vertical speed, and instrument power source. To satisfy the FAR 29 stability requirements, the *Griffin* incorporates an electrohydrostatically-actuated fly-by-wire control system and a state-of-the-art helicopter autopilot and stability augmentation system developed by Chelton Flight Systems. Unlike other systems, whose components may generate cost overruns or schedule delays,[41] this unique Automatic Flight Control System (AFCS) is currently certified for rotorcraft in *Griffin*'s weight class. It provides true hands-off capability with a force-feel trim system and embedded provisions for attitude, altitude, and airspeed hold as well as GPS way-point and glide slope tracking capability.[42] Integrated main rotor blade trailing edge flaps improve occupant comfort by reducing vibration to levels unattainable by passive or other active suppression methods. Additional FAR-required IFR equipment includes rotor blade de-icing, anti-ice provisions for flight equipment sensors, multiple static grounds, an overvoltage disconnect, and battery charge disconnects.

9.6 Internal Communications

Although cabin noise has been minimized, prolonged exposure to the sound pressure levels within the aircraft may cause discomfort or harm to the occupants. Internal noise levels may similarly disrupt timely communication. As such, BOSE Aviation Headset X's are provided for each crewmember. These headsets offer full-spectrum active noise reduction and feature an integral automatic smart shutoff boom microphone.[43] Headset ports are available for the pilot and passenger/co-pilot on the overhead center console and provisioned for intercommunications system (ICS) and external radio communications. ICS ports for aft passengers are located on the rear cabin wall, though this arrangement can be modified depending on the aircraft mission configuration.

9.7 Sensor Configuration

The information presented on the flight displays is collected through a sensor suite consisting of magnetometers, gyroscopes, accelerometers, a pitot-static system, numerous navigational aids, thermocouples, strain gauges, magnetic particle detectors (MPDs), and the full-authority digital engine electronic controls (FADECs). These sensors provide input to the *Griffin*'s flight control system and operator as shown in Fig. 9.1.

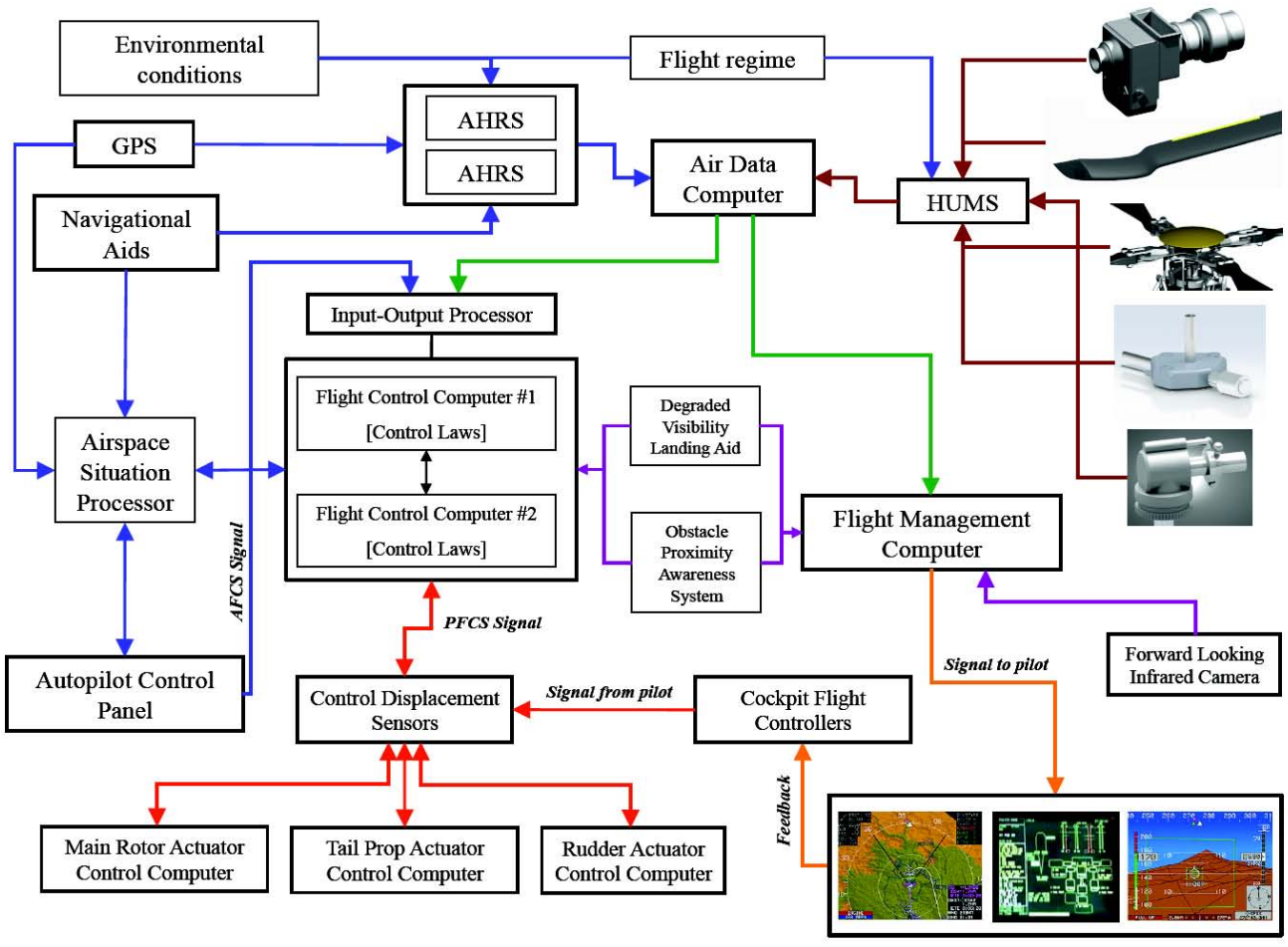

Figure 9.1: Avionics sensor architecture.

9.8 Flight Management Computer (FMC)

The FMC processes and integrates a wide array of vehicle and flight data for display. Vehicle status, navigation and flight control data is passed through fiber-optic cabling, thus eliminating the need for heavy EMI shielding while maintaining MIL-STD-4618 compliance. Attitude sensor information is fed directly to the dual Attitude and Heading Reference System (AHRS) units, in which an efficient recursive Kalman filter estimates the helicopter state from potentially noisy or incomplete positional data. The output is relayed to the ADC, in which the mean of the incoming signals is compared to the value provided by each independent AHRS unit. An internal voting scheme determines ADC input to the flight management and control computers. All data transfer is conducted in accordance with MIL-STD-1553B as individual sensors interface with the FMC via RS-232 communications protocol, while higher level communication is performed via RS-422 protocol.

9.9 Attitude Heading and Reference System (AHRS)

Griffin employs advanced MEMS technology to provide redundant AHRS with a mass penalty of only 4.6 lb per unit. These units are highly reliable and FAA-certified for use in over 100 aircraft.[44] This state-of-the-art system provides attitude and heading measurement with static and dynamic accuracy superior to traditional spinning mass vertical and directional gyros. By incorporating redundant units with 95% nominal reliability and 1000 hours mean time between failures (MTBF), the *Griffin* will have at least one unit operational during 99.9% of flight operations and offer 1 million hours of operation between total system failures. This system is currently FAR 23 certified and is expected to meet FAR 29 requirements within the next three years.[44] The AHRS used on *Griffin* are stand-alone units and incorporate three-axis accelerometers, gyroscopes, and magnetometers in a magnetic sensing unit and an external temperature sensor to provide a precise digital output of aircraft position rate, vector, and acceleration. This highly accurate state estimation enables the flight control system to reject higher frequency excitations resulting in smoother flight during automated flight modes, and a smooth display of attitude information for manual flight.

9.10 Auxiliary Power

Energy to power the avionics suite is provided by a generator mounted to the front of the main transmission. Failure of the generator - however unlikely - does not constitute total avionics system failure. Because of their exceptional energy and power density, eight lithium-polymer (Li-Po) battery cells - each contributing 3.7 V at a maximum of 4.6 kW - are arranged as an auxiliary power unit (APU). The cells output 29.6 V and can provide up to 20 minutes of full power to all navigation and communications electronics, HUMS, and AFCS with a five percent margin for line losses. This method of power supply avoids the step-down/step-up circuitry that would be required to regulate the line voltage for avionics power with a traditional APU, greatly decreasing system complexity. The energy density of Li-Po batteries permits a total battery weight of only 2.4 lb. APUs on comparable vehicles typically provide only half the reserve power at a significantly higher weight penalty. As an added feature, lithium polymer batteries do not suffer from “adverse memory effects” associated with not fully charging or discharging them, thus further improving system capability. To minimize the risk of overcharging, the battery charge is monitored and current is interrupted automatically at full charge. The battery pack is encased in a titanium housing to mitigate the effects of the unlikely fire. The *Griffin*’s auxiliary power pack truly maximizes operator and crew safety, permitting increased productivity.

9.11 Additional Avionics Equipment

9.11.1 Degraded Visibility Landing Aid (DeVLA)

Obscuration of external visual cues and subsequent pilot disorientation from brownout, whiteout, or excessive salt spray during the landing phase is a major safety concern. To mitigate this potentially disastrous risk, the *Griffin* relies on the DeVLA to provide a real-time representation of the terrain below the aircraft to significantly enhance pilot situational awareness and enable safe landings during degraded visibility operations. Four lightweight digital cameras observe the ground and transmit

their images to a central processing unit which, in turn, combines the images to create a three-dimensional map of the terrain beneath. Based on the defined GPS location, the onboard topographical data stored in the Airspace Situation Processor is then correlated with the updated camera-derived map data. *Griffin*'s flight dynamics data from the Air Data Computer and HUMS is incorporated into an embedded flight simulation along with the composite terrain data. The simulation contains a detailed helicopter model capable of estimating and filtering the effects of the particles entrained in the rotor downwash, permitting a representative display of the terrain - as the pilot should see it - in the cockpit.

9.11.2 Obstacle Proximity Awareness System (OPAS)

The precise positions of a helicopter's dynamic components are rarely known by the operator in the cockpit. During confined area operations, the inability to spatially identify the outer limits of the aircraft significantly increases the risk of striking objects and has contributed to countless flight mishaps. To improve the pilot's situational awareness and alleviate this potentially catastrophic risk, the *Griffin* employs the OPAS. This unique system leverages advances in commercially-available infrared laser technology to provide a real-time cockpit representation of objects relative to *Griffin*'s footprint. Four lightweight, low-power, and eye-safe infrared lasers observe the surrounding perimeter of the aircraft when the aircraft descends below 100 feet absolute altitude. Any detected returns from the emitted infrared energy pulses are transmitted to a dedicated digital microprocessor which then combines the signals and – based on their Doppler shift – generates a notional object location map. The position of the receivers and frequency of the transmitted energy pulses are tuned to ensure that only reflected signals from objects within 20 feet of the *Griffin*'s rotor system are detectable. The representation is then overlaid on the pre-programmed dimensions of *Griffin*'s rotor system and fuselage to display any objects in the vicinity of the aircraft to the pilot.

9.11.3 Health and Usage Monitoring System

Current helicopter maintenance practices are limited to:

- *Hard-Time*: Preventative measures performed at fixed intervals on a calendar or hourly basis.
- *On-Condition*: Replacement of suspect components identified through regularly scheduled inspections.

Time phasing of these maintenance actions hamstring operators and can negatively impact mission readiness by reducing aircraft availability. Moreover, replacing components without regard to their remaining life unnecessarily increases material and maintenance costs. Condition Based Maintenance (CBM) offers an attractive method to overcome these limitations. By continuously sampling the status of a particular system or component, corrective measures can be applied only when necessary. Central to such a maintenance approach is a properly configured Health and Usage Monitoring System (HUMS). As shown in Fig. 9.2, *Griffin*'s advanced HUMS was designed to monitor critical VERITAS performance parameters, as well as system components. This system optimizes *Griffin*s readiness, safety, and availability by enabling true CBM.

By integrating electronic logbook interface capability into the *Griffin*'s HUMS, the maintenance tasks required to certify continued airworthiness have been substantially reduced. This inevitably increases availability, improves flight safety, and reduces sustainment costs.[45] As an added benefit, the HUMS increases *Griffin*'s safety and reduces insurance costs. Ultimately, the CBM achieved with *Griffin*'s HUMS lowers direct operating and overall life cycle costs by nearly 5% compared to the baseline EC145.

The HUMS employed onboard the *Griffin* consists of a suite of 64 sensors. The drivetrain sensors are detailed in Fig. 9.3. These sensors collect and transmit aircraft status data to dual Data Acquisition Units (DAUs) and a Vibration Analysis Computer (VAC). The data collection rate was tuned to ensure appropriate system observation in a time-synchronous manner. The Control and Storage Computer (CSC) processes and saves the data for post-flight recall, while simultaneously transmitting pertinent flight data to the ADC for further processing and transmission to the cockpit vehicle status display. The system thus consists of two elements:

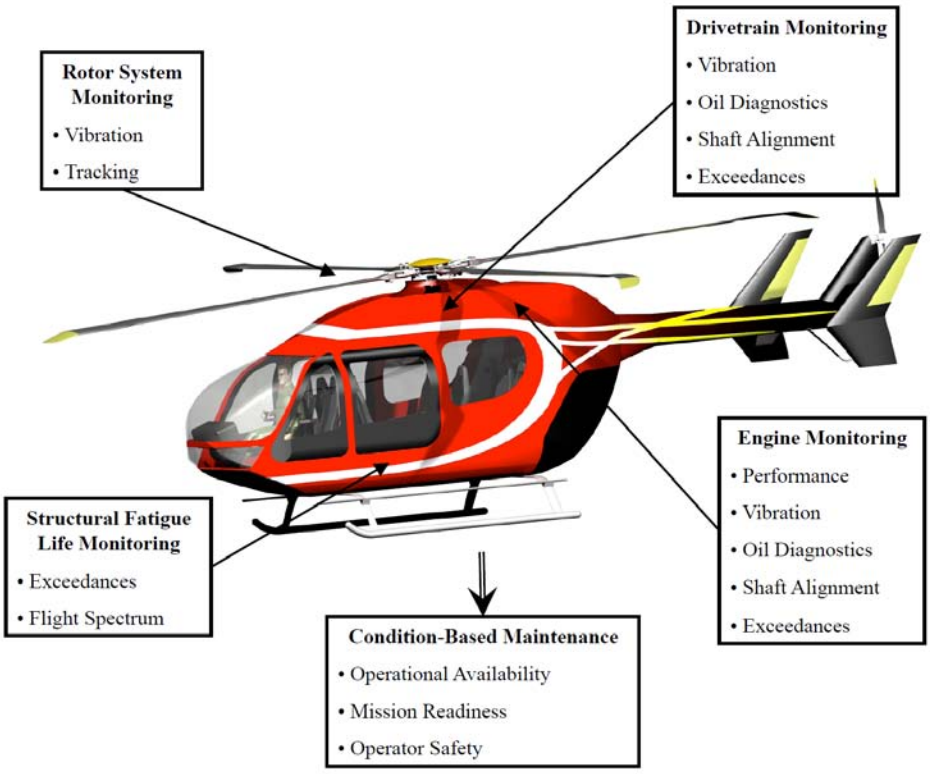

Figure 9.2: HUMS functionality.

- *In-Flight*: On-line processing components collect, condense, and display real-time drivetrain and flight spectrum usage data. Information that does not require extensive processing - such as average and instantaneous fuel consumption rates and remaining mission radius - is provided to increase the operator's awareness of the current aircraft status.
- *Post-Flight*: Ground processing components collect, analyze, process, and store data critical to updating the life limits of dynamic components, tracking structural strength, and determining the next necessary maintenance actions.

The primary subsystems that provide input to the HUMS are:

- **Main rotor**
  - *Trailing edge flaps*: monitored for actuator failure and loss of vibration suppression authority.
  - *Blade roots*: monitored for bending load exceedances.
  - *Rotor hub shaft*: monitored for misalignment vibration signatures.
- **Engine**
  - Full Authority Digital Engine Controls (FADECs) independently monitor for torque exceedances.
  - Temperature-sensitive magnetic particulate detectors (MPDs) permit oil temperature monitoring and provide early warning of impending engine malfunctions.
  - A driveshaft azimuth sensor, accelerometer, and thermocouple mounted to the reduction gear race housing provide insight into engine bearing health.

Figure 9.3: HUMS sensor configuration.

- **Transmission**
  - *Oil Diagnostics*: The oil pressure and temperature are monitored, as are critical component surfaces, to offer insight into potential gear and/or bearing defects. Two capacitance-based fluid level gauges are also employed to alert the operator to a fluid loss situation. Additionally, an MPD is mounted to the transmission fluid reservoir.
  - *Vibration Characteristic Tracking*: An azimuth sensor measures the main rotor rotational speed and accelerometers are mounted on the housing surrounding each shaft to which a gear is connected. The vibrations observed are time-synchronously averaged using an azimuth sensor pulse train and the values are periodically saved by the CSC. Though early stages of failure may not always generate a HUMS indication, this configuration ensures indication of gear tooth fatigue cracking and surface breakdown, rim/web cracking, liner/casing slippage, and shaft/coupling eccentricity and imbalance.[46]
- **Tail Gearboxes**: The tail prop gearboxes have similar instrumentation as the main transmission, though size limits the number of sensors employed.
- **Driveshafts**: Accelerometers are mounted at the bearing supporting each end of driveshafts.
- **Structure**: Ruggedized strain gauges are mounted at critical stress points of the main load bearing structures. Monitoring the loads imposed at these flight critical joints permits localized structural weight reduction while simultaneously reducing the likelihood of catastrophic failure. When coupled with vibration data, such structural health monitoring significantly reduces the time required to ascertain the root cause(s) of performance limitations and improves aircraft availability.

10 Flight Control and Stability

10.1 Flight Mechanics

It is important to ensure that the stability characteristics of the helicopter are not adversely affected by the operation of the variable-speed main rotor. The *Griffin* rotor differs from the baseline EC145 in that it features a semi-articulated hub design, with a small flapping hinge offset. This leads to smaller cross-coupling effects between the longitudinal and lateral modes of the vehicle than the hingeless design of the EC145. This translates to potentially superior handling qualities of the helicopter.

A systematic analysis was developed in order to study the flight dynamics of the *Griffin* in level flight.[36] The vehicle response was modeled using the coupled rigid body Euler equations and the equations of blade flapping. Contributions from the fuselage, horizontal and vertical stabilizers as well as the tail rotor were also modeled. The system was linearized about a trim state at different flight speeds and the eigenvalues of the system were calculated.

Table 10.1: Control derivatives (normalized)

Main rotor					
	Hover	**Cruise**		**Hover**	**Cruise**
X_{θ_0}	1.5465	-2.0812	Y_{θ_0}	0.2089	-0.8087
$X_{\theta_{1c}}$	0.2639	0.2838	$Y_{\theta_{1c}}$	2.0055	2.0150
$X_{\theta_{1s}}$	-5.9930	-5.8687	$Y_{\theta_{1s}}$	0.0883	-0.2610
Z_{θ_0}	-52.3453	-82.9820	L_{θ_0}	0.3118	-2.3838
$Z_{\theta_{1c}}$	-0.0002	0.0000	$L_{\theta_{1c}}$	5.1729	5.1953
$Z_{\theta_{1s}}$	-0.0012	-37.0095	$L_{\theta_{1s}}$	0.2278	-0.8101
M_{θ_0}	-0.9251	1.9153	N_{θ_0}	-12.1328	-7.5059
$M_{\theta_{1c}}$	-0.1774	-0.1907	$N_{\theta_{1c}}$	2.7198	2.4590
$M_{\theta_{1s}}$	4.0290	4.1742	$N_{\theta_{1s}}$	0.1196	1.5310
Tail rotor					
	Hover	**Cruise**		**Hover**	**Cruise**
X_{θ_t}	0.0000	0.0000	L_{θ_t}	0.4277	0.6302
Y_{θ_t}	0.7949	1.1712	M_{θ_t}	0.0000	0.0000
Z_{θ_t}	0.0000	0.0000	N_{θ_t}	-7.6343	-11.2488

10.1.1 Stability and Control Derivatives

Table 10.2: Stability derivatives (normalized)

Longitudinal			**Lateral**			**Lateral-longitudinal coupling**					
	Hover	**Cruise**		**Hover**	**Cruise**		**Hover**	**Cruise**		**Hover**	**Cruise**
X_u	-0.0069	-0.0827	Y_v	-0.0086	-0.3344	X_v	-0.0005	0.0131	Y_u	0.0005	0.0485
X_w	0.0002	0.1410	Y_p	-0.0717	-1.9899	X_p	-3.5608	-3.7494	Y_w	-0.0003	-0.0114
X_q	0.0720	1.9936	Y_r	-0.2581	-73.4775	X_r	0.0048	14.3008	Y_q	-3.5608	-3.7524
Z_u	-0.0006	-0.1059	L_v	-0.1809	-0.8749	Z_v	0.0000	-0.0642	L_u	-0.2782	0.3812
Z_w	-0.8356	-1.0096	L_p	-16.9124	-16.4444	Z_p	0.0130	0.7378	L_w	-0.1069	-4.2435
Z_q	0.5013	74.7643	L_r	-0.4627	5.2465	Z_r	0.2269	0.0725	L_q	11.8050	10.0469
M_u	0.0374	0.0675	N_v	0.0174	1.1276	M_v	-0.0593	-0.0781	N_u	-0.0415	-0.0391
M_w	-0.0035	-0.7637	N_p	-2.3728	-1.7763	M_p	-2.5048	-2.3627	N_w	-0.1576	-0.9704
M_q	-3.6042	-6.1629	N_r	-1.0038	-8.0065	M_r	0.0008	-0.2872	N_q	1.6567	1.3334

The stability derivatives consist of the force and moment derivatives with respect to body translational velocities and angular rates (Table 10.2). The derivatives X_u and Y_v primarily result from tilts of the rotor tip path plane following perturbations. Both are stabilizing for the *Griffin*. The H-tail surfaces provide additional lateral stabilizing effects.

Z_w, the heave damping, describes the vertical gust response, and is again stabilizing for the *Griffin* and increases with increase in speed. The 'speed' and 'incidence' stability derivatives M_u and M_w are important for longitudinal stability and handling qualities. A positive M_u (mainly due to the horizontal tail) and a negative M_w indicate static stability, which is the case for the *Griffin* across all speeds. Lateral/directional stability in gusts is given by the dihedral effect L_v and weathercock stability N_v,

which is positive (stabilizing) due to the tail rotor and vertical fins (Table 10.2). The coupling terms X_v and Y_u result from the finite flapping hinge offset and are smaller than those of the EC145.

Of the angular rate derivatives, the pitch and roll damping, M_q and L_p are most significant due to their direct effect on short-term, moderate amplitude handling qualities. Both are stabilizing for the *Griffin*, due to the c.g.-rotor hub offset. The yaw damping N_r is strongly influenced by the tail rotor and the fins, and is powerfully stabilizing for the *Griffin*. The main rotor has the dominant effect on each of the derivatives, and with reduced rotor speed, the derivatives reduce in magnitude.

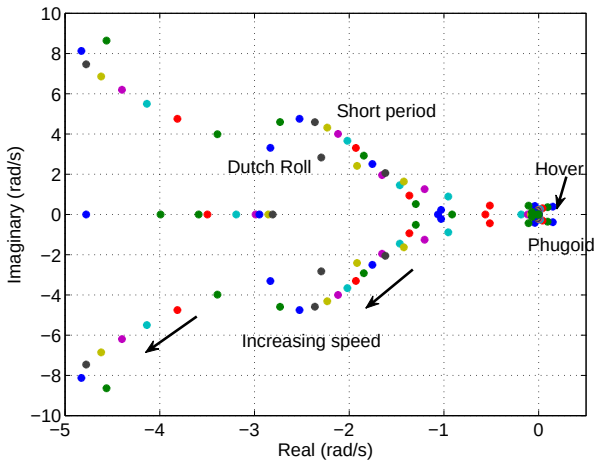

Figure 10.1: Stability of coupled modes of the *Griffin*.

10.1.2 Response Modes

It is common to separate the coupled equations of motion into those relating to the aircraft dynamics in the longitudinal and lateral directions. The response characteristics can then be seen to depend directly on the key stability derivatives.

The root loci of the characteristic equation of the linearized rotor-fuselage system about trim are shown in Fig. 10.1, as forward speed is varied. The rotor roots (in the fixed frame) can be identified easily as those corresponding to the coning/differential flapping and the progressive and regressive flapping modes. The latter is a low frequency wobble of the tip path plane. The other recognizable poles include the longitudinal phugoid pair, which starts off as unstable at hover but stabilizes with speed, and the lateral/directional Dutch roll pair, which is stable for all speeds. With the design vertical H-tail pair, combining for a total vertical stabilizer area of ~ 2 m^2, the Dutch roll modes were stable for all speeds. This stabilizer configuration is present on the baseline EC145, and was specifically optimized for Dutch roll stability.[37] It can be seen (Fig. 10.2a) that a smaller stabilizer would make the low-frequency oscillations unstable, though controllable by the pilot, since it is a mild instability. The roll and yaw damping ensure that the primary roll and yaw modes are stable. Similarly, a smaller horizontal stabilizer than the design stabilizer (of area 1.5 m^2) causes the Phugoid pair to split into a real unstable and a real stable pole at high speeds.

10.1.3 Handling Qualities

Control sensitivity (Table 10.1) and damping of the vehicle's natural modes determine its handling qualities. Preliminary analysis suggests that the *Griffin* possesses good sensitivity to control inputs, described by the derivatives $M_{\theta_{1s}}$, $L_{\theta_{1c}}$ and N_{θ_t} i.e., the sensitivity about the pitch, roll and yaw axes to longitudinal and lateral cyclics and pedal inputs. The damping characteristics as predicted by stability derivatives such as M_q, L_p, N_r and the dihedral effect L_v are also stabilizing in general. Desired responses can be engineered by implementation of model-following methodologies by the AFCS.

The ADS-33[38] standard details the criteria for acceptable handling qualities for rotorcraft. These criteria are based on gain and phase margin specifications for the roll, pitch and yaw axes responses to cyclics θ_{1c}, θ_{1s} and tail collective θ_t respectively. The bandwidth and phase delay characteristics determined from the individual transfer functions are used to assign handling quality 'levels'. For example, the open-loop, short term pitch attitude response of the *Griffin* to longitudinal cyclic was found to have a bandwidth of 0.9 rad/sec and a phase delay of 0.06 sec, implying a Level 2 handling quality in this mode. Similarly, the roll attitude response of the *Griffin* to lateral cyclic was found to have a bandwidth of 1.44 rad/sec and a phase delay of 0.055 sec, which again corresponds to Level 2 behaviour.

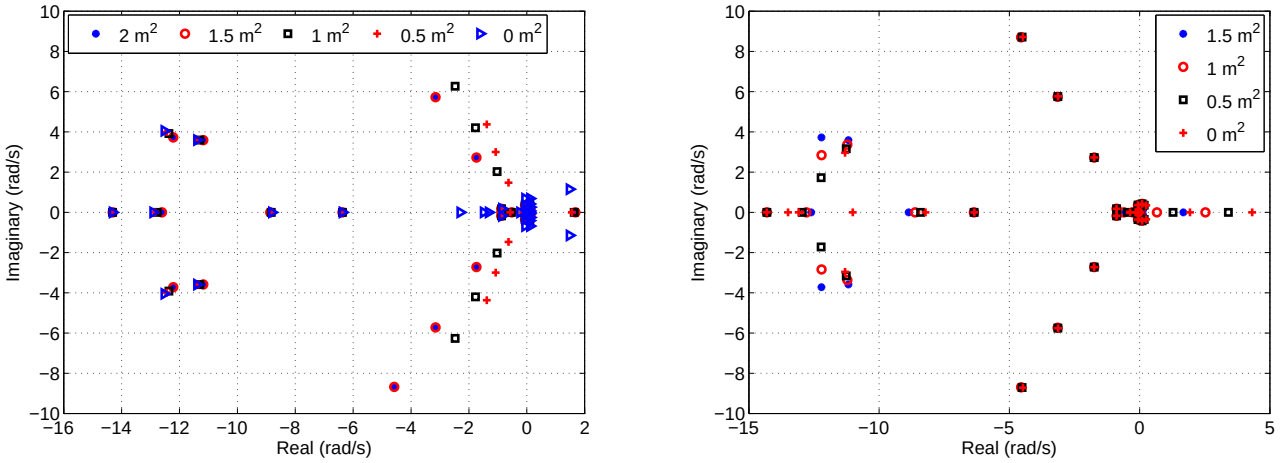

(a) Different vertical stabilizer areas

(b) Different horizontal stabilizer areas

Figure 10.2: Stability of coupled modes of the *Griffin* in forward flight with varying stabilizer areas.

10.2 Flight Control System

Griffin's flight is controlled by an advanced, digital fly-by-wire (FBW) system. It incorporates a unique cockpit controller configuration designed in close coordination with a military helicopter pilot with over 1000 flight hours. A dual-triple redundant architecture based on the one utilized in the Army's latest Blackhawk upgrade (UH-60MU) is employed. As a derivative of the U.S. Army's recently procured EC145 variant, *Griffin* will leverage the extensive rotorcraft flight control and handling qualities analysis capabilities of their Aeroflightdynamics Directorate to reduce developmental and flight safety risks. Innovative, commercially available electrohydrostatic actuators that virtually eliminate the use of hydraulic fluid are used for primary control of the main rotor, rudder, and tail prop. Electromechanical actuation is used for tail prop swiveling. Ultimately, this advanced architecture is implemented to minimize subsystem weight, while optimizing *Griffin*'s safety, capability and reliability.

10.2.1 Flight Control Architecture Selection

Incorporation of FBW flight control systems in new or derivative aircraft has received recent criticism due to perceived negative technical, programmatic, and cost impacts.[41] Nevertheless, a digital FBW architecture was selected for *Griffin*'s flight control system after careful consideration of the parameters detailed in Table 10.3.[47]

Clearly, a FBW system provides a number of distinct advantages over a traditional hydromechanical system. Notably, *Griffin*'s flight control system:

- Nearly eliminates environmentally hazardous hydraulic systems.
- Facilitates incorporation and modification of complex control laws without extensive redesign or remanufacture.
- Reduces maintenance requirements when compared to mechanical linkages that wear with prolonged usage.
- Offers an improved ability to detect and correct system faults.
- Is significantly lighter than a traditional hydromechanical configuration.
- Simplifies provisioning for control redundancy through multiple wiring paths.

Table 10.3: Flight control architecture selection matrix .

Parameter	Weight	**Mechanical**	**Fly-By-Wire**
Handling Qualities	5	4	5
Reliability Flight Safety	5	5	5
Reliability Mission	4	3	5
Maintainability	5	2	5
Availability	4	2	4
Durability	3	1	4
Modularity	3	2	5
Survivability Small Arms	4	2	5
Energy Surge Tolerance	3	5	3
Costs Production	4	3	4
Costs Life Cycle	5	2	4
Weight	5	2	5
		139	**228**

- Increases damage tolerance to permit mission completion and safe recovery.
- Provides greater control responsiveness than mechanical linkages whose fit tolerances decrease over the entire system life cycle.

10.2.2 Cockpit Flight Controls

The *Griffin*'s advanced flight control architecture permits implementation of an innovative cockpit flight control arrangement. Instead of incorporating a traditional cyclic/collective/pedal configuration, *Griffin* employs a unique 3+1 design. A side-mounted control stick is incorporated for three-axis control. Similar small-displacement sidesticks have been shown to generate satisfactory (level 1) Cooper-Harper handling qualities ratings[48,49] and prompted a similar application in the RAH-66. In this arrangement, pitch and roll control is obtained through traditional longitudinal and lateral displacement, respectively. Yaw control is achieved by rotating the controller about its vertical axis. As such, traditional pedals are not required to modulate anti-torque thrust. Rather than employ a four-axis sidestick configuration - which has been shown to yield degraded handling qualities[48] - a small displacement active collective is retained to schedule main rotor collective pitch. The sidestick configuration facilitates ingress and egress and increases the safety of personnel in close proximity of the rotor system on the ground by eliminating the potential for passenger-control interference. Additionally, the side-mounted controller significantly improves operator comfort, further increasing effectiveness and safety. The aircraft system capabilities available to the operator through switches and buttons on the cockpit flight controllers were designed with extensive pilot input to optimize the vehicle-operator interface during critical flight regimes.

10.2.3 Control Mixing

The electronic control mixing implemented in the *Griffin* reduces pilot workload by coupling flight control inputs that are inherently linked through aerodynamic or physical interactions. *Griffin*'s FCCs thus anticipate the natural single main rotor helicopter responses to given control inputs and schedule appropriate control inputs to compensate for them. The electronic implementation of this control mixing is significantly lighter and more robust than traditional mechanical systems, requires less maintenance, and contains fewer parts. As such, this arrangement contributes to reduced life cycle costs and increased reliability. To improve control responsiveness, reduce operator effort, and enhance vehicle performance, the following primary couplings are incorporated:[50]

- **Collective stick to tail prop blade pitch**: An increase in collective requires an increase in tail prop thrust to counter the main rotor torque change and maintain yaw orientation. When the tail prop is providing thrust compounding at higher airspeeds, increasing collective requires an increase in prop thrust to reduce the rotor loading and limit the extent of retreating blade stall.
- **Collective stick to longitudinal sidestick**: In forward flight, increasing main rotor thrust by raising the collective stick leads to increased advancing blade angle of attack. This uneven blade loading causes the tip path plane to tilt back, generating a nose up pitching moment. To compensate for this pitching tendency, nose down sidestick is coupled to an increase in collective stick.
- **Collective stick to negative lateral sidestick**: An increase in collective stick increases the main rotor coning, effectively increasing the loading of the blade over the nose. The result is an upward flapping response of the retreating blade and a right tilt to the rotor disk. To compensate for the resulting right rolling moment, left lateral sidestick is coupled to an increase in collective.

10.2.4 Flight Control System Architecture

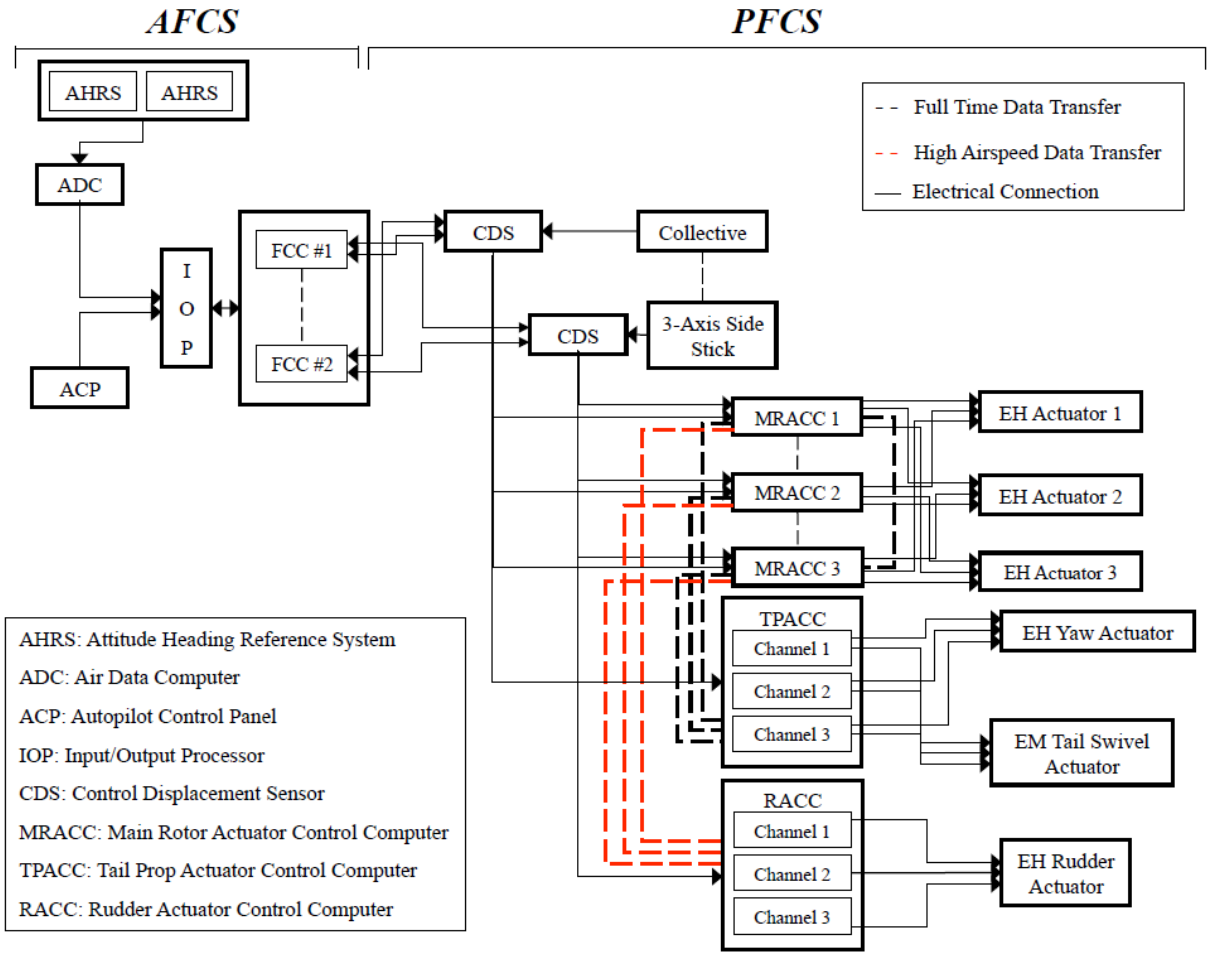

Figure 10.3: Flight Control System Architecture.

Griffin employs a multiple computer architecture for flight control processing, as detailed in Fig. 10.3. In contrast to the single processor approaches of early flight control systems, this configuration limits the scope of software that can affect flight safety to the primary control functions. As such, rapid software verification and validation can be achieved, greatly reducing technical and flight safety risks. *Griffin*'s multiprocessor approach also enhances failure coverage by direct comparison of two independent computations rather than relying on a self-check of a single processor. The triple channel, duplex redundant processor approach achieves the failure coverage of a quadruple cross-channel monitored system without the danger of cross-channel failure propagation or the complication of a quad voter.[47]

10.2.5 Automatic Flight Control System (AFCS)

Griffin's AFCS will endow the advanced rotorcraft capabilities of aircraft significantly larger and more costly. Implementation of Chelton Flight System's HeliSAS - an all-digital, full-authority stability augmentation system (SAS) with autopilot[42] - will reduce pilot workloads and improve handling qualities beyond that of comparable helicopters. Moreover, incorporation of dual flight control processors in a fail-passive architecture increases safety, redundancy and reliability of the advanced rotorcraft. Most importantly, however, *Griffin*'s system weighs approximately 20% of that employed on competing aircraft.[37] The ADS-33E-PRF compliant system centers on the three-channel, duplex redundant, independent digital flight control computers (FCCs) and is fully integrated with the installed navigational aids and mission equipment. The FCCs manage the attitude hold stability augmentation capability through a force-feel trim system. The ACP enables designation of the desired system functionality, including altitude and heading hold, bearing tracking from GPS, VOR, localizer, and ILS signals, synthetic visual navigation through the Airspace Situation Indicator, close proximity obstacle auto-avoidance, and waypoint tracking.[42] HeliSAS is also FAR certified for ILS glideslope and instrument approach navigation to weather minimums. And while pre-set attitude limits prevent inadvertent control inputs that could result in an unusual attitude, the operator can override system inputs at all times. Nevertheless, should the pilot release the control stick after an extreme input, the *Griffin* will recover to a near-level attitude. Such an attitude command-attitude hold capability facilitates low-speed and hover operations - especially in response to gusts and in degraded visibility conditions. Since the system interfaces with the rotor control actuator computers, *Griffin* is capable of flight director-controlled flight in instrument meteorological conditions for a single pilot. Additionally, the employed architecture permits rapid integration of subsequent advancements in automatic flight capability. Ultimately, *Griffin*'s AFCS enhances safety and increases productivity by minimizing pilot workload with reduced weight, life-cycle cost, and technical risk.

10.2.6 Primary Flight Control System

Griffin implements an advanced PFCS designed to mimic the capabilities offered by the systems employed on the UH-60MU and RAH-66. The Flight Control Computers (FCCs) are the backbone of the system and are responsible for all flight critical operations. An input/output processor (IOP) distributes tasks to the FCCs to enable primary flight control functionality, and the Autopilot Control Processor handles threads tied to the AFCS functions detailed above. This configuration maximizes safety and fault tolerance by partitioning flight-critical and mission-critical control laws. Each FCC employs three dual-core COTS processors. Two of the units are manufactured by Intel while the third is supplied by AMD. The intentional incorporation of processors from alternate manufacturers reduces the potential for correlated failures and significantly increases the level of redundancy and reliability of the system. This dissimilar, multiple processor configuration has yielded a flight safety reliability of 1 failure in 28.7 million hours, including fault detection and isolation rates of 97 and 96%, respectively. This translates to a mission reliability of only 1 abort in 2885 1-hour missions[47] - a remarkable 726% improvement over a single, self fault-detecting processor.

10.2.7 Control Law Architecture

Griffin employs an innovative control law scheme to ensure satisfactory handling qualities across the anticipated flight envelope. These control laws vary with flight regime, as detailed in Fig. 10.4, and have been implemented to optimize *Griffin*s capabilities, but can be easily tailored to the mission and aircraft configuration.

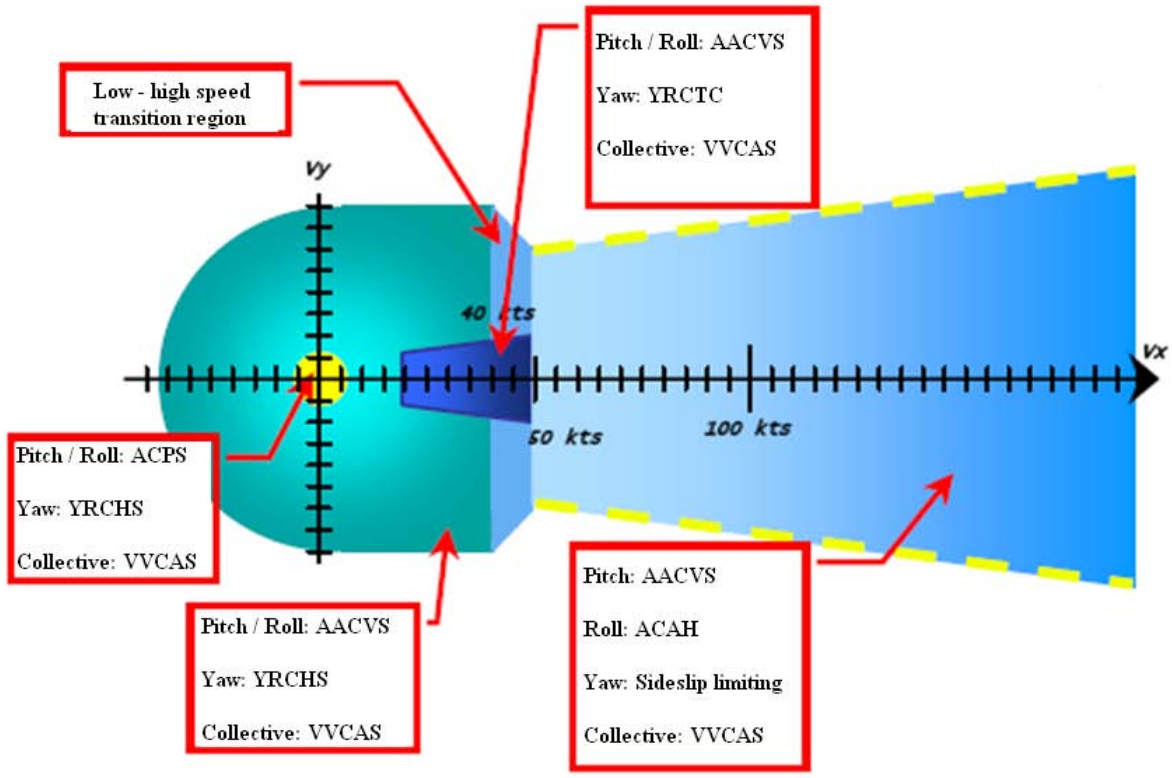

Figure 10.4: Control Law Map.

Near hover, *Griffin* employs:

- Attitude command/position stabilization (ACPS) in the longitudinal and lateral axes
- Yaw rate command/heading stabilization (YRCHS) in the directional axis
- Vertical velocity command/altitude stabilization (VVCAS) in the vertical axis

In this flight regime, inputs to *Griffin*'s sidestick or collective are proportional to the controller displacement, providing agreeable control responsiveness. Position and heading stabilization ensure maintenance of a newly-established reference heading and over-ground position upon returning the cockpit controllers to their center positions. Altitude stabilization employs radar altitude hold once vertical velocity is arrested by controller position centering.

Below 50 knots groundspeed, *Griffin* employs:

- Attitude and acceleration command/velocity stabilization (AACVS) in the longitudinal and lateral axes
- Yaw rate command/heading stabilization (YRCHS) in the directional axis below 20 knots
- Yaw rate command/turn coordination (YRCTC) in the directional axis above 20 knots
- Vertical velocity command/altitude stabilization (VVCAS) in the vertical axis

As in near hover conditions, inputs to the sidestick or collective are proportional to the controller displacement - though only initially. If *Griffin*'s sidestick is continuously held away from center, the rate of pitch and/or roll acceleration becomes proportional to controller deflection. Heading stabilization maintains a constant velocity vector when *Griffin* is below 20 knots - regardless of heading - when the sidestick is centered. Above 20 knots, lateral sidestick induces a heading rate command to eliminate inertial sideslip. Altitude stabilization employs radar altitude hold as in near hovering flight, though at higher speeds, the force-feel trim system provides a tactile cue of the level flight collective position for the pilot-defined groundspeed.

Above 50 knots groundspeed, *Griffin* employs:

- Attitude and acceleration command/velocity stabilization (AACVS) in the longitudinal axis
- Attitude command/attitude hold (ACAH) in the lateral axis
- Passive sideslip envelope protection in the directional axis

In high speed flight, pitch inputs respond with the hybrid behavior found below 50 knots. Lateral sidestick displacement, however, initiates a roll response from which a wings level attitude can be recovered by simply centering the controller. Regardless of controller movement, the extent of the aircraft response to yaw displacement of the sidestick is limited to the maximum sideslip permitted by *Griffin*'s structure.

The *Griffin*'s control laws are executed in a manner similar to that implemented in the UH-60MU flight control system. The goal of the model-following control system employed is to drive aircraft response to pilot inputs in accordance with the dynamics of a simple low-order command model. As such, the true vehicle dynamics are filtered by an approximate inverse of the aircraft dynamics in a forward loop signal. The resulting error between the actual aircraft response and the command model response is then used to provide corrective feedback commands - after a slight delay - to compensate for un-modeled dynamics.[51]

10.2.8 Flight Control Actuation

A hydraulic system has long been recognized as providing superior performance in the operation of flight control components. Unfortunately, the advantages of quick response, precision control and high stiffness were often outweighed by frequent maintenance, nonstandard construction and high life-cycle cost.[52] Similarly, environmental considerations were largely sacrificed for performance. By utilizing electrohydrostatic (EH) flight control actuation, *Griffin* is able to obtain the advantages of hydraulic operation without the conventional drawbacks. In an EH system, a hydraulic motor is matched to a pump and integrated into the actuator housing. *Griffin*'s flight control system thus eliminates external high-pressure hydraulic lines and connections, imbuing the actuators with an innate ability to eliminate the primary leak sources that characterize centralized hydraulic systems. Additionally, the volume of fluid contained in the actuator is significantly less than that required in a traditional hydraulic system. This technology embodies a novel approach to actuator position control by servo-controlling the electric motor driving the pump rather than using a valve to direct the fluid flow.[53] Uniting brushless DC motor controls with a high performance variable displacement pump in this manner provides an efficient, high power density package with excellent reliability. EH actuators permit precision position control and speed ratio regulation in a fail-safe configuration that offers simple redundancy management. Low maintenance, low power consumption and rugged components are inherent in the design. Any actuation failure is confined to a single device that can be removed and replaced without extensive intrusion into other aircraft subsystems. Although complete elimination of environmentally hazardous hydraulics is desirable, no other actuation methodology - including electromechanical - offers the frequency response, or the stroke, load, and duty cycle capabilities[54,55] required for flight control actuation. As such, three electrohydrostatic actuators designated for main rotor control are mounted to the main transmission and attached to the stationary swashplate. A fourth EH actuator is mounted to the tail gearbox and permits tail prop collective pitch modulation through all flight regimes. An additional actuator is provisioned for yaw control of the vertical tail through a simple bellcrank assembly when the tail prop is swiveled to provide propulsive force in high airspeed regimes. Because of its relatively low duty cycle, tail prop swiveling is controlled by an electromechanical actuator.

Due to their extensive rotorcraft control system experience, *Griffin* employs electrohydrostatic actuators designed and manufactured by Moog to specifically to meet the load, stroke, and frequency requirements of *Griffin*s primary flight control devices - while remaining within the size constraints imparted by the existing airframe. The technical specifications of these devices were calculated and independently confirmed by engineers at Hydramotion, Inc.[52] and Moog, Inc.[56] Dynamic peak-to-peak loads on H-60 pitch control rods were scaled and, with a small safety factor for FAR 29 compliance, utilized to obtain the forces required to manipulate the stationary swashplate. Maximum collective pitch angles from the *Griffin* performance code were correlated with the designed pitch horn length to determine maximum linear displacement needed to satisfy the calculated control angles. The entire swashplate assembly was treated as a rigid link with no deformation for both calculations. This data was correlated to available actuator sizing statistics[47][57] to ascertain physical dimensions, weight, and power requirements. The three main rotor actuators each provide 3.2 in total stroke at a penalty of 7 lb, and require 510 W from 125 VDC. A full-load extend speed of 0.8 in/sec can be achieved. Through similar flight load analysis, the tail prop actuator was designed as a 5.5 lb unit that offers 1.1 in of stroke at a maximum load extension rate of 1.5 in/sec from 440 W. *Griffin*s flight control system enhances safety and vehicle performance. These productivity-improving advantages are amplified by an overall weight reduction and minimal technical risk.

10.2.9 Redundancy Management

Removal of the direct mechanical linkages between the cockpit controllers and flight control actuators, and replacement with electrical direct motion signaling commands provides a significant reduction in subsystem weight and mechanical complexity. To achieve the same level of integrity as that achieved with traditional hydromechanical systems, multiple signal sources and several lanes of computing are necessary to provide redundancy. *Griffin*'s flight control signals must be cross-monitored to facilitate isolation of any failed equipment. The system relies heavily on both cross-lane and in-lane monitoring to achieve robust integrity and ensure safe system operation. This monitoring concept involves the use of two identical signal paths in each channel between the cockpit controls and the actuator input. If a discrepancy occurs that is greater than a pre-defined tolerance level, that channel is considered to have failed and is shut down.[47]

10.3 Enhanced Flight Readiness

Checklist design and pre-flight procedures for the *Griffin* were streamlined to minimize the time required to ready the helicopter for flight while retaining the safety of a thorough flight preparation. A fully integrated built-in-test capability permits component and subsystem status pre-flight checks on reserve battery power immediately prior to the pilots visual inspection. All relevant pre-programmed component strength and system limit exceedances that have occurred since the last performed maintenance can be displayed. The number of hours until maintenance action is required for each flight critical life-limited component can also be displayed. Rather than rely on the often erroneous[58] design flight spectrum usage, this output is determined directly from component fatigue data. Once the main aircraft electrical system is online, the embedded HUMS sensors re-examine the main structural elements of the frame, transmission, engines, main rotor, tail prop, and electrical system to determine flight readiness of all instrumented components. This capability permits take-off within 5 minutes of aircraft positioning for flight.[59] The *Griffin* is similarly capable of thorough examination of post-flight checklist items while the pilot conducts a visual inspection. In this manner, the *Griffin* offers a "walk-up and start" pre-flight and a "land and walk-away" post-flight capability unmatched by other rotorcraft.

Table 10.4: Component Weight Comparison.

Instrument	Griffin		EC-145	
	Quantity	Total Mass (kg)	Quantity	Total Mass (kg)
VHF / UHF	4	2.72	2	9.80
IFF	1	0.45	1	4.20
TACAN	1	2.95	1	4.10
VOR / ILS	2	0.54	2	13.40
GPS / INS	2	1.09	1	3.80
AHRS	2	4.17	2	20.70
ADC / FMC	2	2.49	2	8.50
MFD	3	6.12	2	23.80
ESFI	1	0.45	1	6.60
Radar Altimeter	1	2.13	1	3.00
AFCS	1	5.44	1	31.20
ELT	1	1.36	1	3.90
V/HUMS	1	6.80	1	7.60
Batteries	8	1.09	1	3.40
External Antennas	9	1.53	11	10.24
Searchlight	1	2.99	1	4.50
PFCS / Actuators	5	38.70	3	60.00
		81.1		**218.7**

10.4 Weight Reduction

The weight penalty associated with the equipment required for the autonomous capability offered by the *Griffin* has, to date, limited widespread incorporation in production helicopters in this weight class. The rapid development of MEMS sensors and components changes this paradigm. These devices are cheaper to manufacture and lighter than their traditional counterparts. Similarly, electrohydrostatic actuators are commercially available in the load and stroke range required for application to *Griffin*'s flight control system. These advanced devices minimize maintenance down-time and environmental impact, while improving mission flexibility and damage tolerance. Most importantly, however, the avionics suite and flight control system decreases the baseline EC145 subsystems weight without sacrificing capability. This weight reduction directly contributes to *Griffin*'s achievement of speed, range, endurance, and payload capabilities that rival much larger and more expensive aircraft. Table 10.4 details *Griffin*'s avionics and flight control components that are directly comparable to those installed in the EC145 with Avionics Solution C. Although not an exhaustive listing, the advantage offered by the MEMS-based sensors and innovative flight control system employed in *Griffin* is clear a 63% reduction in installed component weight.

Installation of multiple communications systems supports the main and auxiliary missions of *Griffin* by increasing interoperability within dynamic environments. The use of a robust HUMS package permits reduction of the installed redundancy without sacrificing operator or crew safety. In fact, inclusion of this capability dramatically reduces the direct operating costs of *Griffin* - in the form of maintenance and insurance premiums when compared to competing aircraft. MEMS-based sensors contribute to a significant reduction in overall avionics system weight, while simultaneously increasing aircraft capability. Ultimately, the effectiveness of the *Griffin*'s operator will be enhanced by these advanced avionics and flight controls, decreasing workload and augmenting single pilot capability with a higher level of autonomy than previously encountered in any helicopter.

11 Airframe Design

To maintain its true derivative nature, structural modifications of the *Griffin* were limited to those required to support integration of the Variable Energy Rotor and Innovative Transmission ArchitectureS (VERITAS). As such, changes to the baseline EC145 airframe were only made for three reasons:

- Weight reduction through introduction of structural elements with higher strength-to-weight ratios.
- Price reduction from more cost-effective materials and manufacturing processes.
- Environmental hazard reduction through use of eco-friendly materials and fabrication techniques.

Since the *Griffin* was designed with a maximum takeoff weight (MTOW) nearly identical to that of the EC145, structural strengthening of the *Griffin*s airframe was not required. Nevertheless, lighter and stiffer bulkheads were designed and the powerplant deck was strengthened to better support the VERITAS. Corrosion-resistant materials were employed to ensure the *Griffin* could withstand operating within the harsh maritime environment. To support the performance improvements required by the RFP, the hub, exhaust, and cabin roof were streamlined to reduce drag. Additionally, the *Griffin*'s tailboom was lengthened to support integration of the tail prop drive shaft. The front windscreen and cabin windows were also modified to improve crew safety and passenger comfort.

Environmentally friendly materials were employed to simultaneously reduce energy consumption and life cycle costs while increasing material strength-to-weight and stiffness-to-weight ratios. As such, the *Griffin*'s airframe was designed to be energy conscious, structurally rigid, and cost effective. In fact, *Griffin*'s airframe was designed to be fabricated with a considerable amount of composite materials and lightweight aluminum alloys to decrease vehicle weight without modifying existing molds and tooling. Designed to comply with Directive 2000/53/EC of the European Parliament, which requires that 85% of all vehicles, by weight, must be recycled by 2015, *Griffin* is positioned as an industry leader in the effort to minimize the environmental impact of materials processing, manufacturing, and disposal.

11.1 Structural Modifications

The *Griffin* consists of three modules: the cockpit, the central fuselage, and the tailboom and empennage. There are three primary bulkheads, two keel beams, two upper longitudinal beams, and a transmission/engine deck to provide structural integrity and support to the cockpit and the cabin floor. The primary bulkheads, which inter-connect the modules, support the engine and transmission deck, and bear the loads and bending moments. Rotor thrust and mast moments transmit loads to the airframe structure through the transmission. Since the bearing inside the main gearbox is very close to the transmission deck, the rotor mast loads are then transmitted to the deck through the strut assembly. The loads through the struts are transmitted to the bulkhead, which serves as a vertical element that transfers the load to the keel beam. The keel beam and the upper longitudinal beam that support the transmission deck act as horizontal elements that distribute the lateral forces to the vertical bulkheads. This structure reinforces the transmission structure in critical areas and allows the use of a lightweight panel for the transmission deck. The *Griffin*'s airframe was designed to support the same hoist and external loads as the baseline EC145.

In addition, there are secondary bulkheads to maintain shape and frame openings. As shown in Fig. 11.1, the first primary bulkhead connects the cockpit to the center fuselage and houses the front attachment bracket for the skid landing gear. The second and third bulkheads offer immediate support to the transmission deck, and the third bulkhead encloses the rear attachment bracket for the skid gear. Furthermore, the third bulkhead connects the central fuselage to the tail. The secondary bulkheads are located forward of the first bulkhead and aft of the third bulkhead. The first one is connected to the first primary bulkhead and supports the large windscreen and the cockpit side doors. The next secondary bulkhead is connected to the third primary bulkhead and serves as a structural support for the rear "clamshell doors. This secondary bulkhead is also attached to stringers, which connect to the tailboom bulkhead.

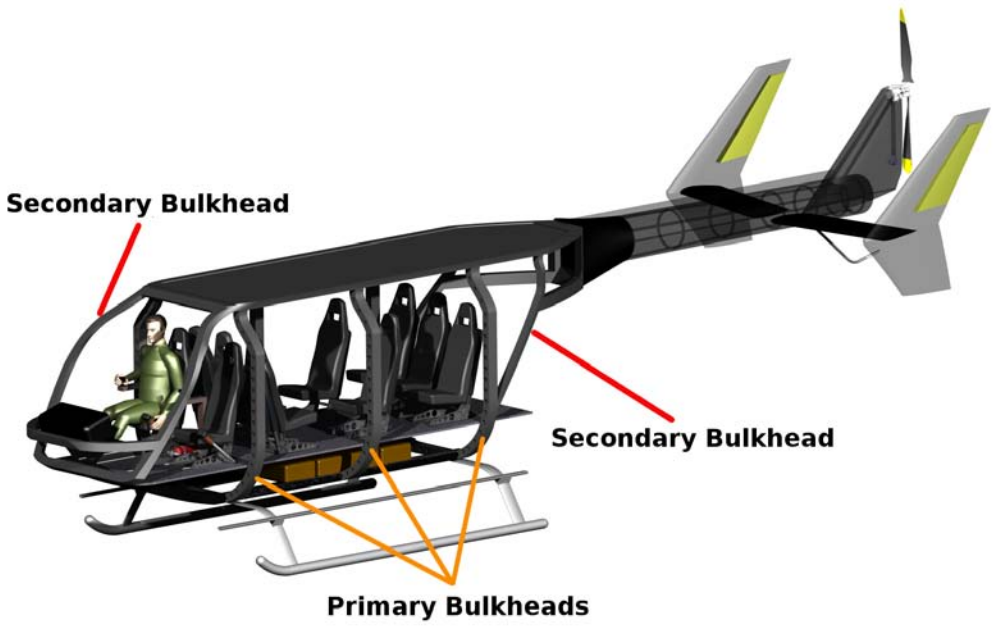

Figure 11.1: The *Griffin*'s internal structure.

11.1.1 Tailboom

The tailboom monocoque and empennage are cantilevered to the tail bulkhead and the vertical fins are connected to the tailboom. Internal structure of the tailboom, consisting of frames and stringers, was added, strengthened, and extended to the quarter-chord of the central vertical fin, as shown in Fig. 11.2. This modification supported the integration of an extended tail drive shaft that operates the swiveling tail prop.

11.1.2 Windows and Windscreen

The two small side windows on the baseline EC145 were converted into one large main window on each side of the *Griffin*, as shown in the Griffin's Exterior Layout Foldout, to enhance passenger visibility and facilitate emergency egress. Several horizontal and vertical frames and stringers supporting the original windows were removed, and one large frame was redesigned to attach a larger side window. The second and third bulkheads were used as vertical support for the *Griffin*'s large windows. Additionally, the front windscreen of *Griffin* was modified by removing the central panel supporting the wipers and enclosing flight control actuator cables. The advanced "dual-triple" redundant fly-by-wire flight control system implemented on *Griffin* permitted removal of this non-structural and vision obscuring panel. To satisfy FAR Part 29 requirements, polycarbonate was retained as the material for all windows. The windscreen was, however, coated with a replaceable mylar laminate for debris and corrosion protection. The tear-away film is clear, water resistant, and reduces the need for changing the *Griffin*'s windscreen. The film costs about $100 per application and a single layer can last up to a year if the helicopter is stored away from extreme conditions.[60] Should the maritime environment require more frequent replacement, the cost is justified by the $7000 or more required to replace the windscreen.

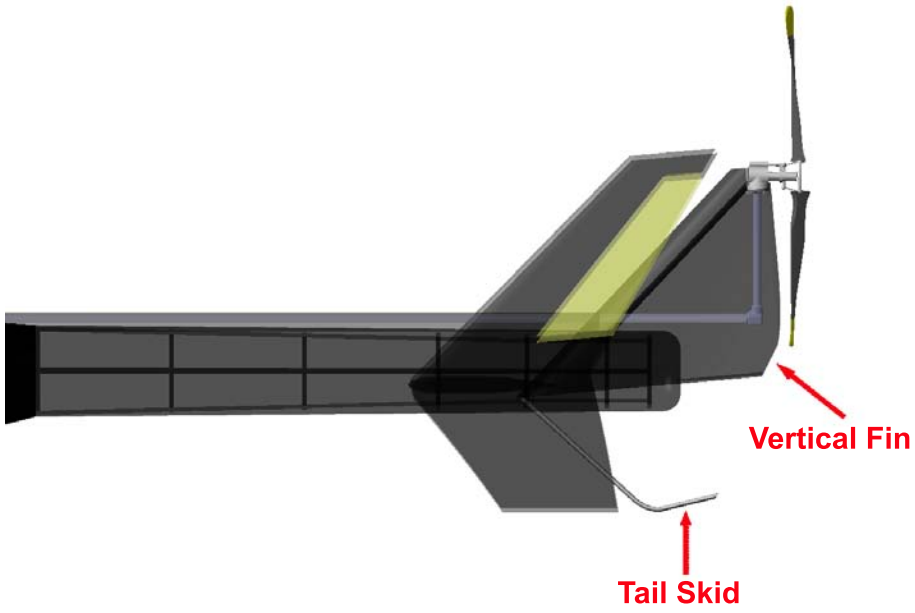

Figure 11.2: The *Griffin* tailboom internal and external structural modifications.

11.1.3 Crashworthiness

To satisfy FAR 29 requirements, each primary bulkhead was designed with a safety factor of 1.5 of the limit loads experienced during landing, flight, takeoff, ground handling, and rotor operations. Landing loads received particular scrutiny since the *Griffin* will likely encounter a variety of unprepared landing areas, pitching and rolling ship decks, and adverse weather conditions during its primary mission. Additionally, every structural element of the *Griffin* was designed to meet or exceed the fatigue load requirements of FAR29.571.

11.2 Materials Selection

Although the *Griffin*'s airframe received minimal structural changes, the materials utilized were driven by the RFP and primary mission requirements. The critical design drivers were material properties such as strength- and stiffness-to-weight ratios, corrosion resistance, ease of fabrication and manufacturing, and disposal options. Indeed, the environmental impact of the vehicle was an important aspect that influenced materials selection. The material decomposition shown in Fig. 11.3 delineates numerous standard components affecting *Griffin*'s environmental footprint. Engine and transmission components, avionics, fuel system, batteries, volatile organic compound (VOC) and hexavalent chromium-free paints, furnishings, windows and wires are detailed. Although aluminum is the primary contributor to the empty weight of *Griffin*, over 60% of *Griffin*'s components were designed for composite materials to optimize strength- and stiffness-to-weight ratios and minimize environmental impact. Aluminum alloys were utilized extensively as primary structural members within the fuselage, while the fuselage skin, tailboom and empennage were designed for trouble-free composite fabrication.

11.2.1 Lightweight, Cost-Effective Aluminum Alloys

Aluminum alloys were selected for the airframe based on cost, fracture toughness, survivability, maintainability, and environmental considerations. The *Griffin*'s primary and secondary structures, as well as the skid landing gear, account for 31% of

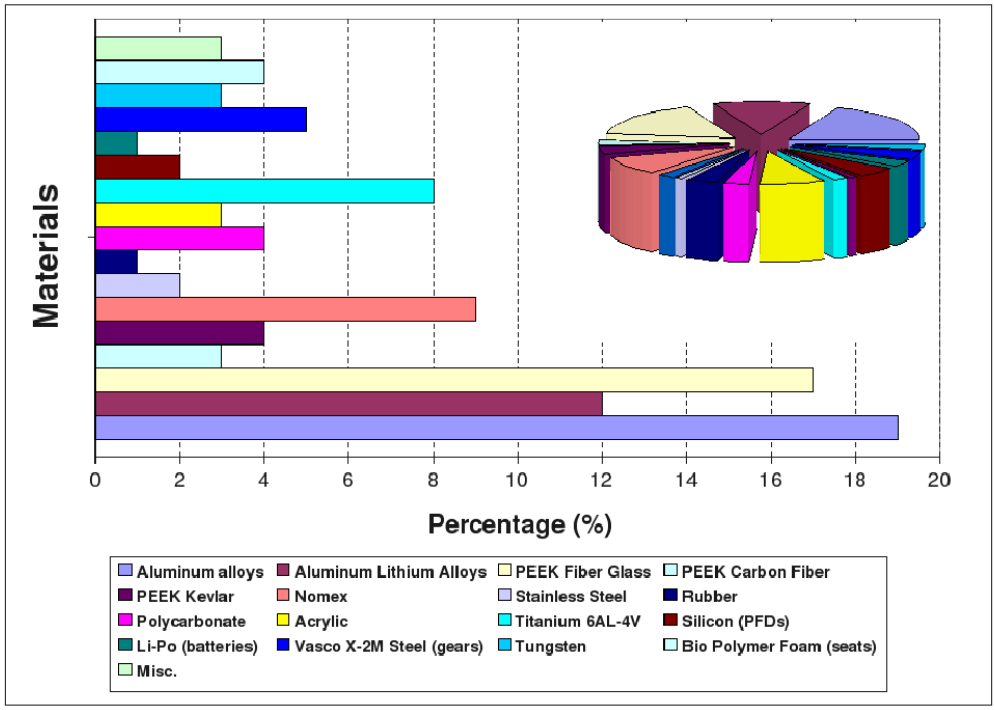

Figure 11.3: Breakdown of the *Griffin* total materials (by percent empty weight).

the alloys used. The primary and secondary bulkheads, as well as the longitudinal and keel beams of the *Griffin* were made of a commercially available aluminum lithium (Al-Li) alloy, Weldalite 049. Use of this material drove a weight reduction in the structural members without changing their shape. As such, no additional tooling would be required to support this modification. Although some Al-Li alloys exhibit reduced ductility and fracture toughness in the short transverse direction, Weldalite 049 was selected based on its excellent strength, corrosion and fatigue resistance, and crack propagation resistance. In addition, Weldalite 049 is weldable and displays no discernable cracking in highly restrained weldments.[61] This capability will permit many of *Griffin*'s components to be welded rather than attached with mechanical fasteners, which lowers part count and contributes to fatigue reduction. As a result, *Griffin*'s primary structure would be significantly easier and cheaper to manufacture and maintain, a significant consideration in both the commercial and marine operating environments. Although the method of fabrication and recycling are similar to conventional aluminum alloys, a one-time end-of-life-cycle investment is required to recycle the lithium.[61] This cost is amortized into the $5.73 million acquisition cost of the *Griffin*. Ultimately, the lithium reduces the weight of the aluminum alloy by about 3% for each percent added. Weldalite 049 contains just over 2% lithium, which results in a 7% reduction in density and a 10% increase in elastic modulus. These advantages directly support the RFP payload improvement requirement, without incurring any structural changes.

The engine and transmission deck of the *Griffin* was designed to be fabricated from titanium alloy because of its high strength-to-weight, excellent salt water and oil corrosion resistance, and superb heat and fire resistance. Even though titanium has long been considered a costly material, an advanced and currently feasible extraction process - as discussed in the "Production and Manufacturing" section - offers a potential cost reduction and significantly reduces environmental impacts.

11.2.2 Environmentally-Friendly, Cost-Effective Composites

11.2.2.1 Matrix Selection: Thermoplastic versus Thermoset The current aerospace industry "composite revolution" is driving substitution of composites for various metals used on earlier designs. As such, a significant number of helicopter airframe components on the baseline EC145 and other aircraft in the *Griffin*'s weight class are constructed of fiber reinforced composites, such as carbon fiber reinforced plastic.[62] These fiber reinforced materials can be separated into two categories: thermoset and thermoplastic polymer-based matrix composites. *Thermoset* polymers have strongly cross-linked molecular structures which decompose, instead of melt, with application of heat and upon solidification. These polymers include epoxides, which are typically formed as a two-part mixture of resin and hardener. Their molecular structure prevents thermosets from being reshaped.[63] *Thermoplastic* polymers have strong intramolecular bonds but weak intermolecular bonds, resulting in reversible melting and solidification processes and allowing reshaping of the material.[63] These polymers include materials such as polyether-ether ketone (PEEK) and polyphenylene sulfide (PPS). The aerospace industry typically implements fiber reinforced thermoset (FRTS) composites since the low pre-cure viscosities of the thermoset matrix at room temperature enables the reinforcing fibers to be impregnated at low pressures. The EC145 utilizes FRTS composites for the majority of its airframe skin. Thermoset polymeric composites also lend themselves to intricate shaped parts because of their pre-cure drapability and ample handling time to form the material around sharp contours of a mold. However, thermoset composites have several deficiencies, such as the need for long processing time, high-touch labor, large and expensive autoclaves,[64] as well as the inability to be readily reshaped or recycled. Recent advancements in composite manufacturing technology have, however, increased the adaptability of thermoplastic composites and the ability to fabricate elaborate parts. Through feasible automated manufacturing practices and resin transfer molding (RTM), which does not require an autoclave, thermoplastics can now achieve the same - if not better - performance than thermosets in conforming to complex composite parts.[65] The transition to thermoplastics is industry-wide as aerospace companies demand automated and repeatable manufacturing processes. For these reasons, thermoplastic polymers were selected for implementation on the *Griffin*.

Table 11.1: Relative advantages of thermoplastics over thermosets.

Material Properties	Relative Advantage	
	Thermoplastics	Thermosets
Corrosion resistance	xxx	xxx
Creep	xxx	xxx
Damage resistance	xx	x
Design flexibility	xxx	xxx
Fabrication	xx	xx
Fabrication time	xxx	xx
Final part cost	xxx	xx
Finished part cost	xxx	xx
Moisture resistance	xx	x
Physical properties	xxx	xxx
Processing cost	xxx	xx
Raw material cost	x	xx
Reusable scrap	xx	O
Shelf life	xxx	x
Solvent resistance	xxx	xx
Specific strength	xxx	xxx
Strength	xxx	xxx
Weight saving	xxx	xx

Note: xxx-best, xx-good, x-fair, O-Not applicable

11.2.2.2 Thermoplastic Advantages Fiber reinforced thermoplastic (FRTPs) composites offer the possibility of reusing industrial products as raw materials for new applications instead of being discarded.[66] This introduces the idea of "closed-loop" recycling, which saves valuable resources. As suggested by Kemmochi et al.,[66] after a FRTP component reaches the end of its useful life, it can be chopped up into shorter length fibers and remolded with the application of heat and pressure into a new product. Consequently, the useful life of a raw material can be extended from 20 to 80 years, considerably reducing the impact on the environment. In addition to recyclability, thermoplastics have a 10% higher specific strength than thermosets and offer improved fatigue strength. Localized repairs with minimal curing times are possible with thermoplastics. In addition, FRTPs are less sensitive to moisture-induced aging than thermosets. These are significant considerations in the maritime environment where maintenance capabilities are often limited. Additional advantages of thermoplastics are summarized in Table 11.1.[67]

11.3 Production and Manufacturing

11.3.1 Production Energy

Material production carries environmental penalties such as carbon dioxide (CO_2), waste heat, or dust. For each primary material in the *Griffin*, approximate values of the production energy and the corresponding CO_2 emissions were calculated. These values, as shown in Table 11.2[69] are *conservative* approximations based on current technology. As such, most of the values are expected to become more favorable before the *Griffin*s initial operational capability in 2015. This is particularly true for aluminum since the U.S. Department of Energy has committed to and demonstrated improvements in the emissions, reduction of cost, and reduction of the energy required for smelting - the most energy intensive part of aluminum production.[68] Table 11.2 also highlights a number of important factors governing material selection. When compared to aluminum alloys, PEEK based composites are not favorable from an energy or CO_2 standpoint. While manufacturing processes have advanced to viably permit an entirely PEEK composite airframe, the environmental impact was deemed excessive despite *Griffin*'s design goals of enhanced performance. As such, *Griffin* sacrifices some performance for environmental considerations, a growing trend in the rotorcraft industry. Furthermore, in places where the composites were used, glass reinforced PEEK was chosen wherever material stress requirements permitted. This minimized the cost, environmental impact and production energy required for the composite-based parts of the helicopter.

Table 11.2: Energy required and CO_2 emissions for the production of various materials.

Materials	**Primary Griffin Uses**	**Energy** (Btu/lb)	**Energy** (MJ/kg)	**CO_2** Burden (lb/lb)	**Notes**
Aluminum alloys	Skid gear, engine, hub, gearbox housing	81,700	190	12	
Al-Li Alloys	Primary bulkheads	87,290	203	12.8	
PEEK Fiber Glass	Main rotor, doors, empennage	141,900	330	20.7	
PEEK Carbon Fiber	Main rotor	218,870	509	33.7	
PEEK Kevlar	Tailboom	267,890	623	35.7	Ref.[70]
Nomex (nylon)	Main rotor, stabilizers	45,150	105	4	
Steel	Engine gears	10,750	25	2	
Stainless Steel	Fuel lines, tail skid	27,950	65	5.4	
Natural Rubber	Hub bearings, fuel tanks	17,200	40	-0.5	Negative CO_2 burden
Butyl Rubber	Hub bearings	34,400	80	2.1	
Polycarbonate (PC)	Front windshield, windows	47,300	110	4	
Titanium 6AL-4V	Engine, main rotor shaft, transmission deck	380,550	885*	41.5*	Current methods of extraction impact environment
Silicon (PFDs)	Avionics	24,467	56.9	3.2	
Lithium Polymer	Batteries	29,240	68	N/A	SO_x is primary pollutant
VASCO X-2M Steel	Transmission gears	55,900	130	8	
Tungsten	Main rotor blade nose weights	134,590	313	19.7	
Bio Polymer Foam	Seat Cushions	29,197	67.9	1.2	Scaled based on biofoams
Iron	Electric motors	7,052	16.4	1	
Copper	Wiring, slip-ring	27,090	63	4	
Epoxy	Paint, tail prop	38,700	90	3.2	Hexavalent chromium-free

*Subjected to change considerably with the use of the FFC Cambridge Process for extraction

The primary pollutants generated during production of lithium-polymer (Li-Po) batteries are sulfur oxides (SO_x), nitrous oxides (NO_x), and particulates such as soot. The amount of volatile organic compounds (VOC) created, however, is relatively low. Although the ability to reuse or recycle these batteries is quite poor, Li-Po batteries were selected because of their exceptional energy density. These batteries power the self-diagnostics of the advanced avionics suite and Health and Usage Monitoring System (HUMS) prior to engine startup and permit up to 20 minutes power for all installed electrical equipment in emergency situations - at a penalty of only 2.4 lb. In addition, Li-Po batteries are less flammable than lithium-ion batteries since the lithium is encased in a flame resistant polymer rather than metal.

As mentioned above, titanium was selected for *Griffin*'s transmission deck because of its high strength-to-weight ratio, excellent corrosion resistance, and superb heat and fire resistance. Titanium is ten times stronger and six times lighter than steel, but is very expensive because of its energy-intensive extraction method. Extracting titanium contributes to almost half of its final cost and more than 60% of the energy consumed during its production. Current methods of extraction include the Kroll process, which is very costly and energy intensive because the titanium is extracted with pyrometallurgy. Most pyrometallurgical processes require energy input to sustain the temperature at which the process occurs, and the energy is usually provided in the form of fossil fuel combustion, exothermic reaction of the material, or from electrical heat. As such, the Kroll process requires approximately 86,000 Btu to extract a single pound (200 MJ/kg) of titanium. The innovative yet feasible Fray-Farthing-Chen (FFC) Cambridge process permits titanium extraction through powder metallurgy for only about 10,750 Btu/lb (25 MJ/kg). The FFC Cambridge process is a new extraction method for titanium and its alloys from solid oxides by molten salt electrolysis. The titanium remains in solid phase and, unlike in pyrometallurgy, retains all of its properties. In addition to reducing energy consumption during titanium production, this process is also a potential energy reduction measure during manufacturing and recycling of titanium components at the end of their life cycle since the titanium is processed from a salt-like state. The FFC Cambridge process can thus reduce titanium costs by 40%. Implementation of this process not only contributes to the RFP and mission requirements, it demonstrates *Griffin*'s environmental conscience in an increasingly energy-dependent global community.

11.3.2 Manufacturing Energy

Table 11.3: Energy required at the manufacturing stage for various materials and processes.

Component Material	**Energy Cost (Btu/lb)**	**Energy Cost (MJ/kg)**
Aluminum	8,170	19
Steel	2,795	6.5
Epoxy-Based Composites		
Prepreg Production	17,200	40
Autoclave	258,000	600
Closed-Die	4,343	10.1
PEEK-Based Composites		
Prepreg Production	17,200	40
Resin Transfer Molding	5,504	12.8
Sheet Molding Compound	1,505	3.5

In addition to the energy consumed and pollution generated during the production of the materials, penalties accompany manufacturing raw materials into the specific parts used in the *Griffin*. While the expended energy and pollution vary considerably by process and component, an estimate for common processes related to the major components of the vehicle is shown in Table 11.3. Although thermoset composites are not used to any significant extent in the *Griffin*, their values are provided for comparison. Since manufacturing PEEK-based composites does not require energy- and time-consuming autoclaving, the manufacturing energy of thermoplastics is substantially reduced. This benefit is somewhat offset by the high energy required to produce PEEK as a raw material. The extreme energy consumption during the thermoset curing process, however, negates

the disparity in material acquisition cost. As such, PEEK composites are substantially more cost effective to produce and manufacture than their epoxy counterparts.

The significantly advanced capability realized through the *Griffin*'s Variable Energy Rotor and Innovative Transmission ArchitectureS (VERITAS) was critical to satisfying the performance improvements demanded by the RFP and required close scrutiny of the structural design and selected materials. To maintain its true derivative nature, the structural modifications of the *Griffin* were limited to those required to facilitate integration of the VERITAS to support the RFP and mission requirements. Several exposed components were streamlined for drag reduction and the tailboom was extended and strengthened to support the tail prop drive shaft. The front windscreen and cabin windows were also modified slightly to improve safety and passenger comfort. Lighter, stiffer and environmentally-friendly materials were implemented where possible. The *Griffin*'s airframe was designed to reduce energy consumption and life cycle costs, while maximizing component strength-to-weight and stiffness-to-weight ratios. Lightweight aluminum-lithium alloys and a significant amount of thermoplastic composite materials were implemented to support the RFP performance requirements and to lower fuel consumption. Designed to comply with Directive 2000/53/EC of the European Parliament, *Griffin* is also positioned as an industry leader in the effort to minimize the environmental impact of materials processing, manufacturing, and disposal.

12 Landing Gear Design

Helicopter landing gear enables safe landing and facilitates ground handling. Two primary functions define the design space: 1) absorbing vertical energy from impact while landing; 2) providing a resilient and stable suspension while avoiding ground resonance.

12.1 Landing Gear Classification

Helicopter landing gear can be classified into two main categories: 1) skid type and 2) wheel type. Skid landing gear is mechanically simple to design, light in weight, requires little maintenance, and is thus less costly than wheeled landing gear. Skid type landing gear suffers, however, from ground resonance effects and higher parasitic drag. Typical skid landing gear consists of forward and rear cross tubes and two skid tubes. Replaceable wear plates are typically added to the bottom of the skid tubes to prevent damage to the load bearing members. Provided that the landing velocities remain within the limits established by FAR Part 29, the energy generated is absorbed and attenuated through displacement of the cross tubes.

12.2 Landing Gear Selection

Table 12.1: Landing gear selection Pugh matrix.

Parameters	**Weights**	**Fixed Tricycle Gear**	**Retractable Tricycle Gear**	**Floats**	**Fixed Skids**	**Retractable Skids**	**Folding Skids**
Speed	5	2	5	1	3	4	3
Mass	5	3	1	3	5	1	2
Crashworthiness	4	4	3	4	4	3	3
Maintenance	3	2	1	3	4	1	1
Ground handling	3	5	5	2	2	2	2
Life Cycle Cost	5	2	1	2	4	2	3
Recyclability	3	2	2	3	4	3	3
Simplicity	2	3	1	3	4	2	3
Drag Penalty	4	2	5	1	3	4	3
NO_x Emisions	3	1	1	3	4	3	3
Weighted Total		95	96	89	**138**	94	97

The selection of the landing gear was based on the RFP requirements. The overall functionality of the landing gear within *Griffin*'s primary mission environment and the safety of the vehicle occupants were other critical design drivers. To aid the selection process, a Pugh matrix was constructed. As shown in Table 12.1, several key performance parameters spanning three broad categories were selected and subjectively weighted based on the RFP and mission requirements. The first parameter category addressed compliance with safety and structural demands while the second included the financial considerations of life cycle cost and required storage space. The last category focused on the environmental impact of the landing gear from "cradle-to-cradle."

Several landing gear designs were included in the Pugh matrix decision space and the impact of each performance parameter on the potential configurations was ranked. A rank of five was used to signify critical importance, while progressively lower values were used to indicate reduced importance. Based on the weighted totals calculated in the Pugh matrix in Table 12.1, the fixed skid landing gear was chosen for implementation on the *Griffin*.

12.3 Static Stability Angle Analysis

(a) Tip-over angle.

(b) Pitch angle

Figure 12.1: Center of gravity envelope of *Griffin*.

The position of the ground contact points in relation to the center of gravity of the helicopter defines the pitch and roll static stability angles. To ensure static lateral stability of the helicopter, the roll stability angle must be less than 60°.[72] Similarly, static pitch stability is guaranteed when the pitch angles is less than 30°. *Griffin*'s landing gear was designed to ensure pitch and roll stability. As shown in Fig. 12.1b, the roll/tip over angle is 56.2°, and the pitch angle is 26.8°.

12.4 Frequency Placement for Ground Resonance

When any helicopter is in contact with the ground, the phenomenon of ground resonance can occur if a natural frequency of the fuselage couples with the regressing lag mode of the rotor. This can occur at any rotor speed within the operational range. The *Griffin*'s landing gear was designed to avoid ground resonance by including adequate damping and carefully placing body natural frequencies. Should ground resonance occur, however, the pivot joint attaching the rear cross tube to the helicopter frame is adjustable[73] and offers that operator the capability of moving the coalescence of natural frequencies away from the critical ranges outlined in Fig. 5.17a.

12.5 Cross Tube Sizing and Fairing

The loads transmitted to the landing gear during a crash constitute the design load, as this is the largest force applied to the structure. To satisfy FAR 29.737, the limit load rating of each cross tube must equal or exceed the maximum limit load. *Griffin*'s maximum load was determined from the stroking distance of the energy absorbing seats and the allowable G-forces experienced by the occupants. The landing gear was thus designed to fail at a load equal to 25Gs applied to a single cross tube member. In the unlikely event of a crash, the gear was designed to break away from the fuselage while absorbing part of the energy. The fuselage and stroking seat would then be required to attenuate the remaining energy to the extent that a non-lethal deceleration would be transferred to the passengers and crew.

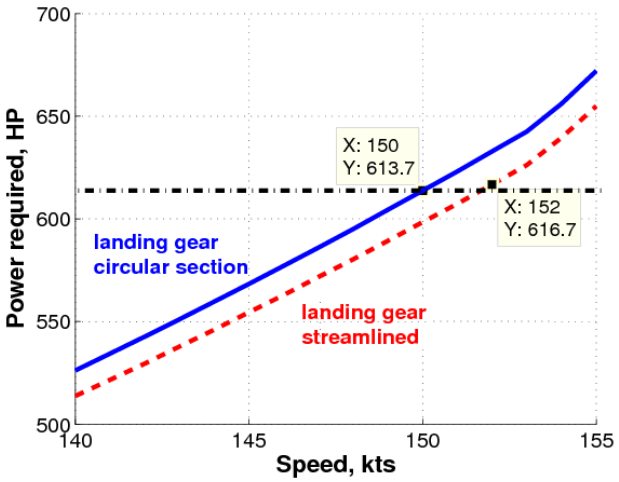

Figure 12.2: Contribution of the streamlined crosstube to *Griffin*'s speed increase.

The landing gear cross tube on the *Griffin* was designed as a hollow streamlined tube. By keeping the same circumference and material as that found in the circular aluminum alloy cross tube on the EC145, *Griffin*'s streamlined tube retained the identical moment of inertia and physical properties. D&E Aircraft of Florida currently manufactures streamlined aluminum struts[74] that could be readily implemented on *Griffin* for under 10% greater cost than the existing tubes on the EC145. Although slightly more costly, changing the effective cross-section of the landing gear cross tubes offers a significant localized drag reduction. Indeed, cylindrical structures have the same drag as an airfoil section with a thickness 25 times the cylinders diameter.[2] By implementing streamlined cross tubes, the equivalent drag flat plate area of the landing gear was reduced from 1.08 ft^2 to 0.61 ft^2, decreasing the total drag contribution of the landing gear of *Griffin* by 43%. As shown in Fig. 12.2, this simple modification increased forward cruise speed by 2 knots. The higher speed increases endurance by 2 minutes and 38 seconds and extends *Griffin*'s range by 9 nm. As such, the minimal changes made to the *Griffin*'s landing gear contributed directly to RFP requirements compliance by increasing speed, endurance, and range.

Figure 12.3: Skid landing gear designed for the *Griffin*.

The circular cross-section of the skid tube was retained to facilitate inclusion of a variety of mission-specific skid extension kits that are readily available for EC145 helicopters. These kits support *Griffin*'s primary mission and increase the overall utility

of the advanced rotorcraft. Indeed, emergency floats can be easily attached to the skid tubes for maritime operations and skid shoes can be added to increase the contact area for landing on soft terrain or mountain rescue missions. Ultimately, the critical design drivers extracted from the RFP, coupled with safety and environmental concerns, prompted the final landing gear design shown in Fig. 12.3.

13 Crash Safety and Comfort

13.1 Crashworthy Seat Design

Occupant safety is of critical importance in the unlikely event of a crash. Although *Griffin*'s landing gear skids were designed to absorb a significant amount of crash loads, energy absorbing systems were designed into the occupants seats to further limit the deceleration loads to non-lethal levels. Although a variety of energy absorbing seat technologies are available, they can be broadly categorized as Fixed Load Energy Absorbing (FLEA), Variable Load Energy Absorbing (VLEA), Variable Profile Energy Absorbing (VPEA), or Adaptive Energy Absorbing (AEA). Table 13.1 provides an overview of the energy absorbing seat concepts used in current operational rotorcraft.[75]

Table 13.1: Energy absorbing systems available for occupant seats.

Energy Absorber	Load Adjustability	Additional Weight
FLEA	No	Minimal
VLEA	Finite	Minimal
VPEA	Finite	Minimal
AEA	Continuous	Heavy

FLEA seats decelerate the occupant under a predetermined fixed load, as designed for the 50th percentile male, to maximize the effectiveness over a range of occupant weights.[75] Lighter occupants experience higher deceleration levels (g's) whereas heavier occupants experience lower g's, but risk a harmful end-stop impact. The g-level experienced by the seat occupant determines the risk of spinal injury[76] and should be limited to a maximum of about 12. VLEA and VPEA seats improve upon the FLEA concept by allowing finite adjustment of the stroking load and load profile, respectively. This approximately maintains the desired g-level in a crash across the entire occupant weight range. AEA seats utilize real-time sensing to monitor the crash environment and offer optimal load isolation through devices such as magnetorheological (MR) fluid dampers. These systems are, however, inherently geometrically bulky and have large weight penalties.[77]

After evaluation of the existing technology available for crashworthy occupant seats, a lightweight VLEA configuration was chosen. This concept will permit *Griffin* to accommodate the broadest range of occupant weights while maintaining the desired g-level for all personnel. These seats exceed current FAR Part 29 certification standards that limit maximum compressive lumbar loads to 1500 lb for a 50th percentile male occupant (170 lb or 77 kg). This loading is intended to limit spinal injury rates for non-military occupants to 20%.[75] The *Griffin* seat design is capable of attenuating lumbar loads to 12 g's or less for the entire anticipated occupant weight range: the 5th percentile female to the 95th percentile male. This design enhances safety by minimizing the risk of spinal injury in crash situations, ultimately contributing to lower insurance rates for *Griffin*'s operators.

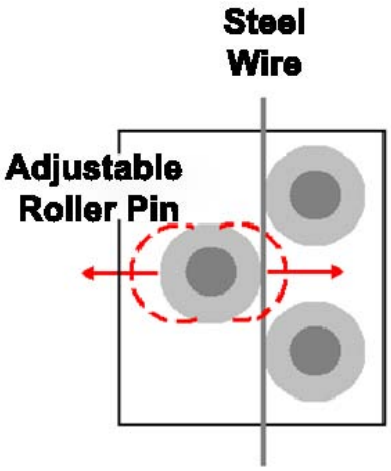

Figure 13.1: Adjustable roller pins for wire bender VLEA.

Griffin's VLEA seat employs a wire bender system designed to fit inside the

structure of the seat. This arrangement has negligible impact on cabin volume due to its compact geometric profile. Other energy absorber designs, such as inversion tubes, tube and die apparatuses, or crushable composites require more intricate mechanisms to offer adjustability. Figure 13.1 illustrates the adjustable roller pins for the wire bender VLEA concept. The system adjusts the limit load by simply positioning a roller pin with respect to the wire to increase or decrease the impedance of wire stroking motion. A load cell sensor determines the occupant weight and appropriately positions the roller pin to one of four pin settings. The 5th percentile female was used to determine the maximum available stroke necessary to ensure the seat did not bottom out. As such, *Griffin*'s seats stroke 8.3 in (21 cm) under a 9.5 g deceleration.

13.2 Vibration Isolation

Helicopter pilots and passengers are subjected to whole body vibration which causes physical fatigue, loss of situational awareness, and discomfort.[78] This is a topic of growing concern since most in-service helicopter seat systems are only designed to meet crashworthiness requirements.[78] As such, seats in current operational rotorcraft are typically rigidly attached to the airframe with no vibration isolation. Magnetorheological (MR) fluid dampers, however, offer a potential solution by isolating occupant seat vibration throughout the entire frequency spectrum[77] through a semi-active control strategy. Indeed, dominant rotor-induced (4 per revolution) vibrations have been experimentally reduced[79] by 90% for the 50th percentile male through the use of lightweight, controllable MR isolators. Although the *Griffin*'s rotor system employs trailing edge flaps to reduce vibration in the rotating frame, the low weight penalty of seat-mounted MR dampers justified inclusion of this technology in all seats to optimize vibration attenuation and occupant comfort.

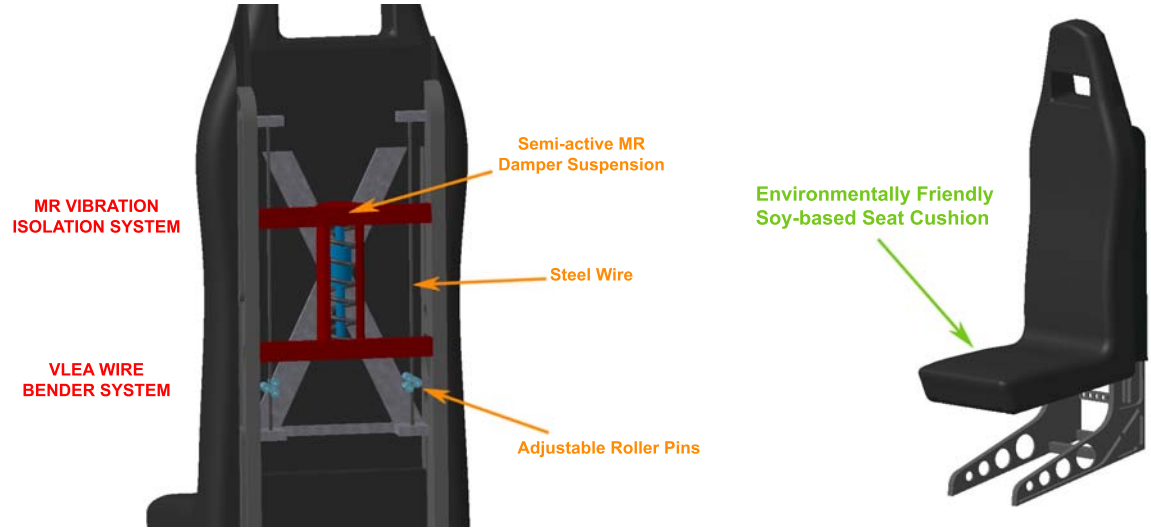

(a) Back view.

(b) Front view.

Figure 13.2: Cabin occupant seat design.

The *Griffin*'s advanced crashworthy seats' MR vibration isolators were integrated in-series with the VLEA wire bender system.[80] The vibration load path passes through the VLEA system to the MR isolation suspension, but the VLEA wire bender does not stroke until the requisite g-level is exceeded. In the event of a crash, the MR isolation suspension bottoms out inside its housing - effectively removing it from the load path - and allows the VLEA wire bender to stroke at the appropriate g-level to protect the seated occupant. Figure 13.2a details the occupant seat design, with the included VLEA and MR vibration isolator. Each MR damper contributes only 5.5 lb (2.5 kg) to the 28 lb (12.7 kg) total weight of each of *Griffin*'s seats. As designed, therefore, the enhanced crashworthiness and vibration reduction achieved in *Griffin*'s seats weighs less than the cockpit seats in the baseline EC145 and only 6 lb (2.7 kg) more than the cabin seats.

In addition to occupant safety and comfort, the *Griffin*'s seats were designed to minimize their impact on the environment.

Currently, vehicular seat manufacturers primarily use 100% petroleum-based polyol foam material - also called flexible polymer foam - for seat cushions, seat backs, head restraints, and arm rests. The extensive use of the foam results in 9 billion pounds of the material being consumed annually.[82] Recently the Ford Motor Company, an automobile manufacturer, conducted extensive research focused on replacing 40% of its seat foam composition with soy-based materials with the intent of reducing total environmental impact of the foam by 75% while offering a significant material cost savings.[82] Substitution of sustainable resources in this manner reduces dependency on petroleum while providing an end product with properties comparable to pure petroleum-based foam seat components. As such, all of the *Griffin*'s occupant seats incorporate this environmentally friendly technology. Not only then does *Griffin* offer exceptional performance, it is a leader within the rotorcraft industry in the continuing effort to reduce detrimental environmental effects.

14 Weight Analysis

14.1 Weight Breakdown

The weight estimates, based on the analysis of each respective section, is provided in Table 14.1. Lateral center of gravity (l.c.g.) is referenced from the nose of the aircraft. Vertical center of gravity (v.c.g.) is referenced from the ground.

Table 14.1: Weight breakdown

Component	(kg)	% GTOW	l.c.g., m	v.c.g., m
Airframe and Cowling	440.2	12.3	3.41	1.86
Engine	264.5	7.4	4.59	2.69
MGB	252	7.0	3.49	2.50
IGB	13	0.4	10.00	2.45
TGB	14.3	0.4	10.20	3.06
Main Rotor System	287.7	8.0	3.59	2.99
Tail rotor system	13.5	0.4	10.20	3.06
Tail rotor shaft	13.3	0.4	6.95	2.43
Prop Actuation Mechanism	5	0.1	10.20	3.06
Avionics	82.7	2.3	0.50	0.00
Landing Gear	72.8	2.0	3.12	0.28
Fuel System	68.7	1.9	3.25	0.71
Oil etc	53.4	1.5	4.59	2.69
Control System	38.3	1.1	3.49	2.50
Electric System	31.1	0.9	4.00	0.00
Empennage	4.2	0.1	9.26	2.37
Unusable fuel	15.1	0.4	3.25	0.71
Furnishings et al	83.6	2.3	2.90	1.42
Empty	**1753.4**	**49**	**3.71**	**2.07**
Fuel	694	19	3.10	0.71
	2447.4	**68**	**3.54**	**1.69**
Pilot	80	2.2	1.64	1.42
	2527.4	**70**	**3.48**	**3.31**
Cargo	1060	30	3.40	2.99
MTOW	**3587.4**	**100**	**3.46**	**3.22**

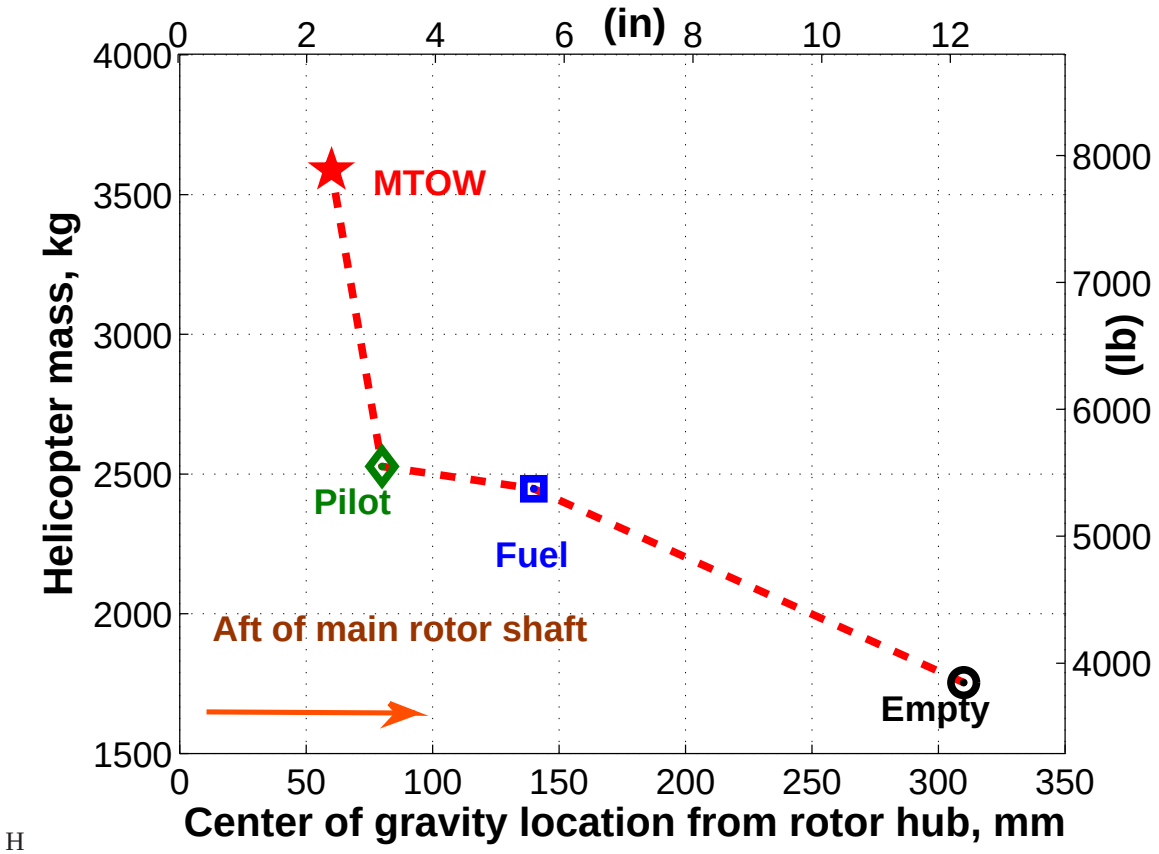

H

Figure 14.2: Center of gravity envelope.

14.2 Weight and Balance

The longitudinal center of gravity envelope for the *Griffin* is provided in Figure 14.2. Aftmost value for the center of gravity translation is 310 mm aft of the main rotor shaft. The resulting range of bending moments about the mast is well within the range of the controls.

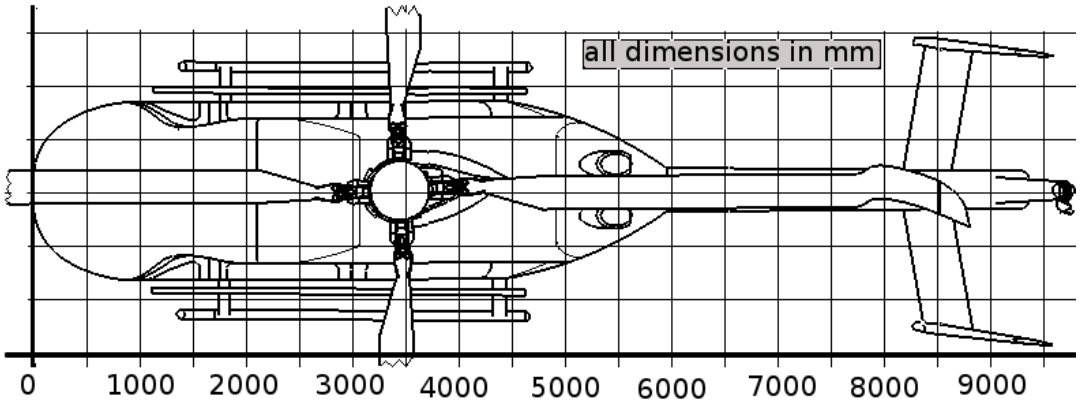

Figure 14.1: *Griffin* Station diagram.

15 Life Cycle Cost Analysis

The overall "cradle-to-cradle" cost of any helicopter can be subdivided into four independent expenses:

- *Research and development.*
- *Production.*
- *Operations and maintenance.*
- *Disposal and recycling.*

To mitigate technical developmental risk and reduce costs, *Griffin* relies extensively on proven commercial off-the-shelf (COTS) technologies. Lean manufacturing techniques are implemented where feasible to optimize acquisition costs and alleviate production risks. The ease of maintenance inherent in *Griffin*'s Variable Energy Rotor and Innovative Transmission ArchitectureS (VERITAS), combined with extensive HUMS sensor coverage, significantly reduces maintenance costs. The reliability of *Griffin*'s subsystems greatly increases the operational safety and service life of the vehicle. As such, the cost to insure *Griffin* would be lower than competing aircraft. Thoughtful consideration of the recyclability of materials early in the design process diminishes the challenges associated with disposal. The care taken in the design of *Griffin* ultimately lowers the helicopter's life-cycle costs by nearly 5% from those of a comparably equipped EC145. Acquisition, direct and indirect costs estimated from historical data and empirical models support this claim.

15.1 Acquisition Cost

The initial helicopter cost was estimated from the formula given by Harris and Scully[8789] and validated by subsystem cost relationships provided by Bell Helicopters. Though Harris and Scully's equation was originally derived in constant 1994 dollars, the consumer price index (CPI)[90] was utilized to correct calculations to current values. The actual costs of 72 helicopters from the Helicopter Blue Book[91] permitted the coefficients of Harris and Scully 's formula to be updated to:

$$\text{Base Price} = \$330 \times H \times {N_b}^{0.2106} \times {W_0}^{0.49996} \times P^{0.6018}$$

In this formula, H is a function of the number of rotors, engine type and number, country of manufacture, landing gear type, and whether the cockpit and/or cabin is pressurized.[87] N_b is the number of rotor blades, W_0 is the empty weight of the aircraft and P is the rated power of the installed engines.

When adjusted for inflation with the CPI, this relationship underestimated the cost of the baseline EC145, Agusta Westland 's A109E, Bell's 430, and Sikorsky's S-76C++ by an average of 5.2%. These calculated costs are detailed in Table 15.1. An average difference of 12.2% between equipped and base prices is noticeable. Incorporating the average errors between Blue Book and calculated base price and equipped prices, Harris and Scully's formula estimated the cost of *Griffin* to be $5.73 million (2009). This includes all equipment capable of cost estimation. *Griffin* costs about 9% more than a fully equipped EC145, yet out-performs other aircraft costing nearly twice as much.

Table 15.1: Comparison of actual and estimated base prices.

Million$ 2009	AW109E	EC145	Bell430	S-76C++
Blue Book Base Price	$4,291,109	$4,441,471	$7,360,723	$8,109,003
Estimated Base Price	$4,154,868	$4,238,474	$6,803,345	$7,660,245
Equipped Price	$4,713,150	$5,264,303	$8,643,079	$8,942,008
Equipped Price		$5,559,452		

Cost relationships provided by Bell Helicopter in the 2002 American Helicopter Society Student Design Competition RFP were used to validate the data obtained from the initial pricing calculations. The equations employ historical cost data, component

weight, aircraft production quantity and rate, and subsystem technology level from an amalgam of primary and secondary aircraft systems to estimate the average recurring cost to manufacture. Assuming an identical manufacturing rate of 75 aircraft per year for 450 total helicopters, these relationships were used to estimate manufacturing costs for the EC145 and *Griffin*. The sales price of the equipped aircraft was obtained by increasing the manufacturing cost by 50% to account for tooling amortization and profit, as recommended by Bell Helicopters.

15.2 Direct Operating Costs (DOC)

Because of the innovative nature of the *Griffin*'s VERITAS, extensive flight testing is anticipated. The potential market for remanufacturing over 470 existing or planned EC145 airframes, however, permits amortization of the estimated $18 million (2009) required for *Griffin*'s fatigue testing and performance envelope determination. As such, $38,500 is added to the final cost of each *Griffin*. Table 15.2 details the results of this analysis. If the remanufacturing of over 400 existing BK-117 airframes were included in this analysis, the flight testing costs could be reduced to less than $21,000 per aircraft.

Table 15.2: Cost estimation methodology validation.

Million $ (2009)	**EC145**	**Griffin**
Estimated Base Price	$4,238,474	$5,073,532
Equipped Price (1)	$5,264,303	$5,730,273
Equipped Price (2)	$5,559,452	$5,873,966

(1) Harris and Scully Method
(2) Bell Helicopter Method

Direct Operating Costs vary in direct proportion to flight hours. These expenditures consist of consumables, such as fuel, fuel additives, and lubricants; inspection costs; replacement and spare parts; and maintenance costs. A Life Cycle Cost program from *Conklin & de Decker Aviation Information*[5] was used to generate detailed financial data for a service life of 20 years and an annual usage rate of 400 flight hours. A 3% per year inflation rate was applied throughout the analysis.
DOC were initially calculated for the baseline EC145, and its cost fraction is shown in Fig. 15.1. Maintenance labor is the most dominant factor and consumes 30% of the total DOC because of the need for experienced technicians to conduct "hard time" and "on-condition" maintenance actions at high per-labor-hour fees. Fuel costs $3.99 per gallon of Jet-A as of May 2009[92] comprise a 27% share of total DOC and were derived directly from available data on the engines installed in each aircraft. The cruise fuel burn rate was calculated from the specific fuel consumption at maximum continuous power. Jet-A was assumed for all aircraft. At recommended cruise speed, *Griffin* consumes 49.1 gallons of Jet-A every hour. This represents a 17% reduction from the 59.2 gallons/hour required by the engines installed in the EC145 and demonstrates the vital need to reduce fuel consumption or at least optimize the engine and transmission operating conditions.

Eurocopter's recommended maintenance schedule for EC145 was used as a basis for the maintenance cost analysis. *Griffin* will require similar hourly inspections as the baseline aircraft, but because *Griffin* is virtually an all electric helicopter integrated with Health Usage Monitoring System (HUMS), maintenance costs for VERITAS as well as the airframe, dynamic components, and avionics is substantially reduced. Compared to EC145, total maintenance requirements are reduced by approximately 20% through implementation of Condition Based Maintenance. Also, *Griffin* 's advanced electrohydrostatic flight control actuators contribute to a lower overall part count and fewer life limited components.

Griffin's estimated DOC are compared with those of EC145 in Fig. 15.1. Table 15.3 provides a detailed comparison of average cost per flight hour during the 20 year life-cycle of *Griffin*, EC145, AW109E, S-76C++, and Bell 430. It is notable that the direct costs are approximately 9% lower than those of the EC145.

It must be noted that the method by which the DOC were calculated averaged per flight hour over 20 inflation-adjusted years of service life with 400 annual flight hours also includes the inevitable increase in maintenance costs as the vehicle ages. The values provided in Table 15.3, therefore, are much higher than the traditional DOC provided by the manufacturer. Table 15.4 details the difference between the 20 year, flight-hour-averaged, and inflation adjusted DOC with those of the first operational year.

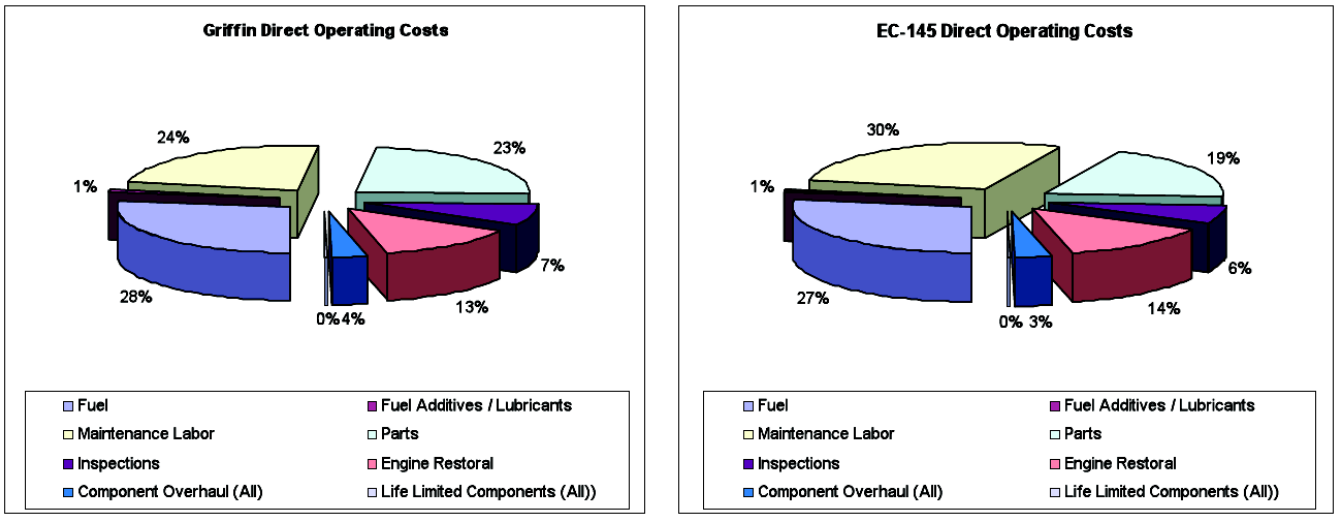

Figure 15.1: Direct operating costs for *Griffin* and the EC145.

Table 15.3: Comparison of direct operating costs (20-year average).

Direct Operating Cost ($/FH)	AW109E	EC-145	Bell 430	S-76C++	Griffin
Fuel / Lubricants	256	327	344	393	272
Maintenance Labor	356	337	383	490	337
Inspections	64	72	42	22	72
Parts	253	227	309	370	227
Engine Overhaul	260	162	308	216	115
Component Overhaul	50	41	79	226	42
Total	1239	1166	1465	1717	1065

Table 15.4: Comparison of life-cycle averaged DOC with 1st operational year DOC.

Direct Operating Cost ($/FH)	AW109E	EC-145	Bell 430	S-76C++	Griffin
20 Year Average DOC	1239	1166	1465	1717	1065
DOC for 1st Operational Year	285	326	352	482	285

15.3 Indirect Operating Costs (IOC)

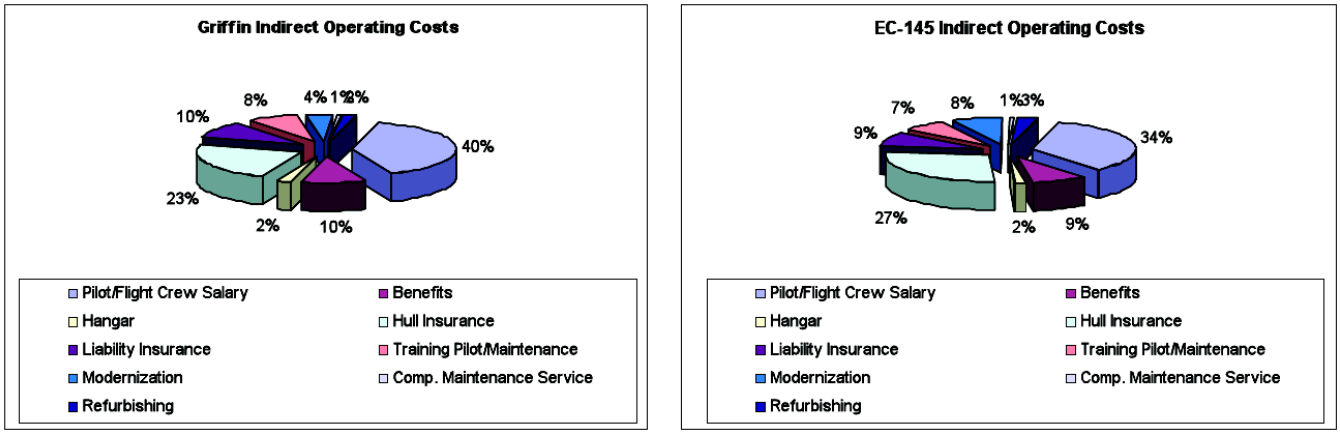

Figure 15.2: Indirect operating costs for *Griffin* and the EC145.

Indirect Operating Costs (IOC) are those expenses not associated with operating aircraft. Typically, IOC are comprised of two components: daily operating costs and fixed costs. Daily operating costs are those that are directly proportional to the number of days the helicopter is performing its mission, like salaries and benefits for flight crew and maintenance personnel. They may also include day-based maintenance costs associated with calendar-driven maintenance actions, if required. Fixed costs comprise the infrastructure and support systems required to sustain the aircraft, such as hangars, management personnel pay, insurance fees, and vehicle depreciation.

The IOC for *Griffin* and EC145 were also calculated using the *Conklin & de Decker* Life Cycle Cost program. Starting with the same assumptions, the results of the analysis are detailed in Fig. 15.2. The largest percentage of IOC is consumed by operator salaries and benefits. These comprise nearly 50% of *Griffin*'s total IOC and are based on qualification level and flight hour experience required for the type, model and series of rotorcraft. Hull and liability insurance comprise another 33% of *Griffin*'s IOC. The liability insurance cost is currently rated at $25,000 per year and is equal for all types of helicopters. Hull insurance cost, however, is calculated as a percentage of insured value. As such, these insurance fees vary with the initial acquisition cost. This disparity is clear in Fig. 15.2, as EC145's hull insurance consumes over 27% of IOC.

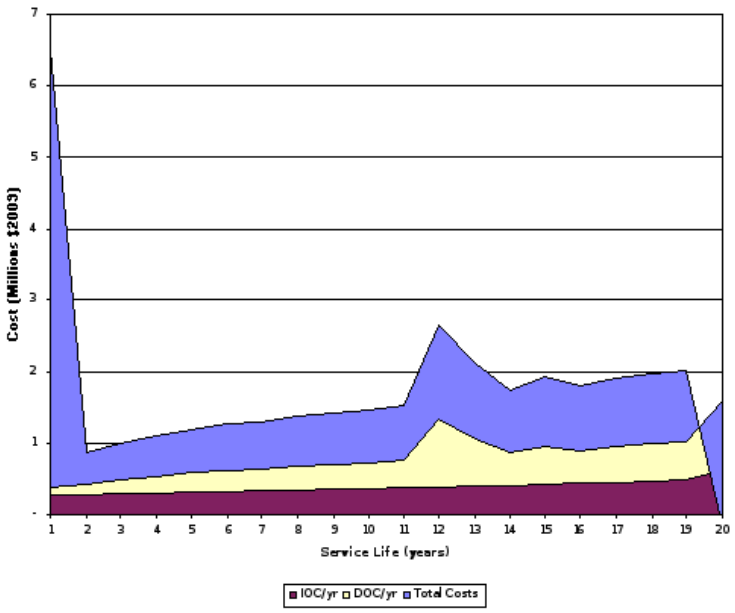

Figure 15.3: Cumulative Ownership Costs for *Griffin*.

The salary *Griffin*'s pilot is assumed to equal that of the EC145's operator due to the derivative nature of *Griffin* and the resultant physical similarities. Hull insurance percentage was also held equal to the 1.5% of insured value used for EC145. As detailed in Table 15.5, *Griffin*'s life-cycle averaged indirect operating costs per year are virtually

identical to those of the EC145. The slightly increased hull insurance expense accompanying *Griffin*'s greater acquisition cost is offset by the reduction in modernization and refurbishment costs required over the life cycle of this state-of-the-art rotorcraft.

The *Conklin & de Decker* Life Cycle Cost program also provided cumulative costs of operation on an annualized basis. *Griffin*'s cumulative ownership costs and annual operating costs per flight hour are highlighted in Fig. 15.3. Table 15.6 compares the ownership costs of *Griffin* with several other helicopters in the 3 to 5 ton weight class. The dominating initial value in Fig. 15.3 represents the initial acquisition cost of *Griffin*. The large operating cost peak near year 12 corresponds to significant maintenance actions notably overhaul of the engines, transmissions, and several life-limited dynamic components at 5000 total flight hours.

Table 15.5: Comparison of indirect operating costs.

Indirect Operating Cost ($/FH)	**AW109E**	**EC-145**	**Bell 430**	**S-76C++**	**Griffin**
Pilot/Flight Crew Pay	$167,940	$167,940	$167,940	$167,940	$167,940
Hangar	$6,718	$6,718	$6,718	$6,718	$6,718
Hull Insurance	$94,622	$106,090	$171,598	$176,485	$114,704
Liability Insurance	$33,588	$33,588	$33,588	$33,588	$33,588
Training	$26,870	$26,870	$26,870	$26,870	$26,870
Modernization	$26,870	$31,349	$31,349	$31,349	$25,078
Refurbishing	$9,472	$12,629	$12,629	$15,155	$10,103
Total	$366,079	$385,184	$450,691	$458,105	$385,001

The smaller peak following the main rework phase is driven by life-limited component inspection, overhaul, or replacement. *Griffin*'s residual value of over $3.5 million significantly reduces the ownership costs near the end of its service life. The total cost of ownership over the 20 year service life with a 400 annual flight hour usage rate is thus calculated to be $18.6 million for *Griffin*. This represents a 4.5% savings in total cost of operation when compared to EC145's $19.5 million. Ultimately, careful materials selection, system design, fabrication techniques, and implementation of advanced yet reliable COTS components has provided *Griffin* a quantum leap in helicopter capability at a lower cost to own and operate.

Table 15.6: Cumulative ownership cost comparison.

Ownership Cost ($/FH)	**AW109E**	**EC-145**	**Bell 430**	**S-76C++**	**Griffin**
Acquisition	$4,713,200	$5,264,300	$8,514,800	$8,942,000	$5,691,700
DOC	$9,916,700	$9,327,000	$11,720,000	$13,737,700	$8,521,800
IOC	$7,508,600	$7,903,000	$9,283,100	$9,436,600	$7,908,500
Residual	$3,135,900	$3,034,400	$5,172,900	$5,474,300	$3,528,000
Total	$19,002,600	$19,459,900	$24,345,000	$26,642,000	$18,594,000

GRIFFIN

Mission Capabilities

16 Mission Capabilities

The *Griffin's* enhanced capabilities provide it with great versatility. The multi-mission capable *Griffin* can be outfitted to provide exceptional performance in the execution of several roles: humanitarian aid, VIP transport, mountain search and rescue, border patrol, and unmanned surveillance. In all missions, the *Griffin* is provided with 20 minutes of reserve fuel.

16.1 Humanitarian Aid

The *Griffin* was designed to provide the performance necessary to execute a ship-based humanitarian aid mission to provide rapid disaster relief. The mission profile calls for the transport of 2340 lb of supplies to a relief site 125 nm away at a speed of 176 kts. Since the relief site may be difficult to locate, 2 hours of loiter time are provided at the site before the *Griffin* is to return to the ship for landing.

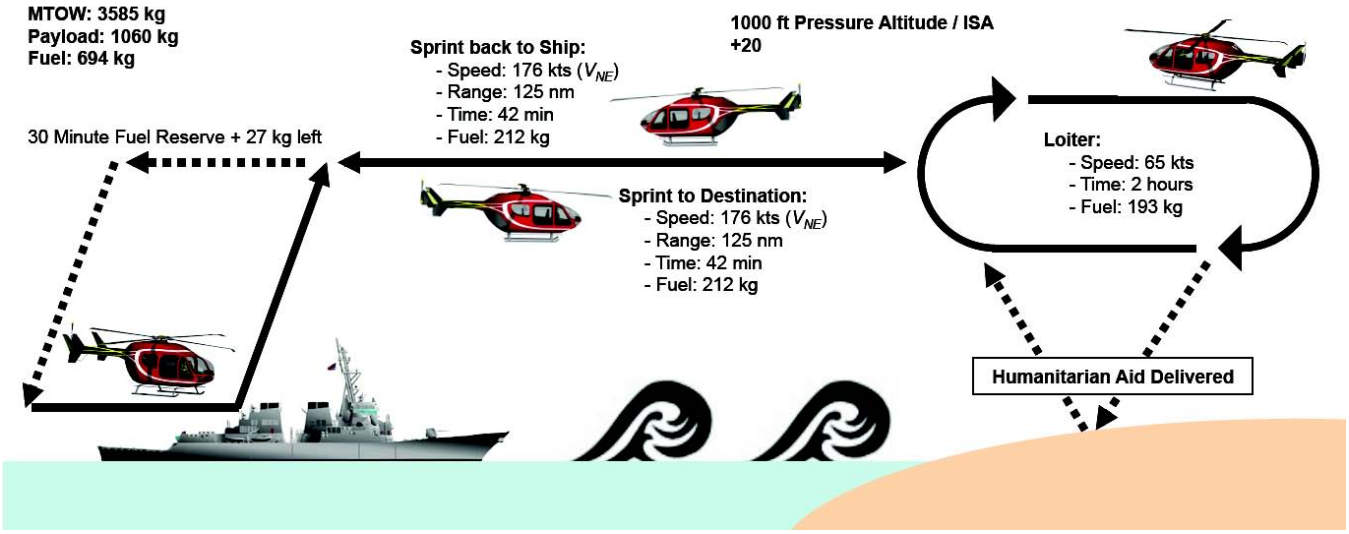

Figure 16.1: Humanitarian mission profile.

16.2 VIP Transport

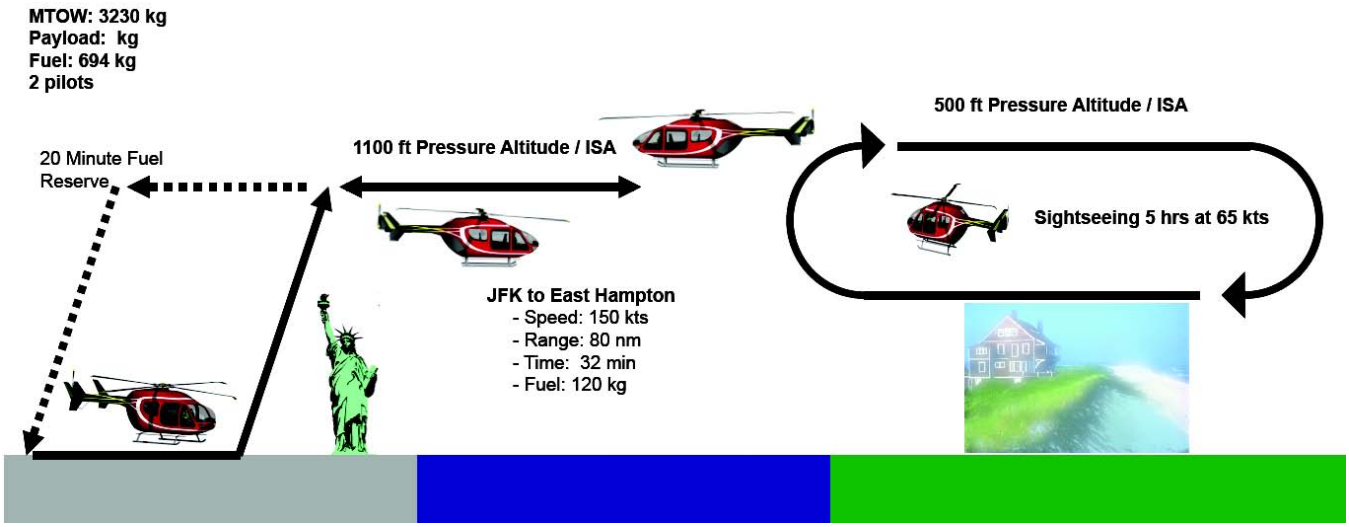

Figure 16.2: VIP mission profile.

In the VIP transport role, the *Griffin* is designed to comfortably carry four passengers. Special care is taken in this configuration to isolate the cabin from noise and preserve cabin space. The additional weight of furnishings and equipment for this mission are listed in Table 16.1.

Figure 16.3: VIP mission - seating.

Table 16.1: Mission equipment for VIP configuration.

VIP mission equipment	Weight (lb)	Weight (kg)
VIP cabin layout	59.5	27.0
Cabin upholstery	44.0	20.0
Soundproofing	11.5	5.2
Cabin carpet	9.5	4.3
Cabin washable cover	8.8	4.0
Protective carpet cover	4.9	2.2
Total	**138.2**	**62.7**

16.3 Mountain Search and Rescue

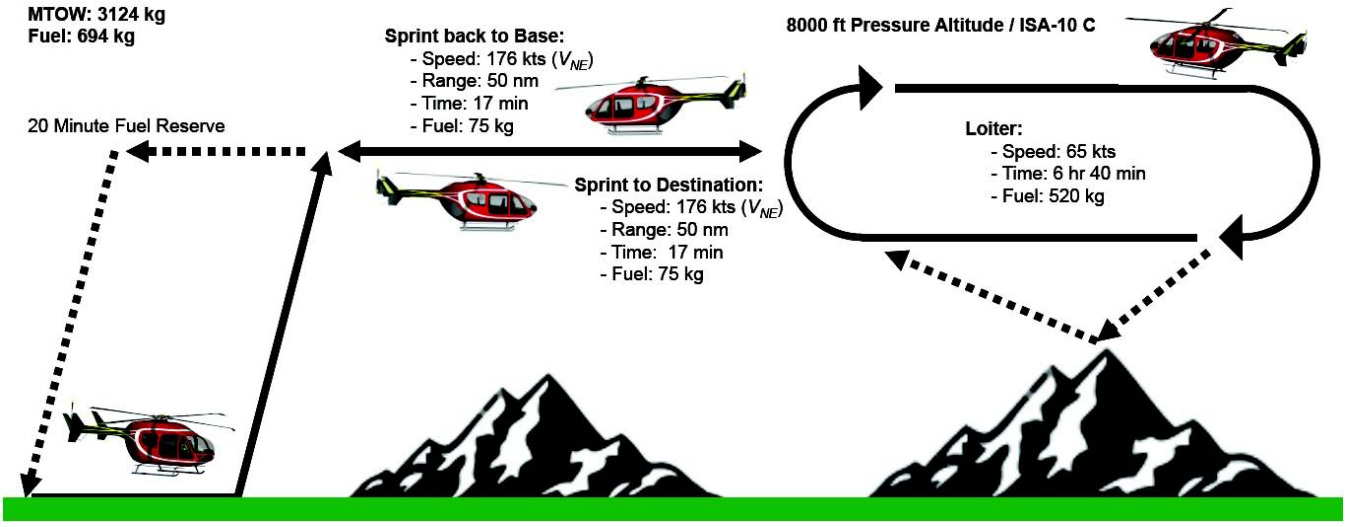

Figure 16.4: SAR mission profile.

The *Griffin* is well suited to performing Search And Rescue (SAR) missions, even at high altitude. In the mountain search and rescue role the *Griffin* ascends to an 8000 ft altitude with a pilot, co-pilot, and two crew members to operate a rescue hoist. The efficient VERTIAS allows the *Griffin* to loiter for an extended period of time, despite the high density-altitude. Searchlights

and Foward Looking InfraRed (FLIR) allow successful missions to be executed at night or in poor weather. Table 16.2 lists the mission equipment provided for this configuration.

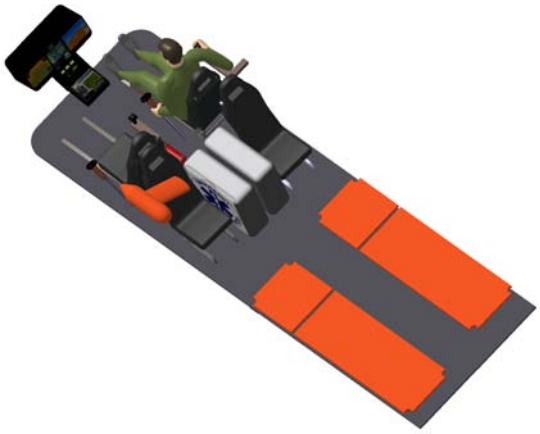

Figure 16.5: Mountain SAR mission - seating.

Table 16.2: Mission equipment for mountain SAR configuration.

Mountain SAR mission equipment	Weight (lb)	Weight (kg)
FLIR systems	45.2	20.5
Searchlight and mount	34.7	15.5
Strobe lights, white	4.4	2.0
Night vision goggle compatible light	9.9	4.5
Night vision goggle compatible cockpit	2.6	1.2
Loudspeaker / siren	22.3	10.1
Quick change EMS kit, Aerolite	73.9	33.5
Hoist with observation light	177.5	80.5
Tactical radio	11.0	5.0
IRIDIUM satellite phone	11.0	5.0
Total	**392.4**	**178.0**

16.4 Border Patrol

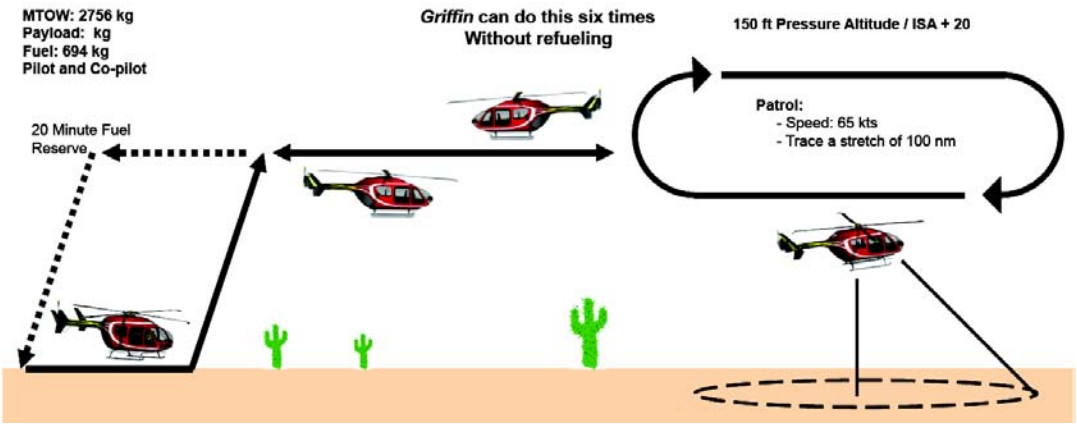

Figure 16.6: Border patrol mission profile.

The *Griffin* is a powerful asset during border patrol operations because of the high efficiency of VERITAS. In this role, the *Griffin* can fly back and forth across a 100 nm stretch at 65 kts three times in each direction before needing to refuel. In this fashion, a small fleet of 17 *Griffins* could patrol the entire 1700 nm US-Mexico border for 6 hours, 15 minutes. The mission equipment for this role is shown in Table 16.3.

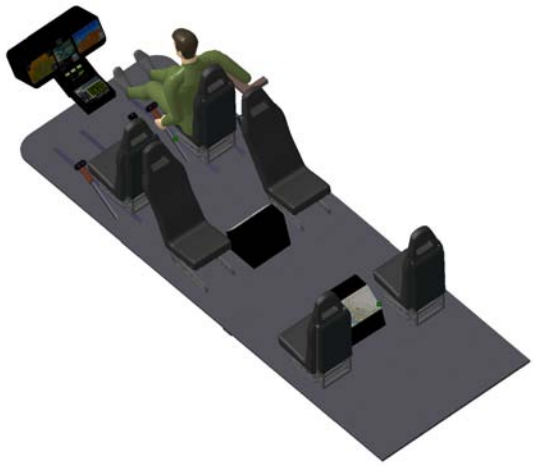

Figure 16.7: Border patrol - seating.

Table 16.3: Mission equipment for border patrol configuration.

Border patrol mission equipment	Weight (lb)	Weight (kg)
Enhanced co-pilot controls / avionics	12.3	5.6
FLIR systems	45.2	20.5
Searchlight with IR filter and mount	77.4	35.1
Strobe lights, white	4.4	2.0
Night vision goggle compatible light	9.9	4.5
Night vision goggle compatible cockpit	2.6	1.2
Loudspeaker / siren	22.3	10.1
Rappelling kit	38.6	17.5
Tactical radio	11.0	5.0
IRIDIUM satellite phone	11.0	5.0
Total	**243.0**	**110.2**

16.5 Unmanned Surveillance

The *Griffin* may also be converted to autonomous operation as an Unmanned Air Vehicle (UAV). All internal furnishings are removed in this configuration in order to install addition fuel tanks in the cabin for a total fuel capacity of 3,953 lb. Combined with the high efficiency of the *Griffin*, this allows for an extremely long endurance of 18 hours, 37 minutes. At a speed of 65 kts, the *Griffin* UAV could cover over 1200 nm without refueling.

Non-conventional Features of Griffin

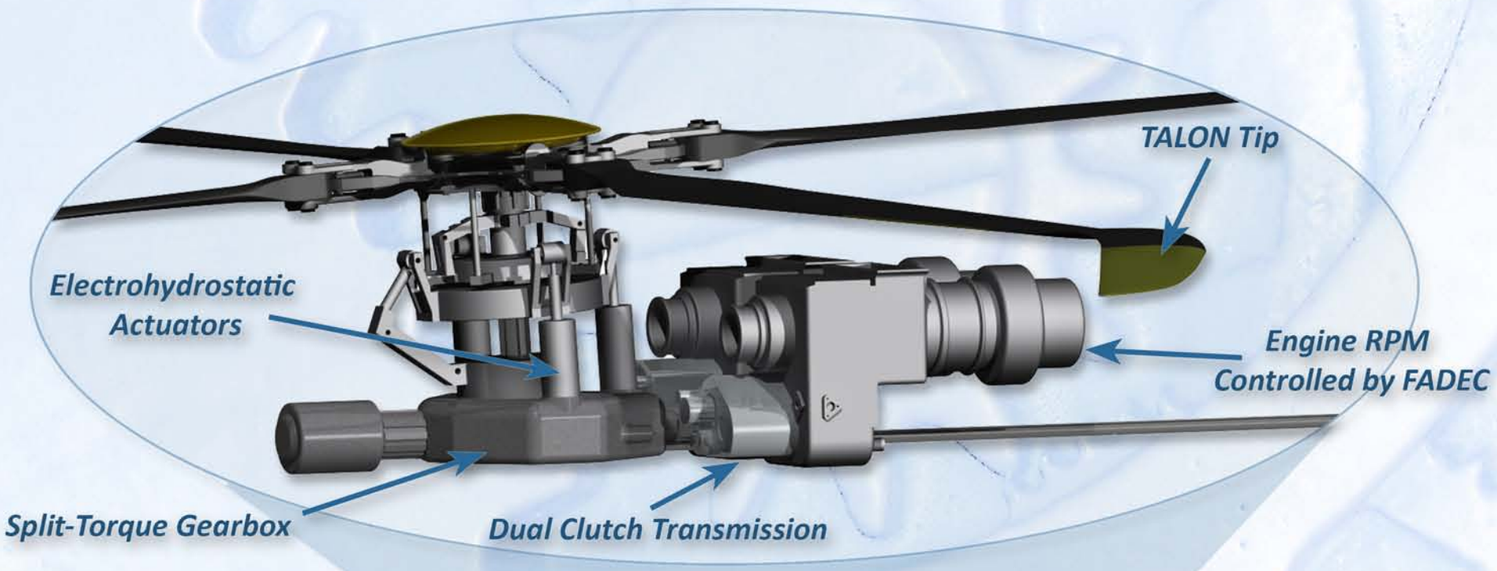

Griffin's Rotor/ Drive System: Variable Energy Rotor and Innovative Transmission ArchitectureS (VERITAS)

17 Summary

Bridging the capability gap between hover and forward flight performance has often been attempted, but never realized without significant penalties in the utility of the helicopter. The *Griffin* succeeds where others have not, through a dedication to innovative yet practical engineering. The VTOL technologies of variable tip speed and thrust compounding were identified through quality function deployment as the best parameters to increase the speed, payload, range, endurance, and reduce noise signature. Rather than employing disparate technologies, the effects of modulating tip speed and propulsive force are complementary. Together, they form a variable *energy* rotor system that, when optimally modulated by the non-conventional drivetrain, endows the emphGriffin truly exceptional performance. The capability of the Variable Energy Rotor and Innovative Transmission ArchitectureS is strikingly clear. Compared to the baseline EC145, *Griffin* cruises 15

Consistent with the RFP requirements, the *Griffin* is a derivative aircraft in every sense of the word. Its MTOW is within 4 lbs of the EC145 and implementing the non-conventional rotor/drive system VERITAS requires no significant structural changes. The modest weight gains from the VERITAS drivetrain are reclaimed by utilizing state-of-the-art materials in the *Griffin* airframe and a low-weight comprehensive MEMS-based avionics package.

Beyond its performance improvements, the *Griffin* also sets the bar high in environmental considerations. The EC145 hydraulic flight control system is replaced with triple-redundant fly-by-wire controls, and so the possibility of hydraulic oil leakage is eliminated. Materials selection is done with a cradle-to-cradle philosophy in mind so most components of the *Griffin* are recyclable. And in such energy conscious times, how appropriate is *Griffin*s superior capability at lower fuel requirements!

In closing, the evidence of the superiority of the *Griffin*is quite clear. The *Griffin*s capability of truly exceptional hovering and forward flight performance is the key to its success, and the nonconventional rotor/drive system VERITAS enables this capability. Recent programs, such as DARPAs Mission Adaptive Rotor Program, support the idea that flight-adaptive rotor systems will be the future of rotorcraft. But, with *Griffin*, that future is now.

Table 17.1: **Data sheet**

		Griffin	EC145
Standard Accommodation		1 + 9	
WEIGHTS			
Design Gross Weight	lb (kg)	7891 (3587)	7887 (3585)
Empty Weight		3858 (1753)	3951 (1792)
Payload (no fuel)		2332 (1060)	2242 (1019)
Fuel		1527 (694)	
SPEEDS			
Speed for Best Endurance	kts (kmph)	65 (120)	
Speed for Best Range		100 (185)	110 (204)
Recommended Cruise Speed		150 (278)	131 (243)
Never Exceed Speed		176 (326)	150 (279)
PERFORMANCE			
Maximum Range	nm (km)	590 (1093)	360 (666)
Maximum Endurance	h:min	07:24	04:12
HOGE Ceiling	ft (m)	7400 (2256)	9200 (2800)
Rate of Climb @ VBE	ft/min (m/min)	2600 (793)	1800 (549)
MAIN ROTOR			
Diameter	ft (m)	36.08 (11)	
Chord		1.05 (0.32)	
Number of Blades	–	4	
Tip Speed (hover)	ft/s (m/s)	723.5 (220.6)	
TAIL PROP/ROTOR			
Diameter	ft (m)	5.74 (1.75)	6.43 (1.96)
Chord		0.43 (0.13)	0.66 (0.20)
Number of Blades	–	2	
Tip Speed	ft/s (m/s)	751.4 (229.1)	730.1 (222.6)
POWERPLANT (x 2)			
Model	–	RR 250-C30	TM Arriel 1E2
Weight	lb (kg)	253 (115)	276 (125.5)
Takeoff Power	hp (kW)	650 (485)	748 (550)
Max. Continuous Power		557 (416)	701 (516)
SFC @ TOP	lb/hp/hr (kg/kw/hr)	0.592 (0.361)	0.573 (0.349)
LIFE CYCLE COSTS			
Acquisition Cost (base)	2009 USD	5.07M	4.24M
Direct Operating Cost / FH		1065	1166
Indirect Operating Cost /Year		0.36M	0.36M

References

[1] M. N. Tishchenko, V. T. Nagaraj and I. Chopra, "Preliminary Design of Transport Helicopters," *Journal of the American Helicopter Society*, Vol. 48 (2), April 2003, pp. 7179.

[2] R. Prouty, K. P. Krieger *Helicopter Performance, Stability, and Control*, 1st ed., Publishing Company, Florida, 1995.

[3] W. Johnson, G. K. Yamauchi and M. E. Watts, "Design and Technology Requirement for Civil Heavy Lift Rotorcraft," *Proceedings of the American Helicopter Society Heavy Lift Aircraft Design Conference*, San Francisco, CA, Jan 2006.

[4] F. Farassat, "Linear Acoustic Formulas for Calculation of Rotating Blade Noise," *AIAA Journal*, Vol. 19(9), 1981, pp. 1122-1130.

[5] "Conklin & de Decker Aircraft Cost Evaluator," http://www.conklindd.com.

[6] J. Davis, "Design Methodology for Developing Concept Independent Rotorcraft Analysis and Design Software," M. S. Thesis, Georgia Institute of Technology, Nov. 2007.

[7] "New Transient Limit and Power Turbine RPM (NP) Steady State Operation Avoidance," Bell Helicopter Service Bulletin 230-05-33, June 2005.

[8] S. Rao and Y. Xiong, "A Hybrid Genetic Algorithm for Mixed-Discrete Design Optimization," *J. Mech. Des.*, Vol. 127, pp. 1100, 2005.

[9] A. Bellocchio, "Drive System Design Methodology for a Single Main Rotor Heavy Lift Helicopter," M. S. Thesis, Georgia Institute of Technology, Dec. 2005.

[10] P. Marklund and R. Larsson, "Wet Clutch Friction Characteristics Obtrained from Simplified Pin on Disk Test," *Tribology International*, Vol. 41 (9), 2008, pp. 824-830.

[11] T. Brown and H. Rothblatt, *Machine Design Handbook*, McGraw Hill, New York, 2006.

[12] G. Lechner and H. Naunheimer, *Automotive Transmissions: Fundamentals, Selection, Design and Application*, Springer-Verlag, Berlin, 1999.

[13] R. Handschuh, D. Lewicki and R. Bossler, "Experimental testing of prototype face gears for helicopter transmissions," NASA-TM-105434, Jan. 1992.

[14] F. L. Litvin, J. C. Wang, R. B. Bossler Jr., Y. J. D. Chen, G. Heath, "Application of Face-Gear Drives in Helicopter Transmissions," *J. Mech. Des.*, 116, 672, 1994.

[15] T. Krantz, M. Rashidi and J. Kish, "Split Torque Transmission Load Sharing," NASA-TM-105884, Oct. 1992.

[16] R. Filler, G. Heath, S. Slaughter and D. Lewicki, "Torque Splitting by a Concentric Face Gear Transmission," *Presented at the 58th Annual American Helicopter Society Forum*, Montreal, Canada, June 2002.

[17] R. Bill, "Summary Highlights of the Advanced Rotorcraft Transmission (ART) Program," ADA-302568, Jul. 1992.

[18] R. Niggemann, S. Peecher and G. Rozman, "270-VDC/Hybrid 115-VAC Electric Power Generating System Technology Demonstrator," IEEE CH3007, Feb. 1991.

[19] J. G. Leishman, *The Helicopter: Thinking Forward Looking Back*, 1st ed., College Park, MD, College Park Press, 2007.

[20] D. Lednicer, "The Incomplete Guide to Airfoil Usage," UIUC Applied Aerodynamics Group, 2007, University of Illinois at Urbana-Champaign, 31 Mar. 2009, http://www.ae.uiuc.edu/m-selig/ads/aircraft.html.

[21] W. G. Bousman, "Aerodynamic Characteristics of SC1095 and SC1094 R8 Airfoils," NASA TP-2003-212265, December 2001.

[22] J. G. Leishman, *Principles of Helicopter Aerodynamics*, 2nd ed., New York, NY, Cambridge University Press, 2006.

[23] W. T. Yeager et al., "Peformance and Vibratory Loads Data from a Wind Tunnel Test of a Model Helicopter Main Rotor Blade with a Paddle-Type Tip," NASA TM-4754, May 1997.

[24] M. A. McVeigh, and F. J. McHugh, "Recent Advances in Rotor Technology at Boeing Vertol," *38th Annual Forum of the American Helicopter Society*, Anaheim, CA, May 1982.

[25] R. Harrison, S. Stacey, and B. Hansford, "Berp IV: The design, Development and Testing of an Advanced Rotor Blade," *64th Annual Forum of the American Helicopter Society*, Quebec, Canada, April 2008.

[26] J. Bao, V. T. Nagaraj, I. Chopra and A. P. F Bernhard, "Development of Mach Scale Rotors with Tailored Composite Coupling for Vibration Reduction," *Journal of Aircraft*, Vol. 43(4), pp. 922-931, 2006.

[27] I. Chopra and G. Bir, "UMARC Theory Manual," University of Maryland, College Park, November 1991.

[28] J. L. Smith, E. C. Palacios, and J. L. Rose, Investigation of an Ultrasonic Ice Protection System for Helicopter Rotor Blades," *64th Annual Forum of the American Helicopter Society*, Quebec, Canada, April 2008.

[29] MGC-841 MG Chemicals Super Shield Conductive Coating, http://www.mgchemicals.com/products/841.html, accessed April 23 2009.

[30] P. Konstanzer, B. Enenkl, P. A. Aubourg, P. Cranga, "Recent Advances in Eurocopters Passive and Active Vibration Control," *64th Annual Forum of the American Helicopter Society*, Quebec, Canada, April 2008.

[31] F. Straub, V. Arbabd, T. Birchette and B. Lau, "Wind Tunnel Test of the SMARTActive Flap Rotor," *65th Annual Forum of the American Helicopter Society*, Grapevine, Texas, 2009.

[32] *Aeronautical Design Standard - Requirements for Rotorcraft Vibration Specifications Modeling and Testing*, ADS-27A-SP, United States Army Aviation and Missile Command, May 2006.

[33] I. Chopra, "Review of State of Art of Smart Structures and Integrated Systems," *AIAA Journal*, Vol. 40, No. 11, 2002, pp. 2145-2187.

[34] Maxon Motor, Brushless DC Motor Data Sheets, http://www.maxonmotor.com, 2008.

[35] C. R. Theodore, R. P. Cheng, and R. Celi, "Effects of Higher Harmonic Control on Rotor Performance," *56th Annual Forum of the American Helicopter Society*, Virginia Beach, VA, May 2000.

[36] G. Padfield, *Helicopter flight dynamics: the theory and application of flying qualities and simulation modeling*, 1st ed., Blackwell Pub, 2007.

[37] *EC145 Technical Data*, http://www.eurocopter.com/ec145/TD EC145.pdf, 12 Apr 2009.

[38] "Handling Qualities Requirements for Military Rotorcraft," ADS-33E-PRF, US Army Aviation and Missile Command, 2000.

[39] P. Martin, C. Tung, A. Hassan, D. Cerchie, and J. Roth, Active Flow Control Measurements and CFD on a Transport Helicopter Fuselage," *61st Annual Forum of the American Helicopter Society*, Vol. 61, No. 1, Grapevine, TX, June 2005, pp. 349.

[40] Eurocopter, *EC145 Flight Manual*.

[41] R. Prouty, "Fly-by-wire," *Vertiflite*, Spring 2009.

[42] "Chelton Flight Systems," http://www.cheltonflightsystems.com/HeliSAS.html, 12 Mar 2009.

[43] Bose, http://www.bose.com/, 12 Mar 2009.

[44] "Chelton Flight Systems," http://www.cheltonflightsystems.com, 12 Mar 2009.

[45] *Aeronautical Design Standard (ADS) Handbook for Condition Based Maintenance Systems for US Army Aircraft*, ADS-79-HDBK, United States Army Aviation and Missile Command, Aviation Engineering Directorate, January 2009.

[46] A. Vincent, "New technologies in rotorcraft mechanical and rotor systems," http://www.midlandsaerospace.org.uk/cgi-bin/maa/SISite/data/files/AgustaWestland.pdf.

[47] B. McManus, and K. Landis, "Advanced Scout Helicopter (ash) Fly-by-Wire Flight Control System Preliminary Design volume I: System Design and Analysis," Boeing Vertol, May 1981.

[48] K. Landis, E. Aiken, K. Hilbert., and P. Dunford, "A Piloted Simulator Investigation of Side-Stick Controller/Stability and Control Augmentation System Requirements for Helicopter Visual Flight Tasks," *39th Annual Forum of the American Helicopter Society*, St. Louis, MO, May 1983.

[49] W. DeBellis, *Anthropometric Considerations for a Four-axis Side-arm Flight Controller*, N86-32993, U.S. Army Human Engineering Laboratory Aberdeen Proving Ground, MD.

[50] *Sikorsky Aircraft Engineering Report*, SER-70602, pp. 50-51.

[51] J. F. et al., "UH-60m Upgrade Fly-by-Wire Flight Control Risk Reduction Using the Rascal JUH-60a in-Flight Simulator," *64th Annual Forum of the American Helicopter Society*, Quebec, Canada, May 2008.

[52] Conversation with Dave Walsh of Hydramotion/Maradyne, Inc, 17 Apr 2009.

[53] J. Geisinger, and D. Black, "Electro-Hydrostatic Transmission and Control Technology for Modular D&D Manipulators," Department of Energy, 2001.

[54] "General Electric Aviation Systems," http://www.geaviationsystems.com/, 15 Apr 2009.

[55] Moog, Inc, http://www.moog.com/, 12 Apr 2009.

[56] According to Jim Smith of Moog, Inc., Technical Data Division, (personal phone conversation), 17 Apr 2009.

[57] S. Frischemeier, "Electrohydrostatic Actuators for Aircraft Primary Flight Control Types, Modeling and Evaluation", Hamburg, Germany, 1997.

[58] S. J. P. Maley, and N. Phan., U.S. Navy Roadmap to Structural Health and Usage Monitoring the Present and Future," *63rd Annual Forum of the American Helicopter Society*, Virginia Beach, VA, May 2007.

[59] C. Jarvis, and K. Szalai, "Ground and Flight Test Experience with a Triple Redundant Digital Fly by Wire Control," *Advanced Aerodynamics and Active Controls,* Feb. 1981, pp. 6784.

[60] J. Pappalardo, "Pit-stop smarts: NASCAR windshield laminates gaining military following," http://www.allbusiness.com/, 1 Nov 2004.

[61] J. R., Davis, *Aluminum and Aluminum Alloys: ASM International Handbook*, 1993.

[62] "MBB BK117 Tests Composites, Flight International," http://www.flightglobal.com, June 1989.

[63] Agarwal, B. D., Broutman, L. J, and K. Chandrashekhara, *Analysis and Performance of Fiber Composites*, 1st ed., John Wiley & Sons, Inc., 2006.

[64] C. O'Bradaigh, C. Semprimoschnig, and J. Kilroy "Mechanical and Physical Evaluation of New Carbon Fibre/Peek Composites for Space Applications," *SAMPE Journal*, Vol. 44, No. 3, May 2008.

[65] "Automated Dynamics," www.automateddynamics.com/, March 2009.

[66] K. Takayanagi, H. Nagasawa, C. Takahaski, J. Hayashi, and R. Kemmochi, "Possibility of Closed Loop Material Recycling for Fiber Reinforced Thermoplastic Composites," *Advanced Performance Materials*, Vol. 2, May/June 1995.

[67] M. C. Y., Niu, *Composite Airframe Structures, Practical Design Information and Data*, Conmilit Press Ltd., Honk Kong, 1992.

[68] "United States Department of Energy," http://www.doe.gov/, April 2009.

[69] M. F. Ashby, *Materials Selection in Mechanical Design*, 3rd ed., Elsevier, 2005.

[70] T. Suzuki and J. Takahashi, "Prediction of Energy Intensity of Carbon Fiber Reinforced Plastics for Mass-produced Passenger Cars," *9th Japan International SAMPE Symposium*, Tokyo, Japan, November 2005.

[71] "A Cleaner, Cheaper Route to Titanium," http://www.technologyreview.com/business/16963/, June 2006.

[72] R. Satish, A. P. Viswanath, and S. Selvin, "Helicopter Landing Gear System," RWR&DC, Hindustan Aeronautics Limited, Bangalore-560017.

[73] P. Minderhoud, "Development of Bell Helicopters Model 429 Sleigh Type Skid Landing Gear," Bell Helicopter Textron.

[74] "D&E Aircraft of Florida," http://www.de-aircraft.com/other.html.

[75] S. Desjardins, "The Evolution of Energy Absorption Systems for Crashworthy Helicopter Seats," *Journal of the American Helicopter Society*, Vol. 51, No. 2, April 2006.

[76] S. Zimmermann, R. Bolukbasi, A. Merritt, and N. Desjardins, "Aircraft Crash Survival Design Guide Volume IV," US-AAVSCOM, TR 89-D-22D, December 1989.

[77] G. Hiemenz, "Semi-Active Magnetorheological Seat Suspensions for Enhanced Crashworthiness and Vibration Isolation of Rotorcraft Seats," Ph.D. dissertation, University of Maryland, College Park, 2007.

[78] K. Yniguez, D. Majar, M. Ellenbecker, D. Estrada, N. Geiger, and M. Harrer, Whole Body Vibration Exposure for MH-60s Pilots." *43rd Annual SAFE Association Symposium,* Salt Lake City, Utah, October 2005.

[79] P. Gupta, H. Wei, N. Wereley, and G. J. Hiemenz, Semi-Active Magnetorheological Helicopter Crew Seat Suspension for Vibration Isolation," *64th Annual American Helicopter Society Forum*, Quebec, Canada, April 2008.

[80] G. J. Hiemenz, W. Hu, N. M. Wereley, and P. Chen, Adaptive Energy Absorption System for a Vehicle Seat," U.S. Patented Application Serial No. 11/819,875, 2008.

[81] "BAE Systems : S5000 Seating Lightweight, Energy-Absorbing Crew & Passenger Seat," Data sheets, 2007.

[82] "Ford Develops Foam with 40 Soy-Based Material," http://www.greencarcongress.com/2006/10/ford develops_f.html, October 2006.

[83] Navy Tactics, Techniques, and Procedures 3-50.1, Naval search and rescue (SAR) manual.

[84] L. Hartman and H. Sternfeld, "An Experiment in Aural Detection of Helicopters," ADA-0917355, Dec. 1973.

[85] F. Schmitz, "Reduction of Blade-Vortex Interaction (BVI) Noise through X-Force Control," NASA-TM-110371, Sept. 1995.

[86] C. Cox, "Fly Neighborly Guide," *Helicopter Association International*, Dec. 2008.

[87] F. D. Harris, and M. P. Scully, "Helicopters Cost Too Much," *53rd Annual Forum of the American Helicopter Society*, Virginia Beach, Virginia, April 1997.

[88] DARPA, "Mission Adaptive Rotor (MAR) Program," Pre-solicitation Notice, DARPA-SN-09-14, January 2009.

[89] F. D. Harris, and M. P. Scully, "Supplemental Appendix : Helicopters Cost Too Much," *53rd Annual Forum of the American Helicopter Society*, Virginia Beach, VA, April 1997.

[90] Bureau of Labor Statistics, *Consumer Price Index*, U.S. Department of Labor, Washington DC, 2009.

[91] The Official Helicopter Blue Book, "The Official Helicopter Specification Book and Helicopter Equipment Lists & Prices (H.E.L.P.)," HeliValue$, Inc.

[92] "Average Fuel Prices in a 50 Mile Radius of College Park, MD," http://www.airnav.com/fuel/local.html.